



A University of Sussex DPhil thesis

Available online via Sussex Research Online:

<http://sro.sussex.ac.uk/>

This thesis is protected by copyright which belongs to the author.

This thesis cannot be reproduced or quoted extensively from without first obtaining permission in writing from the Author

The content must not be changed in any way or sold commercially in any format or medium without the formal permission of the Author

When referring to this work, full bibliographic details including the author, title, awarding institution and date of the thesis must be given

Please visit Sussex Research Online for more information and further details

**AN INVESTIGATION INTO THE
FUNCTION OF SUMOYLATION IN
GENOMIC STABILTY IN
*SCHIZOSACCHAROMYCES POMBE***

BRENDA MERCER

A thesis submitted for the qualification of Doctor of Philosophy

University of Sussex

February 2013

I hereby declare that this thesis has not been, and will not be, submitted in whole or in part to another University for the award of any degree. The work described herein is my own work except where otherwise stated.

Brenda Mercer

February 2013

Acknowledgements

I would like to express my sincere gratitude to Dr. Felicity Watts for giving me the opportunity to carry out my doctoral studies in her laboratory and for her invaluable support and guidance throughout this period. I would like to thank to all our collaborators that contributed to my research: Dr. Ewan Main, Dr. Darren Thompson and Dr. Jacob Dalgaard. I would also like to thank everybody at GDSC and especially to the members of the Watts lab for their constant help and support. I am particularly grateful to Dr. Stephanie Schalbetter and Lauren Small for always being there for me as colleagues and friends.

I would like to thank my family for helping and supporting me in many different ways.

Finally, I would like to dedicate this thesis to my husband, for his constant support and encouragement.

UNIVERSITY OF SUSSEX
BRENDA MERCER

AN INVESTIGATION INTO THE FUNCTION OF
SUMOYLATION IN GENOMIC STABILITY IN *S. POMBE*

SUMMARY

Sumoylation is an essential posttranslational modification involved in many cellular processes such as DNA replication, chromosomal stability, cytokinesis, DNA damage responses and many others. The process of sumoylation is conserved in all eukaryotic organisms. This study involves the analysis of various aspects of sumoylation in the unicellular model organism *Schizosaccharomyces pombe*.

The first part of this study is concerned with elucidating the functional and structural importance of a SUMO-like domain (SLD) and a putative SUMO-binding domain (SBM) present in the essential protein Rad60. Biochemical and genetical analysis reveals that SLD2 is required for the DNA damage response function of Rad60 but that the putative SBM3 is a key structural feature of the hydrophobic core of SLD2 and therefore unlikely to function as a SUMO-interacting motif. As Rad60 interacts with the SUMO E3 ligase Pli1, which facilitates overall sumoylation and SUMO chain formation, further analysis was undertaken to identify the function of SUMO chain formation and the function of Pli1 in maintaining chromosomal stability. A SUMO chain mutant, Pmt3-K14R; K30R, was characterized and shown to be sensitive to the DNA replication inhibitor hydroxyurea. Analysis of the *pli1* null mutant reveals that Pli1 dependent sumoylation has multiple functions at the centromeric repetitive sequences as the mutant displays increased gene conversion at centromeric regions and increased loss of an artificial minichromosome rates compared to a wild type strain.

The second part of this study is concerned with identifying specific modified lysine residues in the sumoylation pathway components Fub2, Hus5 and Nse2 and the target proteins Rtf2 and PCNA. After identification of *in vitro* sumoylation sites, an analysis of the sumoylation of the SUMO conjugating enzyme Hus5 and the sumoylation of the Rtf2 protein is carried out. *In vivo* and genetical analysis of the *hus5-K50R* mutant suggests that the sumoylation of the conjugating enzyme is required for maintaining the homeostasis of the pathway and is essential for cell viability when the homologous recombination machinery is impaired. Sumoylation of Rtf2 protein is required for the response to the DNA alkylating agent MMS and, like the sumoylation of Hus5, is essential for cell viability in homologous recombination mutant backgrounds.

ABBREVIATIONS

A	alanine
ade	adenine
APS	ammonium persulphate
ATP	adenosine triphosphate
ADP	Adenosine diphosphate
AMP	Adenosine momophosphate
BER	Base excision repair
bp	base pairs
BSA	bovine serum albumin
CDK	cyclin-dependent kinase
cDNA	complementary deoxyribonucleic acid
CPK	creatine phosphokinase
Da	dalton
DAPI	4, 6-amino-2-phenylindole
DMSO	dimethylsulphoxide
DNA	deoxyribonucleic acid
dNTP	deoxyribonucleotide triphosphate
DSB	double strand break
DTT	dithiothreitol
E. coli	Escherichia coli
ECL	enhanced chemi-luminescence
EDTA	ethylenediaminetetraacetic acid
ELN	extremely low nitrogen
g	gram
G418	geneticin
Gy	Gray
HR	homologous recombination
<i>H. sapiens</i>	<i>Homo sapiens</i>
HU	hydroxyurea
IPTG	isopropyl- β -D- thiogalactopyranoside
IR	ionizing radiation
J/m ²	joules per meter squared
K	lysine
kb	kilobase
kDa	kilodalton
l	litre
LiOAc	lithium acetate
M	molar
MCS	multiple cloning site
ml	milliliter
MMS	methylmethane-sulphonate
μ g	microgram
μ l	microlitre
μ M	micromolar
NAT	nourseothricin sulfate
NER	nucleotide excision repair

NHEJ	non-homologous end joining
OD	optical density
ORF	open reading frame
PBS	phosphate buffered saline
PCR	polymerase chain reaction
PEG	polyethylene glycol
PMSF	phenylmethanesulphonyl fluoride
PPi	2x inorganic phosphate
R	arginine
RPM	revolutions per minute
<i>S. Cerevisiae</i>	<i>Saccharomyces cerevisiae</i>
SDS-PAGE	sodium dodecyl sulphate polyacrylamide gel electrophoresis
TBE	Ttris borate
TBZ	thiabendazole
TCA	trichloroacetic acid
TE	tris aminomethane
TEMED	N, N, N', N'-tetramethyl-ethylenediamine
Ura	uracil
UV	ultra-violet
YE	yeast extract
YNB	yeast nitrogen base
X-gal	5-bromo-4-chloro-3-indol- β -D galactopyranoside

Table of Contents

CHAPTER 1 INTRODUCTION	5
1.1 <i>S. pombe</i> as a model organism	5
1.2 The cell cycle.....	6
1.2.1 S phase	7
1.2.2 M phase.....	9
1.3 Genome integrity checkpoints	10
1.4 The spindle assembly checkpoint (SAC)	13
1.5 DNA damage	13
1.6 DNA damage repair mechanisms	14
1.6.1 Nucleotide excision repair (NER).....	14
1.6.2 Base excision repair (BER).....	14
1.6.3 Mismatch repair (MMR).....	15
1.6.4 Non-homologous end joining (NHEJ)	15
1.6.5 Homologous recombination (HR)	16
1.7 SUMO	18
1.7.1 Post-translational modifications of proteins	18
1.7.2 Ubiquitin.....	19
1.7.3 The Sumoylation pathway	20
1.7.4 The sumoylation pathway components.....	21
1.7.5 SUMO-like domains (SLDs).....	24
1.7.6 SUMO-interacting motifs (SIMs)	24
1.7.7 SUMO targeted ubiquitin ligases (STUbLs).....	25
1.8 SUMO targets	26
1.8.1 RPA.....	27
1.8.2 PCNA	27
1.8.3 Structural maintenance of chromosome complexes (SMCs).....	29
1.8.4 Rad52 and homologous recombination.....	30
1.9 Aims.....	31
CHAPTER 2 MATERIALS AND METHODS.....	32
2.1 <i>S. pombe</i> Methods.....	32
2.1.1 <i>S. pombe</i> Media.....	32
2.1.2 <i>S. pombe</i> strains.....	33
2.1.3 <i>S. pombe</i> vectors	33
2.1.4 Recombination-mediated cassette exchange (Watson <i>et al.</i> , 2008)	35
2.1.5 <i>S. pombe</i> transformation - standard LiAc method.....	35
2.1.6 <i>S. pombe</i> genetic mating crosses	36
2.1.7 Survival Analysis.....	37
2.1.8 DAPI staining of <i>S. pombe</i> cells.....	38
2.1.9 Mutation Rate Determination.....	38
2.1.10 Genomic DNA extraction from <i>S. pombe</i>	39
2.2 BACTERIAL METHODS	40
2.2.1 Bacterial media.....	40
2.2.2 Antibiotics.....	40
2.2.3 Blue-white selection	40
2.2.4 <i>E.coli</i> strains.....	41
2.2.5 Bacterial cloning vectors.....	41
2.2.7 Preparation of competent <i>E. coli</i> cells.....	42
2.2.8 <i>E. coli</i> transformation	43

2.3 DNA METHODS.....	44
2.3.1 Agarose gel electrophoresis	44
2.3.2 Pulse-Field Gel Electrophoresis (PFGE).....	44
2.3.3 PCR-amplifying DNA fragments.....	46
2.3.4 PCR- Site-directed mutagenesis.....	46
2.3.5 PCR purification	47
2.3.6 Ethanol precipitation	47
2.3.7 Restriction enzyme digests.....	47
2.3.8 Purification of DNA fragments from agarose gels.....	48
2.3.9 Ligations.....	48
2.3.10 Amplification of plasmid DNA.....	48
2.3.11 Sequencing by GATC.....	50
2.4 PROTEIN METHODS	50
2.4.1 SDS polyacrylamide gel electrophoresis (SDS-PAGE).....	50
2.4.2 Coomassie Brilliant Blue Staining.....	52
2.4.3 Western Blotting.....	52
2.4.4 Incubation of PVDF membrane with antibodies.....	53
2.4.5 Enhanced Chemi-Luminescence	53
2.4.6 Determining protein expression and solubility.....	54
2.4.7 Bradford assay	54
2.4.8 GST-tagged protein purification.....	54
2.4.9 His-tagged protein purification.....	56
2.4.10 Expression and purification of PCR polymerases.....	58
2.4.11 Protein dialysis.....	60
2.4.12 Protein desalting/buffer exchange	60
2.4.13 Size exclusion chromatography (gel filtration).....	60
2.4.14 Concentrating protein samples	61
2.4.15 Equilibrium Denaturation Studies	61
2.4.16 Dynamic Light Scattering (DLS).....	61
2.4.17 Protein crystallization screening	62
2.4.18 Affinity purification of crude anti-sera.....	62
2.4.19 Total Cell Extracts (TCAs).....	64
2.4.20 <i>In vitro</i> sumoylation assay	65
2.4.21 <i>In vitro</i> GST-pull down assay.....	65
2.4.22 Identification of sumoylated lysine residues by tandem mass spectrometry	67
CHAPTER 3 ANALYSIS OF THE SUMO-LIKE DOMAINS AND PUTATIVE SUMO-BINDING MOTIFS OF RAD60.....	68
3.1 Introduction.....	68
3.2 Structural characterization of Rad60	69
3.2.1 Expression and purification of full length Rad60.....	69
3.2.2 Residues essential for β -GRASP fold are conserved in SLD1 and SLD2	70
3.3 SLD2 interacts with the SUMO conjugator <i>in-vitro</i>	71
3.4 Analysis of putative SBMs.....	72
3.4.1 Putative SBMs do not facilitate Rad60 dimerization <i>in vitro</i>	72
3.4.2 Putative SBMs do not interact with SUMO <i>in vitro</i>	73
3.4.3 Effect of mutating putative SBMs	73
3.5 Putative SBM3 is essential to maintain SLD2 structure.....	74
3.6 Crystallographic studies of SLD2	75
3.7 Discussion.....	76
3.7.1 Structure and function of Rad60	76
3.7.2 Putative SUMO-binding motifs (SBMs)	77

CHAPTER 4 SUMO CHAIN FORMATION IS REQUIRED FOR DNA DAMAGE RESPONSE DURING S PHASE	79
4.1 Introduction.....	79
4.2 <i>In silico</i> analysis of sequence requirement for SUMO chains formation.....	80
4.3 Expression and purification of recombinant sumoylation pathway components and optimization of <i>in vitro</i> sumoylation assay	81
4.3.1 Co-expression and purification of SAE	81
4.3.2 Expression and purification of E2 and E3 enzymes and SUMO-GG	82
4.3.3 Optimization of <i>in vitro</i> sumoylation assay.....	83
4.3.4 Pli1 is more efficient than Nse2 at forming SUMO chains <i>in vitro</i>	83
4.4 <i>In vitro</i> SUMO chain formation occurs at K14 and K30.....	84
4.4.1 Expression and purification of SUMO chain mutants	84
4.4.2 Both K14 and K30 are substrates for SUMO chain formation in the absence of E3 ligases.....	85
4.4.3 E3 ligases facilitate SUMO chain formation at K14 and K30	85
4.5 <i>In vivo</i> analysis of SUMO chains mutants	86
4.5.1 K14 and K30 are substrates for SUMO chain formation <i>in vivo</i>	86
4.5.2 Phenotypic characterization of SUMO chain mutants.....	87
4.6 Discussion.....	90
CHAPTER 5 INVESTIGATING THE FUNCTION OF PLI1.....	92
5.1 Introduction.....	92
5.1.1 <i>S. pombe</i> centromeres	92
5.1.2 Using the artificial minichromosome Ch16 to determine mutation rates.....	93
5.2 Sumoylation mutants show an increased mutation rate.....	95
5.2.1 Sumoylation mutants show an increased rate of minichromosome loss.....	95
5.2.2 Sumoylation mutants show an increased rate of gene loss.....	96
5.3 Different mutant backgrounds display different chromosomal rearrangements..	96
5.4 Minichromosomal rearrangements in <i>pli1Δ</i> cells result in isochromosome formation	99
5.5 Pli1-dependent sumoylation does not prevent isochromosome formation	100
5.6 Discussion.....	101
Chapter 6 HUS5 SUMOYLATION REGULATES THE PATHWAY HOMEOSTASIS.....	103
6.1 Introduction.....	103
6.2 Strategy to identify sumoylated lysine residues by mass spectrometry	104
6.3 Sumoylation pathway components are sumoylated <i>in vitro</i> at specific lysine residues	105
6.3.1 The SUMO activating enzyme Fub2 is sumoylated <i>in vitro</i> at five lysine residues.....	105
6.3.2 The SUMO E3 ligase Nse2 is sumoylated <i>in vitro</i> at three lysine residues.....	106
6.3.3 The SUMO conjugating enzyme Hus5 is sumoylated <i>in vitro</i> at K50	106
6.4 <i>In vitro</i> analysis of sumoylation of Hus5 at K50	107
6.5 <i>hus5-K50R</i> mutant promotes hyper-sumoylation <i>in vivo</i>	108
6.6 Phenotypic analysis of <i>hus5-K50R</i> mutant	108
6.6.1 <i>hus5-K50R</i> is not sensitive to S-phase arrest	109
6.6.2 Hus5 sumoylation is not required for chromosome segregation or protein synthesis	109
6.6.3 <i>hus5-K50R</i> mutant sensitivity to IR is S-phase specific	109
6.6.4 Sumoylation of Hus5 is required for cell viability when homologous recombination is impaired	110
6.6.5 Sumoylation of Hus5 is required for DNA damage response when sumoylation of the Smc5/6 complex is impaired	111

6.6.6 Sumoylation of Hus5 prevents gross chromosomal rearrangements	111
6.7 Discussion.....	112
Chapter 7 Sumoylation of Rtf2 is required for recovery from IR induced DNA damage during early S-phase	112
7.1 Introduction.....	114
7.2 PCNA is sumoylated at specific lysines <i>in vitro</i>	115
7.3 <i>In silico</i> analysis of sumoylation of PCNA in <i>S. pombe</i>	115
7.4 Rtf2 does not function as a SUMO E3 ligase <i>in vitro</i>	116
7.5 Rtf2 is sumoylated <i>in vitro</i> at specific lysine residues.....	117
7.6 <i>In silico</i> analysis Rtf2.....	118
7.7 Creating the Rtf2 sumoylation mutants from a <i>rtf2</i> ⁺ base strain	119
7.8 Phenotypic characterization of <i>rtf2</i> ⁺ sumoylation mutants.....	120
7.8.1 Rtf2 defective in sumoylation is sensitive to MMS and IR	120
7.8.2 Rtf2 sumoylation mutants are lethal with recombination mutants	122
7.9 Discussion.....	122
7.9.1 Sumoylation of PCNA.....	122
7.9.2 Sumoylation of Rtf2	123
CHAPTER 8 DISCUSSION	125
CHAPTER 9 REFERENCES	131
PUBLICATIONS.....	156

LIST OF FIGURES

- Fig. 1.1 Cartoon representation of the Replication Fork
- Fig. 1.2 Homologous Recombination Repair mechanism
- Fig. 1.3 The sumoylation pathway
- Fig. 1.4 Post-translational modification of PCNA regulates post replication repair
- Fig. 1.5 The Smc5/6 complex
- Fig. 3.1 Schematic representation of Rad60 protein
- Fig. 3.2 Sequence alignment of RENi family proteins
- Fig. 3.3 Purification and stability studies of His tagged Rad60_FL
- Fig. 3.4 Purification of GST tagged Rad60_FL
- Fig. 3.5 SLD1 and SLD2 can be modeled onto *H. sapiens* SUMO-1 structure
- Fig. 3.6 Essential structural residues of SUMO-1 are conserved in SLD1 and SLD2
- Fig. 3.7 Purification of His-tagged SLD2
- Fig. 3.8 Solubility trials of SLD2 mutants
- Fig. 3.9 Residues of SUMO-1 required for non-covalent interaction with Ubc9 are conserved in SLD2
- Fig. 3.10 SLD2 interacts with Hus5 *in vitro*
- Fig. 3.11 Rad60 does not interact with Rad60CT or SLD2 *in vitro*
- Fig. 3.12 *In vitro* GST pull down assays of Rad60 fragments
- Fig. 3.13 Rad60 and SLD2 do not interact with SUMO *in vitro*
- Fig. 3.14 Effect of mutating the three putative Rad60-SBMs
- Fig. 3.15 The C-terminal of SUMO-1 has a sequence consistent with a SIM domain
- Fig. 3.16 Mutation of SBM3 results in SLD2 aggregation
- Fig. 3.17 Crystal structure and denaturation studies of SLD2 confirm the structural requirement of putative SBM3 for Rad60 stability
- Fig. 3.18 Purification and stability studies of His tagged SLD2
- Fig. 3.19 Crystallization of SLD2
- Fig. 3.20 Cartoon representations of crystal structure of *Sp* SLD2 and *Hs* SUMO-1
- Fig. 4.1 *Sp* SUMO has an extended, disordered N-terminus
- Fig. 4.2 N-terminal lysines of SUMO proteins are required for SUMO chain formation

Fig. 4.3 Co-expression and purification of Fub2/Rad31 (E2) complex

Fig. 4.4 Expression and purification of His-Pmt3-GG and GST-Hus5

Fig. 4.5 *In vitro* sumoylation assay time course

Fig. 4.6 Expression and purification of SUMO E3 ligases

Fig. 4.7 Pli1 is 20x more efficient than Nse2 at facilitating *in vitro* SUMO chain formation

Fig. 4.8 Expression and purification of SUMO mutants for *in vitro* sumoylation assays

Fig. 4.9 *In vitro* SUMO chain formation occurs at K14 and K30

Fig. 4.10 E3 ligases, Pli1 and Nse2 facilitate *in vitro* SUMO chain formation

Fig. 4.11 Constructs for the integration of SUMO chain mutants into the genome as the sole copy of *pmt3* gene

Fig. 4.12 Effect of SUMO chain mutations on levels of high Mr sumoylated species *in vivo*

Fig. 4.13 SUMO chain mutant display aberrant cell and nucleus morphology

Fig. 4.14 SUMO chains mutants are sensitive to HU

Fig. 4.15 SUMO chain mutant is slow growing on HR mutants background

Fig. 4.16 SUMO protease *ulp2* deletion mutant has more than one suppressor

Fig. 4.17 SUMO-1 has potential SUMO chain substrate lysines at the globular C-terminal

Fig. 5.1 Graphical representation of *S.pombe* chromosomes and the centromeric region of chromosome III

Fig. 5.2 Using the minichromosome Ch16-AGU to determine spontaneous mutation rates

Fig. 5.3 Graphical representation of relative rates of minichromosome loss of SUMO mutants

Fig. 5.4 Graphical representation of relative rates of *ura4* loss of SUMO mutants

Fig. 5.5 Possible intra- and interchromosomal rearrangements following DNA damage

Fig. 5.6 Different mutant backgrounds give rise to different chromosomal rearrangements

Fig. 5.7 Analysis of the breakpoint of Ch160-AGU in *pli1Δ* mutant cells by PCR

Fig. 5.8 Graphical representation of chromosomal rearrangements fractions of wild type, *pli1Δ* and *rad22Δ* strains

Fig. 6.1 Strategy to identify sumoylated lysine residues by tandem mass spectrometry (MS/MS)

Fig. 6.2 *In vitro* sumoylation assay to identify sumoylated lysine residues by tandem mass spectrometry (MS/MS)

Fig. 6.3 MS/MS fragmentation of Fub2 peptide sumoylated at K86

Fig. 6.4 MS/MS fragmentation of Fub2 peptide sumoylated at K172

Fig. 6.5 MS/MS fragmentation of Fub2 peptide sumoylated at K176

Fig. 6.6 MS/MS fragmentation of Fub2 peptide sumoylated at K263

Fig. 6.7 MS/MS fragmentation of Fub2 peptide sumoylated at K282

Fig. 6.8 Mammalian SAE2 is autosumoylated at five lysine residues clustered in the cysteine domain

Fig. 6.9 Comparison of the position of the sumoylated lysines of *S.pombe* Fub2 and mammalian SAE2

Fig. 6.10 MS/MS fragmentation of Nse2 peptide sumoylated at K134

Fig. 6.11 MS/MS fragmentation of Nse2 peptide sumoylated at K229

Fig. 6.12 MS/MS fragmentation of Nse2 peptide sumoylated at K247

Fig. 6.13 Nse2 sumoylated lysine residues are conserved in humans but not *S. cerevisiae*

Fig. 6.14 Structural mapping of the sumoylated lysines of Nse2

Fig. 6.15 MS/MS fragmentation of Hus5 peptide sumoylated at K50

Fig. 6.16 Comparison of the position of the sumoylated lysines of Hus5

Fig. 6.17 Hus5-K50R is not sumoylated *in vitro*

Fig. 6.18 Strategy to create *hus5-K50R* mutant using a *hus5* base strain (bs)

Fig. 6.19 *hus5-K50R* mutant promotes hypersumoylation

Fig. 6.20 *hus5-K50R* mutant display aberrant cell and nucleus morphology

Fig. 6.21 The *hus5-K50R* mutant is not sensitive to S-phase genotoxins

Fig. 6.22 The *hus5-K50R* mutant is not sensitive to protein synthesis and microtubule inhibition

Fig. 6.23 The *hus5-K50R* sensitivity to ionizing radiation is reversed by over-expression of the SUMO protease Ulp2

Fig. 6.24 Sumoylation of Hus5 is required for cell viability in HR mutant backgrounds

Fig. 6.25 *hus5-K50R x nse2-SA* double mutant is hypersensitive to low doses of UV, IR and HU

Fig. 6.26 *hus5-K50R* promotes gross chromosomal rearrangements

Fig. 6.27 MS/MS fragmentation of SUMO peptide sumoylated at K30

Fig. 6.28 Structural representation of non-covalent interaction of sumoylated Ubc9 with SUMO-1

Fig. 7.1 *in vitro* poly-sumoylation of PCNA is facilitated by Pli1 E3 ligase

Fig. 7.2 MS/MS fragmentation of PCNA peptide sumoylated at K13

Fig. 7.3 MS/MS fragmentation of PCNA peptide sumoylated at K164

Fig. 7.4 MS/MS fragmentation of PCNA peptide sumoylated at K172

Fig. 7.5 MS/MS fragmentation of PCNA peptide sumoylated at K253

Fig. 7.6 *S. pombe* PCNA sumoylated lysine residues are sequentially conserved in humans and *S. cerevisiae*

Fig. 7.7 Structural mapping of the sumoylated lysines and possible sumoylation sites of PCNA

Fig. 7.8 Rtf2 does not function as a SUMO E3 ligase *in vitro*

Fig. 7.9 Rtf2 is sumoylated *in vitro*

Fig. 7.10 MS/MS fragmentation of Rtf2 peptide sumoylated at K184

Fig. 7.11 MS/MS fragmentation of Rtf2 peptide sumoylated at K209

Fig. 7.12 MS/MS fragmentation of Rtf2 peptide sumoylated at K224

Fig. 7.13 Sequence alignment of Rtf2

Fig. 7.14 Structural modeling of *S. pombe* and *H. sapiens* Rtf2 protein

Fig. 7.15 Strategy to create an *rtf2*⁺ base strain

Fig. 7.16 Strategy to create *rtf2*⁺ sumoylation mutants

Fig. 7.17 *rtf2Δ* and *rtf2-T* mutants display aberrant cell and nucleus morphology

Fig. 7.18 *rtf2* sumoylation mutants are sensitive to MMS

Fig. 7.19 *rtf2* sumoylation mutants are sensitive to ionizing radiation

Fig. 7.20 *rtf2-T* and *rtf2-1* mutants are sensitive to low dose of IR during early S-phase

Fig. 7.21 Sumoylation of Rtf2 is required for cell viability on HR mutants background

Fig. 7.22 Sumoylation of three lysine residues of Rtf2 is required for cell viability on HR mutants background

Fig. 7.23 Rtf2 contains a N-terminal U-box domain

Fig. 8.1 Rad60 interactions with sumoylation machinery may control the levels of sumoylated Smc5/6 complex

LIST OF TABLES

Table 1.1 Components of the sumoylation pathway

Table 2.1 *S. pombe* strains

Table 2.2 *E. coli* strains

Table 5.1 Mutant strains containing the minichromosome Ch16-AGU used in this study

Table 5.2 Published spontaneous mutations rates obtained by using the Ch16 assay

Table 5.3 Frequency of genomic rearrangements obtained by using the Ch16 assay

Table 5.4 Determination of rates of minichromosome loss of SUMO mutants by fluctuation analysis

Table 5.5 Determination of rates of *ura4* loss of SUMO mutants by fluctuation analysis

Table 5.6 Determination of percentage of different chromosomal rearrangements of wild type, *pli1Δ* and *rad22Δ* strains

Table 6.1 Sumoylated lysine residues identified in Fub2, Hus5 and Nse2

Table 7.1 Sumoylated lysine residues identified in PCNA

Table 7.2 *S. pombe* PCNA possible sumoylation sites are within non-consensus motifs

Table 7.3 Rtf2 possible sumoylation sites are within non-consensus and canonical motifs

CHAPTER 1

INTRODUCTION

The fundamental characteristic of life is the ability of cells to accurately transmit their genomic information to daughter cells. To achieve this, cells employ complex mechanisms to replicate their genomes, prevent and repair DNA damage and faithfully segregate their DNA between two identical daughter cells. Faults in these mechanisms can lead to genetic diseases, carcinogenesis and cell death.

Cancer is still one of the least understood human diseases and technical and ethical difficulties to study human cells complicate the efforts to make progress in preventing and curing cancer. The use of model organisms to study the eukaryotic cell cycle, DNA damage repair mechanisms and to identify genes involved in these cellular processes has contributed greatly to the understanding of genetic defects that can lead to carcinogenesis.

1.1 *S. pombe* as a model organism

Schizosaccharomyces pombe is a single-celled eukaryote belonging to the kingdom of fungi. It usually exists in haploid form and was initially developed as a model organism to study genetics due to the ease of obtaining mutant strains and the strength of the phenotypes (Leupold, 1957). It has a rod-like shape and, during the cell cycle, it maintains its shape and grows exclusively through the cell tips to divide by medial fission and generate two daughter cells of the same size. Given these characteristics and its rapid growth, the fission yeast gained popularity as a model organism to study the mitotic cell cycle of human cells (Mitchison, 1957).

The identification and characterization in *S. pombe* of the cyclins and the cyclin-dependent kinase, Cdc2 (CDK), the conserved proteins responsible for driving and controlling the cell cycle, further highlighted the significance of this model organism (eg. Lee and Nurse, 1987). Following the nearly complete sequencing of its genome (Wood et al., 2002), further studies in *S. pombe* propose that many of the essential eukaryotic genes emerged with the first eukaryotic cell and remained conserved in all cells (Decottignies et al., 2003), with significant homology in cell cycle regulation, DNA replication and DNA damage repair proteins.

1.2 The cell cycle

The cell cycle is driven by oscillations in the concentration of cyclins, which effect oscillations in the activity of CDKs (cyclin-dependent kinases) through their binding. The active cyclin-CDK complexes phosphorylate proteins required to coordinate the entries to the phases of the cell cycle. Each cell cycle transition is driven by a specific CDK, and a particular cyclin activates each CDK. The timely and accurate progression of the cell through the phases of the mitotic cycle is controlled by complex mechanisms known as ‘checkpoints’.

Following the termination of mitosis, the new cell enters the G1 growth phase during which the restriction point (start point in yeast) (Pardee, 1989) determines whether the cell should continue to divide or exit the cycle and enter the vegetative G0 phase. As the cells commit to the cell cycle, they continue to grow and proteins required for DNA replication are synthesized. DNA replication takes place during S phase. The intra-S phase checkpoint is activated if the replication fork stalls or collapses. After the cells complete DNA synthesis, they enter G2 phase. G2 is mainly characterized by cell growth and preparation for mitosis. Two checkpoints are active during G2 phase: the S/M checkpoint, also known as the DNA replication checkpoint, as it ensures that DNA replication is completed before the onset of mitosis, and the G2/M checkpoint, also known as DNA damage checkpoint as it ensures that no DNA damage is present at the initiation of mitosis.

For the purpose of this thesis, S phase and the M phase are described further.

1.2.1 S phase

DNA replication starts at multiple replication origins, known as *oris* or *ARSs* (Autonomous Replication Sequences) in yeast. These are specific chromosomal sites that are bound by the ‘origin-recognition complex’ (Laane et al.). Replication origins, bound by the ORC, are recognized by the DNA helicases MCM (minichromosome maintenance proteins) (Grallert and Nurse, 1996, Kelman et al., 1999). Helicases unwind the double-stranded DNA and create single-stranded DNA (ssDNA). The unwinding of the double helix in a circular unidirectional path creates supercoiled DNA. Topoisomerases release the supercoiling by creating ‘nicks’ in one of the strands, passing the other strand through the nick and resealing the cut. Single-stranded DNA, generated by helicases, is coated by proteins specialized in single-strand binding such as the Replication Protein A (RPA). RPA keeps the homologous strands from re-annealing and interacts with many proteins required for replication fork progression (Henricksen et al., 1994).

DNA polymerases require a RNA primer to start synthesize DNA. RNA primases synthesize RNA primers complementary to the ssDNA (Griep, 1995). Following the establishment of the replication fork (fig. 1.1), DNA elongation is carried out by DNA polymerases. As DNA polymerases can only integrate nucleotides in the 5’ to 3’ direction, one strand is replicated in a continuous manner, the leading strand, while the other strand is polymerized in opposite direction as discrete nucleotides chains (Okazaki fragments) that are synthesized in a 5’ to 3’ fashion (Okazaki et al., 1967). Polymerases form asymmetric dimers to synchronize the replication of both strands. DNA ligases join the Okazaki fragments and seal the gaps in the sugar-phosphate backbone by catalyzing the formation of the phosphodiester bonds in the lagging strand (Ellenberger and Tomkinson, 2008).

To ensure continuous DNA synthesis, polymerases are hold onto the DNA by processivity factors: homo- or hetero-polymers that are capable of traveling along the

Fig. 1.1 The Replication Fork

Cartoon representation of the main components of the replication fork. DNA replication requires a helicase to separate the duplex, a processivity factor (PCNA), a RNA primase and a DNA polymerase. Topoisomerases release the supercoiles that result from the unwinding of the duplex.

The proteins are represented by Pymol software-generated images based on determined structures; ie the helicase is represented by a Pymol-generated image based on the structure of a helicase.

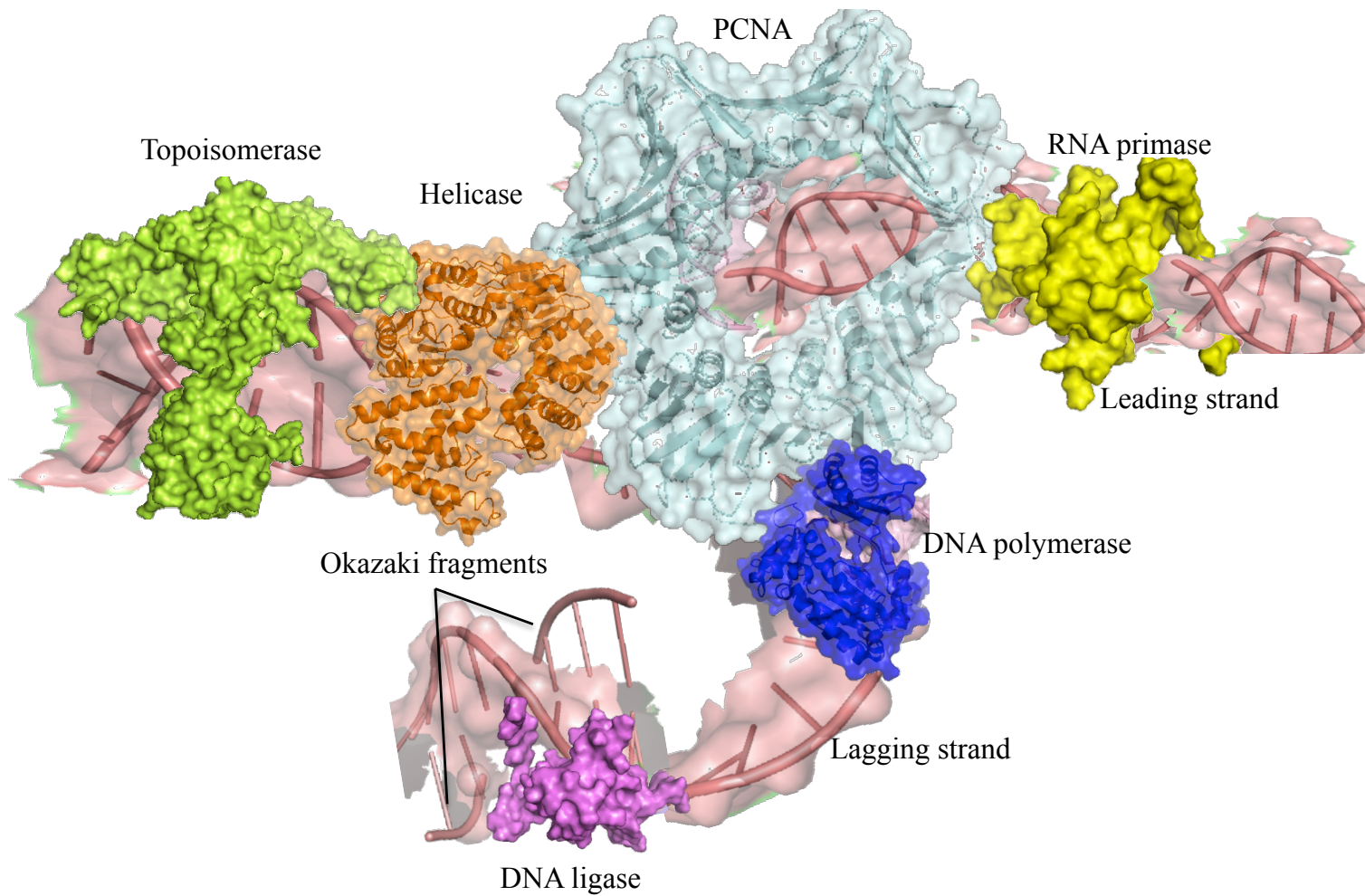


Fig. 1.1 Cartoon representation of the Replication Fork

DNA duplex by encircling it (sliding clamps). One of the most studied processivity factors is the homo-trimeric protein PCNA (Proliferating Cell Nuclear Antigen) (Miyachi et al., 1978, Krishna et al., 1994). Apart of its processive role, PCNA is a key regulator of other replication-associated mechanisms through its interactions with DNA endonucleases (Tom et al., 2000, Guo et al., 2010), helicases (Armstrong et al., 2012) and ligases (Mayanagi et al., 2011). Some of the roles of PCNA are discussed in section 1.5.5. The Replication Factor C (RFC) complex catalyzes the loading of PCNA onto the DNA.

Termination of replication in eukaryotes occurs when two opposing forks merge (Edenberg and Huberman, 1975) or when the fork reaches the end of the chromosomes at the telomeric regions (Lundblad, 2012). Outside of the telomeres, it is believed that replication terminates mostly at random sites where two forks meet, although some specific sites have been identified (Dalgaard et al., 2009). These sites are characterized by protein-DNA complexes that act as replication fork barriers (RFBs) and stall the replication process (Fachinetti et al., 2010). It has been shown that in mammals transcription factors act at ribosomal DNA (rDNA) to stall the fork to avoid collision between the replication machinery and the transcription machinery (Gerber et al., 1997). Most of the research on eukaryotic replication termination has been carried out in *S. pombe* and *S. cerevisiae* (Steinacher et al., 2012). In *S. pombe*, RTS1 (replication termination site 1) has been identified as a replication termination specific site (Dalgaard and Klar, 2001). Several proteins have been identified to function in DNA replication termination at the RTS1 locus: the Swi1-Swi3 complex and the Rtf1 and Rtf2 (termination factor 1 and 2) proteins (Dalgaard and Klar, 2000, Eydmann et al., 2008, Inagawa et al., 2009). Analysis of these proteins in *S. pombe* is relevant to understanding how termination of replication occurs in mammalian cells as the RTS1 locus is closely related to the mammalian rDNA replication barriers (Eydmann et al., 2008).

If DNA damage is encountered during replication, the intra-S phase checkpoint is activated and the replication fork is stalled to allow repair. The intra-S phase checkpoint is discussed in section 1.3. Both replication fork stabilization during stalling, and replication fork restart after stalling, require many replication and DNA damage repair proteins. It has been shown that homologous recombination starts blocked replication

forks by template exchange. The process is mutagenic and results in gross chromosomal rearrangements (GCRs) (Lambert et al., 2010).

1.2.2 M phase

During the mitotic phase, cells separate their newly replicated chromosomes into two identical sets. M phase has several sequential, discrete phases: prophase, metaphase, anaphase and telophase. M phase begins with the condensation of the newly replicated chromosomes in prophase, process requiring the condensin complex (Hirano T, 1994). Prophase is followed by metaphase when the paired chromosomes align in the middle of the nucleus and attach to the microtubules. During anaphase the sister chromatids separate and the daughter chromosomes are pulled towards the poles of the cell. Telophase is characterized by the formation of the daughter nuclei, followed by cytokinesis. While most animal cells have an open mitosis, where the nuclear envelope breaks before the chromosomes separate, *S. pombe* has a closed mitosis, where the chromosomes divide within an intact (“closed”) cell nucleus.

From the end of DNA replication until the onset of anaphase the cohesin complex holds the sister chromatids together (Zou, 2012). Condensin and cohesin belong to the SMC (structural maintenance of chromosome) family of proteins and have multiple functions throughout the cell cycle including roles in DNA replication, DNA damage repair and transcription. During metaphase, the kinetochore assembles at the centromeres of the sister chromatids and attaches to the microtubules that extend from the spindle poles of the cell. The correct positioning of the mitotic spindle at the centromeres ensures accurate distribution of the genetic material between the two daughter cells. Once the centromeres are aligned in the middle of the nuclei, the Anaphase Promoting Complex (APC) (Ostapchuk et al., 1986) triggers a set of events that conclude in the separation of the sister chromatids. The APC targets the protein securin for degradation. Securin forms a complex with separase, a cysteine protease that hydrolyses cohesin. Proteolysis of securin releases separase, which in turn cleaves the cohesion complex and releases the sister chromatids (Yamashita et al., 1999). The spindle checkpoint prevents sister chromatids segregation until all centromeres are properly aligned and attached to the mitotic spindle.

Centromeres are important specialized chromosomal structures required for correct chromosome segregation. While *S. cerevisiae* has simple ‘point’ centromeres (Meraldi et al., 2006), *S. pombe* centromeres are large, complex, transcriptionally silenced heterochromatic structures, more similar to those of humans (Clarke et al., 1986).

1.3 Genome integrity checkpoints

Checkpoints are active at specific times of the cell cycle and are designed to detect stalled or collapsed replication forks that arise during DNA replication, and DNA damage that can occur throughout the cell cycle. When such defects are encountered, the checkpoints generate a cell cycle delay or arrest that allows replication fork restart and/or DNA damage repair (Carr, 2002, Hartwell et al., 1994). Checkpoints also ensure that the phases of the cell cycle occur in a timely order by controlling the completion of essential processes before the initiation of a subsequent process. Checkpoints are organized as signal transduction pathways, with components acting as sensors, mediators and effectors. The term ‘checkpoint’ has been established after research on mutants defective in cell cycle in *S. cerevisiae* (Hartwell and Weinert, 1989).

The G1/S checkpoint

The G1/S checkpoint prevents damaged DNA, present at the beginning of the cell cycle, from being replicated during S phase. It involves the sequential activation of ATM/ATR and the tumor suppressor p53 proteins, followed by down-regulation of CDK2/cyclin E levels.

ATM (Ataxia telangiectesia mutated) and ATR (ATM and Rad3 related) are serine/threonine kinases that are activated by IR-induced DNA double-strand breaks and UV-induced single-strand breaks respectively (Banin et al., 1998). ATM and ATR phosphorylate the tumor suppressor p53, which acts as an effector protein (Banin et al., 1998). Phosphorylated p53 inhibits transcription of S phase-specific proteins by inactivating the CDK2/cyclin complex (Dulic et al., 1994).

The intra-S phase checkpoint

The intra-S phase checkpoint arrests or slows down the replication process until defects encountered by the replication fork are repaired (Bartek et al., 2004). ATM and ATR sense the DNA damage and trigger a signaling cascade that results in inhibition of Cdc25, the phosphatase for Cdk2. Phosphorylated Cdk2 blocks the replication fork progression (Falck et al., 2002), allowing time for DNA damage repair.

The G2/M DNA damage checkpoint

The G2/M checkpoint is activated by DNA damage and ensures that the newly replicated DNA is damage-free before the cell enters mitosis (Lobrich and Jeggo, 2007). Sensor proteins localize at sites of damage and trigger a signaling cascade that results in recruitment of DNA repair proteins. As the genome is duplicated and the sister chromatids are held together in G2, the main mechanism employed for repair is homologous recombination.

The S/M DNA replication checkpoint

The S/M DNA replication checkpoint prevents the cell from entering mitosis with incompletely replicated chromosomes (Corellou et al., 2000). The initiation of this checkpoint does not rely on damaged DNA and it has been shown in *S. pombe* that the replication checkpoint is initiated by the inhibition of the DNA polymerase α (Pol1^{Sp}) (D'Urso et al., 1995).

Checkpoint proteins

Many of the checkpoint proteins were first identified in *S. pombe*, including the Rad proteins (radiation sensitive): Rad1, Rad3, Rad9, Rad26 and Hus1 (hydroxyurea sensitive) (al-Khodairy and Carr, 1992, Enoch et al., 1993).

Rad1, Rad9 and Hus1 form the 9-1-1 complex (Rad9 – Rad1 – Hus1), a PCNA-like sliding clamp that is conserved from yeast to humans (Parrilla-Castellar et al., 2004). The 9-1-1 complex is loaded onto the DNA in response to different stresses and is required for checkpoint activation. Rad26 is the *S. pombe* homologue of the human ATRIP (ATR Interacting Protein) (al-Khodairy et al., 1994). Rad26/ATRIP is phosphorylated by ATR/Rad3 in response to DNA damage, and the two proteins form a complex that responds to DNA damage independent of other checkpoint proteins (Edwards et al., 1999). Rad3 is the *S. pombe* homologue of human kinase ATR (Bentley et al., 1996). Rad3/ATR phosphorylates many substrates in response to DNA damage and is required for activation of S/M, G/M and intra-s checkpoints (reviewed by Humphrey, 2000).

Another important sensor checkpoint protein is ATM (Ataxia telangiectesia mutated). The *S. pombe* homologue of human ATM is the Tel1 protein (Matsuura et al., 1999). ATM/Tel1 is recruited to DNA double-strand breaks by the MRN complex, which directly binds DNA ends (Lee and Paull, 2004). The MRN complex is composed of Mre11, Rad50 and Nbs1 (Xrs2 in *S. cerevisiae*) proteins and is conserved in all eukaryotes. In *S. pombe*, Tel1/ATM checkpoint signaling is activated only when the DNA-end resection is inhibited (Limbo et al., 2010). Rad3/ATR is the major sensor for checkpoint signaling through the main mediators Chk1 and Cds1 (Boddy et al., 1998). ATM and ATR phosphorylate both checkpoint mediators and effectors or directly target proteins. It has been shown that MRN facilitates ATM-dependent phosphorylation of the effectors p53 and Cds1, and the target histone H2AX (Lee and Paull, 2004, Zhao et al., 2008).

Downstream of the sensor proteins are the mediator proteins. Two mediator proteins act downstream of the Tel1^{Sp}/ATM^{Hs} and Rad3^{Sp}/ATR^{Hs} in fission yeast: Crb2 and Mrc1 (Furuya and Niki, 2012). Crb2 is the homologue of human checkpoint mediator 53BP1 (Saka et al., 1997). At sites of DNA double-strand breaks, Rad3/ATR-dependent hyperphosphorylation of Crb2 activates the checkpoint effector Chk1 (Saka et al., 1997). At sites of replication inhibition, Rad3/ATR-dependent phosphorylation of Mrc1 activates the recruitment of Cds1 at stalled replication forks (Tanaka and Russell, 2001). Cds1 and Chk1 kinases are important effectors that function in all checkpoints but act on different substrate in different organisms (Rhind and Russell, 2000).

1.4 The spindle assembly checkpoint (SAC)

The spindle assembly checkpoint controls the M phase to ensure the fidelity of the chromosomes segregation (Musacchio, 2011). It prevents the separation of the sister chromatids until each and every chromosomes is properly aligned and attached to the mitotic spindle. Cdc20, the MAD (mitotic arrest deficient) family of proteins (Mad1, Mad2 and Mad3) and the Bub family of proteins (Hoyt et al., 1991) are the main players in the activation and maintenance of SAC (Shannon et al., 2002). Cdc20 and the SAC proteins are conserved from yeast to humans. Cdc20 and the SAC proteins assemble at the kinetochores before the spindle attachment and maintain the checkpoint active until the kinetochores are properly attached to the spindle. Cdc20, Mad and Bub proteins form a complex that inhibits the activity of the Anaphase promoting complex (Ostapchuk et al.), the ubiquitin E3 ligase that targets cohesin for proteasomal degradation.

1.5 DNA damage

The genome is under constant attack as a result of normal cellular metabolic processes, as well as exposure to exogenous genotoxic agents. Endogenous sources of DNA damage are by-products of hydrolytic and oxidative reactions and other cellular processes that occur under normal physiological conditions. Exogenous sources of DNA damage are: ultraviolet radiation (UV), ionizing radiation (IR) and numerous chemicals from the environment, such as alkylation and methylation agents. These DNA damage sources generate single and double strand breaks and various types of base lesions. In addition to the environmental insults, the process of DNA replication is prone to errors, mainly caused by incorrect nucleotides added by the DNA polymerases. Given the high frequency and the different types of DNA damage, cells have evolved multiple complex mechanisms to repair DNA damage or to by-pass DNA lesions.

1.6 DNA damage repair mechanisms

The main mechanisms involved in single-strand damage are: nucleotide excision repair, base excision repair and mismatch repair. Double-strand break repair occurs mainly by two mechanisms: non-homologous end joining (NHEJ) and homologous recombination (HR).

1.6.1 Nucleotide excision repair (NER)

Nucleotide excision repair removes bulky DNA adducts that result from UV-induced damage or from processes associated with transcription (Kamileri et al., 2012). NER pathway involves the recognition of damage, excision of the oligonucleotide affected, and filling of the resulting gap by repair synthesis. Mutations in NER genes result in several genetic diseases such as Xeroderma Pigmentosum (XP), Trichothiodystrophy (TTD) and Cockayne syndrome (CS). XP and TTD are associated with different mutations in the XP family of genes (Botta et al., 1998) and in the gene encoding for ERCC2, a protein involved in DNA repair and transcription (Taylor et al., 1997).

1.6.2 Base excision repair (BER)

Base excision repair deals with the removal of small, non-bulky base lesions that arise from endogenous chemicals such as reactive oxygen species (ROS) (Robertson et al., 2009). DNA glycosylases remove the damaged bases by hydrolysis of the N-glycosylic bond between the DNA base and the sugar phosphate backbone. The resulting abasic site is processed by endonucleases, and the resulting single-strand break is repaired by DNA polymerases and DNA ligases either by replacing the single nucleotide (short-patch BER) or by synthesizing 2-10 nucleotides (long-patched BER). In humans, the flap endonuclease FEN1, two major ligases, LIG1 and LIG3, two main polymerases, PARP1 (Poly(ADP-ribose) polymerase-1) and Pol β , and the single-strand break repair protein XRCC1 are the main players in BER. The long-patch BER is dependent on the interaction of FEN1 with PCNA (Gary et al., 1999).

Homologues of the human BER components have been identified to function in *S. pombe* BER. *S. pombe* Rad2 is the homologue of FEN1 (Allewa and Doetsch, 1998, Murray et al., 1994), while Rad4 is the homologue of XRCC1 (Fenech et al., 1991). LIG1 ligase is conserved in all eukaryotes while LIG3 is restricted to vertebrates (Ellenberger and Tomkinson, 2008). Recently a PARP1 homologue, Hpz1 (homologue of PARP-type Zn-finger), has been identified in *S. pombe* (Boe et al., 2012). However, Hpz1 does not have PARP activity, but is required for resistance to UV during G1, and resistance to replication inhibition during S phase (Boe et al., 2012)

1.6.3 Mismatch repair (MMR)

Mismatch repair corrects base-pairing errors that arise during the replication process, including small insertions or deletions that occur particularly at highly repetitive sequences (microsatellites) (Jascur and Boland, 2006). In humans, mutations in the DNA mismatch repair genes (MLH1, MSH2, MSH6) are associated with hereditary colorectal cancer (Lynch syndrome) and endometrial cancer (Masuda et al., 2011) and are characterized by microsatellite instability (Banno et al., 2004). The MMR pathway is highly conserved amongst species and defects in the *S. pombe* homologues *mlh1*, *msh2* and *msh6* result in increased nucleotides insertion and deletion mutation rates (Marti et al., 2003).

1.6.4 Non-homologous end joining (NHEJ)

Non-homologous end joining repairs double-strand breaks by directly ligating the ends of the breaks. It is the predominant double-strand break repair mechanism in mammalian cells and is particularly active during the G1 phase in the haploid *S. pombe* (Ferreira and Cooper, 2004), when no homology is available for recombinational repair. In mammalian NHEJ, the heterodimer Ku (Ku70/Ku80) forms a ring that tethers the broken ends, the DNA polymerases Pol λ and Pol μ fill the gap and LIG4 performs the ligation step of the repair (Weterings and Chen, 2008). In *S. pombe* all these proteins are conserved and are the main players in NHEJ repair (Manolis et al., 2001). It has been

shown that in *S. pombe* NHEJ repair at telomeres requires the MRN complex (Reis et al., 2012).

1.6.5 Homologous recombination (HR)

Homologous recombination is a high fidelity DNA repair mechanism that uses the sister chromatids and the homologous chromosomes as templates to repair the double strand breaks (fig. 1.2). *S. pombe* cells generally repair DSBs by gene conversion (GC), in which both ends of the break associate with homologous sequence. In short, the homologous recombination process is initiated by the MRN complex that tethers the ends of the break and interacts with helicases and endonucleases to resect the strands in a 5'-3' fashion to create single strand overhangs. The 3' overhangs are coated by RPA, which recruits the HR protein Rad51 (Rhp51 in *S. pombe*). At one of the 3' overhangs, Rad51 forms single strand nucleoprotein filaments required for fast and efficient search for homologous DNA sequences. After the identification of a homologous sequence, Rad51 facilitates the physical connection of the ssDNA filaments with the template sequence by forming double-stranded nucleoprotein filaments. The strand invasion proceeds with the formation of a displacement loop (D-loop) that allows the DNA polymerases to synthesize new DNA using the invaded strand as a template. This process results in the formation of a Holliday junction (HJ).

Resolution of the HJs can occur by two different mechanisms: the double-strand break repair (DSBR) mechanism takes places with the formation of another HJ by the second 3' overhang with the homologous chromosome; the synthesis-dependent strand annealing (SDSA) mechanism involves the migration of the newly extended strand from the template strand (branch migration) and its annealing to the second 3' overhang of the damaged chromosome, without chromosomal crossover. The double HJ formed by the DSBR mechanism can be resolved either by cutting one HJ at the crossing strand and the other at the non-crossing strand, resulting in chromosomal crossover, or by cutting both HJs at the crossing strand, resulting in chromosomes without crossover (Krejci et al., 2012).

Fig. 1.2 Homologous recombination repair mechanism

Homologous recombination repair of a DBS proceeds through the DBSR mechanism (left), which results in crossover, or through the SDSA mechanism (right), which results in non-crossover. BIR is a HR mechanism that requires DNA replication.

Red and blue represent DNA copies of two different homologues.

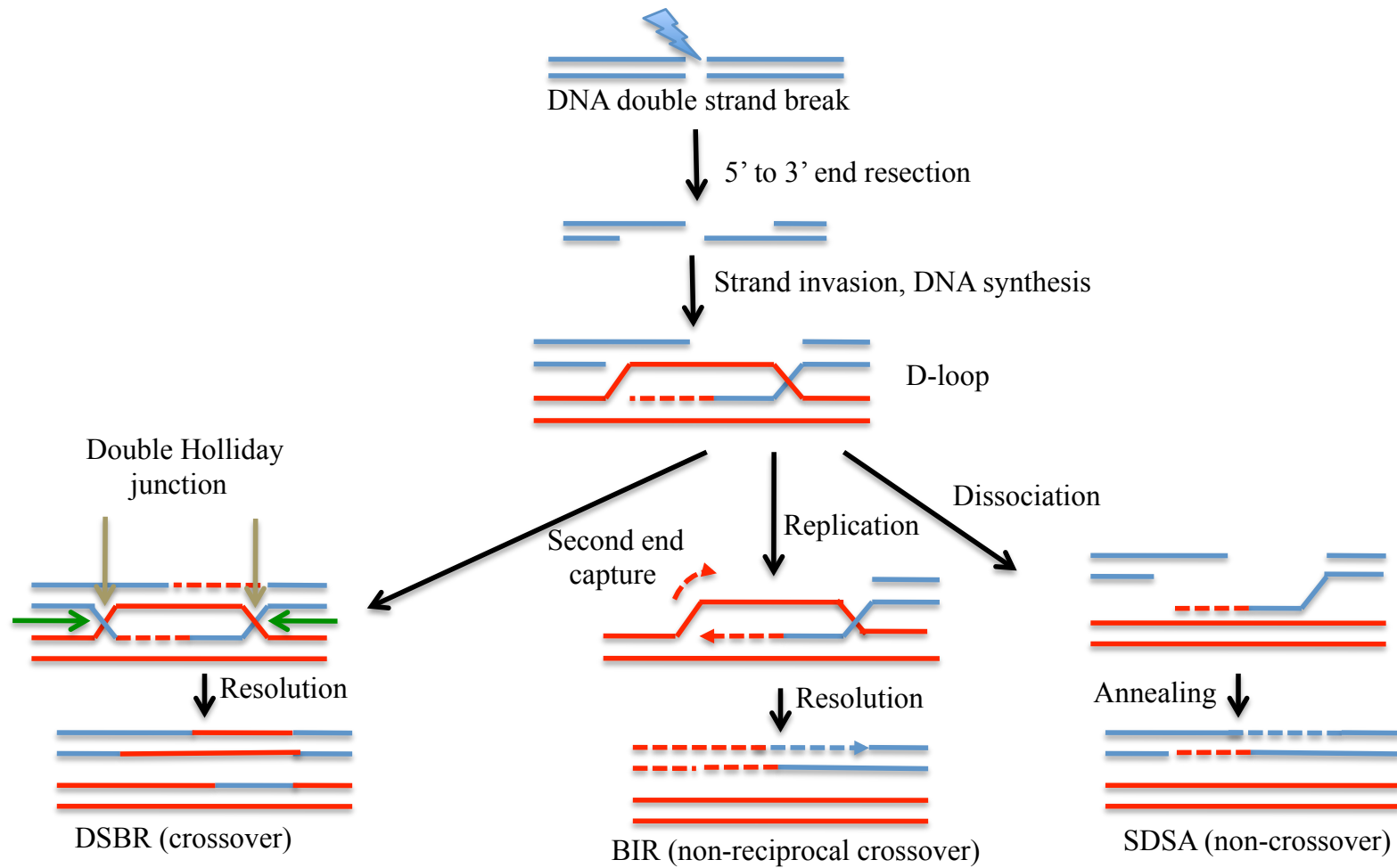


Fig. 1.2 Homologous Recombination Repair mechanisms

RPA has a contributory effect towards the homologous recombination function of Rad51 (Eggler et al., 2002), but it has a higher affinity for ssDNA than Rad51 and this can interfere with the activity of Rad51. To overcome this impediment, the recombination mediator proteins Rad52 (*Sp* Rad22), Rad55 (*Sp* Rhp55) and Rad57 (*Sp* Rhp57) are required to facilitate Rad51-dependent HR repair (Sung et al., 2003). Rad52 is the most studied HR protein as is required for all Rad51-dependent HR pathways and for the Rad51-independent HR pathway single-strand annealing (SSA) (Lok and Powell, 2012).

The SSA mechanism is initiated when double strand breaks occur at repetitive sequences. Complementary single-strands are created adjacent to the break between two repeats and the 3' overhangs align and anneal to each other to restore the continuous double-strand. Rad52 is essential for this process as it binds each of the two repeats at both ends of the break. SSA is the main DSB repair mechanism at the telomeric and centromeric repetitive sequences. The process is mutagenic as it results in the loss of one of the repetitive sequences (chromosomal deletions) (Parsons et al., 2000).

Homologous recombination repair can be employed when only one end of the break shares homology with a template. The HR machinery establishes a unidirectional replication fork that can copy the donor template from the break to the end of the chromosome, process known as break-induced replication (BIR) (Kogoma, 1996). Two pathways of BIR have been identified: a Rad51-dependent BIR, which requires large homology template (several hundred base pairs), and a Rad51-independent BIR, employed when only short homology sequences are present (>30 bp) (Ira and Haber, 2002). The Rad51-independent recombination requires the Rad50 and Rad52 recombinases, and the Srs2 helicase, and proceeds in two steps: first BIR is employed for strand invasion and replication fork initiation, followed by single strand annealing repair (Kang and Symington, 2000). Rad51 inhibits short homology-directed recombination, while Srs2 inhibits Rad51-dependent recombination by dissociating Rad51 from DNA (Antony et al., 2009, Ira and Haber, 2002). BIR has been implicated in restarting stalled or collapsed replication forks during S phase (Michel et al., 2004) and telomere elongation (Lydeard et al., 2007). BIR is an error-prone DNA repair mechanisms and it has been shown to cause chromosomal deletions, translocations and duplications (Hastings et al., 2009).

When the replication fork encounters DNA damage the cells employ the post-replication repair mechanism that allows the fork to bypass the lesion. The process requires the switch of classical replicative polymerases with non-replicative polymerases and is regulated by post-translational modifications of PCNA. Post replication repair is further discussed in section 1.8.2.

Cellular processes, such as cell cycle regulation and DNA replication, and DNA damage response pathways are closely interlinked and share overlapping functions. Specific damage can be repaired by multiple mechanisms, proteins can be shared between repair pathways and replication processes, and intermediates that arise from one repair pathway can be removed by another repair pathway. Proteins with multiple functions, such as PCNA, can switch between pathways by means of post-translational modifications.

1.7 SUMO

1.7.1 Post-translational modifications of proteins

Post-translational modifications of proteins are mostly reversible and modulate the functions of proteins. The first post-translational modification to be identified and functionally characterized was phosphorylation (Burnett and Kennedy, 1954). Phosphorylation is the main post-translational modification in signal transduction pathways as kinases and phosphatases phosphorylate and de-phosphorylate enzymes and receptors to switch their activity off and on. As previously described, checkpoints during the cell cycle are tightly regulated by phosphorylation.

Other post-translational modifications that involve the attachment of a chemical group are hydroxylation, acetylation, alkylation, adenylation (or adenylylation) and many others. Adenylation is the attachment of an adenosine monophosphate group (AMP) to the hydroxyl group of tyrosine, threonine or serine residues of a substrate. AMP is produced during the ATP production and degradation processes. It has been shown that

adenylation is required for the activation of other important posttranslational modifiers, the Ubiquitin like proteins (UBLs) (Schulman and Harper, 2009).

1.7.2 Ubiquitin

Ubiquitin was the first example of a protein acting as a post-translational modifier (Hershko et al., 1982) and it is best known for its catabolic role in protein degradation via the 26S proteasome (Hershko and Ciechanover, 1998). Ubiquitin is a small (76 aa) protein with a compact globular structure, present in large amounts in all eukaryotic cells (ubiquitous) in the nucleus and cytosol. It is highly conserved amongst species, with only three differences in the amino acids sequence between *H. sapiens* and *S. pombe* ubiquitin.

Ubiquitin is involved in post-translational modification by covalently attaching through an isopeptide bond to lysine residues of target proteins (ubiquitination). The isopeptide bond occurs between the carboxylic moiety of the terminal glycine (Gly76) of ubiquitin and the ϵ -amine group of the lysine residues. Ubiquitin can form two types of chains: the canonical K48-linked chains mediate the proteasomal degradation of the target protein (Sun and Chen, 2004); the non-canonical K63-linked chains are involved in modulating the function of the target protein. K63-linked poly-ubiquitination of PCNA switches PCNA-dependent DNA damage repair from an error-prone mechanism to an error-free mechanism (Hoege et al., 2002).

Since the identification of ubiquitin, several proteins, structurally or functionally related to ubiquitin, have been discovered. Some are structurally similar and function in a similar way as post-translational modifiers, known as Ubiquitin –like modifiers (UBLs). Other proteins have ubiquitin-like domains (ULDs) but are not involved in protein conjugation and are known as ubiquitin domain proteins (UDPs) (Jentsch and Pyrowolaski, 2000).

1.7.3 The Sumoylation pathway

SUMO (Small Ubiquitin-like Modifier) is a UBL essential for many cellular processes. A global mapping of sumoylation function, using systematic functional genomics, identified fifteen major biological processes dependent on sumoylation (reviewed by Maknevykh T, 2008). These processes include transcriptional regulation (reviewed by Sapetschnig A, 2002), nuclear transport, DNA replication and repair (reviewed by Morris, 2009, Brnzei D, 2006), cell cycle progression, subcellular localization of targets (Matunis MJ, 1998).

SUMO has only 18% identity with ubiquitin but adopts the same β -grasp fold of ubiquitin and covalently conjugates to lysine residues of target proteins in an analogous manner. There are four SUMO paralogues in mammals (SUMO-1, SUMO-2, SUMO-3 and SUMO-4) and only one SUMO in *S. cerevisiae*, Smt3, and *S. pombe*, Pmt3. The budding yeast SUMO is essential for viability (Meluh PB, 1995), while the fission yeast SUMO null mutant is viable but displays severe growth defects (Tanaka K, 1999). Like ubiquitin, SUMO attaches covalently to target proteins after a cascade of reactions involving SUMO proteases, a SUMO-activating enzyme E1 (SAE), a SUMO-conjugating enzyme E2 and several SUMO E3 ligases (fig. 1.3).

SUMO is translated as a precursor protein that is processed into the mature form by specific proteases. The proteases hydrolyze the C-terminus of SUMO to reveal a double glycine motif. Mature SUMO forms a complex with the adenylated SUMO-activating heterodimer (E1) (fig. 1.4). SAE interacts non-covalently with the conjugating enzyme Ubc9/Hus5 (E2) and SUMO is transferred from the E1 to the E2. Unlike ubiquitination, which requires many substrate-specific E2s, there is only one SUMO conjugating enzyme in the sumoylation pathway. The conjugating enzyme can transfer the SUMO moiety to a substrate directly without the need of a SUMO E3 ligase. E3 ligases are indispensable in ubiquitination and, like E2s, they are more substrate specific. While there are several E3 SUMO ligases in mammals, only two have been identified in *S. pombe*: Pli1 and Nse2. The homologous components of the sumoylation pathway in *S. pombe*, *S. cerevisiae* and *H. sapiens* are listed in table 1.1.

Fig. 1.3 The sumoylation pathway

The covalent conjugation of SUMO is an ATP-dependent process that requires the sequential actions of an activating enzyme (E1), a conjugating enzyme (E2) and, for certain substrates, a ligase (E3). SUMO can attach to a target protein or form chains. Specific SUMO proteases deconjugate SUMO from substrates or disassemble chains.

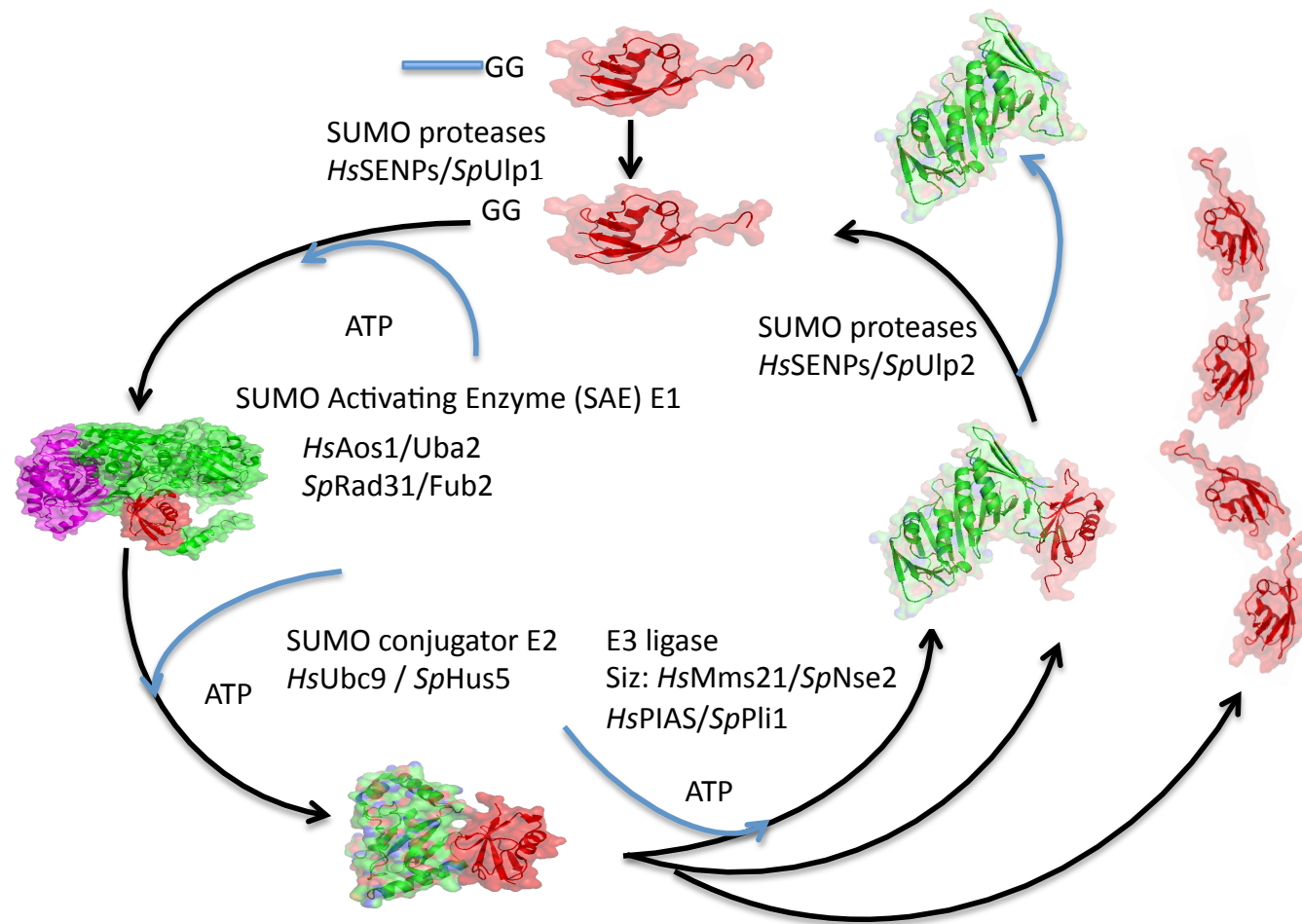


Fig. 1.3 The sumoylation pathway

Component	<i>S. pombe</i>	<i>S. cerevisiae</i>	<i>H. sapiens</i>
SUMO	Pmt3 (Tanaka K 1999)	Smt3 (Meluh and Koshland 1995)	SUMO-1 (Matunis et al, 1996) SUMO-2/3 (Lapenta et al., 1997) SUMO- 4 (Bohren et al., 2004)
Activating enzyme	Fub2/Rad31 (Shayeghi et al., 1997)	Aos1/Uba2 (Johnson et al., 1997)	SAE1/SAE2 (Gong et al., 1999)
Conjugating enzyme	Hus5 (al-Khodairy et al., 1995)	Ubc9 (Johnson and Blobel, 1997)	Ubc9 (Desterro et al., 1997)
Ligases	Pli1 (Xhemalce et al., 2004) Nse2 (Andrews et al., 2005)	Siz1/2 (Johnson and Gupta, 2001) Mms21/Nse2 (Zhao and Blobel, 2005) Zip3 (Cheng et al., 2006)	PIAS1 (Liu et al., 1998) PIAS3 (Chung et al., 1997) PIASy (Gross et al., 2001) Mms21/Nse2 (Potts and Yu, 2005) Pc2 (Kagey et al., 2003) RanBP2 (Pichler et al., 2002) TOPORS (Weger et al., 2005)
Protease Isopeptidases	Ulp1 (Taylor et al., 2002) Ulp2 (Watts lab, University of Sussex, unpublished data)	Ulp1 (Takahashi et al., 2000) Ulp2 (Li and Hochstrasser, 2000)	SEN1 (Gong et al., 2006), 2, 3, 5, 6, 7 SEN2-8 (Gong and Yeh, 2006)

Table 1.1 Components of the sumoylation pathway

1.7.4 Sumoylation pathway components

SUMO proteases

SUMO proteases, known as Ulp1 (ubiquitin-like protein-specific proteases) in yeast and SENPs (sentrin/SUMO-specific proteases) in mammals, are responsible for SUMO maturation and for the de-sumoylation of SUMO conjugates (reviewed by Mukhopadhyay and Dasso, 2007).

In *S. pombe*, Ulp1 is required for both SUMO maturation and SUMO de-conjugation (Taylor et al., 2002) while Ulp2 functions in de-sumoylation of substrates and SUMO chains disassembly (Kosoy et al., 2007). Ulp1 is not essential for cell viability but is required for normal cell cycle progression and an *ulp1* null mutant displays severe cellular and nuclear abnormalities (Taylor et al., 2002). In *S. cerevisiae* Ulp2 is required for recovery from HU-induced checkpoint arrest (Mukhopadhyay and Dasso, 2007) and for the de-sumoylation of PCNA (Stelter and Ulrich, 2003). In mammals, SENP1 and SENP2 function as C-terminal hydrolases (Gong et al., 2000, Nishida et al., 2001), while SENP3 and SENP5 hydrolyze the isopeptide bond between SUMO and substrates (Gong and Yeh, 2006). SENP6 and SENP7 are required for SUMO chain editing (Mukhopadhyay et al., 2006).

SUMO activating enzyme (E1)

S. pombe Rad31 protein was first identified as an ubiquitin-like activating enzyme that functions in a common pathway with Hus5, the *S. pombe* SUMO conjugating enzyme E2 (Shayeghi et al., 1997). Rad31, the homologue of *S. cerevisiae* and mammalian Aos1/SAE1, is not essential for viability but the null mutant displays slow growth and mitotic defects. Rad31 forms the heterodimeric SAE with the essential protein Fub2, the homologue of *S. cerevisiae* and mammalian protein Uba2/SAE2. The heterodimeric structure and the function of SAE has been characterized in *S. cerevisiae* (Johnson et al., 1997) and mammals (Azuma Y, 2001) and the crystal structure of human SAE has been determined (Lois and Lima, 2005). In *S. cerevisiae* and mammals both components of SAE are essential for cell viability (Azuma Y, 2001, Johnson et al., 1997).

SUMO conjugation enzyme (E2)

The SUMO-conjugating enzyme, Ubc9/Hus5, was first identified in yeast (al-Khodairy et al., 1995, Seufert et al., 1995). It is highly conserved from yeast to mammals and is essential for cell viability in all eukaryotes. Hus5/Ubc9 interacts covalently and non-covalently with SUMO and physically associates with the substrate for its sumoylation (Rodriguez MS, 2001). Two *S. pombe* mutants, *hus5-17* and *hus5-62*, are defective in the cellular response to replication inhibition and in recovery from S-phase arrest respectively (Ho and Watts, 2003). Recently it has been shown that Cdk1-dependent phosphorylation of Ubc9 enhances its sumoylation activity (Su et al., 2012).

SUMO E3 ligases

Ubiquitination involves many E3 ligases necessary for the conjugation to specific substrates. Only a few SUMO E3 ligases have been identified and they are not essential for the SUMO conjugation as the conjugating enzyme E2 is generally able to directly interact with the substrates. The first identified SUMO E3 ligases were the Siz1 and Siz2 proteins in *S. cerevisiae* (Johnson ES, 2001). They belong to the PIAS [protein inhibitor of activated STAT (signal transducer and activator of transcription)] family of proteins characterized by an SP-RING [Siz-PIAS RING (really interesting new gene)] which is required for the SUMO ligase activity (Takahashi Y, 2005). However, proteins that lack SP-RING domains but have SUMO ligase activity have been identified: Pc2 (polycomb) protein (Kagey MH, 2003), the histone deacetylases HDAC4 (Gregoire S, 2005) and HDAC7 (Gao C, 2008), and the nucleoporin RanBP2 protein (Pichler A, 2002). In *S. pombe* two SUMO E3 ligases have been identified: Nse2 (Andrews EA et al., 2005) and Pli1 (Xhemalce B, 2004), both belonging to the PIAS family of proteins.

Pli1

Pli1 (Pmt3 ligase 1) belongs to the Siz/PIAS (Protein Inhibitor of Activated Stat) family of proteins represented by SIZ1/SIZ2 in *S. cerevisiae* and four paralogues in mammals (PIAS1, PIAS3, PIASx and PIASy). They are characterized by a N-terminal SAP (SAF-A/B, Acinus and PIAS) domain with DNA binding capacity (Aravind and Koonin, 2000), a PINIT (Proline Isoleucine Asparagine Isoleucine Threonine) domain, required

for nuclear localization (Duval et al., 2003) and a central SP-RING (Siz/PIAS-RING) required for E3 SUMO ligase activity (Hochstrasser, 2001).

Pli1 is 31% identical to the *S. cerevisiae* Siz1 and 22% identical to the human PIASy, with the highest level of sequence identity around the RING domain. The *pli1* null mutant is viable and has a phenotype similar to that of a *pli1* mutant defective in sumoylation (Xhemalce et al., 2004). Both mutants behave like a wild type strain in response to most DNA damaging agents but are sensitive to TBZ (thiabendazole), a microtubule poison that prevents the spindle pole body clustering (Xhemalce et al., 2004). Overall sumoylation levels are drastically reduced in both mutants, suggesting that the SUMO ligase activity is the only function of Pli1 and that Pli1 targets a large pool of substrates. Both mutants display increased rates of loss of an artificial minichromosome, reduced silencing at centromeres and elongated telomeres, and are unviable following deletion of HR genes *rad22/RAD52* and *rhp51/RAD51*. These phenotypes implicate Pli1-dependent sumoylation in DNA damage repair mechanisms involved at heterochromatic regions of chromosomes, characterized by large inverted repeated sequences (Xhemalce et al., 2004). Pli1 has been shown to enhance the sumoylation of several proteins: the homologous recombination protein Rad22, Top1 and Top3 topoisomerases, the NHEJ protein Ku70, and the recQ helicase Rqh1/Sgs1. (Watts FZ, 2007).

In *S. cerevisiae* Siz1 facilitates selective sumoylation of PCNA at K164, through its PINIT domain (Yunus and Lima, 2009), and non-selectively at K127, and formation of SUMO chains on PCNA (Hoege et al., 2002, Windecker and Ulrich, 2008, Stelter and Ulrich, 2003). The SAP domain of Siz1 is required for PCNA sumoylation (Reindle et al., 2006).

Nse2

Nse2 is essential for cell viability. This is due to its structural association with the essential SMC5/6 complex rather than its SUMO E3 ligase function. A mutant defective in sumoylation (*nse2-SA*) is viable but sensitive to IR, HU and MMS. Unlike *pli1Δ*, *nse2-SA* cells have similar levels of sumoylation as wild type cells. It has been shown that Nse2 facilitates the sumoylation of several components of the SMC5/6 complex:

Smc6, Nse3, and Nse4 (Pebernard S, 2008, Andrews et al., 2005, Pebernard et al., 2004). Nse2 is also required for the sumoylation of components of cohesin (McAleenan et al., 2012).

1.7.5 SUMO-like domains (SLDs)

A bioinformatics approach has identified the RENi (Rad60-Esc2-Nip45) family of proteins characterized by two SUMO-like domains (SLDs) at their C-terminal (Novatchkova et al., 2005). Rad60 and NIP45 are essential proteins in *S. pombe* and mammals respectively. NIP45 (NF-AT interacting protein) is a transcription factor (Hashiguchi et al., 2013). The *S. cerevisiae* protein Esc2 is not essential but is required for genome integrity, sister chromatid cohesion (Ohya et al., 2008) and regulation of transcriptionally silenced heterochromatin through its interaction with the silencing protein Sir2 (Yu et al., 2010).

The *rad60*⁺ gene was identified in a screen for mutants hypersensitive to MMS and synthetically lethal with *rad2*^{Sp} (*FEN1*^{Hs}). Rad60 protein is required for cell viability and recombination-mediated DNA double-strand breaks (Morishita et al., 2002). Its activity is regulated by the checkpoint kinase Cds1 and it has been proposed that it interacts with the DNA repair complex Smc5/6 (Boddy et al., 2003).

1.7.6 SUMO-interacting motifs (SIMs)

Apart from its covalent interaction with substrates, SUMO can also interact non-covalently with target proteins. The first motif identified to interact non-covalently with SUMO, named SUMO-interacting motif, SIM, contained two serine residues separated by another amino acid, SxS (Minty et al., 2000). NMR analysis carried out on complexes between SUMO-1 and synthetic peptides, based on the PIASX and PML sequences, identified an hydrophobic sequence proximal to a SxS motif that interacts with SUMO (Song et al., 2004). This SIM, characterized by the V/I-x-V/I-V/I sequence, was further shown to interact with a positively charged surface region of SUMO. This

suggests that the negatively charged residues identified by Minty *et al.* could be necessary for the interaction. Genomic and proteomic analysis of *S. cerevisiae* by two-hybrid screening identified a series of proteins interacting non-covalently with SUMO (Hannich *et al.*, 2005). Some of the potential SIMs identified in these proteins are related but not identical with the ones identified by Song *et al.*, and they are near a sequence of acidic amino acids on the C-terminal side, similar to those reported by Minty *et al.*

Resolved structures of two complexes of SUMO and SIMs, one by NMR (pdb id 2ASQ) (Song *et al.*, 2005), another by X-ray diffraction (Reverter and Lima, 2005), showed that the sequence V/I-x-V/I-V/I and its reverse V/I-V/I-x-V/I forms a β sheet that interacts with residues on the β 2 sheet and α helix of SUMO and fits in the groove form by these two secondary structures. Further, the sequence V/I-x-V/I-V/I adopts a parallel orientation to β 2 sheets of SUMO while the reverse sequence, V/I-V/I-x-V/I, arrange itself into an antiparallel position.

Many proteins have been identified as having the consensus sequences of SIMs and many more have been shown to interact non-covalently with SUMO through sequences similar but not identical to a SIM (Li *et al.*, 2010). Three putative SIMs, named SUMO-binding motifs (SBMs), have been identified in Rad60 protein, two of them within the SLD1 and SLD2 respectively, and proposed that they are required for normal Rad60 function (Raffa *et al.*, 2006).

1.7.7 SUMO targeted ubiquitin ligases (STubLs)

STubLs are a family of ubiquitin E3 ligases that facilitate the ubiquitination of sumoylated proteins or proteins that contain SUMO-like domains (SLDs) (Prudden *et al.*, 2007). At their N-terminal, STubLs contain SUMO interacting motifs (SIMs) that interact with SUMO or SLDs. STubL-mediated ubiquitination promotes de-sumoylation and/or degradation of the target, thus maintaining the physiological levels of cellular overall sumoylation.

Fission yeast cells lacking the STUbL heterodimer Slx8-Rfp accumulate sumoylated proteins and subsequently show genomic instability and hypersensitivity to genotoxic stress. STUbLs are highly conserved as proved by the restoration of the SUMO pathway following expression of human STUbL, RNF4, in *S. pombe* cells lacking the STUbL heterodimer Slx8-Rfp. Mutants of the *slx8* and *rnf* genes, *slx8-1* and *rnfΔ*, display similar phenotypes, suggesting that Slx8 and Rfp work as a heterodimer. However, they work in different manners: Rfp contains SIMs not present in Slx8, while the latter displays RING-dependent E3 ubiquitin ligase activity, not shown by the Rfp protein. The Slx8-Rfp heterodimer interacts strongly with the Rad60 protein and *slx8* and *rnf* mutants display hypersensitivity to DNA-damaging agents at levels similar to those shown by *rad60* mutants. The deletion of the SUMO E3 ligase Pli1 suppresses the phenotype of the *slx8* and *rnf* mutants (Prudden et al., 2007) suggesting that hypersumoylation is responsible for this phenotype.

A mutation at a predicted SIM-binding pocket of SLD1 of Rad60 abolishes the interaction between Rad60 and the STUbL. *In vitro* pull-down assays showed that Rad60 is ubiquitinated by the E3 enzyme Slx8 through its RING domain and that the heterodimer SLX-Rfp increases the ubiquitination of Rad60. The mutant complex Slx8-Rfp Δ SIM (defective in SUMO-interaction) showed strong autoubiquitination but was defective in ubiquitinating Rad60, demonstrating that Slx8 ubiquitinates Rad60 through SIM motifs of Rfp.

Slx5 and Slx8 proteins were identified in *S. cerevisiae* (Mullen et al., 2001) from a synthetic-lethality screen with a mutant of the DNA helicase Sgs1. The heterodimer Slx5-Slx8 has been shown to function as an ubiquitin E3 ligase when activated by sumoylated homologous recombination protein Rad52 (Xie et al., 2007).

1.8 SUMO targets

Since the detection and characterization of the sumoylation pathway, many proteins, with functions in various cellular processes, have been identified as targets of sumoylation. RanGAP, a GTPase required for many cellular processes including mitotic

spindle formation (Becker et al., 1995), was the first identified SUMO target (Mahajan et al., 1997). The sumoylation of RanGAP1 is essential for its interaction with the NPC (Nuclear Pore Complex) proteins (Mahajan et al., 1997). The sumoylation of RPA, PCNA, Smc5/6 complex and Rad52 proteins is briefly discussed.

1.8.1 RPA

It has been shown in human cells that sumoylation of RPA facilitates DNA damage repair by homologous recombination, but inhibits RPA replication function (Dou et al., 2010). During S phase, RPA is maintained in a hypo-sumoylated state through its interaction with the SUMO specific protease SENP6 (Dou et al., 2010). Replication stress dissociates SENP6 from RPA, allowing RPA to be modified by SUMO-2/3. RPA sumoylation facilitates recruitment of Rad51 protein to the DNA damage foci to initiate DNA repair through homologous recombination (HR). Cell lines that expressed a sumoylation defective RPA mutant are defective in HR and display an increased sensitivity to camptothecin (CPT), a Top1 inhibitor. These results demonstrate that the sumoylation levels of RPA play a critical role in the regulation of DNA repair through homologous recombination (Dou et al., 2010).

1.8.2 PCNA

Apart from its function in DNA replication, PCNA is required for post-replication repair of DNA damage that occurs proximal to the replication fork (Lehmann, 1972). The type of post-translational modification on PCNA determines which sub-pathway of PRR is employed to bypass the damage (fig. 1.4). Mono-ubiquitination of PCNA at K164 triggers translesion synthesis mechanism, while attachment of K63 linked ubiquitin chains at K164 activates the template switching (TS) mechanism. Further, mono-ubiquitination-dependent template switching is inhibited by the sumoylation of PCNA at K164 (Hoege et al., 2002).

Translesion synthesis is employed when the replication fork encounters a DNA lesion and the classical DNA polymerases cannot accommodate the lesion in their active site. The process bypasses the damage and requires the exchange of the classical

Fig. 1.4 Post-translational modification of PCNA regulates post replication repair

Following DNA damage, PCNA is mono-ubiquitinated on lysine K164 in an error-prone repair process that is dependent on Rad6 and Rad18. Poly-ubiquitination on K164 initiates an error-free repair mechanism dependent on Rad5, Mms2 and Ubc13. Sumoylation on K164 prevents ubiquitination.

Figure created using cartoon representations, generated by Pymol software, of structures of PCNA, SUMO and a model of Srs2 helicase. The model of Srs2 was generated using the on-line modeling engine PHYRE.

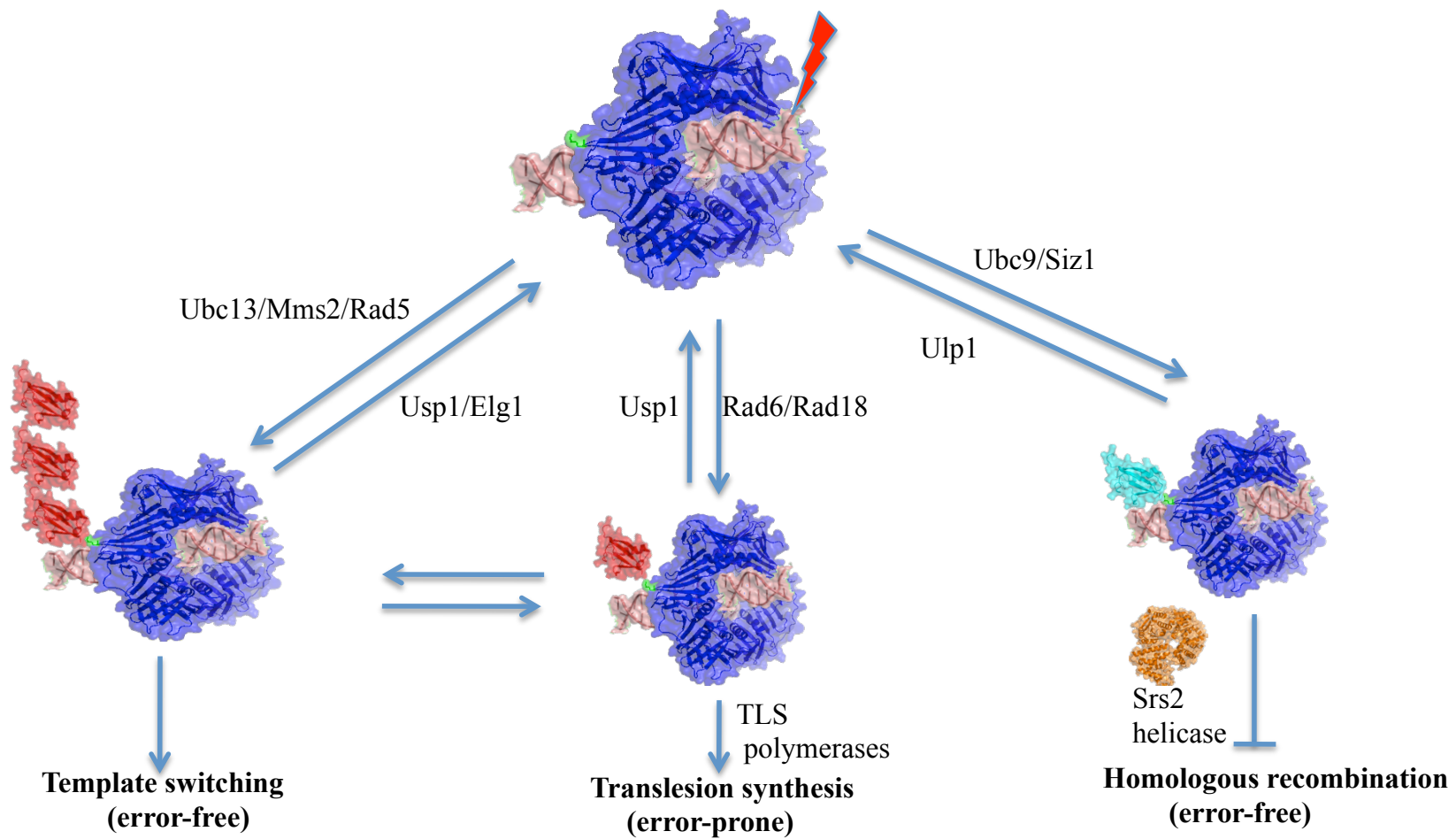


Fig. 1.4 Post-translational modification of PCNA regulates post replication repair

polymerases with non-classical polymerases, which are able to incorporate nucleotides across from a DNA lesion. After the damage bypass, the specialized TLS polymerases are exchanged for the replicative polymerases and the replication fork is restarted (Lehmann et al., 2007). Translesion synthesis is an error-prone damage bypass mechanism as the non-classical polymerases allow structural distortions due to DNA lesions by compromising the fidelity of nucleotide incorporation.

The template switching mechanism (TS) (sometimes referred to as homology-directed repair) is error free as it employs the homologous chromosome or the sister chromatid to copy the correct genomic information (Adar et al., 2009). Homologous recombination can be used to enable template switching to bypass replication fork barriers (RFBs) or to promote replication restart if the fork has collapsed (Branzei and Foiani, 2008).

Both TLS and TS are regulated by Rad6/Rad18 dependent ubiquitination of PCNA (Hoege et al., 2002), but poly-ubiquitination of PCNA requires the ligase activity of Rad5 (Parker and Ulrich, 2009). Initially it was argued that mono-ubiquitinated PCNA is an intermediate for poly-ubiquitination (Hoege et al., 2002). Recent *in vitro* studies suggest that an *en block* transfer of ubiquitin chains to unmodified PCNA is possible (Masuda et al., 2012). An RFC-like protein, Elg1, and the ubiquitin protease Usp1 control de-ubiquitination of PCNA. In humans, USP1 forms a complex with a protein that contains two SUMO-like domains, UAF1. The SLD2 of UAF1 interacts with SIMs present in Elg1 to promote PCNA de-ubiquitination.

K164-sumoylated PCNA recruits the Srs2 helicase to the replication fork (Papouli et al., 2005). Srs2 inhibits homologous recombination by preventing the accumulation of Rad51-dependent recombination intermediates (Liberi et al., 2005). Sumoylation of PCNA at K164 in *S. cerevisiae* was observed during undisturbed S-phase (Hoege et al., 2002) and in response to DNA damage (Stelter and Ulrich, 2003). Sumoylation of PCNA at K127 prevents its interaction with an essential cohesion factor, Eco1 (Moldovan et al., 2006). In humans, PCNA-SUMO prevents double strand break formation at stalled replication forks (Yang et al., 2011).

1.8.3 Structural maintenance of chromosome complexes (SMCs)

The structural maintenance of chromosomes (SMC) proteins assemble into three complexes with different functions: the SMC1/3 complex, or cohesin (Losada A, 1998), maintains sister chromatid cohesion until anaphase, the SMC2/4 complex, or condensin (Hirano T, 1994), promotes condensation of chromosomes and sister chromatids segregation, and the SMC5/6 complex, involved mostly in chromosome maintenance processes that require homologous recombination (HR) (Fousteri MI, 2000.).

Initially, subunits of the SMC complexes were identified as SUMO targets from global proteomics analysis of sumoylated proteins in *S. cerevisiae* (Hannich et al., 2005, Panse et al., 2004). Condensin and cohesin are directly regulated by Nse2/Mms21-dependent sumoylation, and sumoylation of condensin is essential in cells deficient in Top2 sumoylation or lacking Top1 (Takahashi et al., 2008). Sumoylation of cohesin is required for the establishment of sister chromatids cohesion after DNA replication (Almedawar et al., 2012) and for DNA damage-induced cohesion (McAleenan et al., 2012). Recently, Nse2/Mms21-dependent sumoylation of the cohesin component Scc1 at K15, was shown to be required for sister chromatid recombination at DNA damage sites (Wu et al., 2012).

The Smc5/6 complex

The Smc5 and Smc6 proteins form a stable complex with six non-SMC proteins, Nse1-Nse6 (fig. 1.6) (Sergeant J, 2005, Pebernard S, 2006). Smc5 and Smc6 form a heterodimer. Both proteins have two Walker nucleotide binding motifs at their N- and C-termini. The central domains are organized as two long anti-parallel coiled-coil domains separated by a 'hinge' sequence where Smc5 and Smc6 interact (Melby et al., 1998). The hinge domain is flexible and allows the opening and closing of the heterodimer (Hirano et al., 2001). Nse1, Nse3 and Nse4 form a heterotrimeric subcomplex, Nse5 and Nse6 form a heterodimeric subcomplex (Palecek et al., 2006) and Nse2 interacts directly with the coiled-coil region of Smc5 (Duan et al., 2009a). Nse1-Nse3-Nse4 subcomplex binds to the head domain of Smc5 and the Nse5-Nse6 subcomplex bind to the hinge region of Smc5 and Smc6 (Duan et al., 2009b).

Early studies observed that mutations in any of the components of the SMC5/6 complex induce cell sensitivity to DNA damaging agents such as HU, IR, UV and MMS, suggesting that the complex is involved in DNA replication, DNA recombination repair and recovery after genotoxic stress (Lehmann AR, 1995, Fousteri MI, 2000.). It has been shown that the SMC5/6 complex accumulates at telomeres following MMS treatment. This process is dependent on sumoylation of Nse4 by the SUMO ligase Nse2 (Pebernard et al., 2008). Nse1 has a RING domain characteristic to ubiquitin ligases (Santa Maria et al., 2007). Human Nse3 belongs to the MAGE (melanoma-associated antigen) and it has been shown that the RING-MAGE complex function as an E3 ubiquitin ligase (Doyle et al., 2010). Nse4 belongs to the EID (E1A-like inhibitor of differentiation) family of transcriptional repressors (Guerineau et al., 2012). Nse1 has been shown to be required for Rad52-dependent post replication repair of UV-induced DNA damage in *S. cerevisiae* (Santa Maria et al., 2007).

1.8.4 Rad52 and homologous recombination

The main homologous recombination proteins, Rad51 and Rad52, have been shown to interact with the SUMO conjugating enzyme Ubc9 and SUMO in *S. cerevisiae* two-hybrid analyses (Li et al., 2000). In *S. pombe*, the sumoylation of the Rad52 homologue, Rad22, is facilitated by the E3 ligase Pli1 (Watts et al., 2007). SUMO modified lysine residues have been identified in *S. cerevisiae* Rad52 (Sacher et al., 2006). Sumoylation of Rad52 in *S. cerevisiae* is facilitated by the E3 ligase Siz1 and it has been shown to be required for maintaining the activity of Rad52 and for inhibiting Rad52 proteasomal degradation (Sacher et al., 2006). In humans, the sumoylation site of Rad52 has been identified and shown to be required for Rad52 localization at the nucleus, but not for its recombination activities (Saito et al., 2010). In *S. cerevisiae*, sumoylation of Rad52 prevents hyperrecombination at ribosomal DNA (rDNA) by facilitating its nucleolar exclusion, and the MRN and Smc5/6 complexes regulate this process (Torres-Rosell et al., 2007).

1.9 Aims

The objective of this thesis was to obtain a better understanding of the functions of the sumoylation pathway in maintaining genomic stability. Specifically, this study aimed at gaining insights into the structure and function of the SUMO-like domains (SLDs) and putative SUMO-binding motifs (SBMs) of the essential protein Rad60. Secondly, a study of SUMO chain formation in *S. pombe* was undertaken. A third aim was to analyze the function(s) of the SUMO E3 ligase, Pli1, in maintaining genomic stability.

The aims of the second part of this thesis were to use mass spectrometry to identify specific sumoylated lysine residues. Having identified lysine residues targeted by sumoylation in the SUMO conjugating enzyme, Hus5, and the target protein Rtf2, the final aim was to characterize the phenotypic consequences of mutating these residues.

CHAPTER 2

MATERIALS AND METHODS

2.1 *S. pombe* methods

2.1.1 *S. pombe* media

2.1.1.1 Rich media

Yeast Extract (YE)

20 g/l Glucose

200 mg/l Adenine

100 mg/l Leucine, uracil, histidine, arginine

For solid YE media, 25 g/l DIFCO agar was added.

2.1.1.2 Sporulation media

Extra low nitrogen (ELN)

27.3g/l Formedium Edinburgh Minimal Medium (EMM)

50 mg/l Ammonium chloride

200mg/l Adenine

100mg/l Leucine

100mg/l Uracil

100mg/l Histidine

100mg/l Arginine

25g/l Difco (Bacto) Agar

2.1.1.3 Selective media

1.9 g/l YNB (Formedium)

4 g/l Ammonium sulphate

20 g/l Glucose

For solid YNB media, 30 g/l DIFCO Bactoagar and 0.2 ml/l 10 M NaOH were added to liquid YNB.

2.1.1.4 *S. pombe* media supplements

The wild-type *S. pombe* strain used in this study has the genotype *ade6-704*, *leu1-32*, *ura4-D18* and media need to be supplemented with adenine, leucine and uracil for normal growth. Strains containing these auxotrophic markers (*ADE6*, *LEU2* and *URA4* genes) can be selected for by using selective media restricted for a particular supplement (e.g. leucine). Apart from *ade6-704* allele, *ade6-210* and *ade6-216* alleles of *ADE6* gene were used for complementation. *ura4* was predominantly used as it can be counterselected for by supplementing media with 5-fluoroorotic-acid (5FOA). Strains marked with an antibiotic resistance gene, e.g. CpG-free *neo* (*geneticin* = *G418*)^r and *nat1* (*nourseothrycin* = *NAT*)^r can be selected for by growing cells in the presence of that particular antibiotic. The same principles can be applied when selecting for plasmid containing cells.

2.1.2 *S. pombe* strains

Table 2.1 indicates the *S. pombe* strains used during this study. All *S. pombe* strains were stored in 50% glycerol stocks and maintained at –80°C.

2.1.3 *S. pombe* vectors

2.1.3.1 pFA6 vectors- PCR based gene targeting

The pFA6a series of plasmids contain drug resistant cassettes based on the heterologous selectable marker *kanMX6* and are designed to be used as templates for PCR-based gene targeting in *S. pombe* as described by Bahler *et al*, 1998. The pFA6 series include plasmids containing a number of different markers, including the *natMX4* (resistance to clonNAT-Nourseothricin). Through PCR amplification of the heterologous module with primers flanked with 79bp of sequence homologous to upstream and downstream of the target sequences within the *S. pombe* genome, epitopes can be introduced at gene loci via homologous integration.

Table 2.1 *S. pombe* strains

Strain	Genotype
<i>wild type</i>	<i>ade6-704, leu1-32, ura4-D18, h⁺</i>
<i>wild type</i>	<i>ade6-704, leu1-32, ura4-D18, h⁻</i>
<i>nse2.SA</i>	<i>ade6-704, leu1-32, ura4-D18, nse2-SA::ura4⁺, h⁻</i>
<i>nse2.SA</i>	<i>ade6-704, leu1-32, ura4-D18, nse2-SA::ura4⁺, h⁺</i>
<i>rad60.CT</i>	<i>ade6-704, leu1-32, ura4-D18, rad60-CT::kan^r, h⁻</i>
<i>rad60-SBM3</i>	<i>rad60-L401A,V403A, ade6-704, leu1-32, ura4-D18, h⁻</i>
<i>rad60-SBM2</i>	<i>rad60-L348A,V350A, ade6-704, leu1-32, ura4-D18, h⁻</i>
<i>rad60-SBM1</i>	<i>rad60-L243A,V245A, ade6-704, leu1-32, ura4-D18, h⁻</i>
<i>SUMOK14R</i>	<i>pmt3-K14R, ade6-704, leu1-32, ura4-D18, h⁺</i>
<i>SUMOK30R</i>	<i>pmt3-K30R, ade6-704, leu1-32, ura4-D18, h⁺</i>
<i>SUMORR</i>	<i>pmt3-K14R;K30R, ade6-704, leu1-32, ura4-D18, h⁺</i>
<i>pli1Δ</i>	<i>ade6-704, leu1-32, ura4-D18, pli1::ura4⁺, h⁻,</i>
<i>pli1Δ</i>	<i>ade6-704, leu1-32, ura4-D18, pli1::nat^r, h⁻,</i>
<i>pli1Δ</i>	<i>ade6-704, leu1-32, ura4-D18, pli1::kan^r, h⁻</i>
<i>rad22Δ</i>	<i>ade6-704, leu1-32, ura4-D18, rad22::nat^r, h⁺</i>
<i>rhp51Δ</i>	<i>rhp51::ura4, ade6-704, leu1-32, ura4-D18, h⁻</i>
<i>wild type ch.16</i>	<i>leu1-32, ade6-M210, ura4-D18, his3-D1, Ch16-AGU, h-</i>
<i>pli1Δ ch16</i>	<i>pli1::nat^r leu1-32 ade6-M210 ura4-D18 his3-D1 Ch16-AGU h-</i>
<i>rad22Δ</i>	<i>rad22::nat leu1-32 ade6-M210 ura4-D18 his3-D1Ch16-AGU h-</i>
<i>nse2.SA</i>	<i>nse2.SA::ura4⁺ nat leu1-32 ade6-M210 ura4-D18 his3-D1Ch16-AGU h⁺</i>
<i>SUMORR ch.16</i>	<i>pmt3-K14R;K30R nat leu1-32 ade6-M210 ura4-D18 his3-D1Ch16-AGU h⁺</i>
<i>hus5K50R</i>	<i>hus5-K50R, ade6-704, leu1-32, ura4-D18, h⁺</i>
<i>hus5K50R</i>	<i>hus5-K50R;K30R nat leu1-32 ade6-M210 ura4-D18 his3-D1Ch16-AGU h⁺</i>
<i>ulp2Δ</i>	<i>ulp2::ura4, ade6.704, leu1. 32, ura4.D18, h -</i>
<i>rtf2Δ</i>	<i>rtf2::ura4⁺ade6.704, leu1.32, ura4.D18, h⁻,</i>
<i>rtf2K184R</i>	<i>rtf2-K184R ade6-704, leu1-32, ura4-D18, h⁻</i>
<i>rtf2K209R</i>	<i>rtf2-K209R ade6-704, leu1-32, ura4-D18, h⁻</i>
<i>rtf2K224R</i>	<i>rtf2-K224R ade6-704, leu1-32, ura4-D18, h⁻</i>
<i>rtf2T</i>	<i>rtf2-K184R;K209R;K224R ade6-704, leu1-32, ura4-D18, h⁻</i>

2.1.3.2 pAW vectors- Recombinase-mediated cassette exchange system

The pAW series of vectors are for use in the ‘recombinase-mediated cassette exchange (RCME) system’ (Watson et al., 2008) to obtain ‘base strains’. pAW41 and pAW12 are used as PCR templates for generating ‘base strains’ for essential genes in which a ‘loxP-*geneX-ura4⁺*-loxM3’ cassette is introduced into the *S. pombe* genome in a two step process; first the loxP site from pAW41 is integrate upstream of the promoter and then the *ura4⁺* gene and the loxM3 site from pAW12 are integrated immediately downstream of the coding sequence. pAW1 is used for generating base strains for non-essential genes in one step. The ‘loxP-*ura4⁺*-loxM3’ cassette amplified from pAW1 is integrated by homologous recombination immediately upstream of the promoter and immediately downstream of the coding sequence and replaces the gene of interest. pAW8 is a Cre-expression plasmid used for cassette exchange by recombination. All pAW plasmids contain the Amp^R gene for plasmid propagation in *E. coli*.

pAW1 and pAW8 vectors were used to obtain a ‘base strain’ deletion and point mutations for the non-essential *rtf2⁺* gene (see chapter 6.6)

pAW1 contains the ‘loxP-*ura4⁺*-loxM3’ cassette. Through PCR amplification of the heterologous module, with primers flanked with 79bp of sequence homologous to target sequences within the *S. pombe* genome, the cassette was introduced via homologous integration from upstream of the *rtf2⁺* promoter to immediately downstream of the stop codon to obtain the deletion strain (*rtf2::ura4*) .

pAW8 is based on the pUC19 vector and contains the *S. cerevisiae LEU2⁺* gene under the control of *nmt41* promoter (no message in thiamine), the *cre* gene (expresses bacteriophage P1 recombinase) under the control of *nmt1* promoter, and a multiple cloning site (MCS) flanked by the loxP and loxM. When a coding sequence is cloned into the pAW8 plasmid loxP and loxM3 sites consequently flank it. Site-directed mutagenesis on this pAW8 cassette followed by cassette exchange between this plasmid cassette and the chromosomal cassette allows a simple method for integrating point mutations into the target gene.

2.1.4 Recombination-mediated cassette exchange (Watson *et al.*, 2008)

A pAW8 vector containing the sequence for exchange was transformed into the base strain as described in section 2.1.3.1. Following transformation, cells were plated directly onto minimal medium (YNB) containing adenine and uracil (-LEU) to select for cells that took-up the plasmid. Plates were kept at 30°C and when transformants appeared, colonies were re-streaked onto fresh YNB+ade+ura plates. The transformants were grown to saturation in 10 ml YE at 30°C in order for recombination followed by plasmid loss to occur. Two dilutions of the culture (10^{-4} and 10^{-6}) were plated on full media (Yeap *et al.*) such that discernible single colonies are obtained. The resulting colonies were replica-plated onto YEA plates containing 5FOA to select for loss of *ura4+* and onto YNB+ade+ura plates to select for loss of plasmid. Colonies that grew on 5FOA but not on LEU- were re-streaked onto fresh YEA plates containing 5FOA for further analysis.

2.1.5 *S. pombe* transformation - standard LiAc method

S. pombe cells were grown overnight in YE until they were in mid-log phase. 10 ml ($\sim 1 \times 10^8$) cells were used per transformation. Cells were harvested at 3,000 rpm for 5 minutes. The cells were then washed with 1 ml distilled water, followed by two washes with 1 ml of freshly prepared LiOAc /TE solution. The cell pellet was resuspended in 100 μ l LiOAc/TE and ~ 1 μ g plasmid DNA was added. The sample was incubated at room temperature for 10 minutes before adding 260 μ l fresh PEG/TE/LiOAc. The sample was incubated for 30-45 minutes at 30°C followed by heat shock at 37°C for 5 minutes and centrifugation at 13000rpm for 30s. The cell pellet was washed with 1ml of water, resuspended in 100 μ l water and plated onto appropriate media.

LiOAc/TE

0.1M	Lithium acetate pH 7.5
1x	TE

PEG/LiOAc/TE

40%	PEG
0.1M	Lithium acetate pH 7.5
1x	TE

2.1.6 *S. pombe* genetic mating crosses

S. pombe crosses were set up by mixing two strains of opposite mating types on extra low nitrogen (ELN) media. The plates were incubated for 3 days at 25°C until spore-containing asci could be observed by a light microscope.

2.1.6.1 Random Spore Analysis

For mating crosses between strains with different selectable markers random spore analysis was used to select for double mutants. 1 ml of water, with 1 µl helicase (S.P.P. *Helix pomatia* juice) was inoculated with a loop of mating mixture. The sample was incubated on a rotating wheel overnight (minimum 8 hours) at room temperature. Serial dilutions (10^{-4} and 10^{-6}) of the spores were plated onto YEA and incubated at 30°C for 3 days. Colonies were then replica-plated onto selective media plates and double mutants selected.

2.1.6.2 Tetrad Analysis

For mating crosses between strains without different selectable markers tetrad dissection analysis was used to select for double mutants. Following sporulation, a small loop of cells was streaked on one side of a YEA plate and incubated at 30°C for ~3 hours to allow the ascus wall to break down. Each ascus was then micro-manipulated to separate the four individual spores on the YEA plate. The spores were incubated for 3-4 days at 30°C until colonies formed. Depending on the phenotype of the individual mutant strains, double mutants were identified by replica plating onto suitable selection plates and/or exposing to genotoxins and/or UV/IR radiation.

2.1.7 Survival Analysis

2.1.7.1 UV Survival Analysis

Cells were grown in appropriate media overnight to exponential phase and diluted to 5×10^3 cells/ml (or a dilution suitable for the strain). To test UV sensitivity, 100 μ l cells (~500 cells) were plated in duplicate onto yeast extract agar (Yeap et al.) plates and irradiated at a dose of 25 Jm^{-2} /min for doses ranging between (0 and 200 Jm^{-2}). Colonies were counted following incubation for 72 hours at 30°C and percentage survival calculated with reference to the non-irradiated sample.

2.1.7.2 Ionising radiation (IR) survival analysis

Cells were grown in appropriate media overnight to exponential phase and diluted to 5×10^3 cells/ml (or a dilution suitable for the strain). To test γ sensitivity, cells were irradiated with γ rays from a ^{137}Cs source at a dose of 10 Gy/min for doses ranging from 0-1,000 Gy. 100 μ l cells (~500 cells) were plated in duplicate onto yeast extract agar (Yeap et al.) plates. Colonies were counted following incubation for 72 hours at 30°C and percentage survival calculated with reference to the non-irradiated sample.

2.1.7.3 Sensitivity to genotoxins

To determine the sensitivity of cells to DNA damaging agents by spot tests, exponentially growing cultures were adjusted to an equal cell density and four successive tenfold dilutions were spotted onto YEA or YEA plates containing hydroxyurea (HU), thiabendazole (TBZ), cycloheximide (CHX), camptothecin (CPT) or methyl methanesulfonate (MMS). Plates were incubated at 30°C for 3 days. Table 2.3 lists the genotoxins used in this study.

2.1.8 DAPI staining of *S. pombe* cells

1 ml of exponentially growing cells was harvested for 1 minute at 3,000 rpm and the supernatant removed. The cells were washed with 1 ml PBS and resuspended in 1 ml cold methanol. Following centrifugation for 1 minute at 3,000 rpm, the supernatant was discarded and the cells were re-suspended in 100 μ l mounting mix. 5 μ l of the cell suspension was placed on a microscope slide. Once the sample was dry, a small drop of vectashield (Vecta) was added to the slide and covered with a coverslip. The coverslip was sealed with clear nail varnish and the cells visualized with a Delta Vision microscope.

Mounting mix

0.5 μ g/ml DAPI

2.5 μ g/ml Calcofluor

2.1.9 Mutation Rate Determination

To determine the rate of mutation during cell growth, fluctuation tests were utilized (Lea and Coulson, 1949), as modified by Reenan and Kolodner (1992). Single colonies were propagated in 10ml YE and incubated at 30°C (25°C for temperature sensitive strains) on a rotating wheel. After 24 hours the cells were counted and the number of cell cycles calculated. 500 cells were plated on non-selective media as control and higher number of cells (ie 10^3 , 10^4 , 10^5) were plated on selective media. The remaining cultures were diluted and grown further under the same conditions. The procedure was repeated until the cells went through minimum 30 cycles with samples plated after every 24 hours. Plates were incubated at 30°C (25°C for temperature sensitive strains) for 3-5 days followed by colony counting.

Three independent experiments, each using 7 colonies, were performed for each strain to be tested. The method of the median was used to calculate mutation rates; $r_0 = M(1.24 + \ln M)$, where r_0 is the median number of colonies on selective media out of the 7 cultures, and M is the average number of colonies on selective media per culture (Reenan and Kolodner, 1992). Interpolation was used to determine M , and was

subsequently used to calculate the mutation rate using the formula $r = M / N$, where N is the average number of total cells from the 11 cultures (Reenan and Kolodner, 1992). To compare mutation rates, a contingency χ^2 test was used and a P-value of 0.05 or less was considered significant (for three-way comparisons) (Spell and Jinks-Robertson, 2004)

2.1.10 Genomic DNA extraction from *S. pombe*

A 10 ml *S. pombe* culture was grown overnight in YE until the cells reached stationary phase. The cells were harvested at 3000 rpm for 5 minutes and washed once with 2 ml SP1 buffer. The cell pellet was then re-suspended in 2 ml SP1 buffer containing 2 mg/ml zymolyase (T 20,000) and incubated at 37°C for 45-60 minutes until ~80 % cell lysis was observed. Spheroplasting was checked by removing 10 µl of sample onto a microscope slide with 1 µl 10% SDS and viewing by a light microscope. Once the cells were sufficiently lysed the protoplasts were harvested at 3000 rpm for 5 minutes. The pellet was re-suspended in 900 µl 5x TE and 100 µl 10% SDS was added. The sample was incubated for 5 minutes at room temperature before 300 µl KAc was added to the sample. The sample was then incubated for 10 minutes on ice and then centrifuged at 4,500 rpm for 15 minutes. The supernatant was transferred to a clean falcon tube and one volume (~2 ml) of isopropanol was added. After centrifuging at 4,500 rpm for 15 minutes the pellet was washed with 500 µl 70% ethanol. The pellet was air dried and re-suspended in 250 µl 1 x TE.

SP1 Buffer:

1.2 M	Sorbitol
50 mM	Sodium citrate
50 mM	Sodium phosphate
40 mM	EDTA

Buffer was adjusted to pH 5.6 with NaOH

5x TE

50 mM	Tris, pH 8.0
-------	--------------

5 mM EDTA

2.2 BACTERIAL METHODS

2.2.1 Bacterial media

L-Broth (LB)

10 g/l	Tryptone
5 g/l	Yeast extract
5 g/l	NaCl

For solid LA media 8 g/l agar was added.

2.2.2 Antibiotics

To select for plasmids containing a resistance marker, antibiotics were added to media prior to use. All antibiotics were stored at -20°C.

Antibiotic	Stock Concentration	Working Concentration
Kanamycin	100 mg/ml in water	100 µg/ml
Spectinomycin	50 mg/ml	50 µg/ml
Gentimycin	50 mg/ml	50 µg/ml
Ampicillin	100 mg/ml in water	100 µg/ml
Chloramphenicol	34 mg/ml in ethanol	34 µg/ml

2.2.3 Blue-white selection

For blue-white selection using insertional activation of the LacZ gene, IPTG and X-Gal were added to media containing the appropriate selective antibiotic. Both IPTG and X-Gal were stored at -20°C.

Additive	Stock Concentration	Working Concentration
IPTG	20 mg/ml in water	40 µg/ml
X-Gal	20 mg/ml in dimethylformamide	100 µg/ml

2.2.4 *E.coli* strains

The *E. coli* strains used in this study are listed in table 2.2

2.2.5 Bacterial cloning vectors

pGEM-T Easy (Promega)

The pGEM-T Easy cloning vector is a high copy number plasmid that can be used for the cloning of blunt-ended PCR products. The vector have a 3' terminal thymidine at both ends providing a compatible overhang for PCR products generated by polymerases, which add single deoxyadenosine, to the 3'-ends of the amplified fragments. The vectors contain both T7 and SP6 RNA polymerase promoters in addition to the α -peptide coding region of the enzyme β -galactosidase. Insertional inactivation of the α -peptide allows selection of recombinant clones by blue-white screening.

The bacterial expression vectors used in this study are under the control of the T7 promoter, which is activated by the T7 polymerase. The bacterial expression strain BL21-CodonPlus (Stratagen) is a λ DE3 lysogen containing an integrated copy of the T7 polymerase gene, which is under the control of the *lacZ* promoter. Expression of the T7 polymerase, and therefore the protein of interest, is induced by the addition of IPTG.

Table 2.2 *E. coli* strains

NM522	F ⁻ lacI ^q D(lacZ)M15, <i>proA</i> ⁺ <i>B</i> ⁺ / <i>supE</i> , <i>thiD</i> , (<i>lac-proAB</i>) <i>D</i> , (<i>hsdMS-mcrB</i>)5.
BL21 C+	(λDE3 lysogen/pLysS) F ⁻ <i>Amp</i> ^r <i>r</i> _B ⁻ <i>m</i> _B ⁻

pET-15B (Novagen)

The pET-15B vector carries a 6xHis-tag allowing affinity purification of N-terminally tagged proteins on Ni^{2+} agarose beads. A thrombin cleavage site allows cleavage of the tag following purification. An Amp^r gene allows selection of the plasmid.

pET28a (Novagen)

The pET-28a vector carry an N-terminal His Tag / thrombin / T7 Tag configuration plus an optional C-terminal 6xHis Tag sequence. A Kan^r gene allows selection of the plasmid. pET28a was used for co-expression with pGEX vector (Amp^r and Kan^r selection)

pGEX (Pharmacia Biotech)

The pGEX vector encodes a 26 kDa GST tag allowing purification of the N-terminally tagged proteins on glutathione sepharose beads. A thrombin cleavage site allows cleavage of the tag following purification. An Amp^r gene allows selection of the plasmid.

2.2.7 Preparation of competent *E. coli* cells

A single colony was used to inoculate 5 ml LB and grown overnight in a 37°C shaker. The 5 ml pre-culture was used to inoculate 1 litre pre-warmed LB and grown at 37°C with shaking for 2-4 hours until the OD_{595} reached 0.5-0.6. The cells were chilled on ice for 1 hour and centrifuged at 5,000 rpm for 5 minutes at 4°C . The supernatant was discarded and the cell pellet re-suspended in 25 ml ice-cold TRNS 1 solution. The sample was centrifuged at 3,000 rpm for 5 minutes at 4°C . The supernatant was again discarded and the cell pellet re-suspended in 25 ml TRNS 1 solution. After incubating on ice for 5 minutes, the sample was centrifuged at 3,000 rpm for 5 minutes at 4°C . The supernatant was discarded and the cell pellet re-suspended in 6 ml ice cold TRNS 2.

The sample was incubated on ice for 10 minutes before aliquoting into volumes of 300 μ l. The cells were then snap-frozen in liquid nitrogen and stored at -80°C .

TRNS 1 solution

12.1 g/l	RbCl
9.6 g/l	MnCl ₂
1.48 g/l	CaCl ₂
2.88 g/l	CH ₃ COONa
66 ml/l	Glycerol

Solution adjusted to pH 5.8 with acetic acid, and then filter sterilized.

TRNS 2 solution

1.2 g/l	RbCl
11 g/l	CaCl ₂
2.1 g/l	MOPS
66 ml/l	Glycerol

Solution adjusted to pH 6.8 with acetic acid, and then filter sterilized.

2.2.8 *E. coli* transformation

Competent *E. coli* cells were thawed on ice for 15 minutes. Approximately 0.5 μ g of plasmid DNA was added to 100 μ l cells. The sample was incubated on ice for 15 minutes before being ‘heat shocked’ at 37°C for 2 minutes. The cells were then incubated on ice for a further 5 minutes. 0.5 ml L-Broth was added and the sample incubated for 45 minutes at 37°C . After incubation, the cells were spun at 3,000 rpm for 5 minutes and the supernatant tipped off. The cell pellet was re-suspended in 100 μ l LB and the cells plated onto LB agar plates supplemented with the appropriate selective antibiotic. Plates were incubated at 37°C overnight.

2.3 DNA METHODS

2.3.1 Agarose gel electrophoresis

Typically, 200 ml 0.8% agarose gels were used to analyse DNA samples, although occasionally, a 1% agarose gel were used to analyse small (<500bp) DNA fragments. Agarose (Melford) was dissolved, by heating, in 1 x TBE buffer. Prior to pouring in a pre-prepared agarose gel cast, ethidium bromide was added to a final concentration of 0.25 µg/ml. Once set, the gel was submerged in a gel tank containing 1 x TBE buffer. Typically, DNA samples were loaded as a 20 µl volume with one-sixth volume of 6x loading buffer and were run against 1 µl of a 1 kb ladder (Invitrogen). Electrophoresis was carried out at 150 V for ~ 45 minutes or until DNA bands were well separated. The DNA was visualised using a UV transilluminator.

10 x TBE Buffer

108 g/l	Tris base
55 g/l	Boric acid
0.2 M	EDTA, pH 8.

6 x Loading Buffer

0.1%	SDS
40%	Sucrose
1 mM	EDTA
1 mM	Tris, pH 7.5
0.25 %	Bromophenol blue

2.3.2 Pulse-Field Gel Electrophoresis (PFGE)

PFGE was used to resolve *S. pombe* genomic DNA embedded in agarose plugs. Two different conditions were used: *S. pombe* conditions to resolve endogeneous chromosomes and *S.cerevisiae* conditions to resolve artificial minichromosomes.

***S. pombe* conditions:**

DNA agarose plugs were cut to size, washed 3 times in 1.0x TAE buffer and set in a standard casting stand and a 30-well comb (Bio Rad) with a 0.8% InCert agarose (Lonza) in 1.0x TAE. The set up was placed in a CHEF-DR III Variable Angle System (Bio Rad) with 5L of cold 1.0x TAE buffer. The DNA was resolved at 14°C following manufacturer's instructions:

Switch time: 1800 seconds

Run time: 72 hours

Voltage: 1.5V/cm

Angle: 106°

***S. cerevisiae* conditions:**

DNA agarose plugs were cut to size, washed 3 times in 0.5x TBE buffer and set in a standard casting stand and a 30-well comb (Bio Rad) with a 0.8% InCert agarose (Lonza) in 0.5x TBE. The set up was placed in a CHEF-DR III Variable Angle System (Bio Rad) with 5L of cold 0.5x TBE buffer. The DNA was resolved at 14°C following manufacturer's instructions:

Switch time: 60 - 120 seconds (ramped)

Run time: 24 hours

Voltage: 6 V/cm

Angle: 120°

The DNA was visualised using a UV transilluminator after 30 minutes staining in 0.5L of 0.001% EtBr solution.

10 x TBE Buffer: see section 2.3.1

50x TAE buffer:

242 g/l	Tris base
57.1ml/l	glacial acetic acid
0.5 M	EDTA, pH 8.0

2.3.3 PCR-amplifying DNA fragments

PCR was generally carried out using the DNA polymerases *Pfu* (error-free) and *Taq* (error-prone), both expressed and purified in-house (see section 2.4.10). Approximately 50 ng template DNA was used per 50 µl reaction containing; 1 µl forward primer (10 µM), 1 µl reverse primer (10 µM), 5 µl 10 x appropriate buffer, 5 µl 2.5 mM dNTPs, and 1 µl enzyme, which was added last. The PCR programme consisted of 17 - 25 cycles of; 94°C for 1 minute, X°C for 30 seconds and 68°C for Y minutes where X, the annealing temperature, is dependent of the melting temperature of the primer pair, and Y, the elongation time, is dependent on the length of desired product. Typically the extension time was calculated as 2 minutes per kb product. 1 µl of the PCR product was analysed on a 0.8% TBE agarose gel.

10X *Pfu* buffer: 20mM MgSO₄

200mM Tris-HCl (pH 8.8 at 25°C)

100mM (NH₄)₂SO₄

100mM KCl

1% (v/v) Triton X-100

1mg/ml BSA

20mM MgSO₄

10X *Taq* buffer was purchased from Invitrogen.

2.3.4 PCR- Site-directed mutagenesis

Site-directed mutagenesis was carried out based on the 'QuickChange site-directed mutagenesis' technique (Stratagene). Complementary primer pairs were designed to contain the DNA sequence encoding the mutation of choice flanked either side by ~ 12 bases that will hybridise to the original DNA sequence. *Pfu* polymerase was used to amplify the entire template plasmid. Approximately 50 ng template DNA was used per 50 µl reaction containing; 1 µl forward primer (1 µM), 1 µl reverse primer (1 µM), 5 µl 10 x *Pfu* buffer, 3 µl 2.5 mM dNTPs, and 1 µl *Pfu* enzyme, which was added last. The PCR programme consisted of 17 cycles of: 94°C for 1 minute, X°C for 30 seconds and

68°C for Y minutes where X (the annealing temperature) is dependent on the melting temperature of the primer pair, and Y (the elongation time) is dependent on the length of desired product. 1 µl of the PCR product was analysed on a 0.8% TBE agarose gel. The remaining PCR product was digested with 1 µl *DpnI* (New England Biolabs), which digested the methylated parental DNA template, leaving only the newly amplified 'mutagenic' DNA product. 20 µl of the mutagenic PCR product was transformed into *E. coli* NM522 cells and the DNA extracted using a QIAGEN miniprep kit according to the manufacturer's instructions. The presence of the desired mutation was confirmed by sequencing (Section 2.3.11).

2.3.5 PCR purification

PCR products were purified using a QIAGEN PCR purification column according to the manufacturer's guidelines.

2.3.6 Ethanol precipitation

2.5 x sample volumes EtOH (100%) was added to the DNA sample with 1/10th volume 3M NaOAc. Samples were incubated at -20°C for ~ 1 hour and then spun at 13,000 rpm for 10 minutes at 4°C. The supernatant was removed and the DNA pellet washed with 500 µl EtOH. The supernatant was removed and the DNA pellet was dried for ~ 10 minutes before being re-suspended in 50 µl (or desired volume) 1 x TE.

2.3.7 Restriction enzyme digests

Typically, 1 µg of DNA was digested in a total volume of 30 µl. Restriction enzymes (New England BioLabs) were used as according to the manufacturers guidelines with 1 µl restriction enzyme, 3 µl of the relevant 10 x restriction enzyme buffer, and if required 3 µl of 10 x BSA. Digests were incubated at 37°C for minimum 2 hours. For double digests, where the enzyme buffers were not compatible, the DNA was cleaned

following the first enzyme digest using a QIAGEN PCR purification column as according to the manufacturer's guidelines.

2.3.8 Purification of DNA fragments from agarose gels

DNA fragments were isolated by electrophoresis. Typically on a 0.8% TBE gel. For DNA fragments less than 500 base pairs, a 1% TBE gel was used. The DNA fragments were analysed using a UV transilluminator. The DNA band was excised using a clean scalpel and purified from the gel using an 'Easy Pure' gel purification kit (Biozym Scientific GmbH), according to the manufacturer's instructions.

2.3.9 Ligations

Ligations were carried out using a Quick Ligation Kit (New England BioLabs) according to the manufacturer's guidelines. Typically, the vector and insert were ligated in a 1:9 molar ratio with 10 µl 2x ligase reaction buffer and 1 µl DNA ligase (1 unit/µl) in a final reaction volume of 20 µl. The ligation mixture was incubated at room temperature for a minimum of 5 minutes before being transformed into NM522 *E. coli* cells.

2.3.10 Amplification of plasmid DNA

2.3.10.1 DISH minipreps (for DNA checking only)

A 2 ml L-Broth culture, supplemented with the appropriate selective antibiotic was inoculated with a single colony and grown for ~4 hours at 37°C, with shaking. 1 ml of the cell culture was harvested at 13,000 rpm for 5 minutes and the supernatant discarded. The cell pellet was re-suspended in 100 µl DISH I solution. 200 µl DISH II was added and the sample mixed by inversion. 150 µl ice cold DISH III was added and the sample mixed by inversion. 200 µl phenol chloroform was added and the sample vortexed. The sample was then spun at 13,000 rpm for 15 minutes and the top aqueous layer removed to a clean microcentrifuge tube containing 750 µl 100% ethanol. The

sample was spun for a further 5 minutes at 13,000 rpm and the supernatant removed. The DNA pellet was dried for approximately 10 minutes in a dessicator before being re-suspended in 40 µl 1x TE containing 20 µg/ml RNase. 5 µl of the DNA sample was analysed on an agarose gel.

DISH I

9 g/l	Glucose
3 g/l	Tris-base
3.72g/l	EDTA

DISH II

0.2 M	NaOH
1%	SDS

DISH III

3 M	KOAc
11.5%	Glacial acetic acid

Phenol/chloroform

24 Volumes	Phenol
25 Volumes	Chloroform
1 Volume	Isoamyl alcohol.

2.3.10.2 Qiagen minipreps

If the DNA was to be sequenced or further manipulated, minipreps were carried out using a QIAGEN miniprep kit. 5ml *E. coli* liquid culture, with the appropriate antibiotic, was grown to saturation at 37°C. The bacterial pellet was collected by centrifugation at 4000 rpm for 5 min. The plasmid was extracted using the QIAprep Spin Miniprep Kit (Qiagen) according to the protocol provided by the manufacturer. The DNA was stored at -20°C until required.

2.3.11 Sequencing by GATC

DNA samples and sequencing primers were sent to GATC for sequencing. 20 µl DNA (30-100 ng/µl) and 20 µl corresponding primer (30 pmol/µl) were required.

2.4 PROTEIN METHODS

2.4.1 SDS polyacrylamide gel electrophoresis (SDS-PAGE)

SDS PAGE was carried out using Biorad Mini Protean II kits. Protein samples were resolved on 7.5, 10 or 12.5% separating gels. Polymerisation was achieved by the addition of 10% ammonium persulphate (APS) and TEMED to the separating buffer. The pre-polymerised gel solution was poured between glass plates separated with 0.75 mm plastic spacers and left to set for approximately 30 minutes with a layer of distilled water on top to achieve a level surface. Once set, the water layer was poured off and the plates dried with *Whatman* paper. The stacking gel (3%) was poured on top of the separating gel and the gel comb positioned. After approximately 30 minutes the comb was removed and the gel kit assembled. Protein samples were mixed with 5 x sample buffer and denatured at 95°C for 5 minutes. 10-25 µl of sample were loaded into each well. 8 µl of benchmark protein ladder (Invitrogen) was loaded into the end lane as a size indicator. Gels were run in 1 x SDS running buffer at 150 V for approximately 1 hour or until the dye front reached the bottom of the gel.

Separating gels: (To make 2 mini gels)

Separating Gel	7.5%	10%	12.5%
Protogel (ml)	2.5	3.3	4.2
4x separating buffer (ml)	2.5	2.5	2.5
Distilled water (ml)	5.0	4.2	3.3
10% APS (µl)	100	100	100
TEMED (µl)	10	10	10

Stacking gels: (To make 2 mini gels)

Stacking		3%	6%
Protogel	(ml)	0.5	1.0
4x stacking buffer	(ml)	1.3	1.3
Distilled water	(ml)	3.3	2.8
10% APS	(μ l)	50	50
TEMED	(μ l)	10	10

4 x Separating buffer

1.5 M Tris HCl, pH 8.8

0.4% SDS

4 x Stacking buffer

0.5 M Tris HCl, pH 8.8

0.4% SDS

5 x Sample buffer

60 mM Tris HCl, pH 6.8

25% Glycerol

2% SDS

14.4 mM β -mercaptoethanol

10% Bromophenol blue

10 x SDS-PAGE buffer

25 mM Tris HCl, pH 8.3

192 mM Glycine

0.1% SDS

2.4.2 Coomassie Brilliant Blue Staining

An SDS-PAGE gel was placed in Coomassie gel stain at room temperature for ~ 1 hour with gentle shaking. The gel was then briefly washed in water and then placed in destain solution overnight with gentle shaking. To dry the SDS-PAGE gel, the gel was placed on Whatman 3 MM paper and dried for 1 hour on a gel dryer.

Coomassie gel stain

1 g/l	Coomassie Brilliant Blue (Sigma)
45%	Methanol
10%	Glacial acetic acid

Destain solution

10%	Methanol
10%	Glacial acetic acid

2.4.3 Western Blotting

Twelve pieces of Whatman 3 MM paper and one piece of PVDF membrane (millipore) were cut to the same size as the SDS-PAGE protein gel. The Whatman 3MM papers were soaked in blotting buffer and 6 pieces were stacking on top of each other and placed on the Electrobloetter (Biorad). The PVDF membrane soaked in methanol and then placed on top of the 6 Whatman sheets. The protein gel was laid on top of the membrane and the remaining 6 soaked Whatman papers placed on top. Bubbles were removed by rolling a thick marker pan over the stack. The electroblotter was run at 150 mA for 35 minutes per gel. Following blotting the PVDF membrane was transferred to a container containing 4% milk (in PBS) and was blocked for at least 30 minutes at room temperature or overnight at 4°C with gentle shaking.

Semi-dry transfer buffer

48 mM Tris-Base

39 mM Glycine

0.04% SDS

20% Methanol

2.4.4 Incubation of PVDF membrane with antibodies

Following blocking in 4% milk (in PBS), the PVDF membrane was incubated in 10 ml milk containing the primary antibody. Primary antibodies were typically used at a 1:2,000 dilution in 4% milk (in PBS) and incubated overnight at 4°C with gentle shaking. Alterations to this general protocol were made depending on the efficiency of the particular antibody. The blot was washed with 3 x 10 minute washes in PBS containing 0.1% Tween 20 and 1 x minute wash with PBS. Following washing, 10 ml 4% milk (in PBS) was added to the membrane and an HRP-conjugated secondary antibody was added to a final dilution of 1:2,000. The blot was left to incubate at room temperature for approximately 90 minutes with gentle shaking. The previous 10-minute wash steps were repeated (3 x PBS with 0.1% Tween, 1 X PBS) and the proteins detected by ECL (Section 2.4.5).

2.4.5 Enhanced Chemi-Luminescence

Detection was carried out using Western Lightning (PerkinElmer). The blot was incubated for ~1 minute with slight agitation before being removed from solution and wrapped in Saran wrap. In a dark room, the membrane was exposed to X-ray film (Kodaki et al.) for varying lengths of time depending on the intensity of the signal. The film was developed using a LSC50000 machine.

2.4.6 Determining protein expression and solubility

A single BL21-CodonPlus(DE3) colony, carrying the appropriate expression vector, was used to inoculate 2 ml of L-broth media containing chloramphenicol and the appropriate selective antibiotic. The culture was grown overnight at 37°C with shaking. The following morning 1 ml of this pre-culture was used to inoculate 10 ml of medium. The cells were incubated at 37°C, with shaking until an A_{595} reading of ~0.6 was reached. At this point 1 ml of each culture (non-induced) was removed and placed in a fresh tube. Cells in the remaining 9 ml culture were induced with an appropriate concentration of IPTG and grown with the non-induced samples for either a further 1 or 3 hours at 37°C. 1 ml of cells was harvested at 13,000 rpm for 5 minutes and the pellet re-suspended in X ml ($X = A_{595} \text{ reading} / 4$) of an appropriate buffer (NETN (section 2.4.8) for GST-fusion proteins). The sample was sonicated for 15 seconds on ice and then spun at 13,000 rpm for 5 minutes. The supernatant was transferred to a fresh microcentrifuge tube and one-fifth 5x sample buffer added. The pellet was re-suspended in X ml 5 x sample buffer. Samples were boiled for 5 minutes and analysed by SDS-PAGE (Section 2.4.1) followed by Coomassie staining (Section 2.4.2).

2.4.7 Bradford assay

To determine the protein concentration of a sample the Bradford assay reagent (Biorad) was diluted 1 in 5 with water. 1-5 µl protein sample was added to 1 ml of the diluted Bradford reagent. The OD A_{595} was measured as compared to a 1 ml reagent only 'blank'. The protein concentration of the sample was determined by comparing the sample reading against a BSA standard curve.

2.4.8 GST-tagged protein purification

A single BL21-CodonPlus(DE3) colony, carrying the appropriate expression vector, was used to inoculate 2 ml of L-broth containing chloramphenicol and the selective antibiotic (amp). This pre-culture was grown at 37°C with shaking for ~8 hours. 1 ml of this was used to inoculate 100 ml pre-warmed media, which was grown overnight at

37°C. The following day this 100 ml pre-culture was used to inoculate a 1-litre pre warmed culture. When an A₅₉₅ reading of 0.6 was reached, the cells were induced with IPTG at a final concentration of 5mM. After incubating for a further 3 hours at 37°C with shaking cells were harvested at 5,000 rpm for 10 minutes at 4°C and the supernatant discarded. The cell pellet was re-suspended in 10 ml ice cold NETN (freshly supplemented with PMSF to 0.1 mM, and 1 complete protease inhibitor cocktail tablet from Roche per 50 ml buffer). The cells were sonicated on ice 3 times for 15 seconds with 1-minute intervals on ice. The cell extract was cleared by centrifugation at 14,000 rpm for 15 minutes at 4°C. The supernatant was then added to 100 µl pre-washed glutathione-sepharose beads (Amersham) equilibrated with NETN. The beads were incubated for 2 hours at 4°C on a rotating wheel. The beads were washed 7 times in total (3 x 1 ml NETN, followed by 3 x 1 ml wash buffer and 1 x PBS). Washing was carried with a brief spin at 13,000 rpm to pellet the beads. Following this spin, the supernatant was discarded and the beads were incubated with 1 ml of the appropriate buffer on a rotating wheel for 5 minutes at 4°C. Protein was collected either by glutathione elution of the GST-fusion protein or thrombin cleavage of the protein from the GST bound to the beads.

NETN Buffer

0.5%	NP40
1 mM	EDTA
20 mM	Tris-HCl, pH 8.0
100 mM	NaCl
freshly supplemented with:	
0.1 mM	PMSF
1	protease inhibitor cocktail tablet (Roche) per 50 ml buffer

Wash Buffer

100 mM	Tris-HCl, pH 8.0
100 mM	NaCl
1 mM	EDTA

Following the final PBS wash step in the GST-tagged protein purification protocol (Section 2.4.8.1) the GST-fusion protein was eluted from the beads by adding 250 μ l of elution buffer and incubating on a rotating wheel for 30 minutes at 4°C. After a 15 second spin at 2,500 rpm the supernatant was kept. This elution step was repeated a further two times and 5-10 μ l of the elution samples were analysed by SDS-PAGE (Section 2.4.1) followed by Coomassie staining (Section 2.4.2).

Elution Buffer

100 mM	Tris-HCl, pH 8.0
120 mM	NaCl
20 mM	Glutathione

2.4.9 His-tagged protein purification

Ni²⁺ purification

A 10 ml culture of the BL21-CodonPlus strain carrying the appropriate expression vector was grown overnight at 37°C in L-broth containing chloroamphenicol and the selective antibiotic. The pre-culture was used to inoculate a 1 l culture of pre-warmed L-broth, containing the appropriate selective antibiotic. The culture was incubated at 37°C for ~ 4 hours until the OD₅₉₅ reached 0.6-0.8. IPTG was added to a final concentration of 0.1-1 mM and the cells incubated for a further 4 hours at 37°C. The cells were harvested at 5,000 rpm for 5 minutes and the supernatant discarded. The cell pellet was placed at -20°C for at least an hour, before being re-suspended in 20 ml ice-cold binding buffer freshly supplemented with 0.1 mM PMSF. The cells were sonicated on ice for 5x 15 seconds, with 30 second intervals on ice. The cell extract was cleared by centrifugation at 14,000 rpm for 15 minutes at 4°C. The supernatant was gradually applied to 0.5 ml column containing pre-washed Ni²⁺-agarose beads equilibrated with binding buffer at 4°C. Once the supernatant has passed through the column by gravity, the column was washed with 10 column volumes of binding buffer, freshly supplemented with PMSF, followed by 10 column volumes of wash buffer containing PMSF. Elution buffer was added to the column and 0.5 ml fractions were collected on

ice. The protein concentration of each elution was obtained by Bradford assay and ~5 µg protein was analysed by SDS-PAGE.

Binding buffer

5 mM	Imidazole
0.5 M	NaCl
20 mM	Tris HCl, pH 7.5

Wash buffer

20 mM	Imidazole
0.5 M	NaCl
20 mM	Tris HCl, pH 7.5

Elution buffer

500 mM	Imidazole
0.5 M	NaCl
20 mM	Tris HCl, pH 7.5

Co²⁺ purification

A 10 ml culture of the BL21-CodonPlus strain carrying the appropriate expression vector was grown overnight at 37°C in L-broth containing chloroamphenicol and the selective antibiotic. The pre-culture was used to inoculate a 1 l culture of pre-warmed L-broth, containing the appropriate selective antibiotic. The culture was incubated at 37°C for ~ 4 hours until the OD₅₉₅ reached 0.6-0.8. IPTG was added to a final concentration of 0.1-1 mM and the cells incubated for a further 4 hours at 37°C. The cells were harvested at 5,000 rpm for 5 minutes and the supernatant discarded. The cell pellet was placed at -20°C for at least an hour, before being re-suspended in 20 ml ice-cold equilibration/wash buffer. The cells were sonicated on ice for 3 min (5 seconds pulse) on ice. The cell extract was cleared by centrifugation at 14,000 rpm for 15 minutes at 4°C. The supernatant was gradually applied to 0.5 ml column containing pre-washed Co²⁺-agarose beads equilibrated with equilibration/wash buffer at 4°C. Once the supernatant has passed through the column by gravity, the column was washed with 10

column volumes of equilibration/wash buffer. Elution buffer was added to the column and 0.5 ml fractions were collected on ice. The protein concentration of each elution was obtained by Bradford assay and ~5 µg protein was analysed by SDS-PAGE.

Equilibration/wash buffer:

50mM sodium phosphate, pH 7.4
300mM sodium chloride
10mM imidazole

Elution buffer:

50mM sodium phosphate, pH 7.4
300mM sodium chloride
150mM imidazole

2.4.10 Expression and purification of PCR polymerases

Taq polymerase

Taq polymerase was expressed from *pTAQ^{Amp^R}* plasmid (gift from Dr. J. Downs). 2ml culture was inoculated overnight at 37°C and used to inoculate a 1 l culture which was grown at 37°C until OD~0.5. The culture was induced with 1 mM IPTG o/n at 18°C. The cells were pelleted by centrifugation at 5000rpm for 5 minutes and placed at -20°C o/n. The pellet was thawed and resuspended in lysis buffer and the cells were sonicated for 3 min (5 seconds pulse) at 30% amplitude on ice. The debris was spun out at 17000rpm for 20 minutes. The supernatant was heat treated at 85°C for 20 minutes. Ammonium sulfate was added slowly to 30% w/v at room temperature with stirring. The resulting slurry was centrifuged at 17000rpm for 20 minutes and the pellet was resuspended in 5 ml equilibrating buffer. The protein solution was dialysed overnight at 4°C against 5 l of equilibrating buffer, aliquoted and stored at -20°C.

Lysis buffer:

10mM	Tris.Cl, pH 7.9
50mM	KCl
0.5%	Tween
0.5%	NP-40
1mM	PMSF

Equilibrating buffer:

50mM	Tris.Cl, pH 7.9
50mM	KCl
0.1mM	EDTA
50%	glycerol
1mM	DTT

Pfu polymerase

Pfu polymerase was expressed from *pET-Pfu^{KanR}* plasmid (gift from Dr. J. Downs).

2ml culture was inoculated o/n at 37°C and used to inoculate a 1 l culture which was grown at 37°C until OD~0.5. The culture was induced with 1mM IPTG o/n at 18°C. The cells were pelleted by centrifugation at 5000rpm for 5 minutes and placed at -20°C o/n. The pellet was thawed, washed in PBS and resuspended in 20ml PBS300. The cells were sonicated for 3 min (5 seconds pulse) at 30% amplitude on ice. The debris was spun out at 17000rpm for 20 minutes. The supernatant was heat treated at 75°C for 20 minutes and spun out at 15000rpm for 10 mins. The supernatant was applied to 1 ml column of Ni-NTA agarose pre-equilibrated with 10 ml of PBS300.

The column was washed with 20 ml PBS300+15 mM imidazole. 3 ml PBS300+25 mM imidazole was added to the column and 1ml fractions were collected by gravity. 5 ml PBS+500mM imidazole was added to the column and 1ml fractions were collected by gravity. 5 µl of each fraction was run on a SDS gel. Peak fractions were combined and an equal volume of storage buffer was added. The protein solution was dialysed against two changes of 1L of storage buffer at 4°C, aliquoted and stored at -20°C.

PBS300: PBS + 150 mM sodium chloride

Storage buffer:

50mM	Tris, pH 8.0
0.1mM	EDTA
1mM	DTT
0.1%	NP40
0.1%	Tween
50%	glycerol

2.4.11 Protein dialysis

Protein solutions were dialysed using SnakeSkin tubing, MWCO 7K (Thermo Scientific), against minimum 10x volume of the exchange buffer at 4 °C.

2.4.12 Protein desalting/buffer exchange

PD-10 desalting columns (Amersham Biosciences) were used for protein buffer exchange according to the manufacturer instructions.

2.4.13 Size exclusion chromatography (gel filtration)

Prior to gel filtration the elution buffer of protein solutions was exchanged for the equilibrating buffer and the columns, Superdex 75 (10/30 HR) or Superdex 200 (10/30 HR) (Amersham Biosciences), were washed with the equilibrating buffer with a flow rate of 0.5 mL/min. The protein solution was concentrated to 0.5 or 1.0 mL and loaded onto the column. The column was connected to an ÄKTA_{FPLC} system (GE Healthcare) and the protein was eluted at a flow rate of 0.5 mL/min into 1ml fractions according to the manufacturer's instructions. Fractions were monitored using the online UV monitor measuring absorbance at 280nm and by SDS-PAGE.

Equilibrating buffer: 50 mM Tris.HCl pH 8.0
200 mM NaCl

2.4.14 Concentrating protein samples

Proteins were concentrated using Pierce concentrator 7 ml/9K and 7 ml/20K (Thermo Scientific) according to the manufacturer's guidelines.

2.4.15 Equilibrium Denaturation Studies

A stock solution of guanidinium HCl (8 M) was diluted to obtain a large range of denaturant concentrations using a Hamilton Microlab dispenser; 100 μ l of a stock solution of protein (9 μ M) containing 450 mM phosphate, 9 mM DTT (pH 7.0) was added to each denaturant sample (800 μ l). This gave a final buffer concentration of 50 mM phosphate pH 7.0 and a protein concentration of 1 μ M. The protein/denaturant solutions were pre-equilibrated at 25°C for at least three hours. All measurements were performed in a thermostatic cuvette holder at 25°C using Varian Cary Eclipse Fluorescence Spectrophotometer. The excitation wavelength was 280 nm, band passes were set at 5 nm for excitation and emission and the fluorescence was measured at λ_{max} for the denatured state of 352 nm.

2.4.16 Dynamic Light Scattering (DLS)

Dynamic light scattering was used to assess the protein sample dispersity (aggregation) and therefore its suitability for crystallographic studies. 50 μ L of protein solution was centrifuged at 13000rpm for 30 minutes and placed in a disposable solvent resistant micro cuvette (Malvern). Measurements were taken at room temperature or 4°C on a Zetasizer Nano ZS system (Malvern). Scattering data were analysed for peak position and width to identify particle size and polydispersity.

2.4.17 Protein crystallization screening

Protein crystallization screening was performed using the hanging-drop vapor-diffusion method at room temperature in 24-well trays.

1-2 μ l of protein solution was mixed with an equal volume of reservoir solution on a CrystalClene coverslip and sealed with grease upside-down ('hanging drop') on the top of the well containing 400 μ l of precipitant solution to achieve vapour equilibration. As the concentration of the reagent in the drop is smaller than the concentration in the reservoir, water leaves the drop until the two concentrations reach equilibrium and the protein solution reach supersaturation. At this point protein nucleation can take place and crystal growth can occur. Initially, a pre-crystallization screen was conducted in order to optimize the protein concentration. All trays were kept at 4°C and checked daily by microscopy. 10 ml crystallization screens, tools and accessories were purchased from Molecular Dimensions.

2.4.18 Affinity purification of crude anti-sera

Preparation of the affinity column

Affinity purification of crude anti-sera was carried out using the AminoLink®Plus Coupling Gel kit (PIERCE Biotechnology). A column containing 3 ml AminoLink®Plus Coupling Gel was equilibrated with 3 column volumes of Coupling Buffer, pH 10. Purified protein (His-tagged Rad60) was diluted in a 1:3 ratio with coupling buffer, pH 10. The diluted protein sample (final concentration of 1-20 mg/ml) was added to the column. The column was sealed and mixed by gentle end-over-end rocking for 4 hours at 4°C. The column was then washed with 3 column volumes of Coupling Buffer, pH 7.2. 1 column volume of Coupling Buffer, pH 7.2 and 0.02 column volumes of cyanoborohydride solution was added to the column. The column was sealed and mixed overnight by gentle end-over-end rocking at 4°C. The column was allowed to drain and the flow through collected. Protein content was checked by Bradford assay to ensure

protein had been bound. To block the remaining active sites, the column was first washed with 2 column volumes of Quenching Buffer, and then 1 column volume of Quenching Buffer with 0.02 column volumes of cyanoborohydride solution. The column was sealed and mixed gently by end-over-end rocking for 30 minutes. The column was allowed to drain before being washed with 20 column volumes of Wash Solution. To check that the protein would not be immobilised in the elution step, the column was washed with 100 mM glycine, pH 2.3. The flow through was collected and the protein content determined by Bradford assay. To re-equilibrate, the column was washed with 10 column volumes of Quenching buffer followed by 10 volumes of Wash buffer. The column was then washed with 10 column volumes of PBS.

Affinity purification of crude antisera

6 ml crude anti-sera was diluted in one-tenth volume of 10x PBS and added to the column. The column was sealed and incubated at 4°C overnight on an end-over-end rocker. The column was drained and the flow-through collected. The column was then washed with 10 column volumes of PBS. Bound antibody was eluted with 1 column volume of 100 mM glycine, pH 2.3 and the flow through collected in 1 ml fractions. The antibody fractions were neutralised by adding 100 µl 1 M Tris-HCl, pH 7.5. The antibody concentration was analysed by Bradford assay and the purity checked by SDS-PAGE (Section 2.4.1).

2.4.18.3 Regenerating and storing the affinity column

Following elution with glycine, the column was washed extensively with PBS. PBS containing 0.05% sodium azide was added and the column sealed. The column was stored upright at 4°C for future use. To regenerate the column for affinity purification, the column was washed extensively with PBS, followed by 10 column volumes of Quenching buffer, 10 volumes of Wash buffer and 10 volumes of PBS. At this stage the column is ready for the anti-sera to be added.

Coupling Buffer, pH 10

0.1 M	sodium citrate
0.05 M	sodium carbonate

Solution adjusted to pH 10 and then filter sterilized

Coupling Buffer, pH 7.2

0.1 M	sodium phosphate
0.15 M	NaCl

Solution adjusted to pH 7.2 and then filter sterilized

Quenching Buffer

1 M	Tris-HCl
-----	----------

Solution adjusted to pH 7.4 and then filter sterilized.

Cyanoborohydride Solution

Supplied by PIERCE

Wash Solution:

1 M	NaCl
-----	------

2.4.19 Total Cell Extracts (TCAs)

S. pombe cells were grown in 10 ml appropriate medium overnight. 1×10^8 cells were harvested at 3,000 rpm for 5 minutes and washed in 1 ml 20% (w/v) trichloro-acetic acid (TCA). The cell pellet was re-suspended in 200 μ l 20% TCA, transferred to a screw cap ribolyser tube and an equal volume of glass beads was added. The cells were broken to ~ 50% lysis by ribolyzing for 3 x 15 seconds, with 1 minute intervals on ice. 400 μ l 5% (w/v) TCA was added and the bottom of the screw-capped tube was punctured with a hot needle. The cell extract was spun into a clean micro centrifuge tube at 3,000 rpm for 5 minutes. The extract was then spun for a further 5 minutes at 13,000 rpm. The supernatant was discarded and the pellet re-suspended in 200 μ l TCA sample buffer. The sample was then boiled and analysed by SDS-PAGE (Section 2.4.1).

TCA sample buffer

250 mM	Tris HCl, pH 8.0
5%	Glycerol
0.4%	SDS
2.9 mM	β -mercaptoethanol
2%	Bromothanol blue

2.4.20 *In vitro* sumoylation assay

An *in vitro* sumoylation assay as described previously (Ho, 2001) was used to test the sumoylation status of a protein *in vitro*. Typically, 2 μ l of translated protein was incubated with 2 μ l 10x *in vitro* assay buffer, 3 μ g Hus5, 0.5 μ g GST-Rad31/GST-Fub2, 0.12 U inorganic pyrophosphatase and 0.7 U creatine phosphokinase, with or without 10 μ g His-Pmt3. The reaction was made to a final volume of 20 μ l with dH₂O. The reactions incubated at 30°C for 2 hours and analysed by SDS-PAGE (Section 2.4.1).

10x *in vitro* assay buffer

500 mM	Tris-HCl, pH7.5
50 mM	MgCl ₂
50 mM	ATP
100 mM	creatine phosphate

2.4.21 *In vitro* GST-pull down assay

A 100 ml culture of a BL21 strain carrying the GST-expression construct of choice was grown at 37°C, with shaking until A₅₉₅ 0.6 was reached. Cells were then induced with 1 mM IPTG and grown for a further 3 hours at 37°C, with shaking. Cells were harvested at 5,000 rpm for 5 minutes at 4°C and the supernatant discarded. The cell pellet was re-suspended in 1 ml binding buffer freshly supplemented with a protease inhibitor cocktail tablet (Roche). The cells were sonicated on ice for 3 x 15 seconds with 1-

minute intervals on ice. The cell debris was cleared at 13,000 rpm for 3 minutes at 4°C. The supernatant was transferred to a new microcentrifuge tube. 20 µl of this supernatant was added to 180 µl binding buffer and incubated for 1 hour at 4°C with 30 µl glutathione-sepharose beads that had been pre-equilibrated in binding buffer. The beads were then harvested at 3,000 rpm for 5 seconds and washed twice with 1 ml binding buffer containing protease inhibitors. This 200 µl sample was then added to the pre-bound glutathione beads and incubated on a rotating wheel for 1 hour at 4°C. The beads were harvested at 3,000 rpm for 5 seconds and a 10 µl sample of the supernatant was taken (unbound fraction). The rest of the supernatant was discarded and the beads were washed for 15 minutes in wash buffer 1, followed by 15 minutes in wash buffer 2. The protein was eluted by boiling in 30 µl 5 x sample buffer (bound fraction). The input, unbound and bound fraction were analysed by SDS-PAGE (Section 2.4.1)

Binding Buffer

25 mM	HEPES, pH 7.8
150 mM	KCl
0.4 mM	EDTA
2 mM	EGTA
3 mM	MgCl ₂
8%	Glycerol
0.1%	NP-40
0.5 mM	PMSF
0.2 mM	DTT

Wash Buffer 1

25 mM	HEPES, pH 7.8
200 mM	KCl
0.4 mM	EDTA
2 mM	EGTA
3 mM	MgCl ₂
8%	Glycerol
0.1%	NP-40
0.5 mM	PMSF

0.2 mM	DTT
--------	-----

Wash buffer 2

25 mM	HEPES, pH 7.8
100 mM	KCl
0.4 mM	EDTA
2 mM	EGTA
3 mM	MgCl ₂
8%	Glycerol
0.1%	NP-40
0.5 mM	PMSF
0.2 mM	DTT

2.4.22 Identification of sumoylated lysine residues by tandem mass spectrometry

Protein mixtures from *in vitro* sumoylation assays (see section 2.4.20) were separated by SDS-PAGE. Bands corresponding to sumoylated species were excised and subjected to in-gel trypsin digestion (Gygi et al., 2000). Peptide fractions were loaded onto 75- μ m inner diameter fused silica with C18 resin columns and separated using a 35-min gradient from 2.5 to 97.4% CAN (Denison et al., 2005). Eluting peptides were loaded into an HPLC system coupled to a LTQ FT (Linear Ion Trap – LTQ combined with Fourier Transform Ion Cyclotron – FT) mass spectrometer (ThermoScientific) (LC-MS/MS) and full FT-MS scans (m/z range of 300 to 1,400) were acquired. Data were analyzed using the *S. pombe* NCBI database in conjunction with the MASCOT search algorithm (Perkins et al., 1999).

CHAPTER 3

ANALYSIS OF THE SUMO-LIKE DOMAINS AND PUTATIVE SUMO-BINDING MOTIFS OF RAD60

3.1 Introduction

The *S. pombe rad60* gene was first identified as a gene essential for cell viability that is involved in DNA double strand break repair (Morishita *et al.*, 2002). Later, the translation product, the Rad60 protein (fig. 3.1), was shown to have two homologues, Esc2 in *S. cerevisiae* and NIP45 in mammals. These three proteins, known as the RENi family of proteins, have two C-terminal SUMO-like domains (SLDs) closely related to SUMO-1 (Novatchkova *et al.*, 2005) (fig. 3.2). Moreover, at the N-terminal Rad60 has a S-X-S-D/E-D/E-D/E sequence that conforms with one type of SUMO interacting motif (SIM) (Minty *et al.*, 2000) and three hydrophobic regions with sequences of V/I-X-V/I-V/I and V/I-V/I-X-V/I that conform to a second type of SIM (Song *et al.*, 2004). It was proposed that these latter regions, named SUMO-binding motifs (SBMs), facilitate Rad60 self-association by interacting with the proposed SLDs and as a result are required for Rad60 function (Raffa *et al.*, 2006). Two of the three putative SBMs, SBM2 and SBM3, are within SLD1 and SLD2 respectively (fig. 3.1).

Hypomorphic mutations of *rad60*⁺ (represented on fig. 3.1) were identified in various studies: *rad60-1* (K263E) cells are defective in DSBs DNA repair, temperature sensitive for growth, defective in maintaining chromosome structure, elevated loss of a minichromosome, and epistatic with *rhp51^{Sp}/rad51^{Hs}* (Morishita *et al.*, 2002); *rad60-3* (F272V) cells are sensitive to DNA damaging agents (IR and UV) and hypersensitive to HU (Boddy *et al.*, 2003); *rad60-4* (T72A, I232S, Q250R, K312N) is sensitive to HU and is not phosphorylated in response to HU due to failed interaction with Cds1^{Sp}/Chk2^{Hs}, the Rad60 specific effector kinase (Boddy *et al.*, 2003).

In this study I began an *in vitro* functional and structural analysis of the proposed SLDs and SBMs and characterized the phenotypic consequences of mutating the SBMs. In

Fig. 3.1 Schematic representation of Rad60 protein

Highlighted are SUMO-Like Domains: SLD1 (blue) and SLD2 (red); putative SUMO-Binding Motifs: SBM1, SBM2 and SBM3 (green), N-terminal *SXS* motif. Characterized hypomorphic mutations are depicted (★). The C/C (in blue) represents a coil/coil domain.

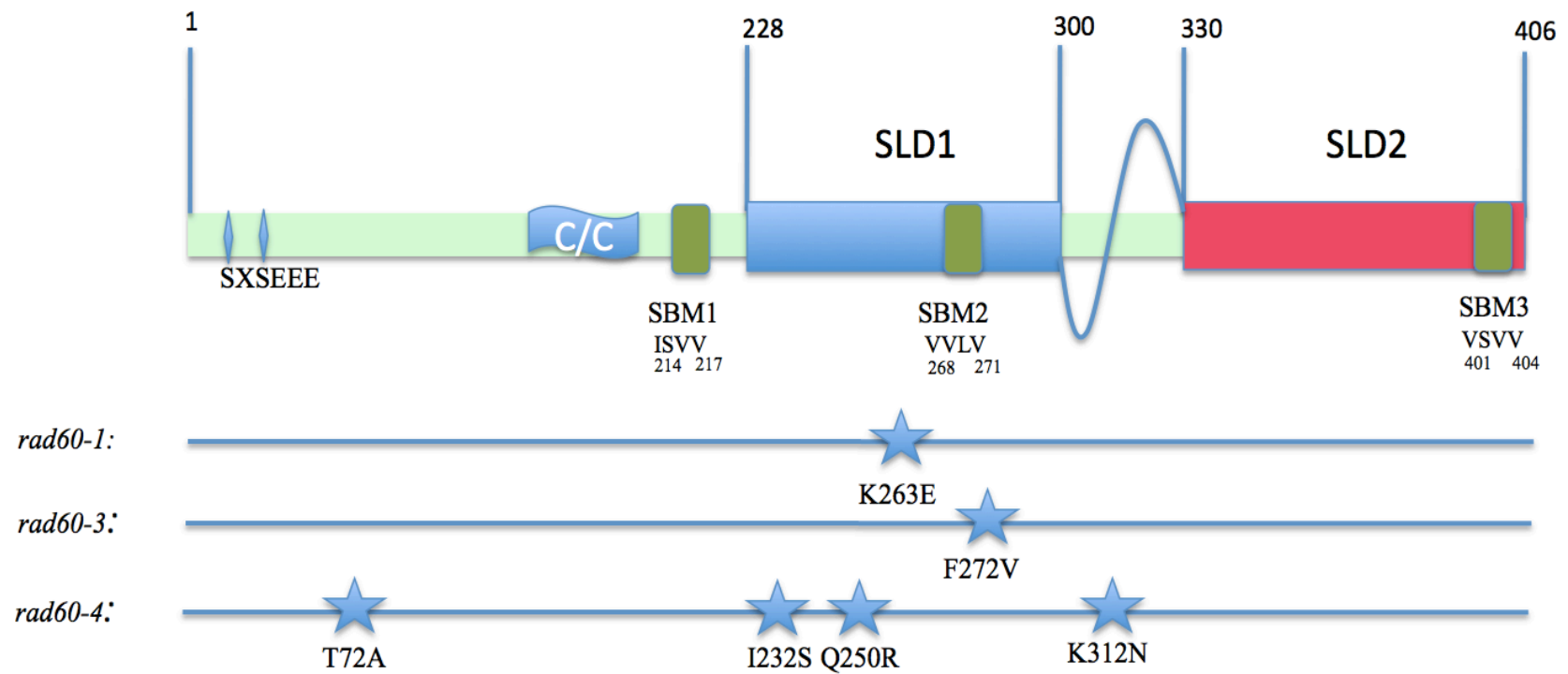


Fig. 3.1 Schematic representation of Rad60 protein

Rad60	1	-----MDNLDEDDLAFFSKPIKPPLN--YAKQLIASSSSEEESELDINKQAL
Esc2	1	MTGTSRSISEPSINLLDPTNISESDENSDDFFMDNSHDIDEIDHSDESNRQSVIVDSKVTV
NIP45	1	-MAEPVGKRGWSSGGSGAGRGGRGGWGCGRRPRAQRSPSRGTLDPVVSVDLVDSDEEIL

Rad60	48	EHINAQKNITHNENKSAEPLSRSTILDADEGNQDVSDTTNACLNEGRHSPKSAISCVT
Esc2	61	PPSKHSTLTLSDESDAKECHQSLSRSSSKNVNIEDITEPKPDKPSGRTRGRSVMKESV
NIP45	60	EVATARGAADEVEVEPEEPGPVVASRDNSNSDSEGEDRRPAGPPREPVRRRRRVLDPGE

Rad60	108	QPVS-----PVYNTRAAANLRNNSIN-----SEAALSTSSLLDDDFARLEE
Esc2	121	VEINSSSDLDDEDKNFPRSRSRSSIRSSIPAGKYKROKSSLLTYDENDDEKELAKE
NIP45	120	APLV-----PVYSGRVKSSLRDIPDD-----LSLLKLYPPGDEEAEALADS

Rad60	151	IDRQVQEFEKSSSDMDVCIHTHKREIEE-----DDNTSADVPLLKHSKSDHSTLYHSKSE
Esc2	181	AKSTTISKESIPDQKRKYNIKFLSKLGTINKAVQVKVLGKYERSKILEAALDGLMKS
NIP45	161	SGLYHEGSPSPGSPWKTKLRTDKKEKKK-----TEFLDLDNSPLSPSPSRKSRTH-

Rad60	207	FST-----NEPVISVVLQAVIGQRTPNSNISLFRDWEAPL-----FFKVKSNQQFRR
Esc2	241	YKIPKVMKDIYKVENVTLYWNNAKLLTFMTCNLSLHIPQDFENEVSTIDVTIVSKEYEKNF
NIP45	214	-----RAKKLSEVVKRLQDLRSCLSPKEPQGQEQGQEDVVLVEGPTLPET

SLD1

Rad60	255	VRLAYSERKK-VDNVVLVFQNCRIWDYGTGKGAGMKVDTRLVVAHACHSDFISLKR---
Esc2	301	EATLESKLKE-DEAALLKEROEMERKLEKKRNEQEESEYREFESELKNVEEIQEIKEND
NIP45	262	PRFFPIKIRCRADLVRLPLRMSEPLQSVVDHMAHIGVSPSRILLGETELSPATPRT

Rad60	311	-IKELVEKLSVIEDSTACTCKLITLLRSSKSE---DLRLSPVLEFTVKDLKRYCTE
Esc2	360	TVNNTKLIOEGGSLSGNSSSMEEVMRTALMGQDNK---KIYVHVRSTPFPSKIAEYYRIQ
NIP45	322	LKUGVADIIICVVLTSPEATETTSQQLCLRVQGREKHQOTLEVSLSRDSPLKTLKSHYEEA

SLD2

Rad60	367	VKLSFHERIRPEFEGEWLDENIQVQSTEEDEDEQVSVVLD
Esc2	417	KQLPQKTRVKLLFDHDELDMECIADQMEDEDMVDVLIID
NIP45	382	MGLSGRK-LSFFFDGTKLSGRELPADLGMESGDLIEVWG-

Fig. 3.2 Sequence alignment of RENi family proteins

Alignment created with *ClustalW* and highlighting of conserved (■) and semi-conserved (◼) residues created with *BoxShade* on-line software .

order to obtain a true 3D structure of the SLDs and SBMs, crystallographic studies were considered for the full length Rad60 (Rad60_FL).

3.2 Structural characterization of Rad60

3.2.1 Expression and purification of full length Rad60

Rad60_FL was first expressed as a His tag fusion protein as the small His tag does not require removal prior to crystallographic trials. The expression was performed with various concentrations of IPTG (0.1 – 1 mM) and the His-Rad60_FL was purified at 4 °C using Co²⁺ beads (fig. 3.3 A). The Coomassie stain of the elutions showed a large number of degradation products suggesting that the protein is not very stable under the purification conditions. Successful crystallization requires high purity protein in a homogeneous, monodisperse state. To further analyze the suitability of the recombinant His-Rad60_FL for crystallography, Dynamic Light Scattering (DLS) was used to assess the polydispersity of the sample and the presence of protein aggregates that might interfere with the crystallization process. The results indicated that the sample was polydisperse and therefore unsuitable for crystallography (fig. 3.3B).

Another possibility was to express and purify the Rad60_FL with a GST tag as sometimes the large GST tag (~26 kDa) stabilizes proteins in solution but requires thrombin cleavage prior to crystallography trials. Unfortunately, GST-Rad60_FL degraded into smaller fragments as well, making it unsuitable for crystallographic studies (fig. 3.4).

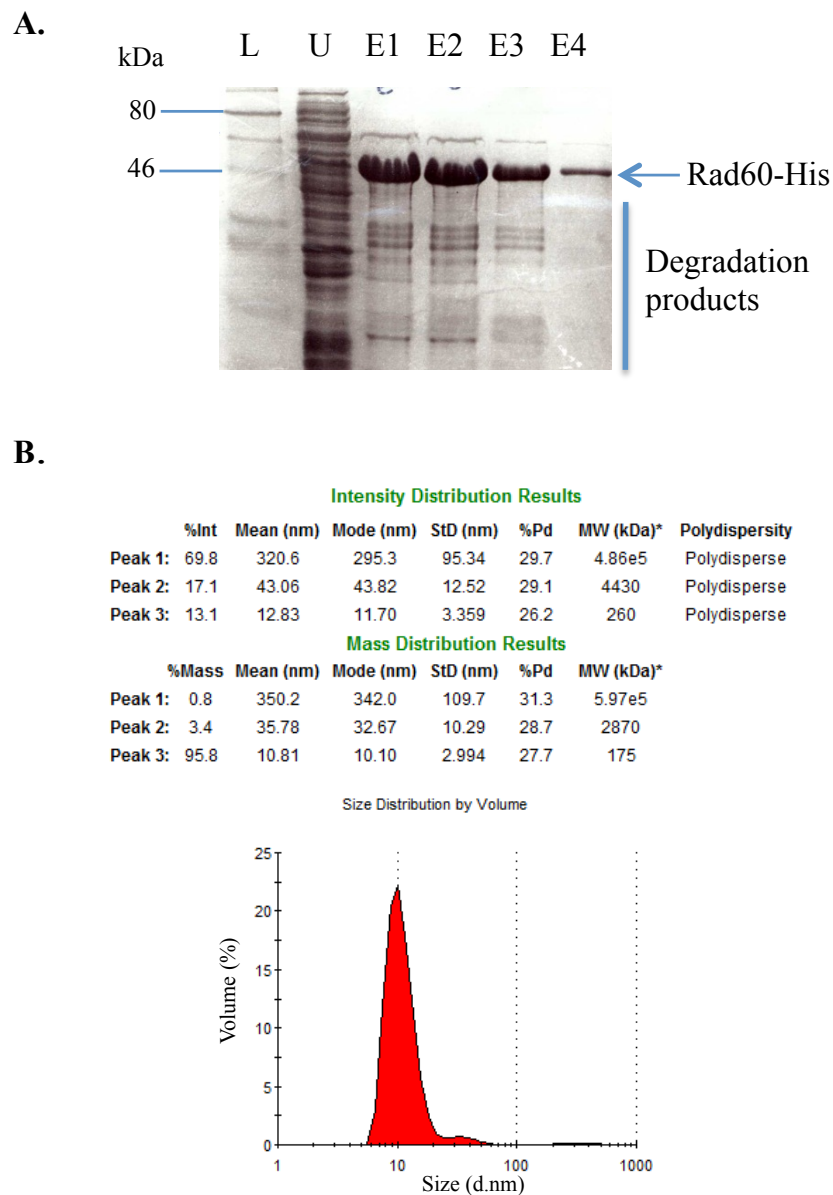


Fig. 3.3 Purification and stability studies of His tagged Rad60_FL

A) SDS PAGE of purified full length Rad60 – His
 L = ladder; U = cell extract unbound to column; E = elution

B) Dynamic Light Scattering tabulated data and spectrum showing polydispersity and average particle size respectively

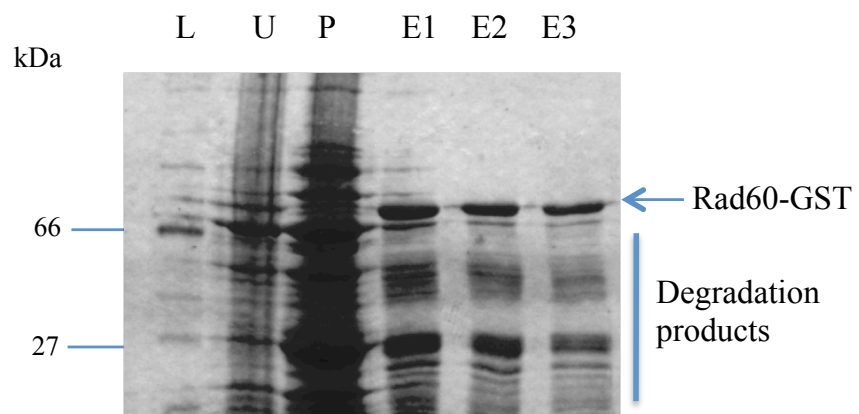


Fig. 3.4 Purification of GST tagged Rad60_FL

A) SDS PAGE of purified full length Rad60 – GST

L = ladder; U = cell extract unbound to column; E = elution

3.2.2 Residues essential for β -GRASP fold are conserved in SLD1 and SLD2

An initial search for proteins homologous to Rad60 only revealed a match between SLD2 and the ubiquitin-2 motif (Morishita *et. al.*, 2002). The ClustalW sequence alignment of both SLDs against SUMO-1 (fig. 3.5 A) revealed an identity of 19.7% for SLD1 and 23.4% for SLD2. Further, the β -GRASP fold ($\beta\beta\alpha\beta\beta\alpha\beta$) shared by SUMO and ubiquitin can be modeled onto both SLDs using the on-line Phyre modelling software (Bennett-Lovsey *et al.*, 2008). The electrostatic surfaces were determined using Pymol software (Liang *et al.*, 2003), with the surface of SLD1 being positively charged, like ubiquitin, while that of SLD2 is negatively charged like SUMO (fig. 3.5 B)

The sequence alignment of SLD1, SLD2 and SUMO-1 shows that residues essential for the β -GRASP fold of SUMO-1, referred to as 'Bayer residues' (Bayer *et al.*, 1998), are conserved/semi-conserved in the SLDs (fig. 3.6). To assess the *in silico* data, expression and purification of recombinant SLD proteins was carried out (L. Boyd, PhD thesis, University of Sussex). The SLD1 domain could not be expressed, while SLD2 was successfully expressed and purified with a His tag (fig. 3.7). Mutagenesis was carried out on the wild-type SLD2 construct (L. Boyd, PhD thesis, University of Sussex) to determine if residues required for the β -GRASP fold are essential for the SLD2 structure. Eight single mutations of key residues at the hydrophobic core of SLD2 matching residues essential for the β -GRASP fold of SUMO-1 (I334G, L336G, L338G, L346G, L348G, I350G, L359G, Y363G) were created in order to determine whether these residues were important for the structure of SLD2. Five of the single mutations, when introduced into the *S. pombe* genome, resulted in unviable cells (L336G, L346G, I350G, L359G, Y363G) while the other three (I334G, L338G, L348G) gave viable but sick cells (L. Boyd, PhD thesis, University of Sussex).

In order to analyse the effect of these mutations on the domain, recombinant proteins for the viable mutants were expressed with a His tag under the conditions that SLD2 wild type was expressed. However they were insoluble under these conditions suggesting that the mutant proteins may be incorrectly folded. Since the pH, salt concentration and the type of buffer heavily influence proteins solubility, new buffers were designed using

Fig. 3.5 SLD1 and SLD2 can be modelled onto *H. sapiens* SUMO-1 structure

- A) ClustalW sequence alignment of SLD1 and SLD2 against *H.sapiens* SUMO-1 (NCIB accession number AAC50996). Highlighted in black are conserved residues and in gray are semi-conserved residues.
- B) Modelling of SLD1 (blue) and SLD2 (red) onto SUMO-1 structure (*pdb: 2uyz*) using *PHYRE* software (Bennett-Lovsey et al., 2008) . On the left: representation of the secondary syructures; on the right: representation of the surface electrostatics, using *PYMOL* software

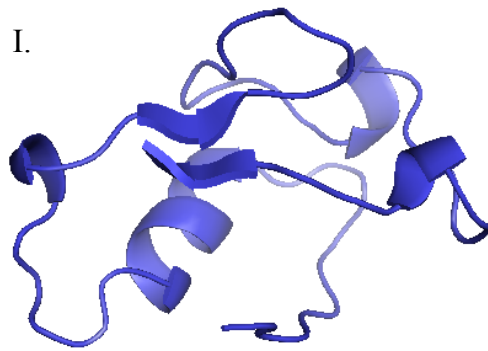
A.

SUMO-1	1	*MSDQEAKPSTEDLGDKKEGEYIKLKVIGQDSSEIHFKVKMTTHIKKLKESYC-QRQGVEM
SLD1	228	-----NSNISLPDWEAPLEFKVKSNNQFRRVPIAMS-ERK--KV
SLD2	330	-----TCKLITILLRSSKSEDLRLSIPVDFTVKDLIKRYCTEVKISFH

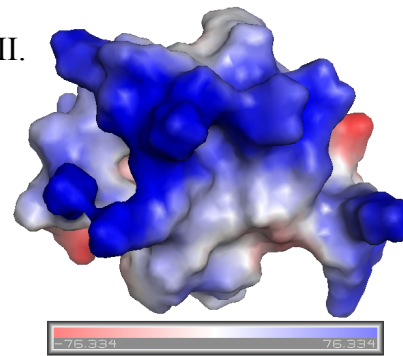
SUMO-1	60	NSLRLEFEGQRITADNHTPKELGMEEDVIEVYQQTGGHSTV
SLD1	266	INVLVLFQNRRLNDYGTPTKGAGMLKVITRIVVHAY-----
SLD2	374	IRIRLEFEGEWLDPNQVQSTLEDEDQVSVVLT-----

B.

I.



II.



III.



IV.

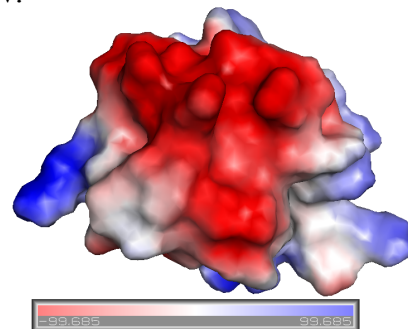


Fig. 3.5 SLD1 and SLD2 can be modeled onto *H. sapiens* SUMO-1 structure

Fig. 3.6 Essential structural residues of SUMO-1 are conserved in SLD1 and SLD2

- A) Essential structural residues of SUMO-1 (Bayer residues) highlighted on the sequence alignment of SUMO-1, SLD1 and SLD2. Conserved, semi-conserved Bayer residues tabulated below

- B) Cartoon representation of Bayer residues and their interactions (green) on the structure of SUMO-1(pdb:1A5R) and the models of SLD2 and SLD1, created using PYMOL software

A.

```

SUMO-1  1  MSDQEAKPSTEDLGDKKEGEYIRKIKVIGQDSSEIHFKVKMTTHIKKLIKESYC-QRQGVPM
SLD1    1  -----NSNLSIPRDWEAPLFEKVKSNQQFRRVFIAYS-ERK--KV
SLD2    1  -----TCKLITLLIRSSKSEDLRLSIPVDFTVKDLIKRYCTEVKISFH
          ★★ ★      ★★ ★      ★ ★
SUMO-1  60  NSLRFLFEGQRADNHTPKELGMEEDVIEVYQEQTGGHSTV
SLD1    38  INVVLVFQNRLEWLYGTPKGAGMLKVDTRLVVHAY-----
SLD2    44  ERIRLEFEGEWLDPNDQVQSTELDEDQVSVVLD-----
  
```

SUMO-1	SLD1	SLD2
I22	S230	I334
L24	I232	L336
V26	L234	L338
I34	L242	L346
F36	F244	L348
V38	V246	I350
L47	V255	L359
Y51	Y259	Y363

B.

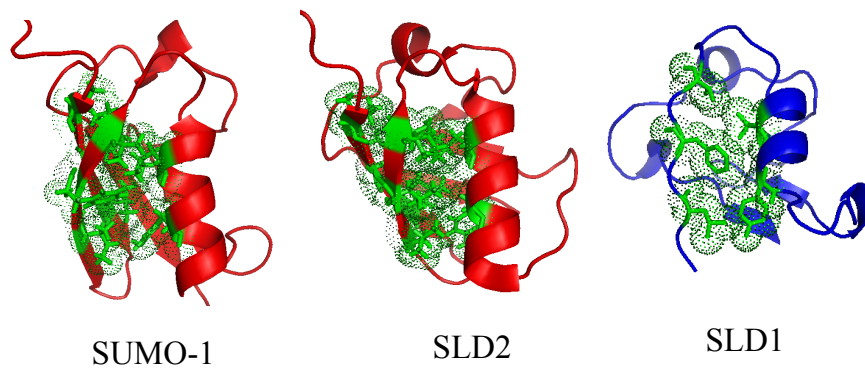


Fig. 3.6 Essential structural residues of SUMO-1 are conserved in SLD1 and SLD2

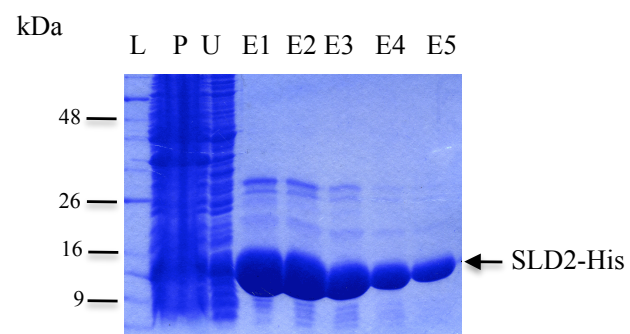


Fig. 3.7 Purification of His-tagged SLD2

Coomassie stain of purified SLD2-His; L = ladder; U = cell extract unbound to column; E = elution

sodium acetate, HEPES and Tris with various concentrations of sodium chloride (0, 0.1, 0.2, 0.3, 0.4, and 0.5 M) and at different pH (5.5, 7.5 and 8.5). All three mutant proteins were insoluble in all conditions (fig. 3.8, not all data shown). These results suggest that ‘Bayer’ residues are required for the structure of SLD2, further confirming the hypothesis that SLD2 adopts a β -GRASP fold like SUMO-1.

3.3 SLD2 interacts with the SUMO conjugator *in vitro*

The phenotypic similarities of *rad60* mutants, including those within the SLD2 domain, to mutants defective in the sumoylation pathway (L. Boyd, PhD thesis, University of Sussex) suggest a functional overlap, with Rad60 as an important SUMO pathway component. Moreover, the residues involved in the non-covalent interaction of SUMO-1 with the SUMO conjugating enzyme, Ubc9^{SpHus5}, (Capili and Lima, 2007) are conserved in SLD2 but not SLD1 (fig. 3.9). To assess the interaction between SLD2 and Hus5 an *in vitro* analysis was carried out. A GST pull-down assay was carried out with recombinant His-SLD2 and GST-Hus5 (fig. 3.10). To check that SLD2 does not interact with the GST tag a pull down assay of SLD2 with GST only was carried out in parallel as a negative control. GST, GST-Hus5 and His-SLD2 were expressed and purified as described (see section 2.4) and loaded as inputs. SLD2-His was added to mixtures of GST and Hus5-GST with glutathione sepharose beads and incubated for 1 hour at 4°C. After centrifugation the supernatant was kept for SDS-PAGE as the unbound fraction (U) and the beads, after washing, were treated with elution buffer to extract the bounded fractions (B).

SLD2 interacts with Hus5 *in vitro*, as it is present in the bound fraction of GST-Hus5 + SLD2 (lane 5) but not in that of GST + His-SLD2 (lane 4). This positive interaction further implies that SLD2 structurally and functionally resembles SUMO. The interaction between SLD2 and Hus5 was later confirmed *in vivo* by *S. pombe* extract precipitation of GST-Rad60 or SLD2 with TAP-Hus5 (Prudden et al., 2009). Using the same method, Prudden *et. al.* also showed that SLD1 interacts with the sumoylation enzymes Fub2, (part of the activating enzyme E1), a Pli1 (an E3 ligase), and with the STUbL complex component Slx8.

Fig. 3.8 Solubility trials of SLD2 mutants

- A) SDS-PAGE of the pellet and the supernatant of an *E. coli* culture expressing SLD2 wild type lysed in the binding buffer for Ni²⁺ purification
- B) SDS-PAGE of pellets and supernatants of *E. coli* cultures expressing SLD2-I334G mutant lysed in NaAc, Tris and HEPES buffers, pH 5.5, 0.2M NaCl
- C) SDS-PAGE of pellets and supernatants of *E. coli* cultures expressing SLD2-L338G mutant lysed in NaAc, Tris and HEPES buffers, pH 7.5, 0.3M NaCl
- D) SDS-PAGE of pellets and supernatants of *E. coli* cultures expressing SLD2-L348G mutant lysed in NaAc, Tris and HEPES buffers, pH 8.5, 0.4M NaCl

L = ladder; P = pellet; SN = supernatant

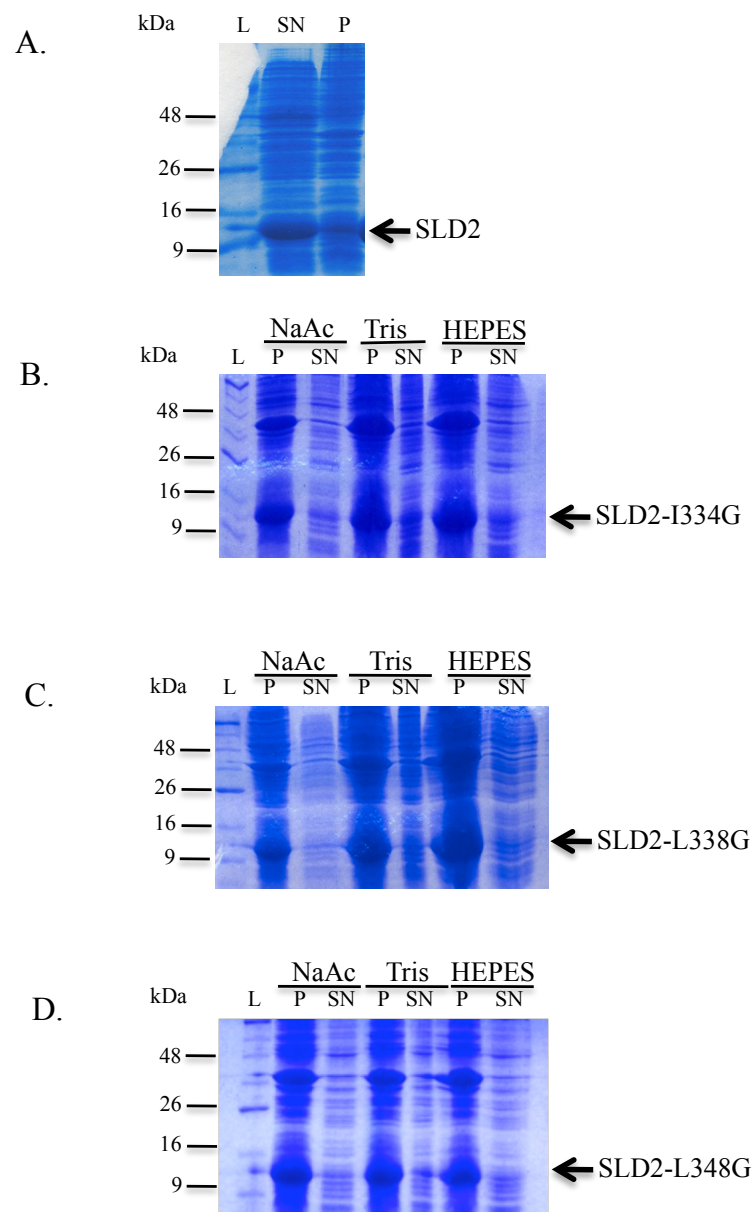


Fig. 3.8 Solubility trials of SLD2 mutants

A.

SUMO-1	1	MSDQEAKPSTEDLGDKKEGEYIKLRKVIQDSSSEIHFKVKMTTHLKKLKESYC-CRQGVPM
SLD1	1	-----NSNLSIPRDWEAPLEFKVKSNNQQRFRVRIAYS-ERK--KV
SLD2	1	-----TCKLITLLLRSSKSEDLRLSLPVDFTVKDLIKRYCTEVKISFH

SUMO-1	60	NSLRFLFEGQRADNHTPKELGMEEDVLEVYQEQTGGHSTV
SLD1	38	INVVLVEQNQLWDYGTGPKGAGMLKVDTRLVVHAY-----
SLD2	44	ERIRLEFEGEWLDENDQVQSTELEDEDQSVVLD-----

B.

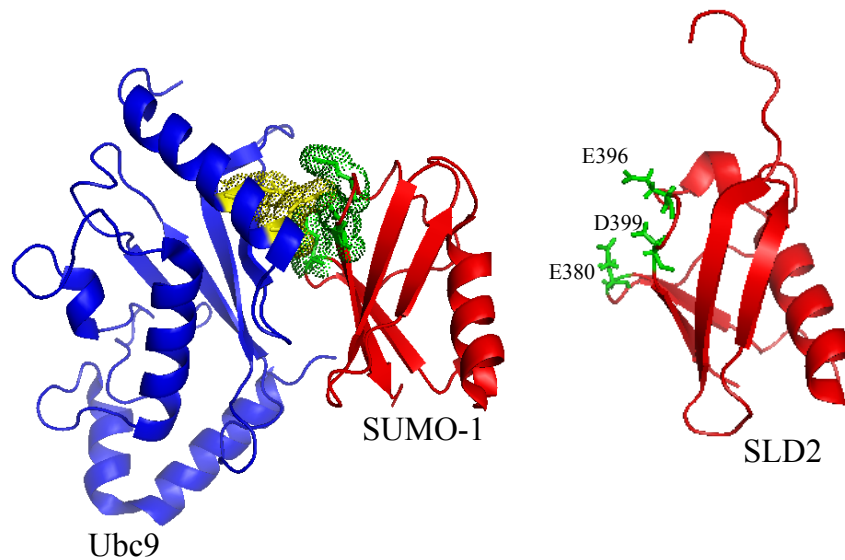


Fig. 3.9 Residues of SUMO-1 required for non-covalent interaction with Ubc9 are conserved in SLD2

A) Sequence alignment of SUMO-1, SLD1 and SLD2. Highlighted (★) are residues required for non-covalent interaction with Ubc9.

B) Cartoon representation of the non-covalent interaction between SUMO-1 and Ubc9 based on the crystal structure of the complex (pdb id 2PE6; left) and the conserved residues highlighted on the SLD2 structure (pdb id 3GOE; right)

Fig. 3.10 SLD2 interacts with Hus5 *in vitro*

GST pull-down assay was carried out with recombinant GST, His-SLD2 and GST-Hus5.

Pull down assay of SLD2 with GST only was carried out in parallel as a negative control (lanes 1 – 4).

GST and GST-Hus5 are represented as loads L (lanes 1 and 8) and His-SLD2 is represented as input I (lanes 2 and 7).

Supernatants resulting after incubation with glutathione sepharose beads are represented as unbound fractions U (lanes 3 and 6).

The fractions eluted from glutathione sepharose beads are represented as bound fractions B (lanes 4 and 5)

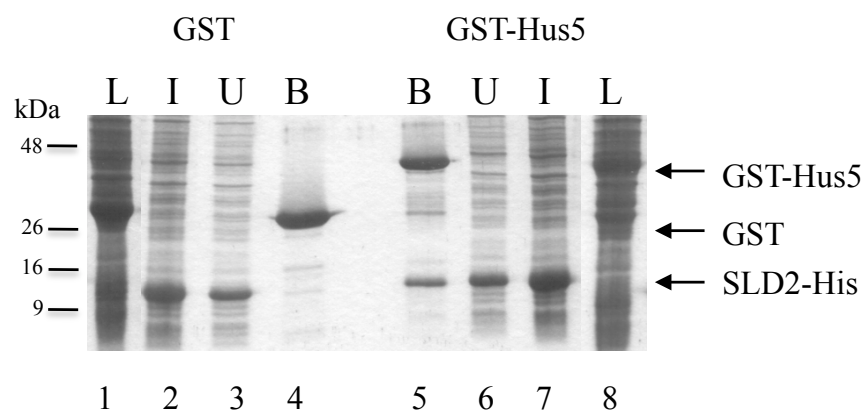


Fig. 3.10 SLD2 interacts with Hus5 *in vitro*

SDS-PAGE of *in vitro* GST pull-down assay of GST and GST-Hus5 with SLD2-His.

L = load; I = input; U = unbound; B = bound

3.4 Analysis of putative SBMs

Apart from the SUMO-like domains and the N-terminal SXS motif, Rad60 contains three hydrophobic regions that correspond to amino acid sequences of SIMs, V/I-V/I-X-V/I or V/I-X-V/I-V/I (see section 1.4.6). It has been proposed that these regions, named SUMO-binding motifs (SBMs), facilitate the homodimerization of Rad60 (Raffa GD et al., 2006). These putative SBMs are located near or within SLD1 (SBM1 and SBM2 respectively) and at the C-terminal of Rad60, within the SLD2 domain (SBM3) (fig. 3.1). Pull-down assays and phenotypic characterization of key mutants were employed to investigate whether these putative SBMs can indeed function as SIMs and, if so, whether they are essential for Rad60 functions by facilitating its homodimerization.

3.4.1 Putative SBMs do not facilitate Rad60 dimerization *in vitro*

To determine whether putative SBMs facilitate Rad60 homodimerization, *in vitro* GST pull-down assays were carried out with Rad60FL, Rad60CT (deleted for SLD2) and SLD2. Recombinant His-Rad60FL, GST-Rad60FL, His-Rad60CT, GST-Rad60CT, His-SLD2 and GST-SLD2 were expressed in *E. coli* and purified as previously described (see sections 2.4.8 and 2.4.9; DNA constructs made by Dr. F.Z.Watts, University of Sussex). Pull-down assays of GST only and the His tagged components were carried out in parallel as negative controls. Firstly, to see if Rad60 homodimerises *in vitro*, the pull down of His-Rad60FL was carried out with GST-Rad60FL. This showed an interaction between the two proteins (fig. 3.11 A, lane 5) confirming previous results obtained from assays carried out on *S. pombe* whole cell extract (Raffa et al., 2006) and was used as a positive control for further pull downs of Rad60FL. If SBMs facilitate Rad60 dimerization by interacting with the SLDs then any fragment of Rad60 that contains an SBM should interact with fragments of Rad60 that contain an SLD, ie Rad60FL should interact with Rad60CT (fig. 3.11 B) and SLD2 (fig. 3.11 C). However, no interactions were observed between Rad60FL and Rad60CT (fig 3.11 B, lane 5) or SLD2 (fig. 3.11 C, lane 5) under the conditions that Rad60FL homodimerizes. Further pull-down assays of GST-Rad60CT with His-Rad60CT (fig.

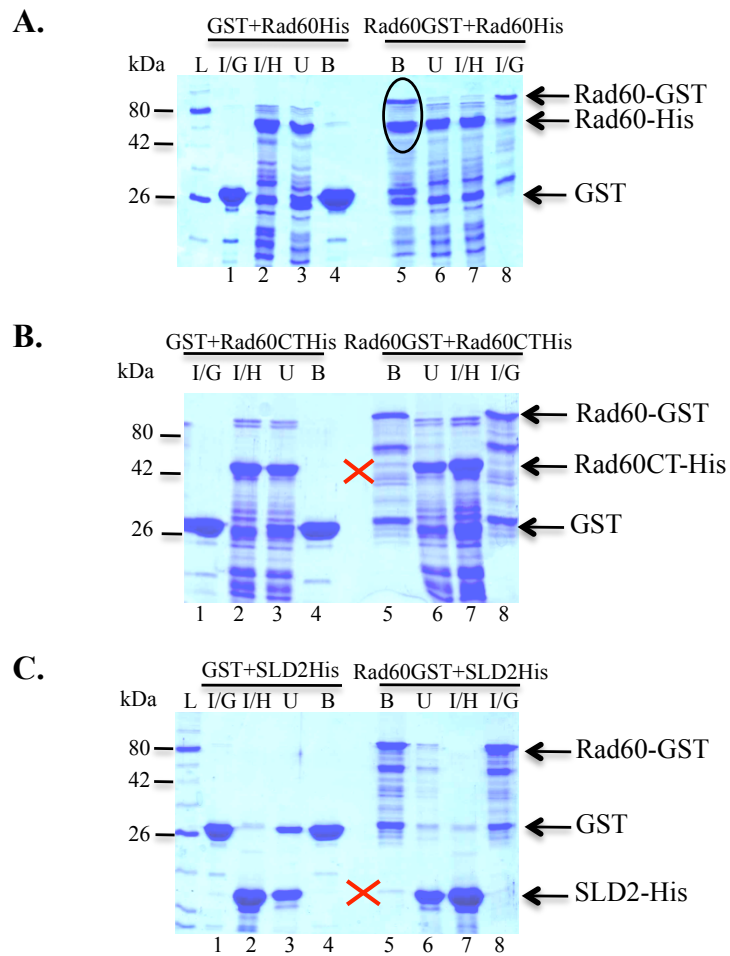


Fig. 3.11 Rad60 does not interact with Rad60CT or SLD2 *in vitro*

- A) SDS-PAGE of *in vitro* GST pull-down assay of GST tagged Rad60FL and His tagged Rad60FL
- B) SDS-PAGE of *in vitro* GST pull-down assay of GST tagged Rad60FL and His tagged Rad60CT
- C) SDS-PAGE of *in vitro* GST pull-down assay of GST tagged Rad60FL and His tagged SLD2

L=ladder; I/G=input GST component; I/H=input His component; U=unbound; B=bound; oval highlights interaction; red cross highlights lack of interaction

3.12 A) and His-SLD2 (fig. 3.12 B), and GST-SLD2 with His-SLD2 (fig. 3.12 C) showed no positive interactions. These data suggest that Rad60 homodimerization does not occur through interactions between SLDs and putative SBMs or/and that full-length protein is required for dimerization.

3.4.2 Putative SBMs do not interact with SUMO *in vitro*

Having determined that the putative SBMs do not facilitate Rad60 homodimerization *in vitro*, the question remained as to whether these hydrophobic regions with sequence homology with SIMs can interact with free SUMO *in vitro*. GST pull-down assays of Rad60FL and SLD2 were carried out with recombinant Pmt3 protein (*S. pombe* SUMO homologue). As the non-covalent interaction between the SUMO conjugating enzyme and SUMO has been recognized (Capili and Lima, 2007, Liu et al., 1999), the *in vitro* pull-down of GST-Hus5 and His-Pmt3 was used as positive control (fig. 3.13 A). Pull-down assays of GST-Rad60FL (fig. 3.13 B) and GST-SLD2 (fig. 3.13 C) with His-SUMO showed no interaction, further suggesting that these putative SBMs do not function as SIMs. To assess the *in vitro* data, *in vivo* analysis of SBMs mutants was carried out.

3.4.3 Effect of mutating putative SBMs

If SBM2 and SBM3 are important functional elements of SLD1 and SLD2 respectively, then mutating them should result in phenotypes similar to those seen in *rad60-SLD1Δ* and *rad60-SLD2Δ* mutants, *i.e.* lethality and sensitivity to DNA damaging agents respectively. Mutations of SBM1, SBM2 and SBM3, where two valine residues of each SBM were replaced with alanine to obtain *rad60-SBM1*, *rad60-SBM2* and *rad60-SBM3* strains (fig. 3.14 A; all strains created by Dr. F.Z.Watts) resulted in viable cells. This indicates that at least SBM2 is not involved in the essential function of SLD1. Interestingly *rad60-SBM3* is slow growing at 36°, suggesting that SBM3 is important for the SLD2 structure. Phenotypic analysis of the SBMs mutants revealed that *rad60-SBM1* and *rad60-SBM2* are not sensitive to HU, MMS or UV, while *rad60-SBM3*

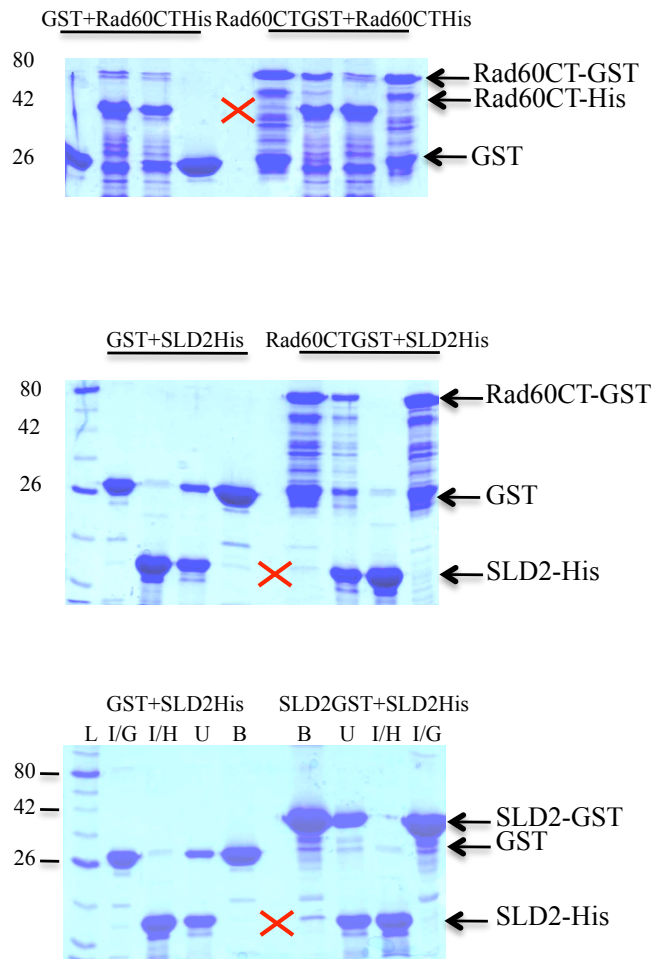


Fig. 3.12 *In vitro* GST pull down assays of Rad60 fragments

- A) SDS-PAGE of *in vitro* GST pull-down assay of GST tagged Rad60CT and His tagged Rad60CT
- B) SDS-PAGE of *in vitro* GST pull-down assay of GST tagged Rad60CT and His tagged SLD2
- C) SDS-PAGE of *in vitro* GST pull-down assay of GST tagged SLD2 and His tagged SLD2

L=ladder; I/G=input GST component; I/H=input His component;
 U=unbound; B=bound; red cross highlights lack of interaction

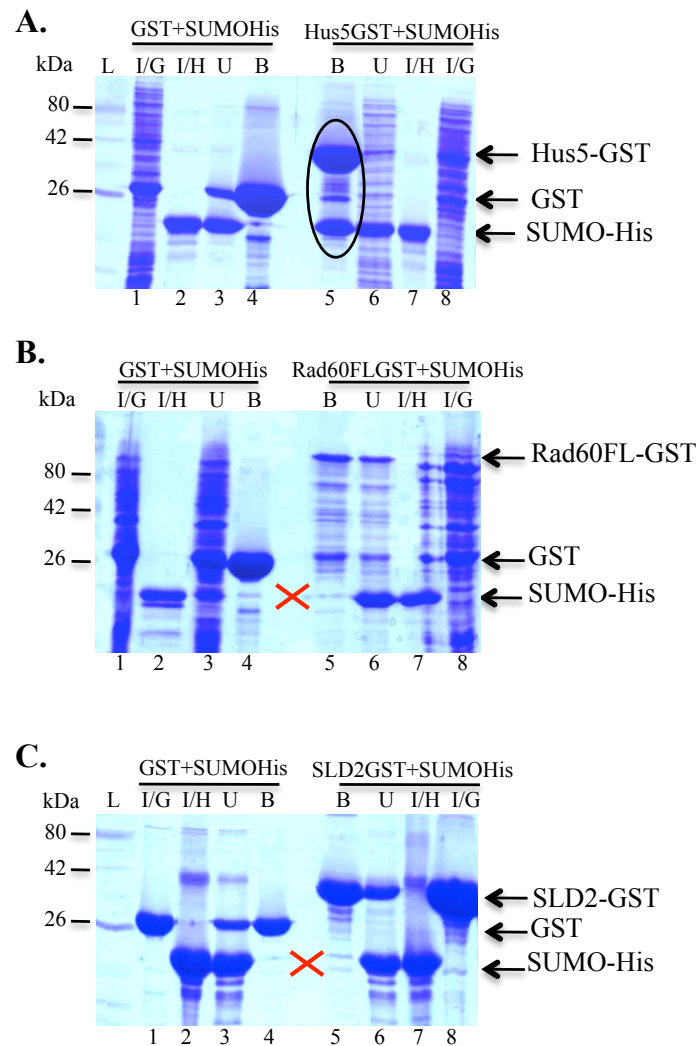


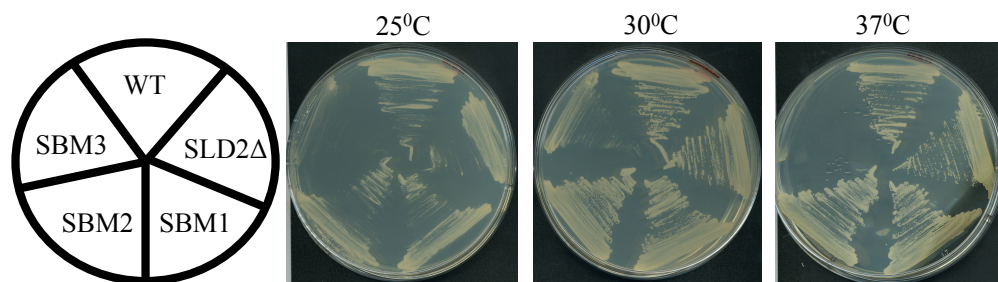
Fig. 3.13 Rad60 and SLD2 do not interact with SUMO *in vitro*

- A) SDS-PAGE of *in vitro* GST pull-down assay of GST tagged Hus5 and His tagged SUMO
- B) SDS-PAGE of *in vitro* GST pull-down assay of GST tagged Rad60FL and His tagged SUMO
- C) SDS-PAGE of *in vitro* GST pull-down assay of GST tagged SLD2 and His tagged SUMO

L=ladder; I/G=input GST component; I/H=input His component; U=unbound; B=bound; oval highlights interaction; red cross highlights lack of interaction

A.

Strain	SBM1	SBM2	SBM3
wild type	ISVV	VVLV	VSVVLD
mutant	ISAA	VALA	ASAVLD



B.

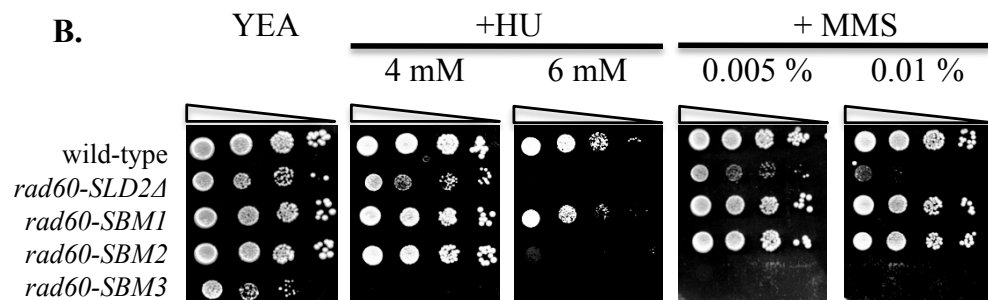



Fig. 3.14 Effect of mutating the three putative Rad60-SBMs

- A) Table of SBMs mutants and their response to permissive and restrictive temperatures. Strains were streaked onto YEA and incubated at the indicated temperatures for 5 days.
- B) Phenotypic analysis of SBMs mutants and SLD2Δ in response to HU and MMS.  represents 10 folds reductions in number of cells plated.

displayed a phenotype more severe than that of *rad60-SLD2A* (fig. 3.14 B). This result was intriguing as SBM3 is within the SLD2 and, given the temperature sensitivity as well, further tests were carried out to identify the structural and/or functional importance of SBM3.

3.5 Putative SBM3 is essential to maintain SLD2 structure

SUMO-1, like SLD2, has an amino acid sequence at the C-terminal that conforms with a SIM (V/I-V/I-x-V/I) (fig. 3.15 A). The crystal structure of SUMO-1 (pdb id: 1A5R) shows that this region forms the β 5 sheet of the β -GRASP fold of SUMO-1 (fig. 3.15 B). The fact that SLD2 adopts the same structure as SUMO-1 suggests that the SBM3 may be required for maintaining the β -GRASP fold of SLD2. To assess this the purification of a His-tagged SLD2_SBM3 mutant was conducted under the same purification conditions as His-tagged SLD2 wild type. Interestingly, while the mutant was soluble in the lysis buffer, the elution of the mutant showed a different pattern compared to that of wild type SLD2, exhibiting high molecular mass species (fig. 3.16 A). The elute fractions of the wild type and mutant SLD2 were run on a Superdex 75 10/300 gel filtration column and the fractions corresponding to observed peaks were checked by SDS PAGE (fig. 3.16 B). Consistent with the previous results, the majority of the mutant eluted earlier off the Superdex 75 10/300 column than the wild type. These fractions correspond to significantly higher molecular weight soluble aggregates. To confirm these results the fractions from the gel filtration were analysed by DLS. The spectrum of the wild type protein shows a peak at approximately 4 nm for the hydrodynamic radius while the mutant spectrum shows a peak at approximately 10 nm (fig. 3.16 C), a difference corresponding to a 16 times increase in volume, further suggesting that the SLD2-SBM3 mutant forms soluble aggregates.

Mapping the putative SBM3 onto the crystal structure of SLD2 shows that, as in SUMO-1, this region forms the β 5 sheet of the β -GRASP fold of SLD2 (fig. 3.17 A). Guanidine hydrochloride induced denaturation of SLD2 was used to measure the change in the stability of the SBM3 mutant relative to that of the wild type. The free energy of the unfolding (ΔG_{U-F}) of wild type SLD2 was calculated from the normalized GuHCl induced denaturation curve (fig. 3.17 B) to be 6.2 kcal/mol (experiments and

A.

SUMO-1	1	MSDQEA	PKSTED	LGDKKE	GEYIK	IKVIGQ	DSSEI	HF	KKMT	THL	KKL	KES	YCQR	QGW	PMN
SLD2	1	-----	CKLIT	LLIR	SSKS	EDLR	LSI	PVDF	TVK	DLIK	RYC	TEVK	ISFH		

SUMO-1	61	S-	LRFI	FEGQR	IADN	HTPK	ELG	MEED	VLEV	YQE	QTGG	HSTV
SLD2	43	ERIR	LEFEG	EWDP	NQVQ	STEL	EDQ	VS	VLD	-----		

B.

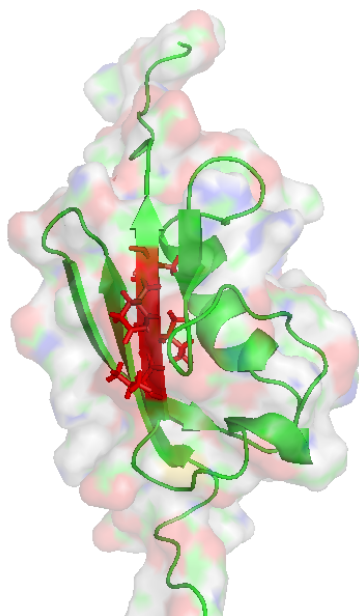


Fig. 3.15 SUMO-1 has a sequence consistent with a SIM at the C-terminal

- A) Sequence alignment of SUMO-1 and SLD2. Highlighted in red are the sequences consistent with SIMs
- B) Representation of amino acids that form the β 5 sheet of the SUMO-1 structure

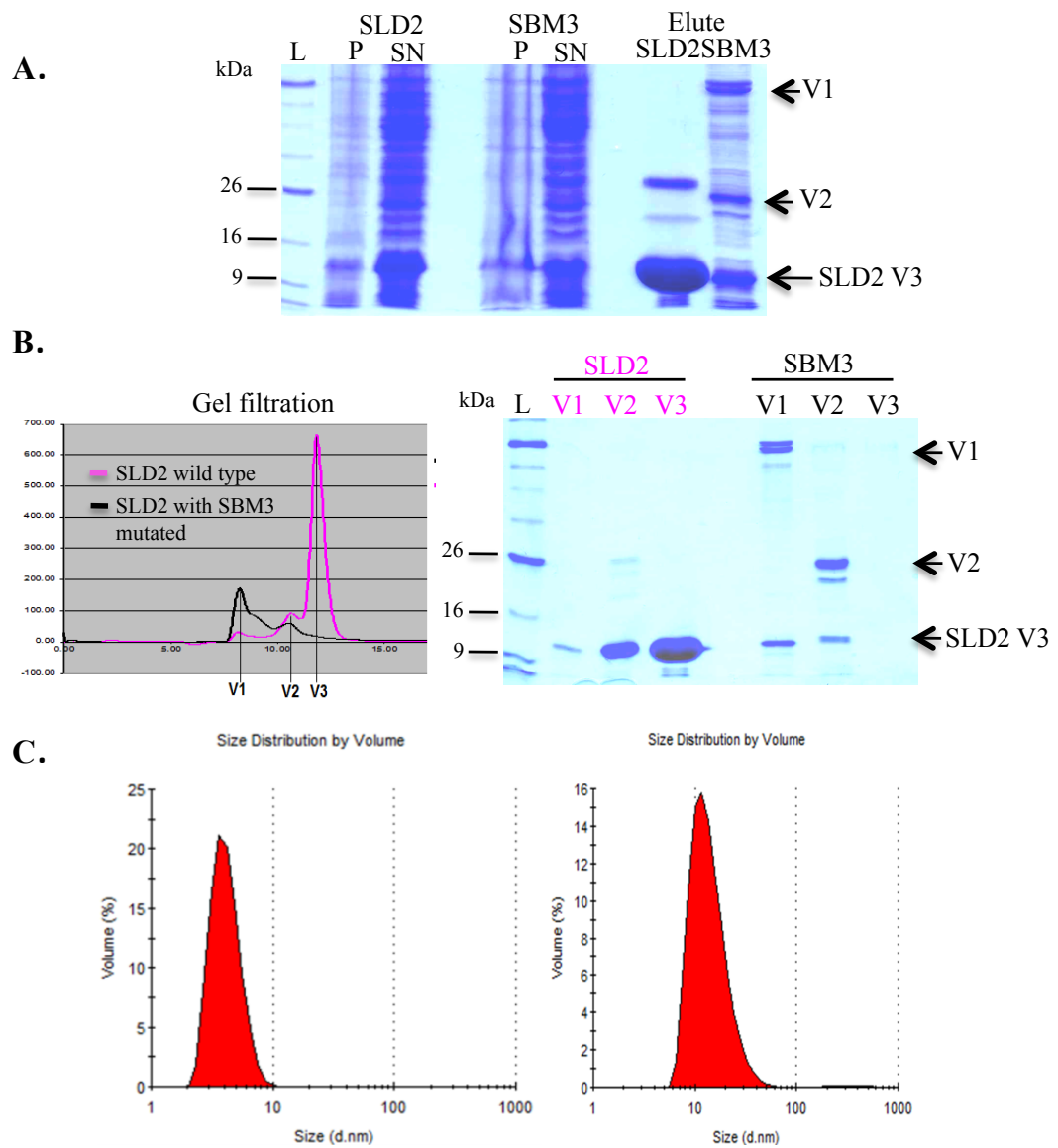


Fig. 3.16 Mutation of SBM3 results in SLD2 aggregation

- A) SDS-PAGE of SLD2 and SLD2 with SBM3 mutated purified from Ni^{2+} agarose (V1, V2 and V3 represent fractions from gel filtration)
- B) Gel filtration chromatogram and SDS-PAGE of fractions of SLD2 and SLD2 with SBM3 mutated
- C) Dynamic Light Scattering spectra of SLD2 and SLD2 with SBM3 mutated

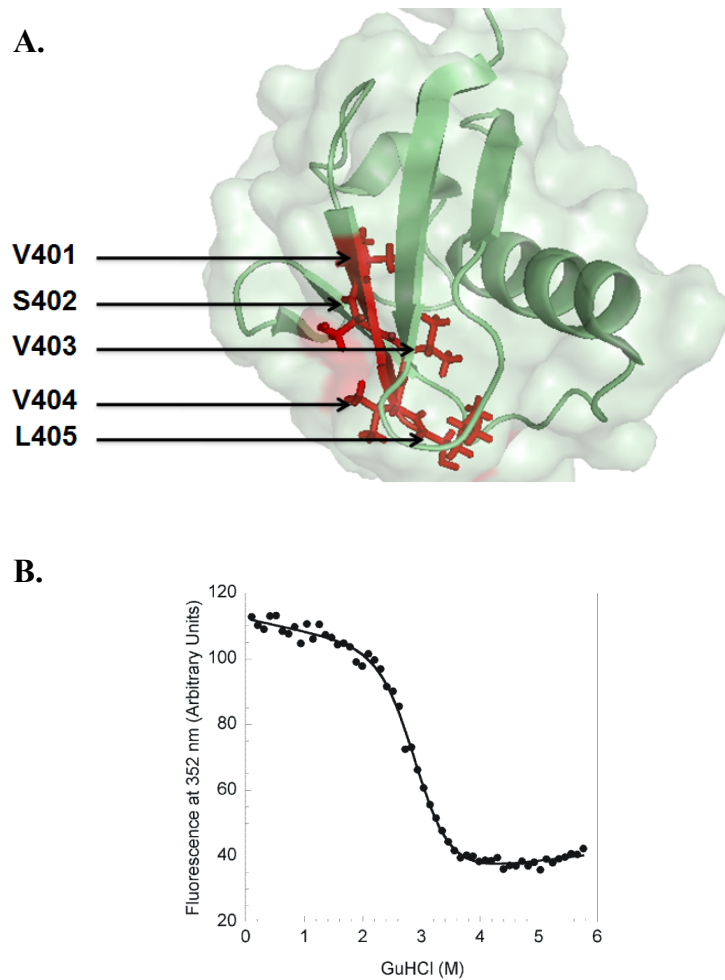


Fig. 3.17 Crystal structure and denaturation studies of SLD2 confirm the structural requirement of putative SBM3 for Rad60 stability

A) Cartoon representation of SLD2 (modeled on pdb id. 3GOE). Highlighted are the residues of β -5 sheet.

B) Guanidine hydrochloride-induced denaturation curve of wild type SLD2.

calculations carried out by Dr. E. Main). It has been shown that the extent of destabilization, or stabilization, of a protein is highly context dependent and the removal of a methylene group side chains of a hydrophobic residue will result in a destabilization energy of 1 ± 0.3 kcal/mol of the protein (Main et al., 1998). Therefore mutation of two valine residues to two alanines removes 4 methylene groups and decreases the overall stability of the protein of approximately 4 kcal/mol. This would result in the SLD2-SBM3 mutant domain being completely unfolded. These biochemical data, together with the severe phenotype observed for the *rad60-SBM3* mutant strongly suggest that the SBM3 region is essential to maintain the β -GRASP fold of SLD2 and the overall structure of Rad60 and that an unfolded SLD2 domain is more damaging to the Rad60 function than the deletion of the domain.

To further identify the features of the SLD2 domain crystallography studies were undertaken.

3.6 Crystallographic studies of SLD2

For crystallographic trials of SLD2, protein purified on Ni^{2+} agarose beads (fig. 3.7) was further purified by FPLC. Firstly, the His elution buffer, unsuitable for FPLC, was exchanged to an equilibrating buffer (50 mM TrisHCl pH 8.0, 10 mM MgCl_2 , 300 mM NaCl) suitable for size-exclusion chromatography (gel filtration), using disposable PD-10 desalting columns (GE Healthcare Life Sciences). Fractions were pooled and concentrated to 0.5 ml using a Pierce concentrator with MCO 3K. The protein was loaded into a HiLoad 16/60 Superdex 75 10/300 GL column (Amersham Biosciences) attached to an ÄCTA_{FPLC} system (GE Healthcare). The column was initially washed with the appropriate equilibrating buffer with a flow rate of 0.5 ml/min. The protein solution was then loaded and fractions collected every 1.2 ml. Fractions were monitored using the online UV monitor measuring absorbance at 280 nm (fig. 3.18 A). Fractions containing SLD2 were checked by SDS-PAGE (fig. 3.18 A) and then pooled and concentrated to 10 mg/ml using a Pierce concentrator with MCO 3K. The resulting protein solution was tested by DLS and the results showed that it was monodisperse, *ie* suitable for crystallography (fig. 3.18 B).

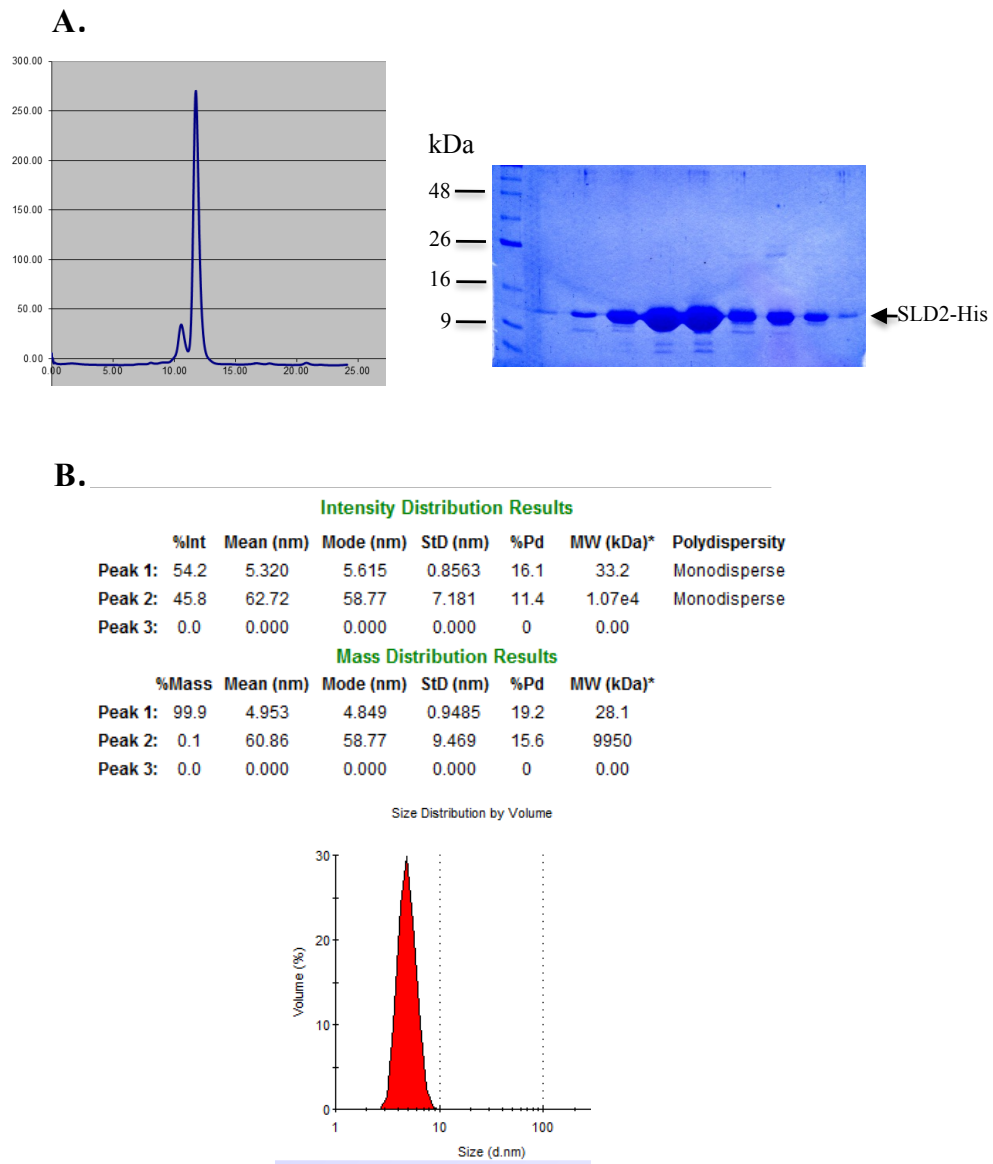


Fig. 3.18 Purification and stability studies of His tagged SLD2

A) Chromatogram of size-exclusion purification of SLD2 and Coomassie stain of fractions containing pure SLD2

B) Dynamic Light Scattering results for SLD2: tabulated data and spectrum showing polydispersity and average particle size respectively

Crystallography screening was conducted using the vapor diffusion ‘hanging drop’ technique based on equilibrating a protein solution against a reservoir containing crystallizing agents at higher or lower concentrations than that of the protein solution in the drop. A pre-crystallization test was conducted to determine the appropriate protein concentration according to the manufacturer’s instructions (kit purchased from Hampton Research). A light amorphous precipitate was obtained with a protein concentration of 8 mg/ml (fig. 3.19 A) and further screening was conducted with this concentration with various sparse matrices (all from Molecular Dimensions). Crystals were obtained with Clear Strategy Screen II (CSS II) matrix, 0.8M Li₂SO₄, pH 6.5, and with Structure Screen I (SS I) matrix, 10% 2-propanol, 0.1 M Na HEPES, 20% PEG4000, pH7 (fig. 3.19 B). The crystals were mounted on a nylon loop of the suitable dimension (Hampton Research), transferred for 5-10 seconds into a stabilising solution containing the cryoprotectant (the reservoir solution plus 30% glycerol), flash-frozen in liquid nitrogen and X-rayed on a Rigaku 007HF rotating anode generator with VariMax-HF mirrors and Saturn 944+ CCD detector. However no diffraction pattern was obtained from these crystals and further optimization of the crystallization screening was considered. At this point, the crystal structure of SLD2 was solved at The Scripps Institute, USA (Prudden et.al.,2009, pdb id: 3GOE, fig. 3.20), and proved the *in silico* prediction that SLD2 adopts a β -GRASP fold like SUMO .

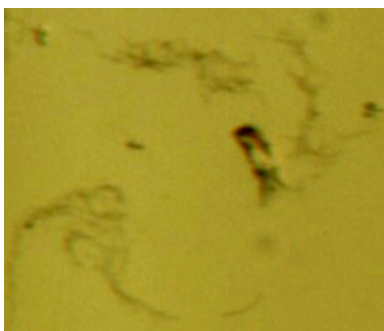
3.7 Discussion

In this chapter I have structurally and functionally characterised a SUMO-like domain, SLD2, and a putative SUMO-binding motif, SBM3, of the Rad60 protein.

3.7.1 Structure and function of Rad60

The crystal structure of SLD2 (Prudden et al., 2009) confirmed the *in silico* and *in vitro* results obtained in this study, that SLD2 mimics SUMO by adopting a β -GRASP fold and interacting non-covalently with the SUMO conjugating enzyme Hus5 through a

A.



B.

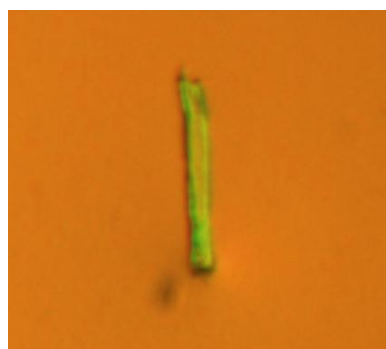
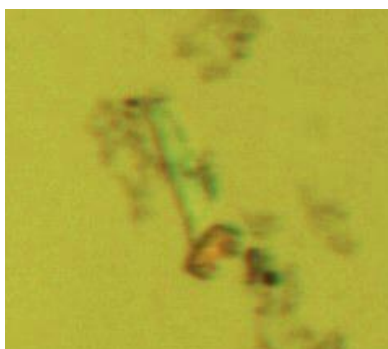


Fig. 3.19 Crystallization of SLD2

- A) Amorphous light precipitate of SLD2 obtained with PCT kit (Hampton research)
- B) Crystals of SLD2 protein obtained with CCSI (left) and SSI (right) matrices (Molecular Dimensions)

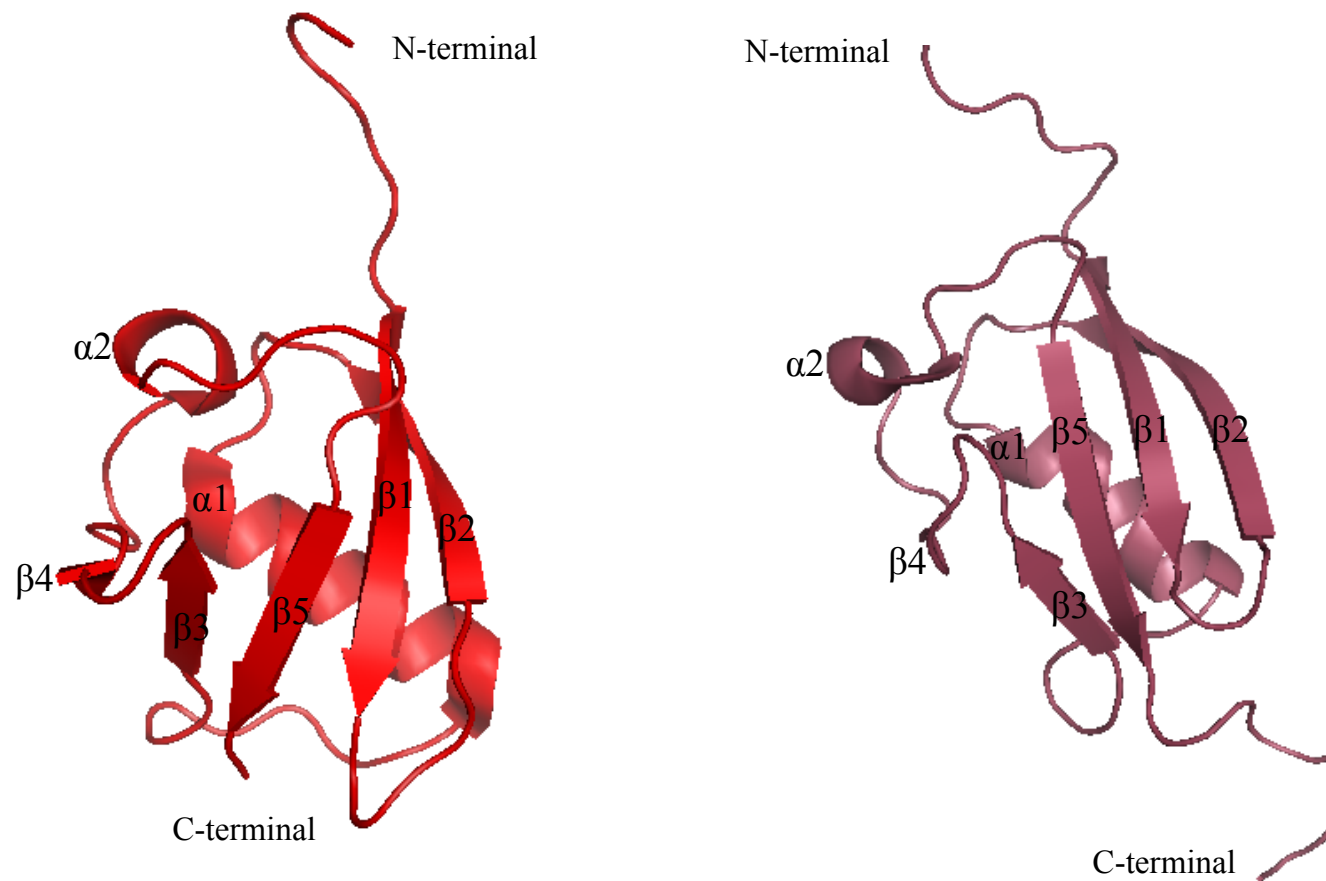


Fig. 3.20 Cartoon representations of crystal structure of *Sp* SLD2 (pdb: 3GOE; left) and *Hs* SUMO-1 (pdb: 1A5R, right).

Depicted are the secondary structure elements in the β -GRASP fold.

conserved surface. While the SLD1 sequence can be modeled onto the SUMO-1 and SLD2 structures, its 3D folding has yet to be defined. This is intriguing as proteins adopting the β -GRASP fold like ubiquitin, SUMO and now SLD2, are very stable and can be easily expressed and purified as recombinant proteins. This suggests that while SLD1 may adopt a similar fold, this is probably somewhat divergent from the classical β -GRASP fold or could be hydrophobic on the surface. Interestingly, a Rad60 fragment deleted for SLD2, Rad60CT, can be expressed and purified as His and GST-tagged recombinant proteins with good yields. Moreover Rad60CT can be modeled using the on-line PHYRE modeling engine (fig. 3.21). The model suggests that SLD1 interacts strongly with the N-terminal of Rad60 and this interaction could stabilize the domain. As a Rad60 full length recombinant protein cannot be purified with good yields and purity, a problem highlighted by the fact that its crystal structure has not yet been defined, crystallographic studies of the Rad60CT could provide insights into Rad60 structure, homodimerization and function.

3.7.2 Putative SUMO-binding motifs (SBMs)

Experimental data show that the SUMO-like domains are essential for the function of Rad60. Deleting SLD1 results in inviable cells while *rad60-SLD2 Δ* is sensitive to DNA damaging agents. Further, it has been shown that these phenotypes are not due to mutation of the putative SUMO-binding motifs within the SLDs (Boyd et al., 2010). However, further analysis of these mutants showed that the SBM3 mutant loses viability at 36° unlike the other two SBMs mutants or *rad60-SLD2 Δ* and shows a more severe phenotype than *rad60-SLD2 Δ* in response to genotoxins. This is interesting as SBM3 is within SLD2. From the crystal structure of SLD2 can be seen that SBM3 forms the β 5 sheet of the β -GRASP fold and its mutation more likely destabilizes the structure of SLD2, which in turn may affect the whole structure of Rad60 more than just deleting SLD2. Moreover, the failure of Rad60 to dimerise in these circumstances could be due to this structural destabilization and not to the abrogation of the interaction between SBMs and SLDs. Further, pull-down assays of Rad60 fragments containing putative SBMs show no interactions with free SUMO. Taken together, these data imply that, from their sequence, the hydrophobic regions appear to be SIMs but do not necessary function as SIMs. The only putative SBM of the RENi family of proteins

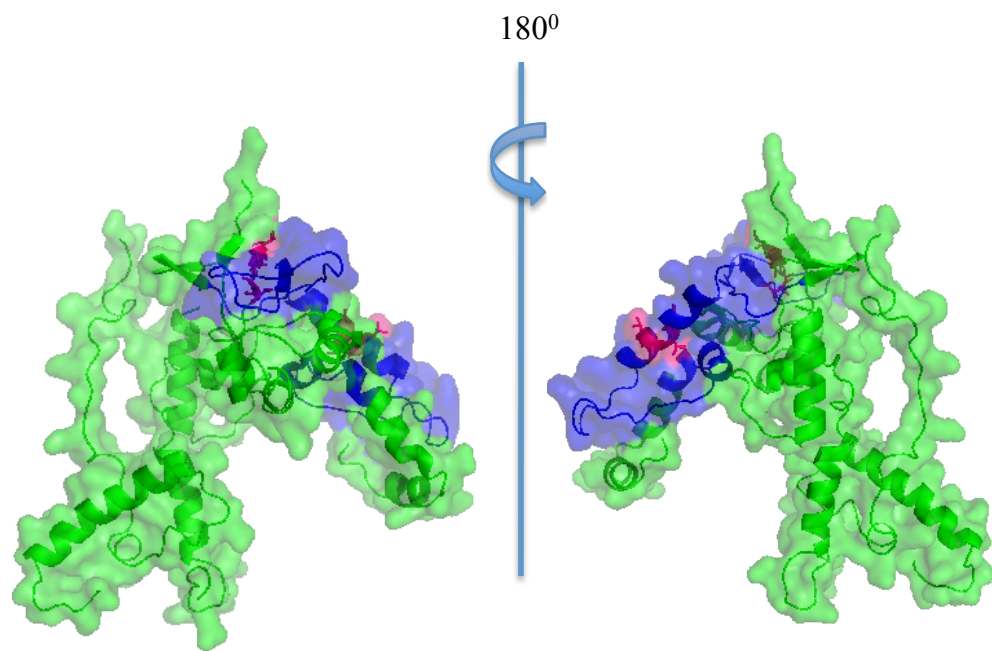


Fig. 3.21 Structural model of Rad60CT (deleted for SLD2)

Green = N- terminal; blue = SLD1; magenta = putative SBM1 and SBM2

shown to interact with SUMO is the SBM1 of Esc2, the *S. cerevisiae* ortholog (fig. 3.22 A) (Yu et al., 2010). This raises the possibility that SBM1 of Rad60 may interact with SLD1 or SLD2. However it has been shown that the SUMO interface that interacts with SIMs is not conserved in SLD2 (Sekiyama et al., 2010). The model of Rad60CT suggests that the SBM1 forms a β -sheet that closely interacts with SLD1 (fig. 3.22 B). If this region is required to maintain the intramolecular structure of Rad60 it is unlikely that it will be available for intermolecular interactions with SUMO moieties or other Rad60 molecules. However, it cannot be excluded that these interactions could be facilitated by an allosteric behavior or environment induced conformational changes of the Rad60 protein.

CHAPTER 4

SUMO CHAIN FORMATION IS REQUIRED FOR DNA DAMAGE RESPONSE DURING S PHASE

4.1 Introduction

Like ubiquitin, SUMO has been shown to form polymeric chains at lysine residues at its extended non-ubiquitin like N-terminal. Chains formed by human SUMO-2 and SUMO-3 were first identified in HeLa cells (Tatham et al., 2001) and later SUMO (Smt3) in *S. cerevisiae* (Bylebyl et al., 2003, Takahashi et al., 2003) and Pmt3 in *S. pombe* (Ho and Watts, 2003). The first identified physiological substrate for SUMO chains was the histone deacetylase HDAC4 (Tatham et al., 2001).

Proteomic investigations into endogenous poly-SUMO conjugates (Bruderer et al., 2011, Golebiowski et al., 2009, Tatham et al., 2011) suggest that proteins involved in DNA replication and DNA damage responses modified by SUMO polymers accumulate in response to various stress stimuli. This is consistent with phenotypes observed for mutants of the sumoylation pathway components such as the SUMO conjugating enzyme, Hus5^{Ubc9}, or the SUMO protease responsible for SUMO chain editing, Ulp2, which display hypersensitivity to a range of genotoxins.

The proliferating cell nuclear antigen (PCNA) clamp protein is essential for DNA damage responses during replication. PCNA is one of the few targets identified as being ubiquitinated and sumoylated at the same lysine residues (Ulrich, 2005). The architecture and assembly of poly-SUMO chains on PCNA was described in *S. cerevisiae* (Windecker and Ulrich, 2008) and mammalian cells (Gali et al., 2012). In humans the poly-sumoylation of PCNA is required for replication fork stabilization at double strand breaks (Gali et al., 2012). In *S. cerevisiae* SUMO polymers can co-exist

with ubiquitin chains on a common PCNA subunit and are dispensable for the PCNA functions in DNA replication and repair (Windecker and Ulrich, 2008).

So far, the best characterized function of SUMO chains is targeting of proteins for proteasomal degradation. SUMO chains anchored to substrates interact non-covalently with tandem SIMs present in RNF/SLX type ubiquitin E3 ligases known as STUbLs (SUMO-Targeted Ubiquitin Ligases, (Prudden et al., 2007). The interaction of conjugated SUMO chains with STUbLs results in the degradation of the substrate proteins by the UPS (Ubiquitin Proteasome System) (Perry et al., 2008, Tatham et al., 2008).

In this study I began an analysis of the sequence requirements for SUMO chain formation in *S. pombe*. Having identified the lysines involved in chain formation and analyzed chain formation in an *in vitro* sumoylation assay, the phenotypic consequences of mutating sumoylated lysines were characterized. The gene coding for the *S. pombe* SUMO protein is referred to as *pmt3*, while for the translation product the general name SUMO was adopted.

4.2 *In silico* analysis of sequence requirement for SUMO chains formation

All SUMO homologues have an extended disordered N-terminus with lysine residues that can potentially act as substrates for polymeric chains (fig. 4.1). In mammals SUMO-2 and SUMO-3 have two lysine residues at the N-terminal, K5 and K11, with K11 within the tetrapeptide consensus motif for SUMO attachment (Ψ KxE) (fig. 4.1). It was shown that K11 only is a substrate for chain formation (Tatham et al., 2001). In *S. cerevisiae* SUMO has three lysine residues at the N-terminal, K11, K15 and K19, all within SUMO acceptor consensus sequences (fig. 4.1) and all involved in polymeric chain assembly (Bylebyl et al., 2003). Interestingly, the *S. pombe* SUMO homologue, Pmt3, has a significantly longer disordered N-terminal region with two lysine residues, K14 and K30, which are not within consensus sequences (fig. 4.1). However, sumoylation at lysines that are not within the consensus sequence has been observed


```

SpPmt3      1  MSSEFSANISDAIKSAITPTTGDTSQGVKISTEHLNKLKVVQGDNNVEVFKIKHTTESK
ScSMT3      1  -----MSDEVNQEAKIEVKEVKEETHINLKVSDGSSEIFFKIKHTTPFR
HsSUMO-2    1  -----MADEKPKKGVKTE-----DHINLKVAGQDGSVVQFKIKHTPLSK
HsSUMO-3    1  -----MSDEKPKKGVKTE-----DHINLKVAGQDGSVVQFKIKHTPLSK

SpPmt3      61  LMKIYCARQGHSMNSRLFLVDGERIRPDQTPAELLMEDGLQLEAVLEQLGGCTHLCL---
ScSMT3      48  LMAFAHARQCKEMDSRLFLVDGERIRADQTFEDLMEDNTDFAHREQIGATY-----
HsSUMO-2    43  LMKAYCERQGLSMRQIRRFDFDGGFINETDTPAQLMEDEDTILVFCQQTGGVY-----
HsSUMO-3    42  LMKAYCERQGLSMRQIRRFDFDGGFINETDTPAQLMEDEDTILVFCQQTGGVPESLAGH

SpPmt3      --
ScSMT3      --
HsSUMO-2    --
HsSUMO-3    102 SF

```

Sp: Pmt3

MSISPSANISDADKSAITPTTGTSDSQDVKPSTHINLKVVGQDNNIEVIFKIKKTTTFISK

Sc: SMT3

MSDSIEVHQIAKPIEVKPKPKPIETHINLKVSDGSSEIIFKIKKTTPLRLMEIAFAKRQGKEM

Hs: SUMO-2

MADEKPKIGVKTIENHHDHINLKVAGQDGSVVQFIKIKRHTPLSKLMKAYCIRQGLSVRQIRF

Fig. 4.1 *Sp* SUMO has an extended, disordered N-terminus

A) ClustalW sequence alignment of *Sp* Pmt3, *Sc* SMT3, *Hs* SUMO-2 and *Hs* SUMO-3

B) *In silico* analysis of N-termini of *Sp* Pmt3, *Sc* SMT3 and *Hs* SUMO-2 using DISOPRED2 software (Ward et al., 2004). Highlighted (□) are lysine residues involved in chain formation in *Sc* and *Hs*, and potential lysine residues involved in SUMO chain formation in *Sp*.

(Lin et al., 2006, Hoege et al., 2002, Pichler et al., 2005, Meulmeester et al., 2008). Additionally it has been shown that SUMO forms chains at K30 (Andrews et al., 2005). This raises the question as to whether both K14 and K30 are substrates for polymeric chains assembly (fig. 4.2). To assess this, recombinant SUMO-K14R, SUMO-K30R and SUMO-RR (both K14 and K30 mutated to arginine) mutants were probed for SUMO chain formation in a previously developed *in vitro* sumoylation assay (Ho et al., 2001).

4.3 Expression and purification of recombinant sumoylation pathway components and optimization of the *in vitro* sumoylation assay

In vitro sumoylation assays have evolved as an important tool for the analysis of this post-translational modification (Desterro et al., 1998, Ho et al., 2001, Okuma et al., 1999, Johnson et al., 1997) as they can be set-up as well defined systems where the components of the sumoylation machinery and targets can be biochemically characterized. Reconstituting SUMO modification *in vitro* requires expression and purification of the recombinant mature form of SUMO (SUMO-GG), the heterodimeric activating enzyme E1 (Rad31 + Fub2), the conjugating enzyme E2 (Hus5), the E3 ligases (Pli1 and Nse2) and the target proteins.

4.3.1 Co-expression and purification of E1

The recombinant SUMO-activating enzyme has been mainly expressed and purified for sumoylation assays from two independent *E. coli* cultures expressing Fub2^{Uba2} and Rad31^{Aos1} either His- or GST-tagged. While this method produces the proteins in good quantity and free of contaminants, the enzymatic activity of the complex, probed by the capacity to form SUMO chains in *in vitro* assays, seemed to vary from batch to batch. As the two proteins may stabilize each other by forming a heterodimer, the variations in the enzymatic activity could be due to some misfolding of the components before they

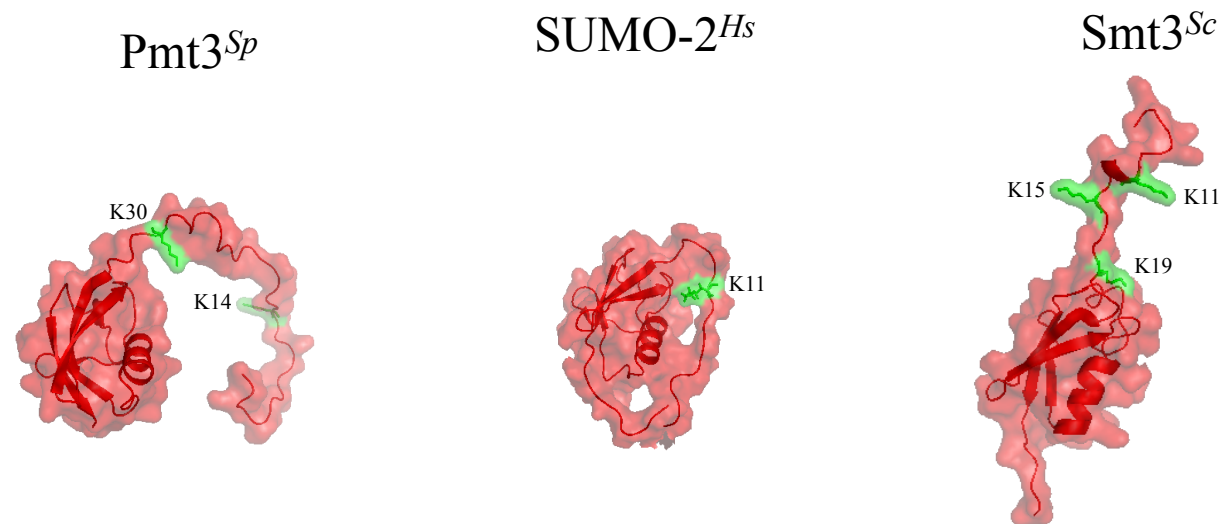


Fig. 4.2 N-terminal lysines of SUMO proteins are required for SUMO chain formation

Lysine residues (green) mapped on the model of SUMO^{Sp} and crystal structures of SUMO-2^{Hs} (pdb id: 1WZ0) and Smt3^{Sc} (pdb id: 1L2N) respectively.

dimerise. To address this problem, co-expression of the components with two different tags followed by two steps purification was carried out.

A *fub2* construct in a pGEX-KGH vector was already available (made by J. Ho). As the pGEX-KGH has a GST tag and the ampicillin selection marker, *rad31* ORF was cloned into the pET28a vector which has a His tag and the kanamycin selection marker. The *rad31* ORF was digested from the pET15b plasmid (construct made by J. Ho) using the *Nde*I and *Bam*HI enzymes (fig. 4.3 A). The *rad31* fragment was gel purified and then ligated in the *pET28a* vector that has been digested with the *Nde*I and *Bam*HI enzymes (fig. 4.3 B). The ligation product was transformed in NM522 *E. coli* cells and transformed cells were plated onto solid medium containing kanamycin. To express the E1 complex, pGEX-KGH-*fub2* and pET28a-*rad31* constructs were co-transformed in BL21Codon+ cells. Transformed cells were plated on solid medium containing ampicillin and kanamycin to select for cells that took up both plasmids. The Fub2-Rad31 complex was first purified on Ni²⁺ column as described (see section 2.4.9). The elution was pooled (~ 1.5ml) and the Ni²⁺ elution buffer was exchanged for GST binding buffer using a PD10 column. The resulting protein solution was incubated with glutathione sepharose beads for GST purification as previously described (see section 2.4.9; fig. 4.3 C). The enzymatic activity of the purified complex was assessed by the capacity to form SUMO chains in *in vitro* sumoylation assay (fig. 4.5).

4.3.2 Expression and purification of E2 and E3 enzymes and SUMO-GG

The SUMO conjugating enzyme Hus5, the SUMO E3 ligases Pli1 and Nse2 and the modified form of SUMO with the double glycine motif at the C-terminal (SUMO-GG) were expressed and purified from previously made DNA constructs (made by J. Ho). Hus5 and Nse2 were expressed from the pGEX-KGH plasmid (constructs made by J. Ho and E. Outwin respectively) as GST fusion proteins. GST purification was carried out as previously described (see section 2.4.8; fig. 4.4 B and fig. 4.6 B respectively) and the elutions concentration was assessed using a Bradford assay. SUMO-GG and Pli1 were expressed from the pET15b plasmid (construct made by J. Ho) as 6 x His fusion proteins. Ni²⁺ purification was carried out as previously described (see section 2.4.9;

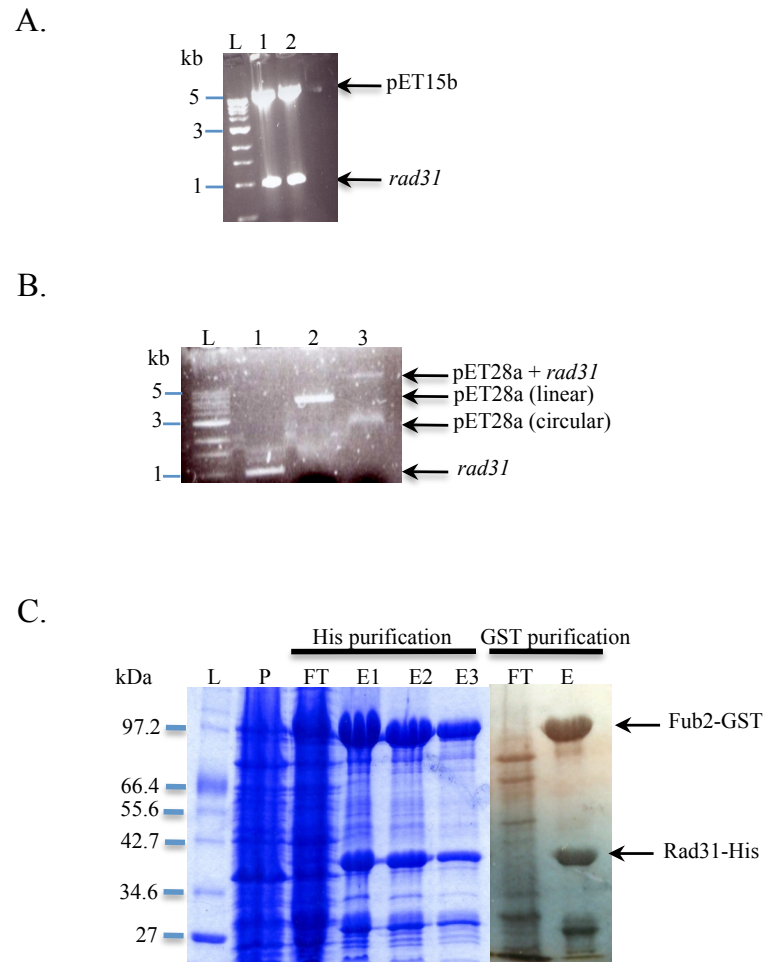
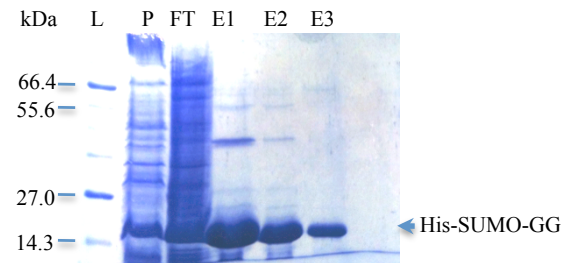


Fig. 4.3 Co-expression and purification of Fub2/Rad31 (E2) complex

- A) Digestion of *rad31* ORF from pET15b plasmid with *NdeI*/*BamHI* enzymes
- B) Ligation of *rad31* ORF into pET28a plasmid digested with *NdeI* and *BamHI* enzymes.
Lane 1: *rad31* ORF digested from pET15b; lane 2: pET28a plasmid digested with *NdeI*/*BamHI*; lane 3: ligation of *rad31* ORF in pET28a
- C) Coomassie stain of Ni²⁺/GST purified Rad31/Fub2 complex;
P = pellet; FT = flow through; E = elute;

A.



B.

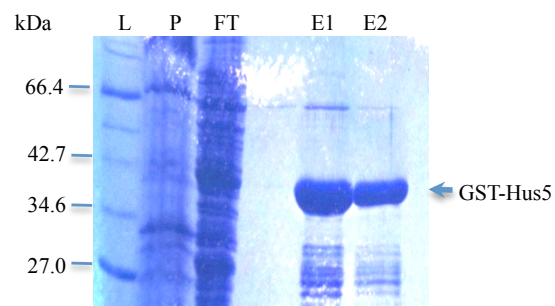


Fig. 4.4 Expression and purification of His-Pmt3-GG and GST-Hus5

A) Coomassie stain of Ni^{2+} purified His-Pmt3-GG

B) Coomassie stain of glutathione sepharose purified GST- Hus5

L = ladder; P = pellet; FT = flow through; E = elute;

fig. 4.4 A and fig. 4.7 A respectively) and the elutions concentration was assessed using a Bradford assay.

4.3.3 Optimization of the *in vitro* sumoylation assay

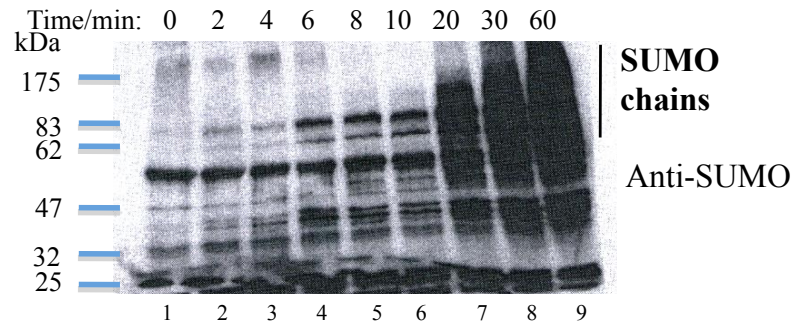
Different incubation conditions have been reported for *in vitro* sumoylation assays: 1 hour at 37°C (Xhemalce et al., 2004), 2 hours at 30°C (Ho et al., 2001) or 1 hour at 30°C (Flotho et al., 2012). To assess the best conditions, assays were carried out at 30°C and 37°C for 2 hours and 1 hour respectively. Samples were taken at various times and probed for high Mr sumoylated species (fig. 4.5). Interestingly high Mr species are formed after just 20-30 minutes at both temperatures but at 30°C they appear gradually while at 37°C they appear abruptly. Given that the most polymeric species were observed at 30°C after 2 hours (fig. 4.5 B lane 8) and that this is the physiological growing temperature of *S. pombe*, these conditions were used for all further assays.

4.3.4 Pli1 is more efficient than Nse2 at forming SUMO chains *in vitro*

Previously it has been shown that E3 ligases enhance SUMO chain formation in *S. cerevisiae* (Takahashi et al., 2003, Johnson and Gupta, 2001) and mammalian cells (Pichler et al., 2002) Having optimized the conditions for the formation of SUMO chains *in vitro* independent of the E3 ligases, the next step was to assess whether Pli1 and Nse2 facilitate SUMO chain formation under these conditions.

His-Pli1, GST-Nse2 and GST-Nse2-SA (ligase dead mutant, fig. 4.6 C) recombinant proteins were expressed from pET15b for Pli1 and pGEX-KGH for Nse2 and Nse2-SA vectors (constructs made by J. Ho and E. Outwin respectively) and purified as previously described (see sections 2.4.8 and 2.4.9 respectively; fig. 4.6 A, B and D). The ligase activities of Pli1 and Nse2 have been previously assessed on target proteins (Ho et al., 2001, Andrews et al., 2005) by reducing the amount of the conjugating enzyme, Hus5, to a tenth, which results in reduction of sumoylation. Adding the SUMO

A.



B.

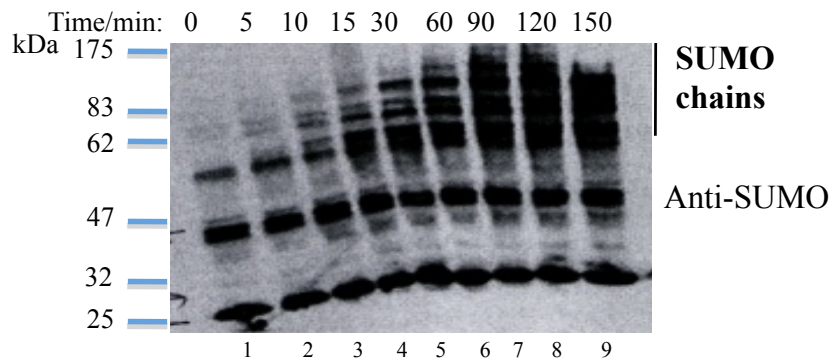


Fig. 4.5 *In vitro* sumoylation assay time course

- A. Western blotting of *in vitro* sumoylation assay carried out at 37°C; samples taken at shown times; probed with SUMO antibodies.
- B. Western blotting of *in vitro* sumoylation assay carried out at 30°C; samples taken at shown times; probed with SUMO antibodies.

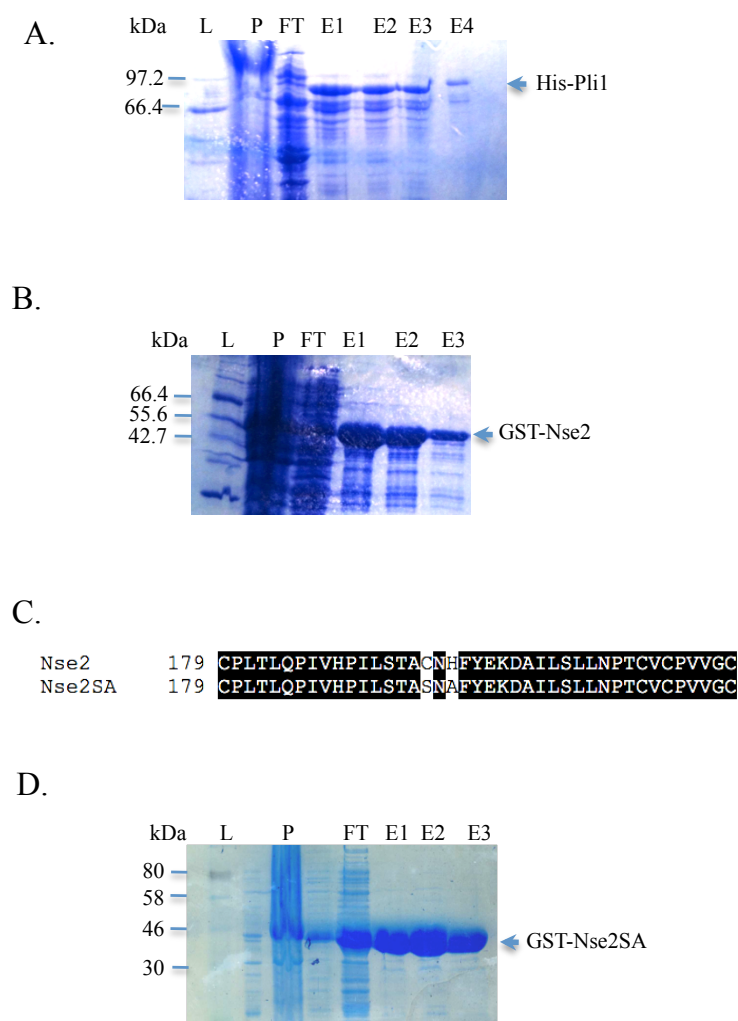


Fig. 4.6 Expression and purification of SUMO E3 ligases

A) Coomassie stain of Ni^{2+} purified His-Pli1

B) Coomassie stain of glutathione sepharose purified GST-Nse2

C) Sequence alignment of Nse2 and Nse2SA highlighting the mutated residues

D) Coomassie stain of glutathione sepharose purified GST-Nse2-SA

P = pellet; FT = flow through; E = elute;

E3 ligases can restore the levels of sumoylation. The same strategy was used to assess the efficiency of SUMO E3 ligases at forming SUMO chains (fig. 4.7). Interestingly, a low level (5 nM) of Pli1 was sufficient to restore the levels of SUMO chains to that obtained using the full amount of Hus5 (fig. 4.7 lane 3) and increased quantities of Pli1 did not further increase the levels of SUMO chains (fig. 4.7 lanes 4 and 5). In contrast, twenty times more (100 nM) Nse2 was required to restore the levels of polymeric SUMO (fig. 4.7 lane 8). The ligase activity of wild type Nse2 was compared with that of Nse2-SA, which has a mutated RING domain (fig. 4.7 lane 9). The lack of high Mr SUMO species when Nse2-SA was used confirms the requirement of the RING domain for the ligase activity.

These results provide evidence that, at least *in vitro*, Pli1 is required in enzymatic quantities to sumoylate substrates, while Nse2 probably act as a scaffold protein to facilitate sumoylation.

4.4 *In vitro* SUMO chain formation occurs at K14 and K30

With the *in vitro* sumoylation assay optimized and the activity of all components assessed, the next step was to determine whether SUMO chain formation occurs at K14, K30 or both. To achieve this, the three mutants, singles and the double, were expressed and purified as recombinant proteins.

4.4.1 Expression and purification of SUMO chain mutants

Purified His-SUMO-K30R protein was already available (work carried out by E. Outwin). His-SUMO-K14R and His-SUMO-RR (K14R, K30R) were expressed from pET15b constructs (made by F.Z.Watts) and purified as described (see section 2.4.9, fig. 4.8 A). The mutants were checked to determine whether they are recognized by anti SUMO antibodies as efficiently as wild-type SUMO (fig. 4.8 B).

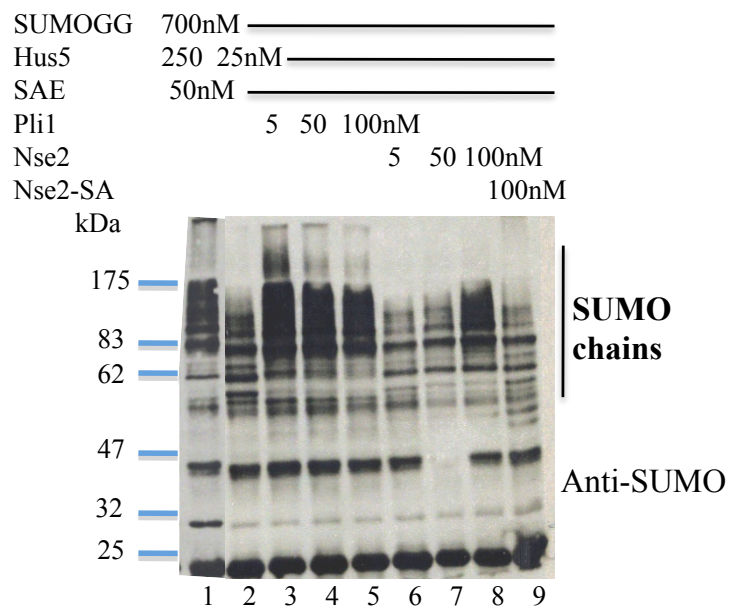
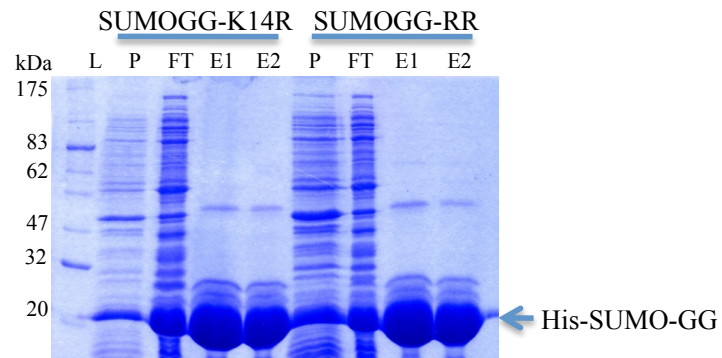


Fig. 4.7 Pli1 is 20x more efficient than Nse2 at facilitating *in vitro* SUMO chain formation

Western blotting of *in vitro* SUMO assay probed with SUMO antibodies. All components are in nanomolar quantities.

A.



B.

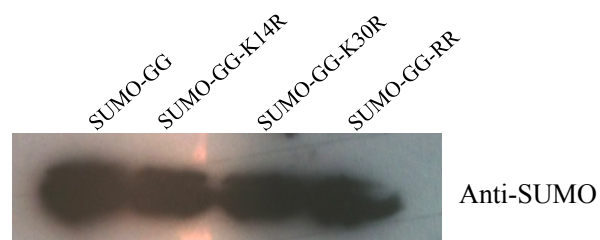


Fig. 4.8 Expression and purification of SUMO mutants for *in vitro* sumoylation assays

A. Coomassie stain of Ni^{2+} purified SUMO mutants.
P = pellet; FT = flow through; E = elute

B. Western blotting of SUMO-GG and SUMO chain mutants probed with SUMO antibodies

4.4.2 Both K14 and K30 are substrates for SUMO chain formation in the absence of E3 ligases

The sumoylation assay was carried out with the SUMO activating enzyme (E1) and the conjugating enzyme (E2) but no E3 ligases. The ability of the mutants to form polymeric chains was compared to that of the wild type protein. Both single mutants, SUMO-K14R and SUMO-K30R, form similar levels of SUMO chains (fig. 4.9 lanes 2 and 3), slightly less than that of the wild type SUMO (fig. 4.9 lane 1). However, the double mutant, SUMO-RR, shows a drastic reduction in SUMO chains (fig. 4.9 lane 4), with few high Mr species visible, possibly representing SUMO conjugated forms of the activating and/or the conjugating enzymes. These results imply that K14 and K30 are the only lysine residues involved in SUMO chain formation, and that if one of them is unavailable for chain formation the other one is sufficient for SUMO polymerization.

4.4.3 E3 ligases facilitate SUMO chain formation at K14 and K30

Having demonstrated that SUMO chain formation occurs at both lysines independently of E3 ligases, the effect of mutating K14 and K30 on chain formation facilitated by E3 ligases was assessed. *In vitro* sumoylation assays were carried out with reduced quantities of the SUMO conjugating enzyme ($1/10^{\text{th}}$) and with the amount of Pli1 and Nse2 required to restore poly-SUMO species (fig. 4.10).

Nse2 displays a drastic decrease in poly-SUMO species when both lysines are mutated (fig. 4.10 A lane 9) compared to SUMO wild type, and lower levels when K30 is mutated (fig. 4.10 A lane 7) than when K14 is mutated (fig. 4.10 A lane 5). This is consistent with previously published data that Nse2 facilitates SUMO chain formation at K30 *in vitro* (Andrews et al., 2005). Interestingly, Pli1 has the opposite effect with a decrease in poly-SUMO species when K14 (fig. 4.10 B lane 5) is mutated while mutated K30 (fig. 4.10 A lane 7) displays similar levels as SUMO wild type (fig. 4.10 A lane 3) with the double mutant, SUMO-RR, (fig. 4.10 A lane 9) showing similar levels as SUMO-K14R.

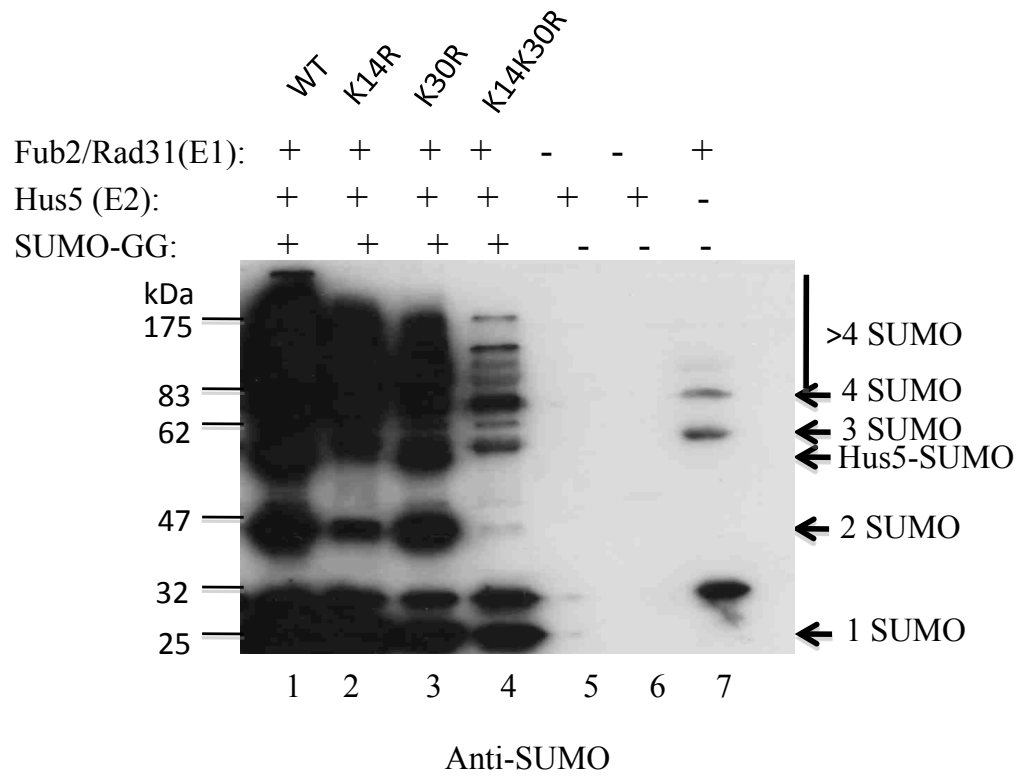


Fig. 4.9 *In vitro* SUMO chain formation occurs at K14 and K30

Western Blotting of *in vitro* sumoylation assay with SUMO and SUMO chain mutants: K14R, K30R, and K14RK30R. Probed with SUMO antibodies.

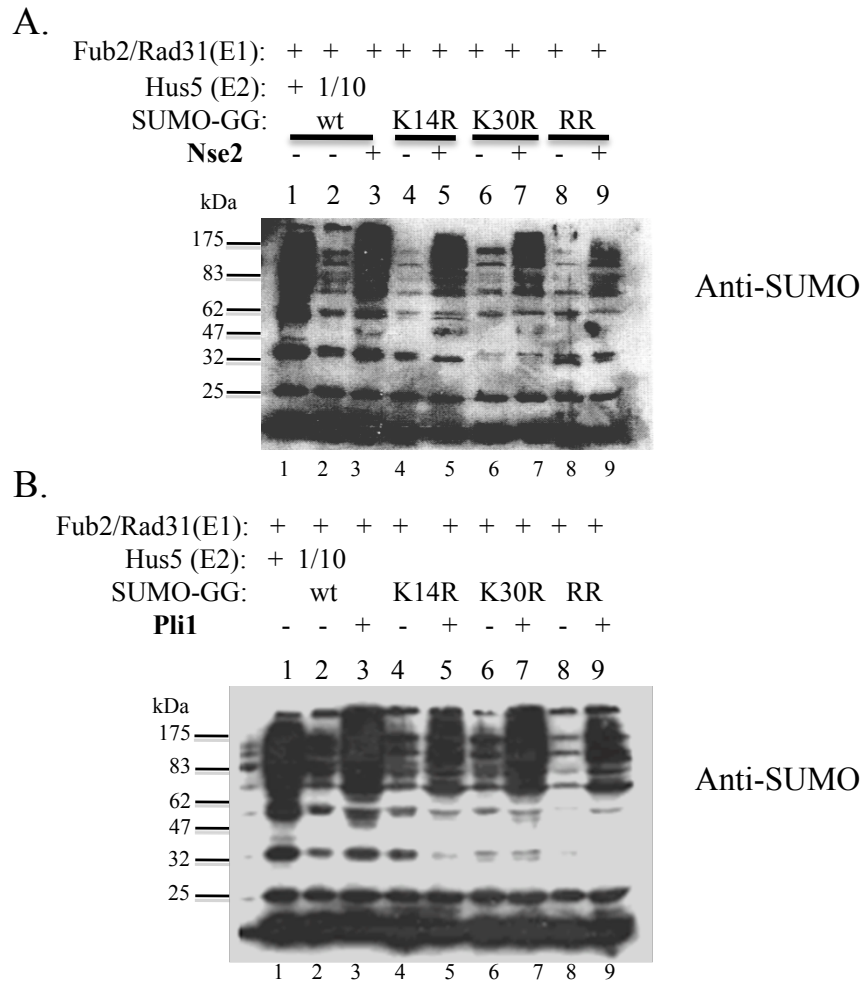


Fig. 4.10 E3 ligases, Pli1 and Nse2 facilitate *in vitro* SUMO chain formation

A. Western Blotting of *in vitro* sumoylation assay with SUMO chain mutants and Nse2 E3 ligase

B. Western Blotting of *in vitro* sumoylation assay with SUMO chain mutants and Pli1 E3 ligase

Probed with SUMO antibodies.

These data suggest that both K14 and K30 are sites of SUMO chain formation *in vitro* in the presence of E3 ligases but with different specificities, with Pli1 preferentially acting on K14 while Nse2 having a higher affinity for K30 than K14.

4.5 *In vivo* analysis of SUMO chains mutants

Given the results from the *in vitro* analysis of sequence requirements for SUMO chain formation, the next step was to determine whether mutating K14 and/or K30 in the genome affects the levels of SUMO modification or chain formation. Strains with mutant alleles present in cells as the sole copies of *pmt3* gene (made by F.Z.Watts, fig. 4.11) were created by site directed mutagenesis on a pET15b-SUMO construct (fig. 4.11 A) followed by digestion of the plasmid with *NdeI/BamHI* restriction enzymes. The product was ligated into a pSTA18-*pmt3* construct digested with *NdeI/BamHI* (fig. 4.11 B). The *pmt3* cassette was excised by digestion with *SphI* (fig. 4.11 B) and the fragment was used to transform a wild type strain to obtain *pmt3-K14R:ura4⁺*, *SUMO-K30R:ura4⁺* and *pmt3-K14RK30R:ura4⁺* (*pmt3-RR*) strains. All SUMO chains mutant strains were viable although the double mutant, *pmt3-RR*, grows slower than wild type. The mutants are not temperature sensitive (fig. 4.12 A), suggesting that mutating K14 and K30 to arginine does not affect the folding of the protein and therefore the phenotype observed is likely to be due to functional defects and not structural aberrations.

4.5.1 K14 and K30 are substrates for SUMO chain formation *in vivo*

To assess whether mutating K14 and/or K30 in the genome affects SUMO modification or chain formation whole cell extracts were prepared using TCA, separated by SDS-PAGE and probed with anti-SUMO antibodies. The effects of the mutations on the levels of sumoylation were compared with wild type sumoylation levels, *pli1Δ* and *nse2-SA* strains (fig. 4.12 B).

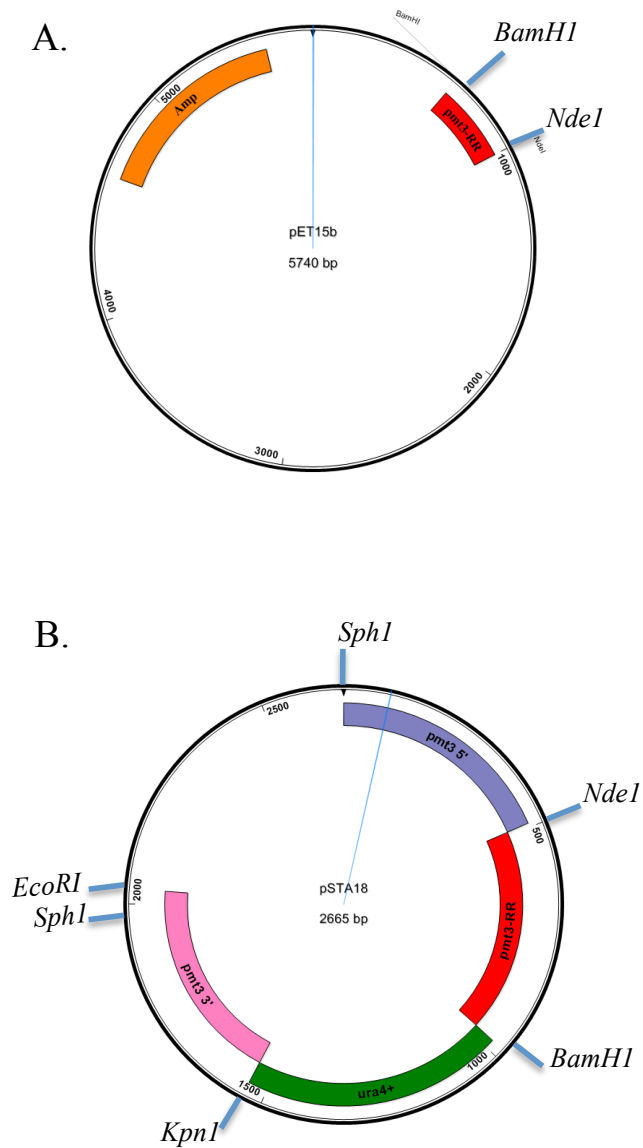


Fig. 4.11 Constructs for the integration of SUMO chain mutants into the genome as the sole copy of *pmt3* gene

A. Map of the *pET15b* – *pmt3*-GG construct

B. Map of the *pSTA18* – *pmt3*-RR construct used for genomic integration

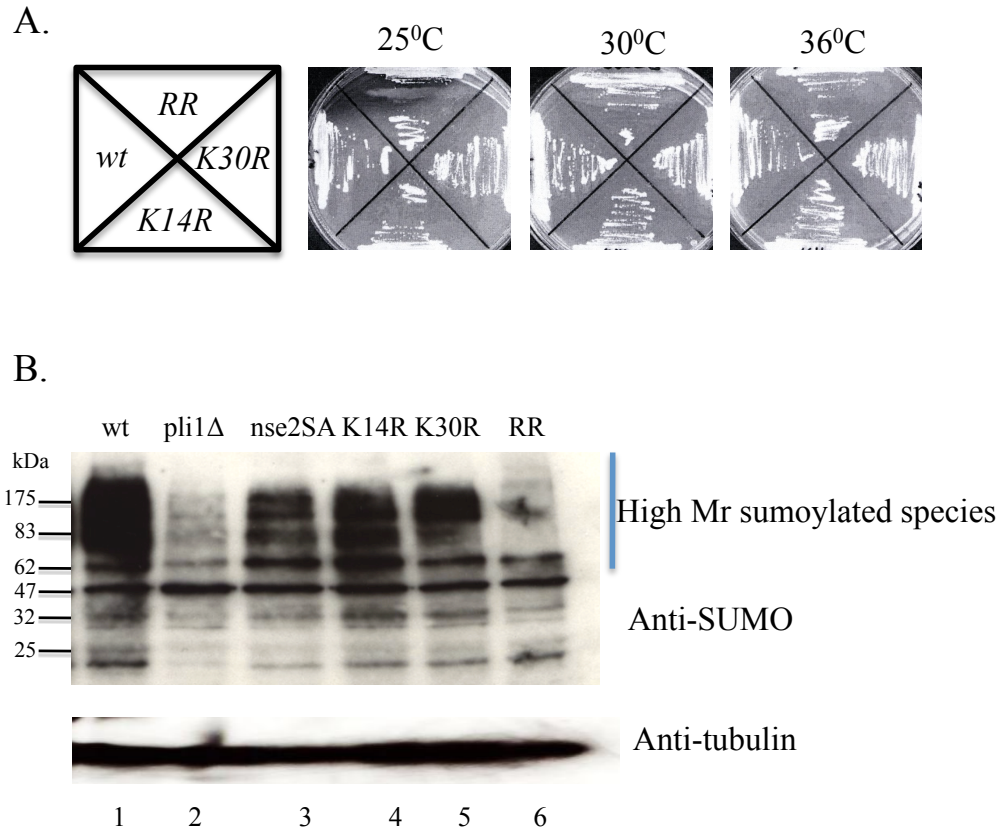


Fig. 4.12 Effect of SUMO chain mutations on levels of high Mr sumoylated species *in vivo*

- A. SUMO chain mutants are not temperature sensitive
- B. Western blot of total cell extracts from wt, *pli1-d*, *nse2-SA* and SUMO chain mutant cells as indicated, probed with anti-SUMO antisera (upper panel) and anti-tubulin antisera (lower panel)

The *pmt3-K14R* strain has a lower level of total sumoylation compared to wild type but higher than *pli1Δ* and *nse2-SA*. The *pmt3-K30R* has lower levels than *pmt3-K14R*, similar to that of *nse2-SA*. The *pmt3-RR* strain displays drastic reduction in the levels of high Mr SUMO-containing species, similar to those of *pli1Δ* strain.

These results are consistent with those from the *in vitro* analysis and show that both lysines are required to maintain normal cellular levels of sumoylation. Further, they are reminiscent of the phenotype of other sumoylation mutants e.g. *rad31Δ* (deleted for the one component of the SUMO activator heterodimer) (Shayeghi et al., 1997) and *hus5-62* (defective in SUMO conjugation) (Ho and Watts, 2003).

4.5.2 Phenotypic characterization of SUMO chain mutants

As previously characterized sumoylation mutants display cellular and nuclear aberrations and are sensitive to genotoxins (Shayeghi et al., 1997, Ho and Watts, 2003) SUMO chain mutants were subjected to microscopic visualization of the cellular and nuclear structures and response to DNA damaging agents.

4.5.2.1 SUMO chain mutant, *pmt3-RR*, displays aberrant cellular and nuclear structures

pmt3-K14R and *pmt3-K30R* have cellular and nuclear morphologies similar to those of wild type cells under normal growth conditions (fig. 4.13, upper panels). However, mutating both lysines to arginine results in elongated cells (fig. 4.13, lower panel, a) and stretched and fragmented chromatin (fig. 4.13, lower panel, b), resembling morphologies of other sumoylation mutants (Shayeghi et al., 1997, Ho and Watts, 2003).

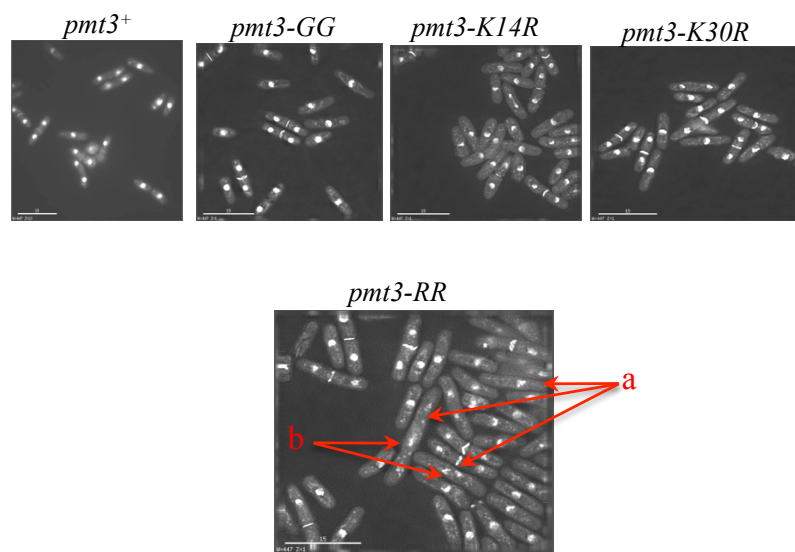


Fig. 4.13 SUMO chain mutant display aberrant cell and nucleus morphology

Morphology of methanol fixed cells, stained with DAPI and calcofluor.

a – elongated cells; b – stretched and fragmented chromatin;

4.5.2.2 *pmt3-RR* is sensitive to hydroxyurea

rad31Δ and *hus5-62* sumoylation mutants are sensitive to a range of genotoxins (Shayeghi et al., 1997, Ho and Watts, 2003) while the *pli1Δ* mutant is sensitive only to TBZ, the microtubule inhibitor. The *pmt3-K30R* mutant resembles wild type cells in response to HU, MMS, CPT, UV and TBZ (fig. 4.14, not all data shown). The *pmt3-K14R* and *pmt3-RR* mutant cells are not sensitive to MMS, CPT, UV or TBZ but are sensitive to high doses (5 mM) of HU (fig. 4.14, not all data shown, sensitivity to HU highlighted in red box).

While the sensitivities of SUMO chain mutants are significantly lower than those of other sumoylation mutants, the results suggest a function for SUMO chain formation in the response to replication arrest.

4.5.2.3 SUMO chain formation is required for normal cell growth when homologous recombination is impaired

The role of sumoylation in DNA damage repair is well documented (Altmannova et al., 2010, Dou et al., 2010). It has been shown that in *S. pombe* Pli1 facilitates the sumoylation of the homologous recombination protein Rad22^{Sp}/Rad52^{Hs/Sc} (Watts et al., 2007). Nse2 is part of and facilitates the sumoylation of components of the SMC5/6 complex, an essential element of the homologous recombination repair machinery (Andrews et al., 2005). To determine whether SUMO chain formation is required for the recombinational repair of DNA, double mutants *pmt3-RR;rad22Δ* and *pmt3-R;nse2-SA* were created (fig. 4.15 A and B respectively) for epistasis analysis. Interestingly, the double mutants (fig. 4.15 A and B respectively, highlighted in red) are strikingly slower growing than the single mutants. These data indicate that *pmt3-RR* is not epistatic with *rad22Δ* or *nse2-SA* and that SUMO chain formation is required for an alternative DNA repair pathway when homologous recombination repair is impaired. Another possibility is that SUMO chains are required for the stabilization of replication forks and defects in both SUMO chain formation and homologous recombination will result in an additive phenotype.

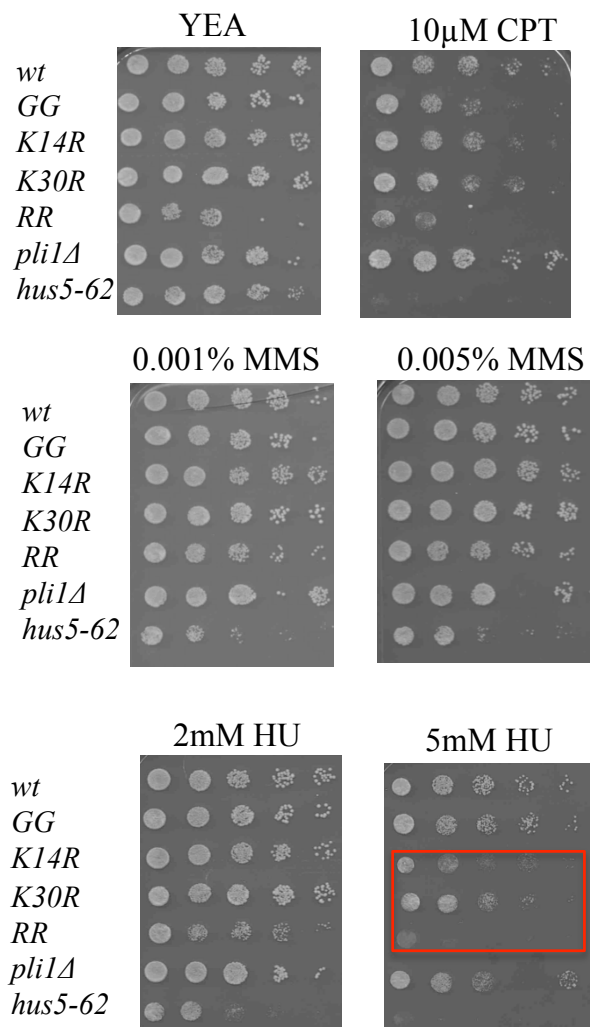
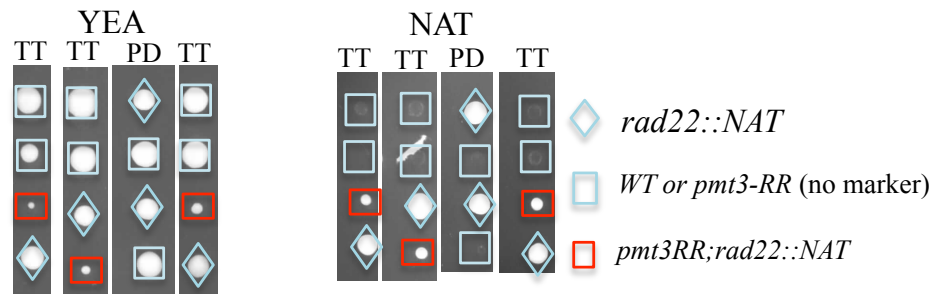


Fig. 4.14 SUMO chains mutants are sensitive to HU

Phenotype of SUMO chain mutants. 10 μl of 10 fold serially diluted cultures were plated onto media as indicated, and incubated at 30°C for 3 days.

A.



B.

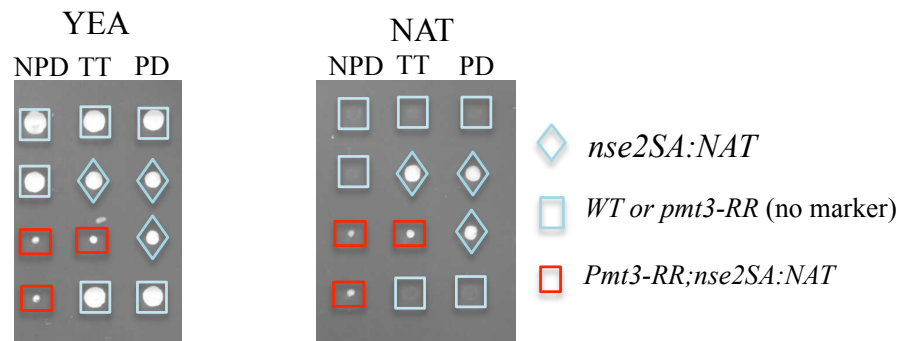


Fig. 4.15 SUMO chain mutant is slow growing on HR mutants background

A. Tetrad dissection to isolate *pmt3-RR;rad22Δ* double mutant

B. Tetrad dissection to isolate *pmt3-RR;nse2SA* double mutant

Represented tetrads were chosen from a pool of 20 dissected tetrads

4.5.2.4 SUMO chain mutant is not a spontaneous suppressor of the *ulp2Δ* mutant phenotype

In *S. cerevisiae* a SUMO chain mutant (*SMT3-allR*) shows no growth defect and no sensitivity to genotoxins but it reverses the sensitivity of the *ULP2* null mutant to hydroxyurea and thiabendazole (Bylebyl et al., 2003). The *ULP2Δ* strains accumulate high Mr poly-SUMO species and the results suggest that its sensitivity to genotoxins is due to the high levels of poly-SUMO species. In *S. pombe* the *ulp2* null mutant readily acquires suppressors and it was reported that a double mutant *ulp2Δ;pmt3-RR* reverses the phenotype of *ulp2Δ* in response to hydroxyurea (Prudden et al., 2011). To see if the spontaneously arising suppressor of *ulp2Δ* is a SUMO chain mutant, a *ulp2::KAN* strain with acquired suppressor(s) was crossed with a wild type strain and tetrads were dissected to isolate the *ulp2Δ* from the suppressor (fig. 4.16 A). The resulting strains (wild type, *ulp2Δ*;suppressor, suppressor and *ulp2Δ*) were assessed for their response to hydroxyurea (fig. 4.16 B). The *ulp2Δ*;suppressor strain behaves like wild type while the *ulp2Δ* strain shows increased sensitivity. Interestingly, the suppressor shows slight sensitivity, similar to that of the *pmt3-RR* strain. To verify that the SUMO chain mutant is a spontaneous suppressor of the *ulp2Δ* phenotype, the *pmt3* gene was amplified from the genomic DNA of the suppressor strain with *pmt3_F* (5'-ATGTCTGAATCACCATCAGC) and *pmt3_R* (5'-CTAAAGGCATAGATGGGTGC) primers and the PCR product was sent for sequencing. Surprisingly, the K14 and K30, the SUMO chain substrates, were not mutated (fig. 4.16 C), suggesting that other spontaneous mutations were suppressing the *ulp2Δ* phenotype. One possibility could be a mutation of *Pli1*, the E3 SUMO ligase that promotes the formation of high Mr SUMO species. Point mutations of its RING domain (C321S/H323A/C326S, (Xhemalce et al., 2004) behave like a *pli1* null strain with a drastic reduction of total sumoylation. Crossing *pli1* mutants with the *ulp2Δ* and/or sequencing the *pli1* gene of the isolated suppressor could provide insights into the homeostasis of SUMO chain formation. Further, only one colony was checked and colonies originating from different tetrads should be checked, as it is possible that *ulp2Δ* has more than one suppressor.

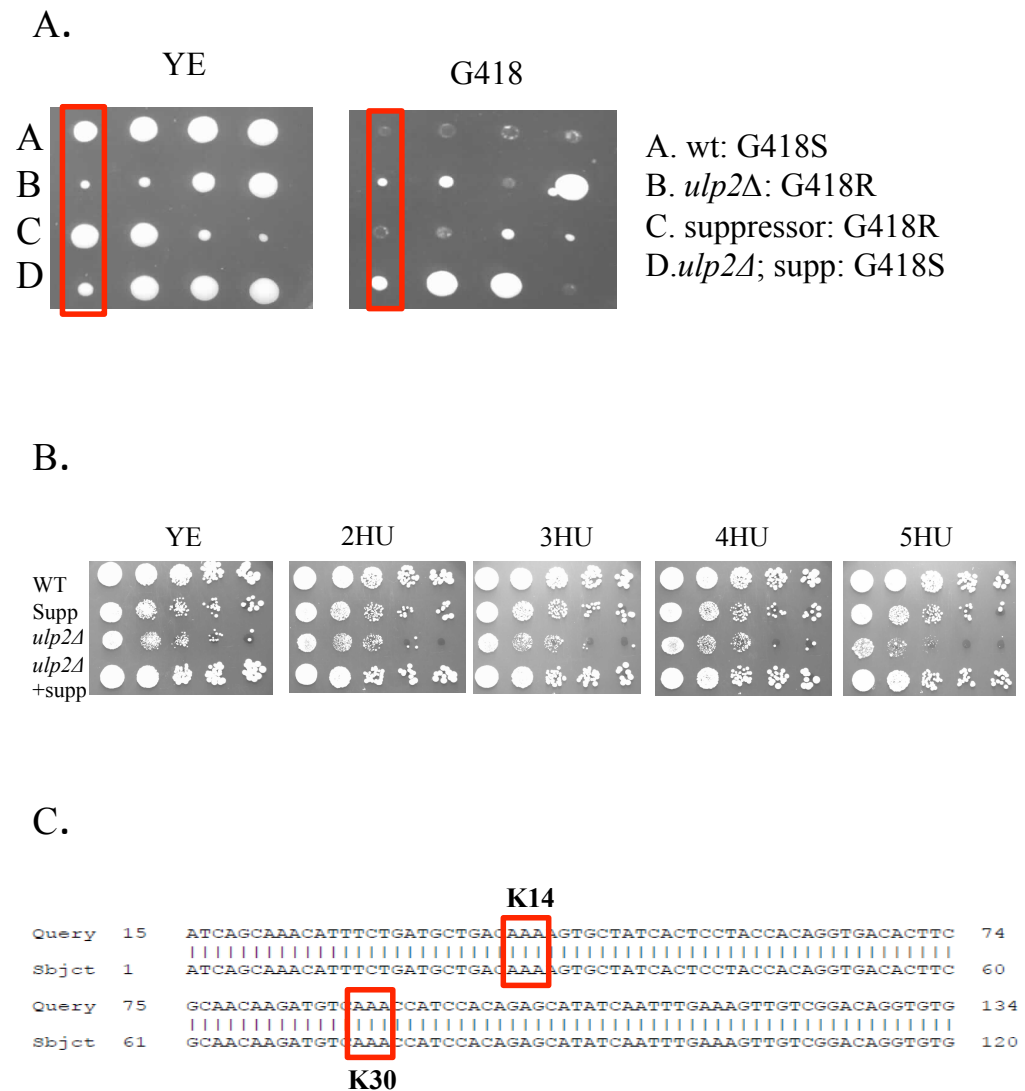


Fig. 4.16 SUMO protease *ulp2* deletion mutant has more than one suppressor

- A. Tetrad dissection to isolate *ulp2Δ* suppressor (represented tetrads were chosen from a pool of 20 dissected tetrads)
- A. Hydroxyurea sensitivity of the *ulp2Δ* suppressor
- B. Sequence alignment of *pmt3* ORF (subject) and suppressor (query). Highlighted are the lysines involved in chain formation

4.6 Discussion

In this chapter I determined the sequence requirements for SUMO chain formation *in vitro* and *in vivo* and phenotypically characterized the mutants defective in SUMO polymerization. The slight sensitivity to HU of *pmt3-RR* mutant suggests that SUMO chain formation function(s) could be S-phase specific. To identify such function(s) experimental work has to be carried out on cells synchronized in S phase. This could be achieved by working with SUMO chain mutants in a *cdc10-M17* mutant background which allows synchronization at G1/S.

Like *S. cerevisiae* Smt3 and mammalian SUMO2/3, *S. pombe* SUMO can form chains at two lysines at the N-terminal. Unlike Smt3 and SUMO2/3, which have the lysines within a SUMO consensus sequence, the *S. pombe* SUMO K14 and K30 are not within consensus sequences. Mammalian SUMO-1 was initially believed not to form chains but to terminate SUMO-2/3 chains. However it has been reported that SUMO-1 forms polymeric chains (Yang et al., 2006, Pichler et al., 2002) and four lysines, K16, K37, K39 and K46, all conserved in Pmt3 (K30, K51, K53 and K60 respectively, fig. 4.17 A, red boxes), have been identified as substrates for chain formation *in vitro* (Cooper et al., 2005). Interestingly, like *S. pombe* SUMO, none of these lysines are within SUMO consensus sequences and intriguingly only K16 (corresponding to K30 in *S. pombe* SUMO) is at the disordered N-terminal (fig. 4.17 B) while K37, K39 and K46 are part of the globular C-terminal albeit at the surface (fig. 4.17 B and C). The same study (Cooper et al., 2005) identified new sites for SUMO-2 chain formation: K5, K7 and K42 (corresponding to K46 in SUMO-1 and K60 in *S. pombe* SUMO). Interestingly the K51, K53 and K60 of *S. pombe* SUMO were identified as substrates for inefficient chain formation *in vivo* when K14 and K30 are mutated (Prudden et al., 2011). This suggests that while lysine residues at the globular C-terminal of SUMO can form chains it is unlikely that this will have functional importance, most probably due to the structural rigidity of the environment.

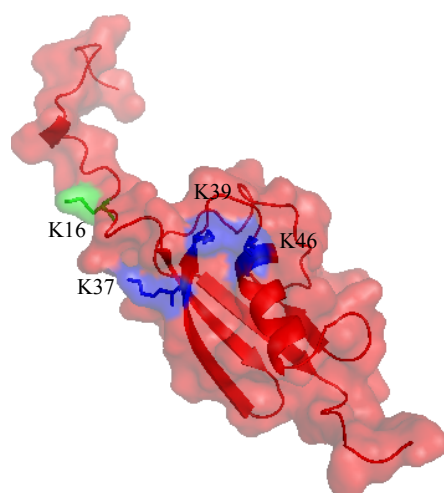
A.

Pmt3	1	MSESPSANISPAKSAITETTTGDTSQQDVKPSTEHINLKVVGDNNVEFEKIKTTTEFSK
SUMO-1	1	-----MSDQPAKPSTEDLGD-----KKEGEYIKLVIGQDSSETHFKVKMTTHLKK
SUMO-2	1	-----MADEKPKEGVKTENN-----DHINLKVAGQDGSVVQEFKIKSHTPLSK

Pmt3	61	LMKTIYCARQGKSMNSLRFLVDGERIRPDQTPAELDMEDGQIEAVLEQLGGCTHICL
SUMO-1	47	LKESYCQRQGVPMNSLRFLFEGQRIADNHTPKELGMEEDLVIEVYQEQTGGHSTV---
SUMO-2	43	LMKEYCERQGLSMRQIRERFDGQFINETDTPAQLEMEDELTIDVFQQQTGGVY----

B.

SUMO-1



C.

SUMO^{Sp}

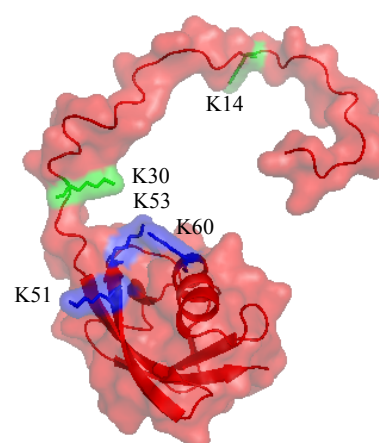


Fig. 4.17 SUMO-1 has potential SUMO chain substrate lysines at the globular C-terminal

A. Sequence alignment of SUMO-1, SUMO-2 and *S. pombe* SUMO. Highlighted are Ks identified as chain substrates in SUMO-1

B. Mapping of Ks identified as chain substrates on the SUMO-1 structure

C. Mapping of conserved Ks identified as chain substrates in SUMO-1 on the *S. pombe* SUMO model.

In this study I demonstrated that a SUMO chains mutant (*pmt3-RR*) is sensitive to hydroxyurea and is defective in an alternative DNA damage response pathway required when homologous recombination repair is impaired.

CHAPTER 5

INVESTIGATING THE FUNCTION OF PLI1

5.1 Introduction

Pli1 was identified from a yeast two-hybrid screen as an interacting partner of Sap1 (Switch-activating protein 1), an essential protein required for chromosome stability (de Lahondes et al., 2003, Xhemalce et al., 2004). Unlike the other *S. pombe* SUMO E3 ligase, Nse2, which is essential for cell viability, the *pli1* deletion mutant has no growth defects and is not sensitive to DNA damaging agents despite the fact that it displays a drastic reduction in cellular levels of sumoylation (see section 4.5.1, fig. 4.13B). It is mildly sensitive to TBZ, a microtubule inhibitor (Xhemalce et al., 2004). Further, the *pli1* null mutant has been shown to be defective in silencing at centromeric heterochromatic repeat sequences and in maintaining an artificial minichromosome. These data, taken together with the fact that a SP-RING mutant has a phenotype similar to that of the deletion mutant (Xhemalce et al., 2004), suggest that Pli1-dependent sumoylation is required for proper centromeric function.

5.1.1 *S. pombe* centromeres

S. pombe centromeres contain a unique central core sequence (*cnt*) flanked by inverted repetitive structures: inner most repeats (*imr*) and outer most repeats (*otr*) (fig. 5.1) (Nakaseko et al., 1987, Clarke et al., 1986, Nakaseko et al., 1986). The outer most repeat further contains two inverted sequences, *dh* and *dg*. The *dg* repeat is the only region that is highly conserved and is essential for centromeric functions in mitosis and

Fig. 5.1 Graphical representation of *S.pombe* chromosomes and the centromeric region of chromosome III

- A. Schematic representation of the *S. pombe* chromosomes
- B. The centromeric region of the Chromosome III as represented on the genedb website;
link:<http://old.genedb.org/genedb/Search?organism=pombe&name=SPCC1259.13&isid=true>
- C. Schematic representation of the centromeric repeats and the tRNA genes of the Chromosome III

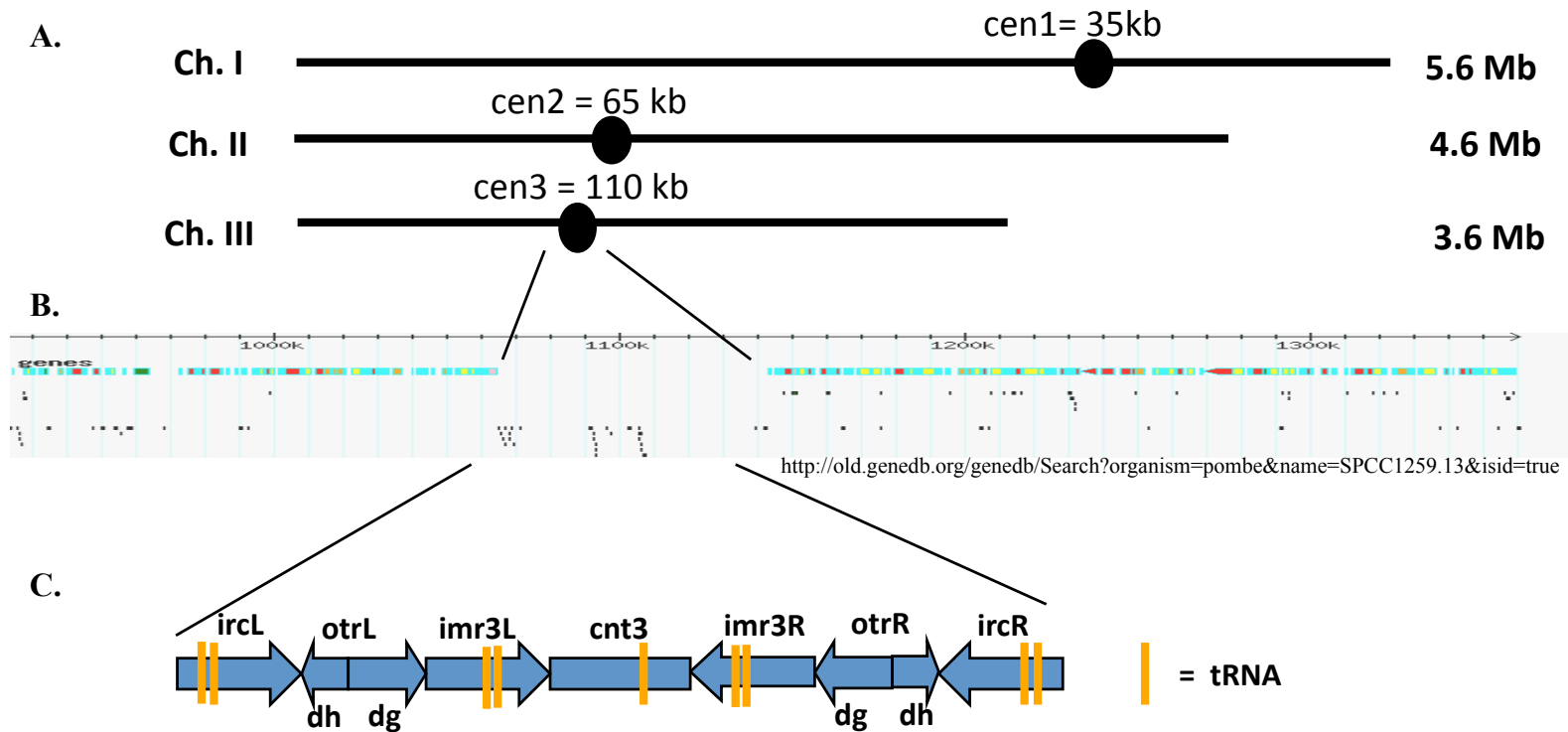


Fig. 5.1 Graphical representation of *S.pombe* chromosomes and the centromeric region of chromosome III

meiosis (Baum et al., 1994). The centromeres are also flanked by single or clustered tRNA genes believed to function as barriers for heterochromatin (Scott et al., 2006). The centromeric regions have been identified as hotspots for gross genomic rearrangements (GCRs) that result in loss of heterozygosity (LOH), a frequent cause of tumorigenesis. Repetitive DNA sequences and tRNA genes are known to be replication fork barriers, the former through formation of unusual DNA structures (Deshpande and Newlon, 1996, Mirkin, 2006). For DNA damage repair and/or stalled replication fork restart, cells employ various mechanisms including homologous recombination; the repetitive structures facilitate hyper-recombination between non-allelic DNA fragments and this can lead to GCRs.

While *S. pombe* centromeres are the best characterized complex centromeres, mainly due to the knowledge of their nearly complete sequence (Wood et al., 2002), given the close relation between fork stalling and DNA damage repair by homologous recombination and the complex structures and mechanisms at centromeric regions, the mechanism by which cells prevent GCRs arising at this region remains unclear.

5.1.2 Using the artificial minichromosome Ch16 to determine mutation rates

The aim of this project was to establish how SUMO chains, Pli1 and Nse2 are involved in processes that maintain a non-essential minichromosome by analyzing spontaneous chromosomal rearrangements using the artificial but stable minichromosome Ch16 that contains the centromeric region of chromosome III (Niwa, 1986, fig 5.2 A).

To look at minichromosome stability, Ch16 was adapted to contain selectable marker genes: an *ade6-M216* allele which complements the *ade6-M210* allele on chromosome III to prevent the accumulation of a red intermediate in the adenine biosynthesis pathway (Leupold, 1964; fig. 5.2 B) and a *kanMX6* gene that confers resistance to genitcin (G418) were introduced on the right arm (construct Ch16-MGH kindly donated by Humphrey lab, Gray Institute), and a *ura4* gene was introduced on the left arm at the *chk1* locus close to the centromere (created by Dr. F.Z.Watts, University of

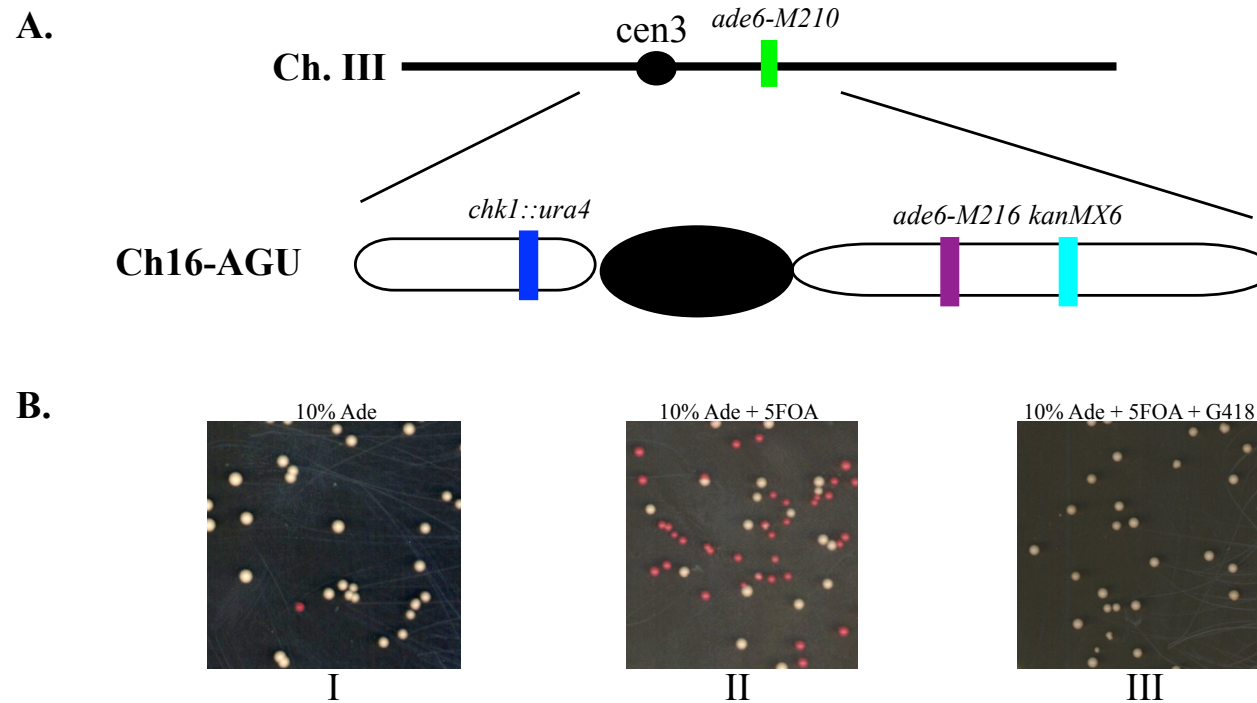


Fig. 5.2 Using the minichromosome Ch16-AGU to determine spontaneous mutation rates

A. Graphical representation of minichromosome Ch16-AGU based on chromosome III

B. Colonies plated on selective media: red colonies denote loss of *ade-216* allele (panels I and II); colonies on 5FOA media lost the *ura3* gene (panels II and III); colonies on G418 media retained the *kanMX6* gene.

Sussex). The mutant strains containing the minichromosome Ch16-AGU were created by crossing and tetrad analysis (see table 5.1). The mutant strains were grown for a minimum of thirty generations to allow for spontaneous mutations to take place. A predetermined number of cells was plated on medium containing a tenth of the required amount of adenine to identify colonies that had retained or lost the *ade6-M216* allele. The loss or maintenance of *ura4* gene was determined on medium containing 5FOA and medium lacking uracil respectively. Spontaneous mutation rates were calculated by selecting colonies that lost the *ura4* gene together with the *ade6-M216* allele and *kanMX6* cassette, or that had lost the *ura4* gene but maintained the *ade6-M216* allele and the *kanMX6* cassette (fig. 5.2 B). The results were expressed as relative to mutation rates of the wild type strain and compared with results from previous studies (table 5.2). Moreover, as Pli1 and Nse2 has been shown to facilitate the sumoylation of the DNA damage repair proteins Rad22 and Smc6 respectively (Ho et al., 2001, Andrews et al., 2005), the mutation rates for the sumoylation mutants were compared to those previously determined for mutants of these proteins (table 5.3).

Concomitant loss of *ura4* and *ade6-M216/kanMX6* is consistent with minichromosome loss while loss of *ura4* and retention of *ade6-m216* and *kanMX6* is consistent with the occurrence of chromosomal rearrangements (Nakamura et al., 2008). It has to be noted that loss of all marker genes due to chromosomal rearrangements, while maintaining the minichromosome, cannot be distinguished from loss of the minichromosome in this assay. However, loss of the minichromosome occurs at a rate of approximately 10^{-3} per cell per generation in wild type cells (some studies reported a lower rate; see table 5.2) while chromosomal rearrangements occur at rates of approximately 10^{-5} - 10^{-6} per cell per generation and therefore loss of all marker genes due to chromosomal rearrangements, while maintaining the minichromosome, are considered negligible and included in the loss of minichromosome rates.

Table 5.1

strain	Selection	Created by
<i>pli1::natMX6</i>	<i>ura4⁺, ade6⁺, KAN^R, NAT^R</i>	F.X. Ogi, University of Sussex
<i>nse2-SA:natMX6</i>	<i>ura4⁺, ade6⁺, KAN^R, NAT^R</i>	F.Z.Watts, University of Sussex
<i>pmt3-RR:leu1</i>	<i>ura4⁺, ade6⁺, leu1⁺, KAN^R</i>	this study
<i>rad22::natMX6</i>	<i>ura4⁺, ade6⁺, KAN^R, NAT^R</i>	F.Z.Watts, University of Sussex

Table 5.1 Mutant strains containing the minichromosome Ch16-AGU used in this study

Table 5.2

strain	Minichromosome loss		<i>ura4</i> loss (GCRs)		Reference
	rate	Relative to wt	rate	Relative to wt	
wild type	2×10^{-3}	1	ND	ND	Niwa <i>et al.</i> , 1989
wild type	3.4×10^{-5}	1	2.9×10^{-5}	1	Nakamura <i>et al.</i> , 2008
<i>pli1Δ</i>	0.012	12	10^{-3}	>10	Xhemalce <i>et al.</i> , 2004
<i>pmt3Δ</i>	0.06	165	ND	ND	Tanaka <i>et al.</i> , 1999
<i>rhp51^{rad51}Δ</i>	1.8×10^{-3}	515	5.6×10^{-3}	192	Nakamura <i>et al.</i> , 2008
<i>swi6Δ</i>	0.05	100	ND	ND	Allshire <i>et al.</i> , 1995
<i>swi6Δ</i>	1.47	>6	ND	ND	Ekwall <i>et al.</i> , 1996
<i>clr4Δ</i>	2.81	40	ND	ND	Bayne <i>et al.</i> , 2010
<i>smc6-X</i>	0.37	74	ND	ND	Murray <i>et al.</i> , 1994
<i>ku70Δ</i>	1.4×10^{-3}	8	ND	ND	Manolis <i>et al.</i> , 2001

ND = not determined

Table 5.2 Published spontaneous mutations rates obtained by using the Ch16 assay

Table 5.3

strain	Minichromosome loss		<i>ura4</i> loss (GCRs)		Determined by
	rate	Relative to wt	rate	Relative to wt	
<i>rad22Δ</i>	6×10^{-3}	30	1.6×10^{-4}	55	F.X. Ogi, University of Sussex
<i>rhp51Δ</i>	2×10^{-3}	10	9×10^{-5}	31	F.X. Ogi, University of Sussex
<i>rad50Δ</i>	0.23	133	3.6×10^{-5}	12	F.X. Ogi, University of Sussex
<i>rqh1Δ</i>	1.2×10^{-2}	60	5.4×10^{-5}	18	F.X. Ogi, University of Sussex

Table 5.3 Frequency of genomic rearrangements obtained by using the Ch16 assay

5.2 Sumoylation mutants show an increased mutation rate

To further investigate the function of SUMO in maintaining the minichromosome, the rates of spontaneous loss of the *ura4*, *ade6-216* and *kanMX6* marker genes in SUMO mutants were compared to those of wild type.

Cell cultures from single colonies were grown in YE liquid medium for a minimum of 30 generations to allow spontaneous events to take place. To obtain statistically relevant data seven cultures from each mutant were grown concomitant with seven cultures of wild-type cells under the same conditions and each experiment was carried out three times. 500 cells were plated on 10% adenine media as a control, 10^5 cells were plated on 10% adenine and 5FOA media to select for colonies that lost *ura4* gene but maintained the *ade-216* allele (white colonies, rearrangements of CH16-AGU) and for colonies that lost both the *ura4* gene and the *ade6-216* allele (pink colonies, loss of Ch16-AGU). To further ensure that loss of *ade-216* allele is due to loss of the minichromosome and not due to homologous recombination with chromosomal *ade-210* allele, 10^5 cells were plated on 10% adenine medium containing 5FOA and G418. All colonies on this medium were expected to be white, confirming that the *ade-216* allele and the *kanMX6* gene are maintained or lost together and in a similar number to the white colonies on the 10% adenine and 5FOA media.

5.2.1 Sumoylation mutants show an increased rate of minichromosome loss

To determine whether the sumoylation mutants *pli1Δ*, *nse2-SA* and *pmt3-RR* are defective in maintaining the minichromosome, red colonies from the 10% adenine and 5FOA media were counted and the relative mutation rates were calculated (table 5.4 and figure 5.3). The mutation rates per cell per generation was calculated by means of Luria-Delbrück fluctuation analysis (Luria and Delbruck, 1943) using the method of median (Lea DE, 1949) (tables 5.4 and 5.5). The heterogeneity of all mutation rates was confirmed by statistical analysis of the results by a paired t-test (95% confidence

Table 5.4

strain	No. of cultures	N_t value ^a	Lea-Coulson m value ^b	Mutation rate (Ch16 loss) ^c	Relative rate (mutant/wt)	T test p value ^d
wt	7	$2 \times 10^9 \pm 10^8$	311.5	2.3×10^{-4}	1	1
<i>pli1Δ</i>	7	$8 \times 10^8 \pm 10^7$	445.5	1.9×10^{-3}	8	0.025
<i>nse2-SA</i>	7	$7 \times 10^7 \pm 10^6$	81.2	1.4×10^{-3}	6	0.043
<i>pmt3-RR</i>	7	$6 \times 10^8 \pm 10^7$	56.0	1.6×10^{-3}	7	0.008

a Final number of cells in the culture.

b Number of mutations per culture.

c Probability of mutation per cell per generation

d T test of significant statistical differences; for $p < 0.05$ the distribution was considered significantly different to wild type;

Table 5.4 Determination of rates of minichromosome loss of SUMO mutants by fluctuation analysis

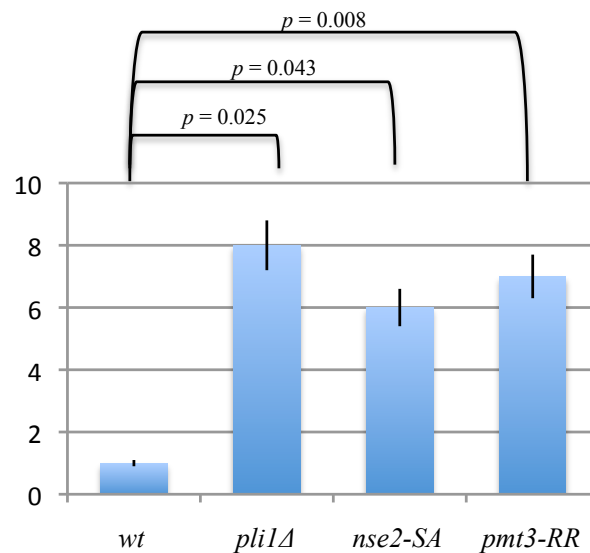


Fig. 5.3 Graphical representation of relative rates of minichromosome loss of SUMO mutants

Bars represent s.e.m from three independent experiments

interval) and a *P* value of 0.05 or less was considered significant for two-way comparison between wild type and mutant strains (Pierron et al., 2011).

All three mutants displayed the same order of magnitude of rate of minichromosome loss, with *nse2-SA* having the highest and the SUMO chain mutant, *pmt3-RR*, the lowest values. The rate for *pli1Δ* was similar to that of previously published data (Xhemalce et al., 2004) but lower than that of the homologous recombination mutant *rad22Δ* (table 5.3). These results suggest that sumoylation is required for cells to maintain the minichromosome.

5.2.2 Sumoylation mutants show an increased rate of gene loss

To determine whether sumoylation mutants are defective in preventing chromosomal rearrangements, white colonies from the 10% adenine and 5FOA and the 10% adenine, 5FOA and G418 plates were counted and the mutation rate calculated as described above (table 5.5 and figure 5.4). The sumoylation mutants display similar relative mutation rates with *nse2-SA* having the highest and SUMO chain mutant, *pmt3-RR*, the lowest values. The rate for *pli1Δ* was similar to that previously published (Xhemalce et al., 2004) but lower than that of the homologous recombination mutant *rad22Δ* (table 5.3).

5.3 Different mutant backgrounds display different chromosomal rearrangements

The homologous recombination protein Rad22/Rad52 has been shown to prevent gross chromosomal rearrangements (Cullen et al., 2007). Further studies identified the homologous recombination proteins Rhp51/Rad51, Rhp55/Rad55 and Rhp57/Rad57 as having roles in break-induced isochromosome formation (Tinline-Purvis et al., 2009) using an induced double strand break assay. Pli1 facilitates the sumoylation of the homologous recombination protein Rad22. Therefore it was of interest to determine

whether *rad22Δ* and *pli1Δ* mutants display the same type of chromosomal rearrangements.

Loss of the *ura4* gene from the minichromosome could be the result of three different mechanisms (fig. 5.5): gene conversion at the *chk1* locus by recombination between the minichromosome and endogenous Ch. III; recombination between the DNA repeats from the left arm with homologous repeats on the right arm and subsequent duplication of the right arm (isochromosome formation) of the minichromosome; recombination between the DNA repeats of the minichromosome left arm with DNA repeats from the chromosome III left arm, followed by replication of the chromosome III left arm (break-induced replication) (fig. 5.5) (Nakamura et al., 2008).

To analyse the structure of the Ch16-AGU that lost the *ura4* marker, agarose embedded chromosomal DNA from wild type, sumoylation mutants and *rad22Δ* white colonies from 10% adenine and 5FOA media were analyzed by PFGE using *S. cerevisiae* conditions (Herschleb et al., 2007). This allows the separation of chromosomal DNA up to 1500 kb. Chromosomal DNA from white colonies from 10% adenine media containing the unmodified Ch16-AGU was used as control and the minichromosome can be visualized, after ethidium bromide staining, at 530 kb (fig. 5.6 A, lane 1, all panels).

Three outcomes can be identified from the wild type and sumoylation mutants: a chromosomal element at the same size as the original Ch16-AGU (Ch16-AG, fig. 5.6 A panel I lanes 5 and 6, panel II lane 4, panel III lane 3, panel IV lanes 2 and 3, panel V lane 4), a larger chromosomal element at approximately 700 kb (Ch16-AG-L, fig. 5.6 A panel I lanes 2, 3 and 4, panel II lane 2, 3 and 5, panel III lane 6, panel IV lanes 4, 5 and 6, panel V lane 2) and a lack of a chromosomal element below 1500 kb (fig. 5.6 A panel III lanes 2, 4 and 5, panel V lanes 3 and 6). A small number of samples displayed two chromosomal elements, a Ch16-AG together with a Ch16-AG-L (fig. 5.6 panel II, lane 6). Interestingly, the types of rearrangements in *pli1Δ* cells differ from those in the homologous recombination mutant *rad22Δ* cells. In *rad22Δ* cells a chromosomal element at the same size as the original Ch16 (Ch16AG, fig. 5.6 A, panel VI, lane 2), was identified but most of the samples displayed chromosomal elements of various

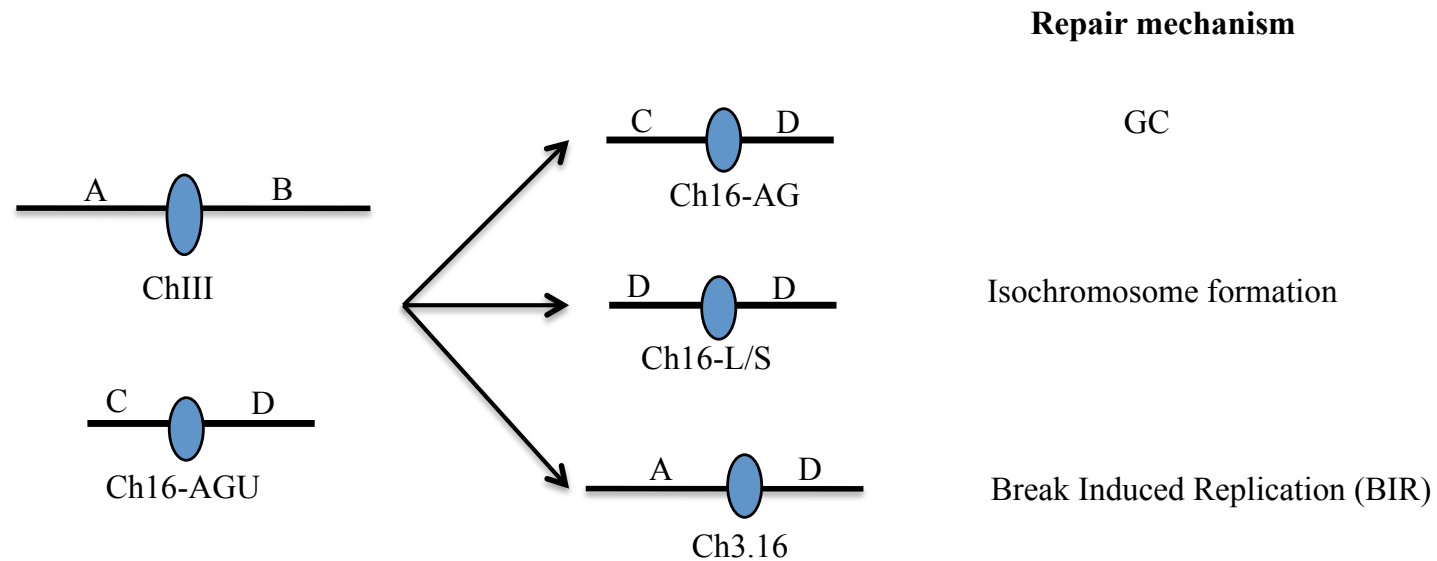


Fig. 5.5 Possible intra- and interchromosomal rearrangements following DNA damage that result in loss of *ura4* gene from the left arm (C) of Ch16-AGU and repair mechanisms involved in each type of rearrangement

Fig. 5.6 Different mutant backgrounds give rise to different chromosomal rearrangements

- A. Ethidium bromide stained chromosomal and minichromosomal DNA separated by PFGE under *S. cerevisiae* conditions. *S. cerevisiae* genomic DNA was used as ladder.
- B. Ethidium bromide stained chromosomal and minichromosomal DNA separated by PFGE under *S. pombe* conditions.

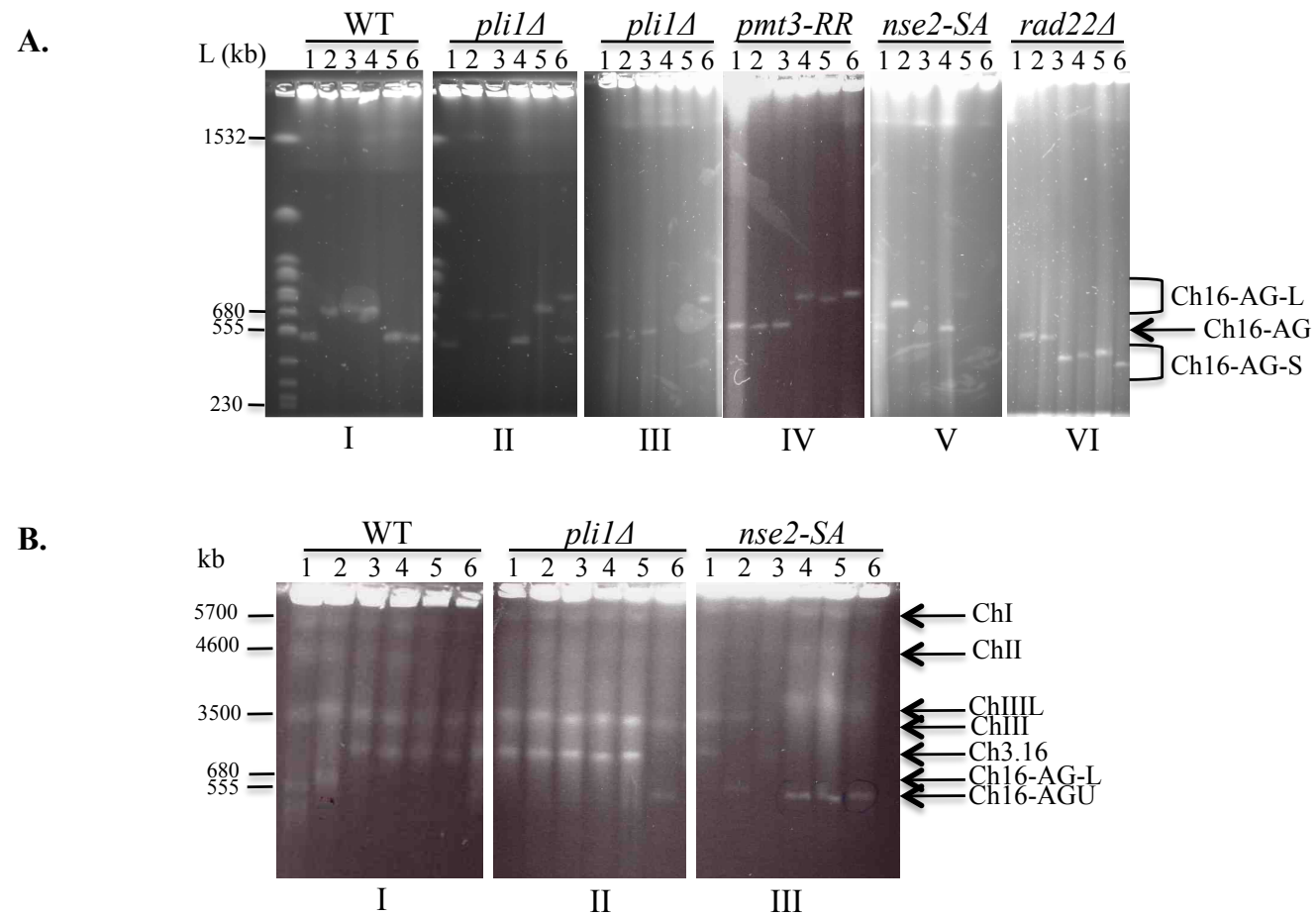


Fig. 5.6 Different mutant backgrounds give rise to different chromosomal rearrangements

sizes, all smaller than the original Ch16-AGU (Ch16-AG-S, fig. 5.6 A, panel VI lanes 3 – 6).

In some DNA samples the minichromosome was not detected. However, all DNA samples originated from strains containing the *ade-216* allele and the *kanMX6* gene. They should therefore contain some sequences deriving from the Ch16-AGU. The samples when such elements could not be identified by electrophoresis using *S. cerevisiae* conditions (fig. 5.6 A, panel III lanes 2, 4 and 5, and panel V lanes 3, 5 and 6), were re-analysed under *S. pombe* conditions. This allows separation of DNA up to 5.7 Mb (fig. 5.6 B). Under these conditions, after ethidium bromide staining, the three endogenous *S. pombe* chromosomes, the original minichromosome Ch16-AGU (fig 5.6 B, panel I, lane 1) and the modified Ch16-AG (fig 5.6 B, panel I, lane 2) can be identified. The samples that did not display a chromosomal element under *S. cerevisiae* conditions, display a minichromosomal element intermediate in size between the Ch.16-AGU and the endogenous Ch.III (Ch16-3) (fig. 5.6 B, panel I, lanes 3 – 6, panel II, lanes 1 – 5, panel III, lane 1). These chromosomal elements are consistent with the occurrence of recombination event between the minichromosome and the endogenous Ch. III. Interestingly, the *nse2-SA* mutant displays a modified chromosome III not identified in either wild type or *pli1Δ* strains. These data demonstrate that *pli1Δ* and *rad22Δ* cells are vulnerable to different types of chromosomal rearrangements. This suggests that Pli1 and Rad22 proteins are involved in different mechanisms that prevent chromosomal rearrangements. Interestingly, the minichromosomal rearrangements in *pli1Δ* strain are similar with those that occur in wild type cells suggesting that Pli1 is required for a general mechanism that prevents chromosomal rearrangements. The *rad22Δ* strain displays smaller size minichromosomal rearrangements, not identified in wild type cells, consistent with extensive deletions of DNA sequences. This suggests that Rad22-dependent homologous recombination inhibits chromosomal rearrangements that result in DNA deletions. Further, *rad22Δ* cells do not exhibit rearrangements between the minichromosome and the endogenous Ch. III, suggesting that Rad22 dependent homologous recombination is essential for this type of rearrangements.

5.4 Minichromosomal rearrangements in *pli1Δ* cells result in isochromosome formation

Previous studies designed to identify spontaneous GCRs in fission yeast detected the *otr* – *imr* centromeric repeats as hot spots for isochromosome formation in wild type cells (Nakamura et al., 2008). While the *irc*, *otr* and *imr* repeats are almost identical in the right and left arms of the chromosome, subtle differences can be identified using specific primers. To determine whether the same pattern of breakpoints occurs in minichromosomal rearrangements in *pli1Δ* cells, modified minichromosomes were recovered from agarose gels and PCR amplification was carried out with previously designed specific primers (fig. 5.7) as described by Nakamura et al., 2008.

Amplification with *irc3-F* and *irc3-R* primers (*irc3-F*: 5'-CATTA AAAATCAACAAGT CTTGTCC; *irc3-R*: 5'-GAAACATTTTGTAGTGTTGTTTCAGG) results in a 440 bp fragment characteristic of the left and right arm of the chromosome (fig. 5.7 A, panel I). However, the left fragment has one *ApoI* digestion site while the right fragment has two *ApoI* digestion sites. Using the unmodified Ch16-AGU four digestion fragments were detected as expected (fig. 5.7 A panel II, lane 1). When the modified minichromosome Ch16-AG from *pli1Δ* cells was used only three digestion fragments were observed, as a 347 bp fragment specific to the left arm is missing (fig. 5.7 A, panel II, lanes 2 and 3). The *imr3-in* (5'-AAGTTTTGATGCTCAACAAATGGC), *cen3-L* (5'- AACCGCAAC AAACGATTAGC) and *cen3-R* (5'-CGGAATTAGAAAGATTGATGATTG) primers are specific to the *imr* – *cnt* junction (*cnt* region is unique) and amplification results in two fragments: a 446 bp fragment specific to the left arm and a 622 bp fragment specific to the right arm (fig. 5.7 panels I and II). When the modified minichromosome Ch16-AG from *pli1Δ* cells was used as substrate both fragments were present (fig. 5.7, panels I and II lanes 2 and 3) as in the unmodified Ch16-AGU minichromosome (fig. 5.7, panels I and II lane 1). These results suggest that the *irc3* of the left arm of the modified minichromosome is missing while the *imr3-cnt3* junction is retained. The analysis of the breakpoint was extended to the *otr3-imr3* junction. Amplification using the *dh* (5'- CGTGTAATAAGGGACAAATAGG) and *imr3-out* (5'- GTGGTTAGAATTGAC AAGC) specific primers results in two fragments: a 917 bp fragment specific to the left arm and a 868 bp fragment specific for the right arm as

Fig. 5.7 Analysis of the breakpoint of Ch160-AGU in *pli1Δ* mutant cells by PCR

- A. Analysis of the *irc3* centromeric repeats on the left and right arm of the minichromosome using PCR;
- B. Analysis of the *otr3-imr3* centromeric repeats on the left and right arm of the minichromosome using PCR;

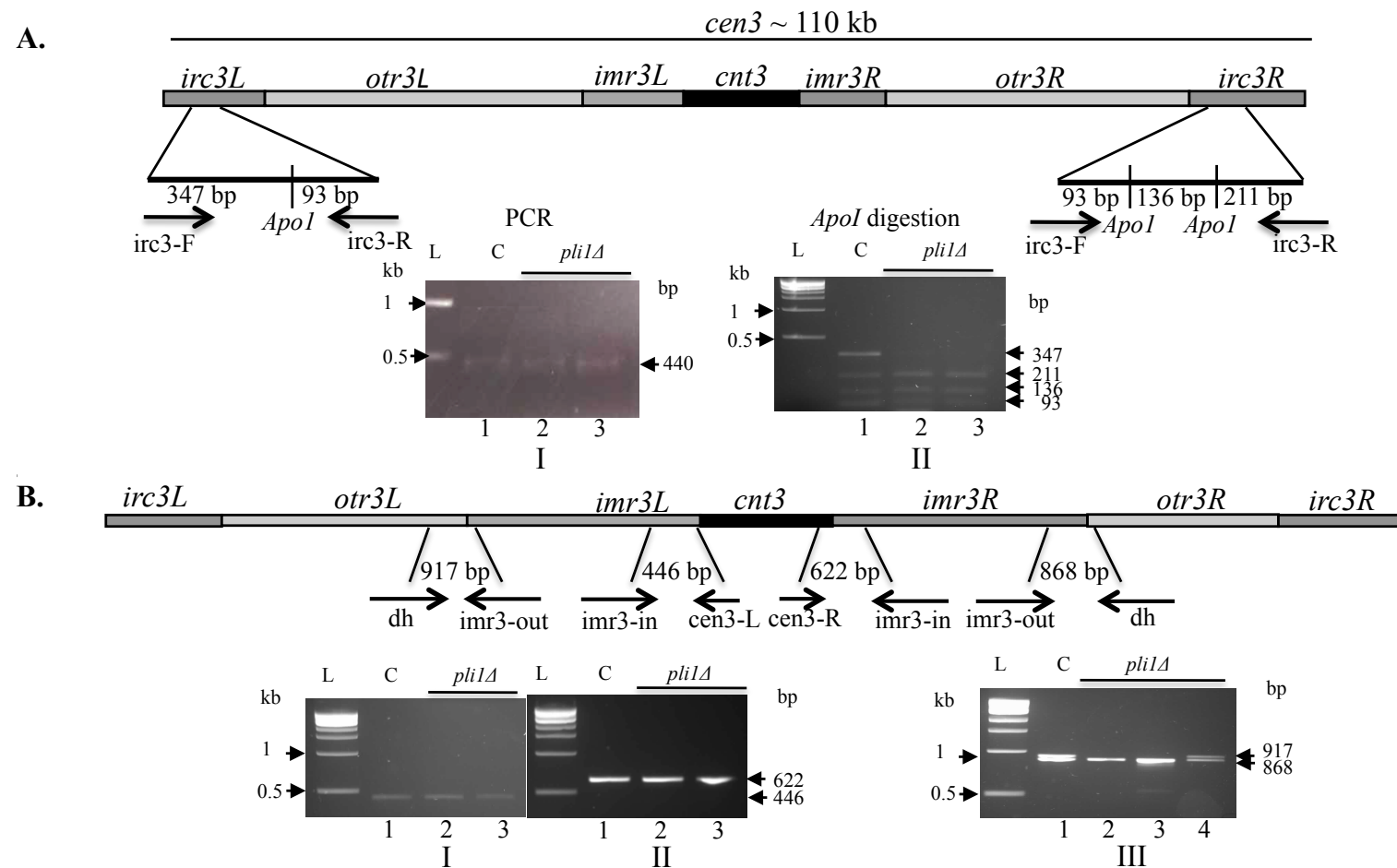


Fig. 5.7 Analysis of the breakpoint of Ch160-AGU in *pli1Δ* mutant cells by PCR

observed for the unmodified Ch16-AGU minichromosome (fig. 5.7 B, panel II, lane 1). Interestingly some isochromosomes retained the 917 bp region specific to the left arm (fig. 5.7 B, panel II, lane 4), while others lost this region (fig. 5.7 B, panel II, lanes 2 and 3).

The results from this analysis of breakpoints in *pli1Δ* cells are consistent with previous results obtained for isochromosome formation in wild type cells (Nakamura et al., 2008). This indicates that the minichromosomal rearrangements in *pli1Δ* cells are isochromosomes and these isochromosomes involve rearrangements at the *otr-imr* centromeric repeats.

5.5 Pli1-dependent sumoylation does not prevent isochromosome formation

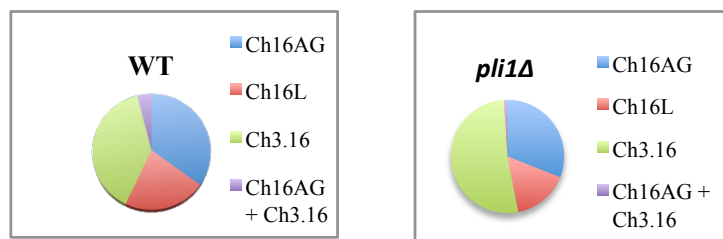
Previous studies suggest that Pli1 dependent sumoylation can prevent isochromosome formation (Xhemalce et al., 2004). To determine whether isochromosome formation occurs at higher frequency in *pli1Δ* cells than in wild type cells, a statistical survey was carried out on 100 samples of each strain.

Agarose embedded chromosomal DNA from wild type, *pli1Δ* and *rad22Δ* white colonies from 10% adenine and 5FOA media were analyzed by PFGE using *S. cerevisiae* and *S. pombe* conditions. The results from the survey are tabulated in table 5.6. Interestingly *pli1Δ* cells do not show an increased frequency of isochromosome formation compared to wild type cells but display an increased rate of recombination between the minichromosome and chromosome III (fig. 5.8 A panels I and II and fig. 5.8 B).

strain	No. of samples	Ch16-AG	Ch16L/S	Ch3.16	Ch16 + Ch3.16
wt	100	35	22	39	4
<i>pli1Δ</i>	100	31	16	52	1

Table 5.6 Determination of percentage of different chromosomal rearrangements of wild-type, *pli1Δ* and *rad22Δ* strains

A.



B.

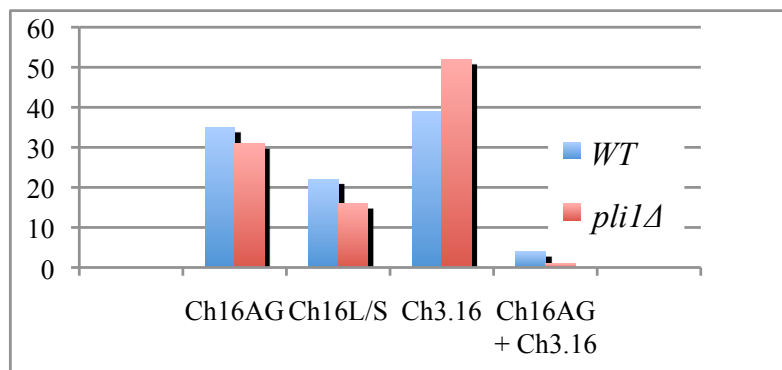


Fig. 5.8 Graphical representation of chromosomal rearrangements fractions of wild type, *pli1Δ* and *rad22Δ* strains

A. Percentage comparison of different chromosomal rearrangements for each strain

B. Percentage comparison of different strains for each type of chromosomal rearrangement

5.6 Discussion

In this study I analysed the function of the SUMO E3 ligase, Pli1, in maintaining chromosomal stability using an artificial minichromosome. The data are consistent with a function of Pli1-induced sumoylation in maintaining an artificial minichromosome and in preventing illicit recombination between the minichromosome and endogenous Ch. III.

The *pli1* null mutant displays similar spontaneous chromosomal rearrangements to those observed in wild type strain but it does not exhibit an increased frequency of isochromosome formation as previously suggested (Xhemalce et al., 2004). This is in contrast with a *rad22Δ* strain, which displays an increased frequency of rearrangements of the minichromosome but no recombination between the Ch.16-AGU and the endogenous chromosome III. The minichromosome rearrangements detected in the *rad22Δ* cells produce species that are smaller than the isochromosomes observed in the *pli1Δ* and wild type strains and smaller than the original minichromosome, suggesting that this type of rearrangement occurs after chromosomal deletions. These results suggest that Pli1-dependent sumoylation of Rad22 does not function in preventing isochromosome formation, chromosomal rearrangements associated with DNA deletions, or in preventing illicit interchromosomal recombination. However, the increases rate of interchromosomal GCRs due to illicit recombination in the *pli1* null mutant strain is consistent with previous data that identify sumoylation as an important mechanism in preventing deleterious recombinogenic events at damaged replication forks (Branzei et al., 2006).

The increased loss of an artificial minichromosome is consistent with failure to repair double strand breaks either during replication or post-replication and/or with defects in chromosome segregation. The increased frequency of the *pli1* null mutant in minichromosome loss and the sensitivity to the microtubule inhibitor TBZ suggest that Pli1 dependent sumoylation is required for proper chromosome segregation. The centromere is packed within the heterochromatin and is the site of the kinetochore. Mutations of heterochromatin proteins, such as Clr4 and Swi6, are characterized by sensitivity to TBZ (Ekwall et al., 1996) and elevated loss of chromosomes (Allshire et

al., 1995). Both Clr4 and Swi6 were identified as SUMO targets *in vivo* and defective sumoylation of Swi6 was shown to cause ineffective silencing at heterochromatin (Shin et al., 2005). While no specific SUMO E3 ligase was identified as facilitating the sumoylation of either Clr4 or Swi6, it cannot be excluded that Pli1 is required for normal levels of sumoylation of these heterochromatic proteins. More recently, the sumoylation of cohesin (the Smc1/3 complex) was shown to be required for the establishment of sister chromatid cohesion in *S. cerevisiae* (Almedawar et al., 2012).

Taken together, the data from this study suggest that Pli1-dependent sumoylation function in maintaining chromosomal stability at the heterochromatic centromeric repeats and this function is independent of the sumoylation of the homologous recombination protein Rad22 that is facilitated by Pli1.

CHAPTER 6

HUS5 SUMOYLATION REGULATES THE PATHWAY HOMEOSTASIS

6.1 Introduction

In recent years it has been reported that sumoylation pathway components E1, E2 and E3s are themselves post-translationally modified by SUMO. The first SUMO pathway component identified to be autosumoylated was the mammalian E3 ligase RanBP2 believed to be specific for SUMO-1 (Pichler et al., 2002). Multiple lysine residues in RanBP2 were identified that were modified by single moieties or chains of SUMO-1 and SUMO-2 using various mass spectrometry techniques (Cooper et al., 2005). The *S. pombe* and human Siz/PIAS type E3 ligases Nse2 have been shown to be autosumoylated *in vitro* but no specific modified lysine residues have been identified (Andrews et al., 2005, Potts and Yu, 2005).

Autosumoylation of the SUMO conjugating enzyme Ubc9 at K14 in human cells was identified as being required for target discrimination and to by-pass the need for an E3 ligase by creating a new interface that interacts with SIMs in the target protein (Knipscheer et al., 2008). The same study identified K153 as the only sumoylation site of the SUMO conjugating enzyme in *S. cerevisiae*. Later K157 was also identified as being modified (Ho et al., 2011). Another study reports that Rhes, a mammalian SUMO E3 ligase, facilitates sumoylation of human Ubc9 at K14, K49 and K153 (Subramaniam et al., 2010). In mammals the sumoylation of the SUMO conjugating enzyme E1 can facilitate or inhibit the sumoylation of a target protein (Knipscheer et al., 2008). In *S. cerevisiae* it has been shown that autosumoylation of Ubc9 reduces the sumoylation of septins (Ho et al., 2011).

The mammalian SAE2 protein, one of the components of the SUMO activating enzyme heterodimer, was found to be autosumoylated at K236 in the absence of Ubc9, and

sumoylated in the presence of the conjugator at four further sites: K190, K257, K271 and K275 (Truong et al., 2012). This is the first example where SUMO attaches covalently to a lysine residue without the need of the SUMO conjugating enzyme.

While it is known that the sumoylation pathway components are sumoylated in *S. pombe* (this study, Chapter 4) (Andrews et al., 2005), no specific modified lysine residues have been identified to date. Having optimized the *in vitro* sumoylation assay (see Chapter 4) this work now focuses in identifying SUMO modified lysines of the sumoylation pathway components by mass spectrometry. After identifying one SUMO modified lysine residue in the SUMO conjugating enzyme Hus5 *in vitro*, biochemical and genetic characterization of the Hus5 sumoylation function was carried out.

6.2 Strategy to identify sumoylated lysine residues by mass spectrometry

Detection of specific post-translationally modified amino acids by tandem mass spectrometry coupled with liquid chromatography (LC/MS/MS) (Larsen et al., 2006) following enzyme digestion is a well-established technique (see section 2.4.22). Trypsine, an enzyme widely used for protein digestion, cuts peptide bonds at lysine and arginine residues but not lysines modified at the ϵ amino group. This results in modified lysines being incorporated in signature peptides.

To identify sumoylated lysines by MS/MS, proteolytic digestion with trypsin was used. To overcome the possibility of modified lysines being incorporated into large peptides, a pET15b-SUMOGG construct (see Chapter 4) was modified such that the threonine residue preceding the di-glycine motif was changed to an arginine residue by site directed mutagenesis (fig 6.1 A, construct made by L. Small, University of Sussex) such that trypsin digestion results in a signature di-glycine motif on the SUMO modified lysine residues of the target protein. *In vitro* sumoylation assays using the SUMO-RGG mutant followed by trypsin digestion result in peptides containing lysine residues modified at ϵ amino group by a di-glycine tag (fig. 6.1 B). Peptides carrying the

Fig. 6.1 Strategy to identify sumoylated lysine residues by tandem mass spectrometry (MS/MS)

- A. Trypsin digestion of a sumoylated protein results in a signature peptide with a di-glycine motif (magenta-red) from SUMO. Orange arrow represent trypsin cleavage at arginine residue (green). Modified lysine of target protein are coloured blue.
- B. MS/MS spectrum of a SUMO modified peptide. The GG tag changes the mass of the peptide by 114.1 Da compared to the unmodified peptide.

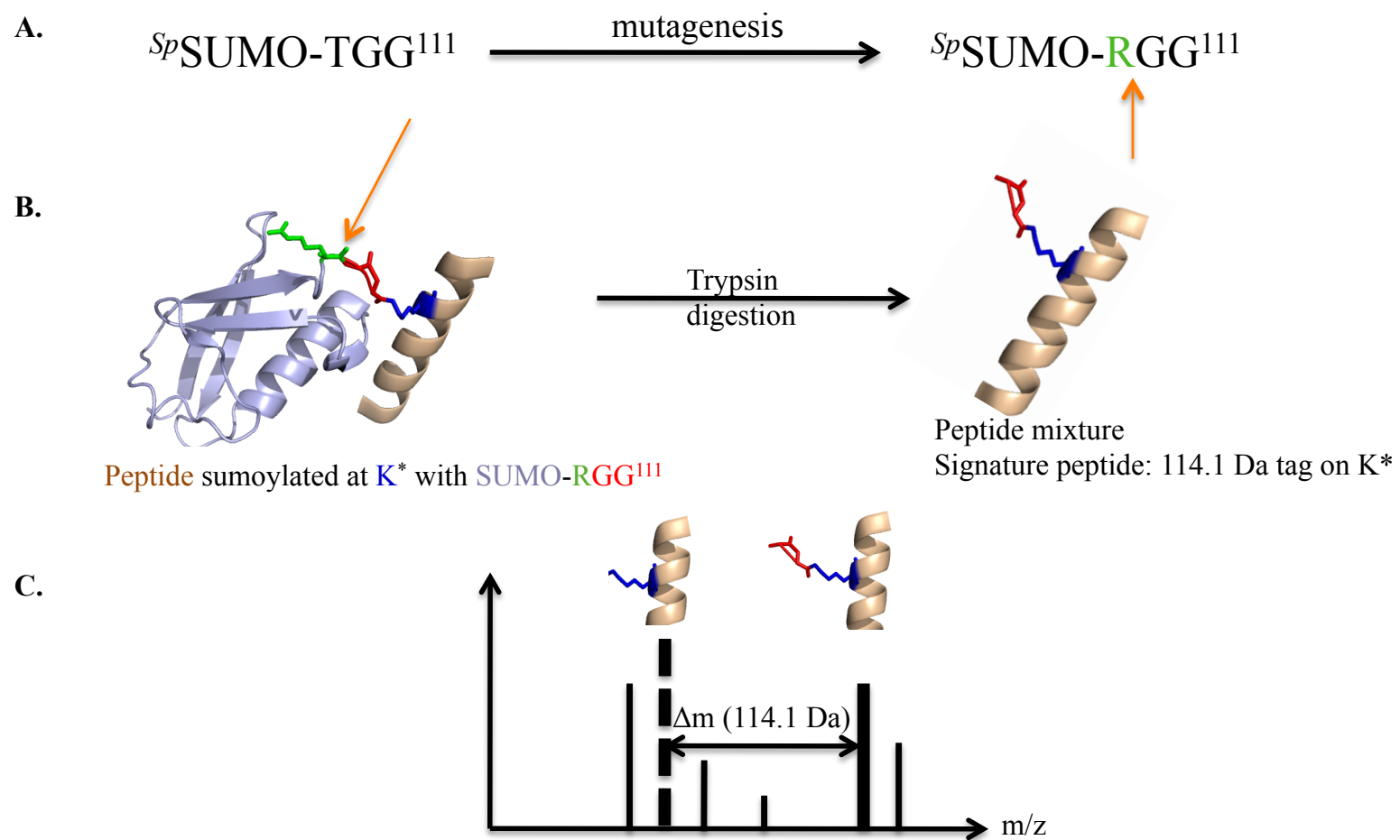


Fig. 6.1 Strategy to identify sumoylated lysine residues by tandem mass spectrometry (MS/MS)

signature di-glycine tag can be identified from mass spectra (fig. 6.1 C) following databases searches using MASCOT software.

Following *in vitro* sumoylation assays, bands were cut out from colloidal blue stained SDS-PAGE and all samples were sent to the mass spectrometry services for in-gel trypsin digestion, LC-MS/MS run and MASCOT searches (Dr. L. Bowler and M. Daniels, Proteomics Department, University of Sussex).

6.3 Sumoylation pathway components are sumoylated *in vitro* at specific lysine residues

The *in vitro* sumoylation assay was carried out as previously described (see Chapter 4) but scaled up from 20 µl to 100 µl so that proteins could be visualized by colloidal blue staining. Two reaction mixtures, one without the SUMO E3 ligase Nse2 (fig. 6.2 A) and one with Nse2 (fig. 6.2 B) were separated by SDS-PAGE and bands believed to contain sumoylated species (fig. 6.2 red boxes) were excised and send to the mass spectrometry services. The lysine residues modified by SUMO identified by MS/MS are listed in table 6.1. This is the first time that a post-translational modification has been identified by mass spectrometry at the University of Sussex.

6.3.1 The SUMO activating enzyme Fub2 is sumoylated *in vitro* at five lysine residues

K86, K172, K176, K263 and K282 of the SUMO activating enzyme Fub2 (SAE2/Uba2) were identified from the MS/MS spectra, peptide mass fingerprints, sequence queries and MS/MS ion searches using the MASCOT search engine (see section 2.4.22; fig. 6.3, 6.4, 6.5, 6.6 and 6.7 respectively) (Perkins et al., 1999). None of the identified sumoylated lysines in *M. musculus* or *S. pombe* are in a sumoylation consensus sequence (Ψ-K-X-E). While the modified lysines in the mammalian SAE2/Uba2 are all clustered in the active cysteine domain (fig. 6.8) (Truong et al., 2012), the model of *S. pombe* Fub2 suggests that K86 is located in the adenylation domain and K172, 176, 263 and 282 are located in the active cysteine domain (fig. 6.9).

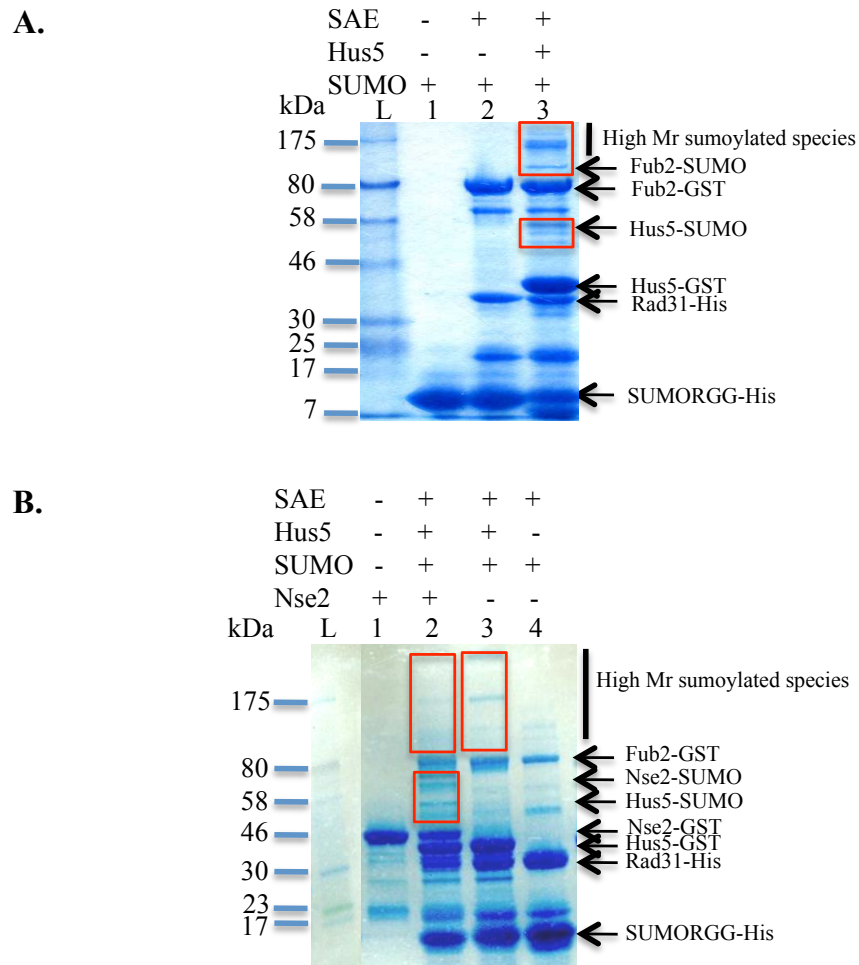


Fig. 6.2 *In vitro* sumoylation assay to identify sumoylated lysine residues by tandem mass spectrometry (MS/MS)

A. Colloidal blue staining of SDS-PAGE of *in vitro* sumoylation assay with SUMO-RGG mutant, SAE and the conjugating enzyme.

B. Colloidal blue staining of SDS-PAGE of *in vitro* sumoylation assay with SUMO-RGG mutant, SAE, the conjugating enzyme and the E3 ligase Nse2.

Red boxes represents excised bands sent to mass spectrometry services.

Substrate	Sumoylated Ks identified in this study	Sumoylated Ks in <i>Hs</i>	Sumoylated Ks in <i>Sc</i>
Hus5/Ubc9	50	14 Knipscheer <i>et al.</i> , 2008 146 Hsioa <i>et al.</i> , 2009 14, 49, 153 Subramaniam <i>et al.</i> , 2010	153, 157 Knipscheer <i>et al.</i> , 2008 Ho <i>et al.</i> , 2011
Fub2/Uba2	86,172, 176, 263, 282	190, 236, 257, 271, 275 Truong <i>et al.</i> , 2012	Not reported
Nse2/Mms21	134, 229, 247	Not reported	Not reported
SUMO	30	11 Tatham <i>et al.</i> , 2001	11, 15, 19 Bylebyl <i>et al.</i> , 2003

Table 6.1 Sumoylated lysine residues identified in Uba2^{Hs/Sc}/Fub2^{Sp}, Ubc9^{Hs/Sc}/Hus5^{Sp} and Nse2^{Sp/Hs}/Mms21^{Sc}

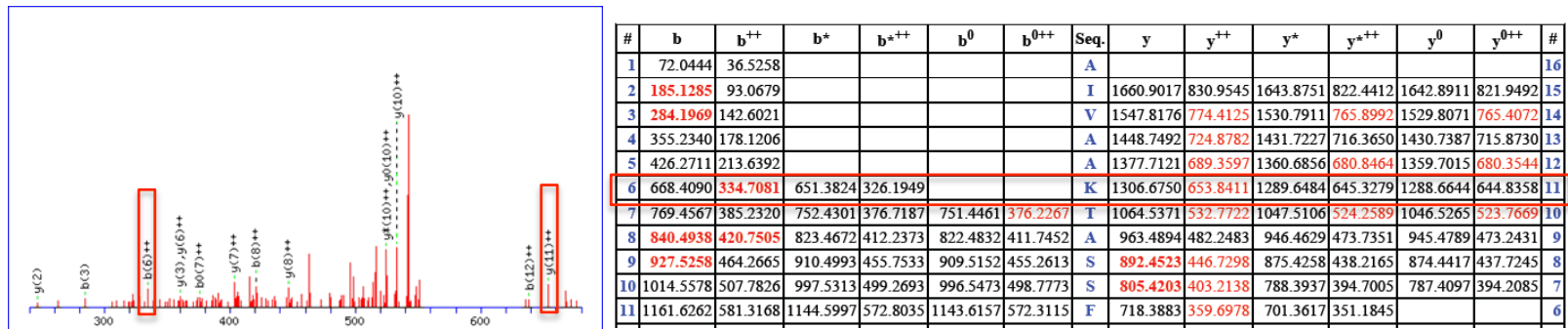
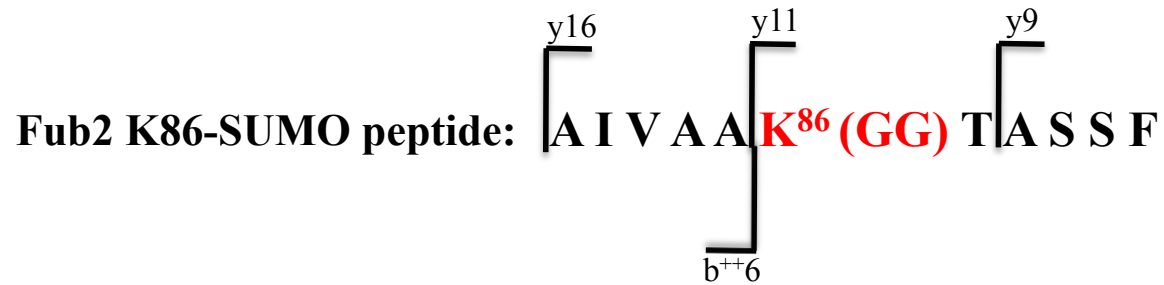


Fig. 6.3 MS/MS fragmentation of Fub2 peptide sumoylated at K86

Highlighted in boxes are the b and y ions corresponding to K86

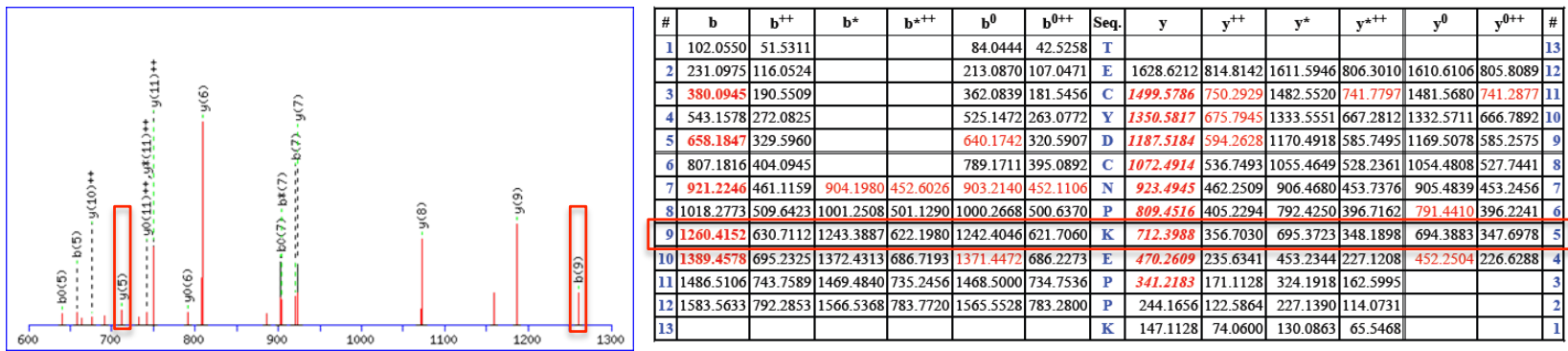
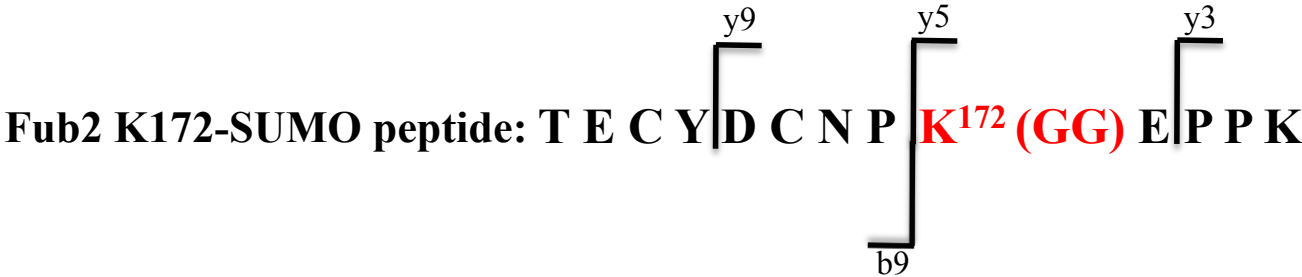
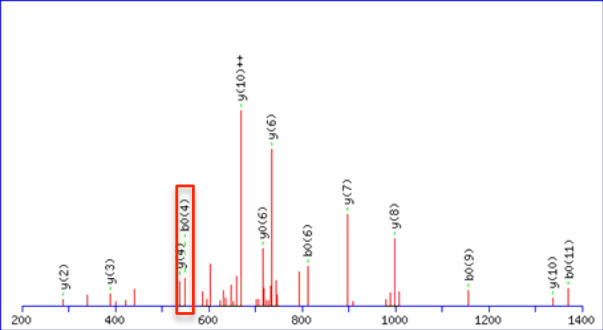
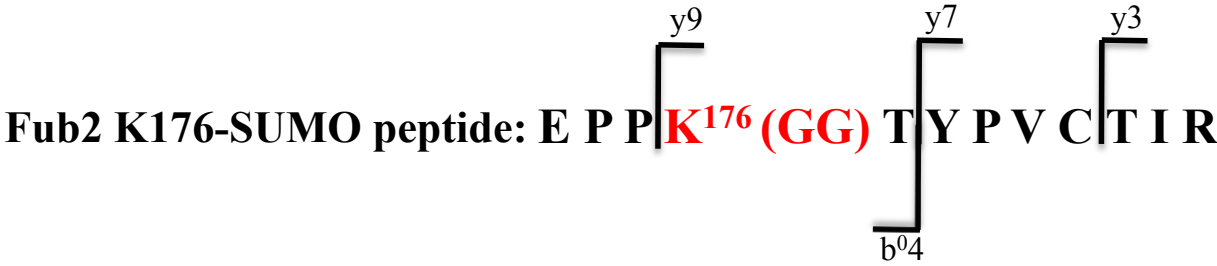


Fig. 6.4 MS/MS fragmentation of Fub2 peptide sumoylated at K172

Highlighted in boxes is the y ion corresponding to K50



#	b	b ⁺⁺	b [*]	b ⁺⁺⁺	b ⁰	b ⁰⁺⁺	Seq.	y	y ⁺⁺	y [*]	y ⁺⁺⁺	y ⁰	y ⁰⁺⁺	#
1	130.0499	65.5286			112.0393	56.5233	E							12
2	227.1026	114.0550			209.0921	105.0497	P	1434.7232	717.8652	1417.6967	709.3520	1416.7126	708.8600	11
3	324.1554	162.5813			306.1448	153.5761	P	1337.6704	669.3389	1320.6439	660.8256	1319.6599	660.3336	10
4	566.2933	283.6503	549.2667	275.1370	548.2827	274.6450	K	1240.6177	620.8125	1223.5911	612.2992	1222.6071	611.8072	9
5	667.3410	334.1741	650.3144	325.6608	649.3304	325.1688	T	998.4798	499.7435	981.4532	491.2303	980.4692	490.7382	8
6	830.4043	415.7058	813.3777	407.1925	812.3937	406.7005	Y	897.4321	449.2197	880.4056	440.7064	879.4215	440.2144	7
7	927.4571	464.2322	910.4305	455.7189	909.4465	455.2269	P	734.3688	367.6880	717.3422	359.1748	716.3582	358.6827	6
8	1026.5255	513.7664	1009.4989	505.2531	1008.5149	504.7611	V	637.3160	319.1616	620.2895	310.6484	619.3055	310.1564	5
9	1175.5224	588.2648	1158.4958	579.7516	1157.5118	579.2595	C	538.2476	269.6274	521.2211	261.1142	520.2370	260.6222	4
10	1276.5701	638.7887	1259.5435	630.2754	1258.5595	629.7834	T	389.2507	195.1290	372.2241	186.6157	371.2401	186.1237	3
11	1389.6541	695.3307	1372.6276	686.8174	1371.6436	686.3254	I	288.2030	144.6051	271.1765	136.0919			2
12							R	175.1190	88.0631	158.0924	79.5498			1

Fig. 6.5 MS/MS fragmentation of Fub2 peptide sumoylated at K176

Highlighted in boxes are the y and b ions corresponding to K176

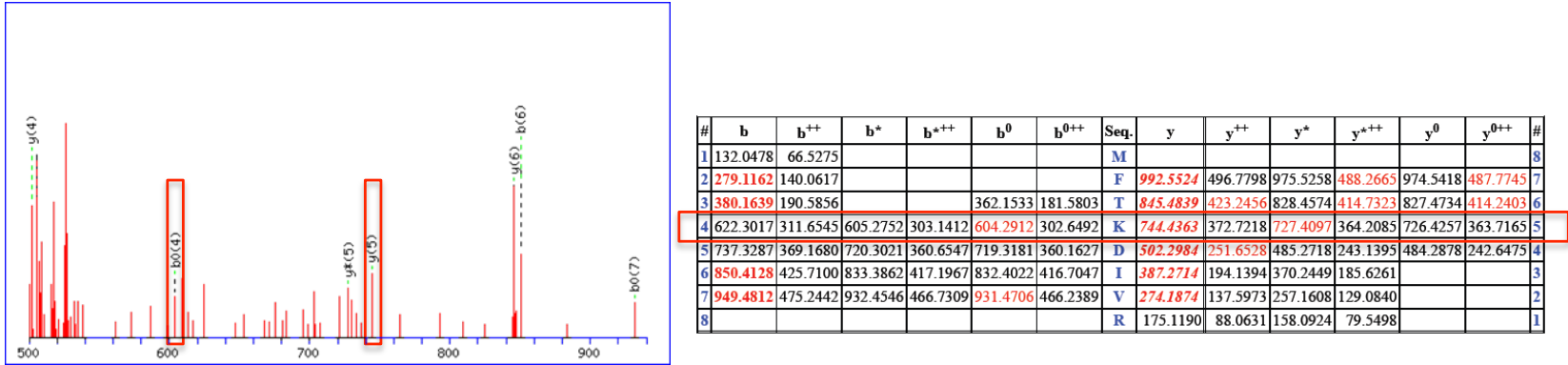
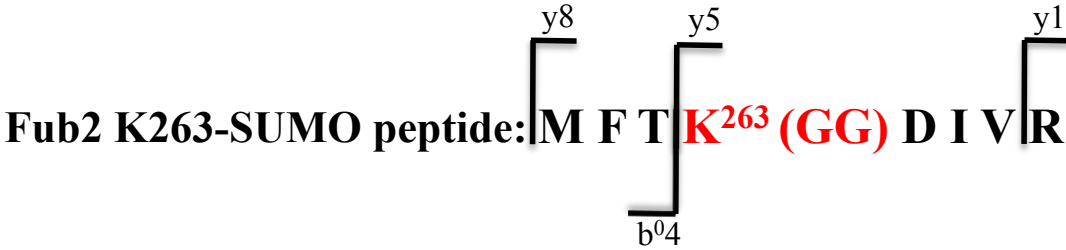


Fig. 6.6 MS/MS fragmentation of Fub2 peptide sumoylated at K263

Highlighted in boxes are the b and y ions corresponding to K263

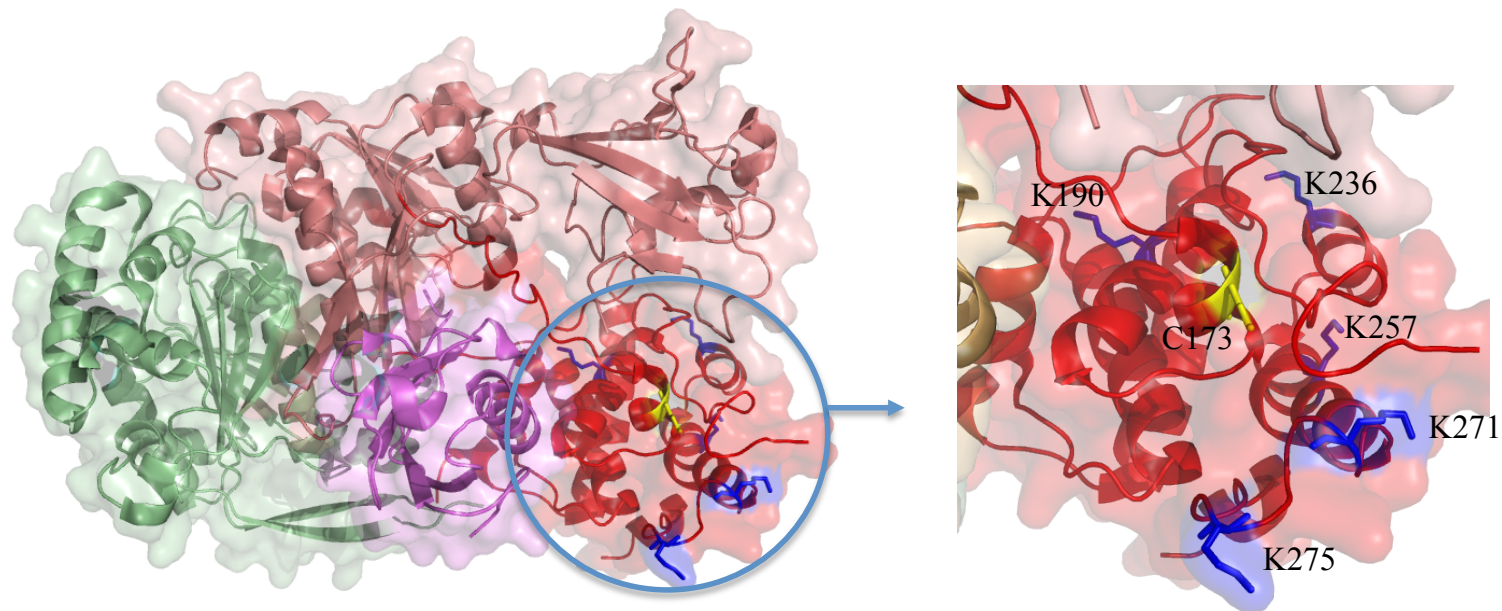


Fig. 6.8 Mammalian SAE2 is autosumoylated at five lysine residues clustered in the cysteine domain

A. Cartoon representation of the human SAE1-SAE2-SUMO-1 complex; SAE1 in green; SUMO-1 in pink; SAE2 in red with cysteine domain in bright red;

B. Cartoon representation of cysteine domain of SAE2.

Highlighted in blue are sumoylated lysine residues and in yellow the active cysteine.

Figures created using PYMOL software based on the crystal structure of the human SAE1-SAE2-SUMO-1 complex (pdb id.: 1Y8R)

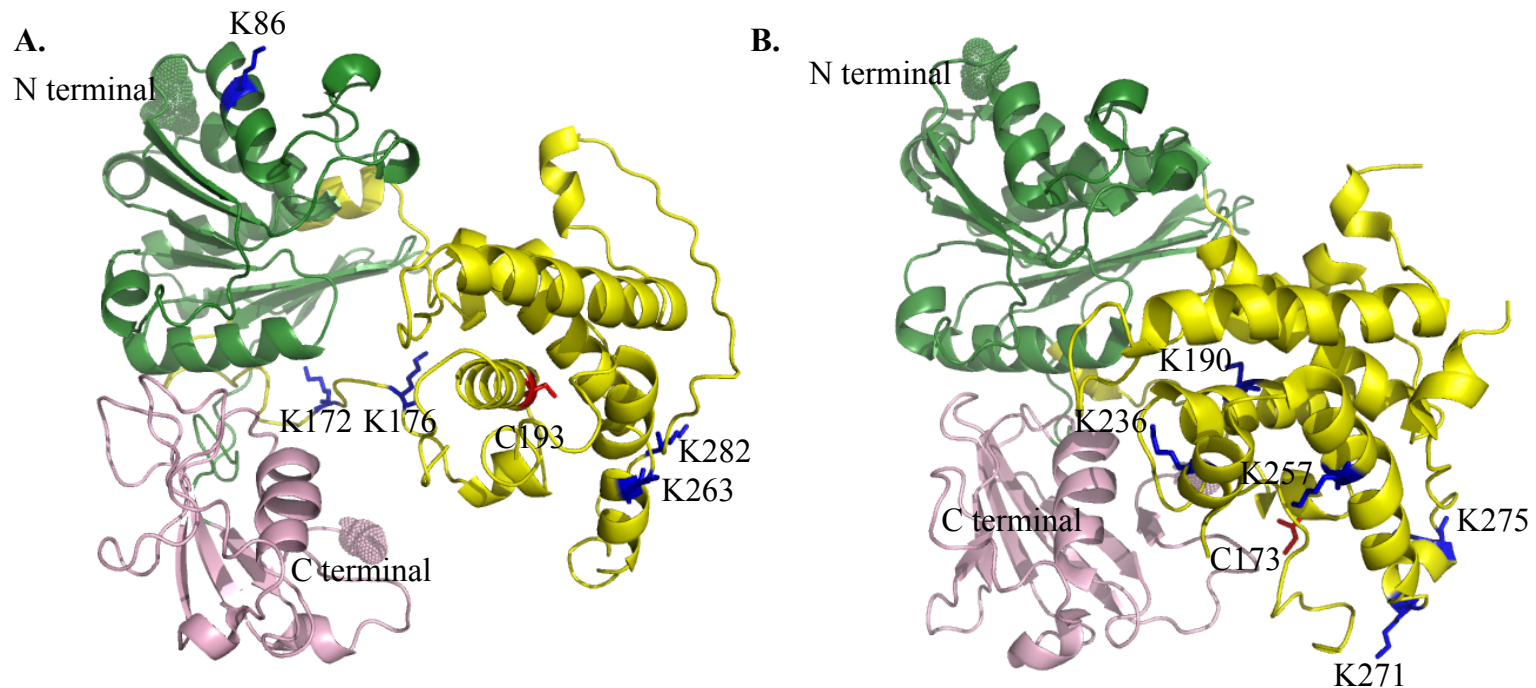


Fig. 6.9 Comparison of the position of the sumoylated lysines of *S.pombe* Fub2 and mammalian SAE2

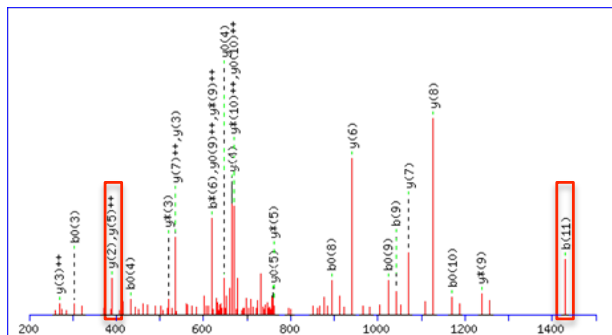
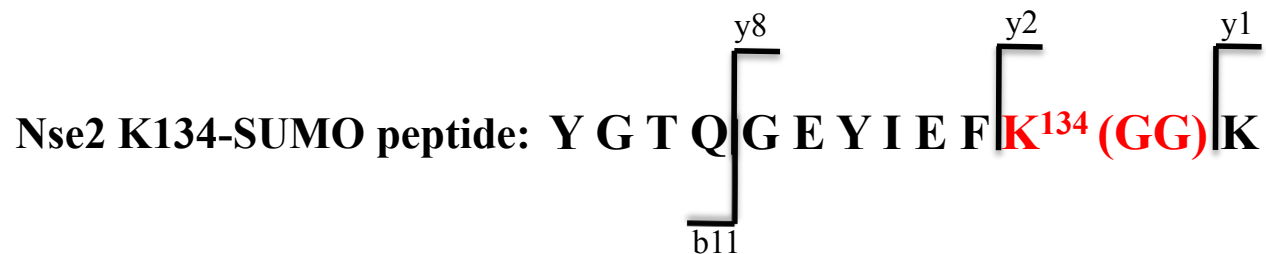
- A. Cartoon representation of the structural model of *S. pombe* Fub2. Model created by PHYRE software based on the structure of human SAE2 (pdb id: 2Y8R).
- B. Cartoon representation of human SAE2 structure (pdb id: 2Y8R). Addenylated domain in green, cysteine domain in yellow with the active Cys highlighted in red. Highlighted in blue are sumoylated lysine residues. Figures created using PYMOL software.

6.3.2 The SUMO E3 ligase Nse2 is sumoylated *in vitro* at three lysine residues

The SUMO E3 ligase Nse2 sumoylated lysine residues K134, K229 and K248 were identified from the MS/MS spectra, peptide mass fingerprints, sequence queries and MS/MS ion searches using the MASCOT search engine (see section 2.4.22; fig. 6.10, 6.11 and 6.12 respectively) (Perkins et al., 1999). All three lysines are conserved in humans but not in *S. cerevisiae* (fig. 6.13), however structural representation reveals that the *S. cerevisiae* homologue Mms21 has lysine residues at similar locations within the 3D structure (fig. 6.14). 3D modeling of *S. pombe* Nse2 based on the crystal structure of *S. cerevisiae* Mms21 reveals that K134 is situated within the domain that interacts with Smc5 at a position close to K111 and K130 in *S. cerevisiae* and mammals respectively. K229 is situated within the RING finger domain again at a location approximate to K189 and K222 in *S. cerevisiae* and mammals respectively. K248 is located just after the RING finger domain at the C-terminal like K258 in *S. cerevisiae* and K242 in mammals. It has to be noted that 3D models are speculative *in silico* analyses and do not necessarily reflect the true 3D structure of the protein. As with Fub2, none of the modified lysines is within sumoylation consensus sequence.

6.3.3 The SUMO conjugating enzyme Hus5 is sumoylated *in vitro* at K50

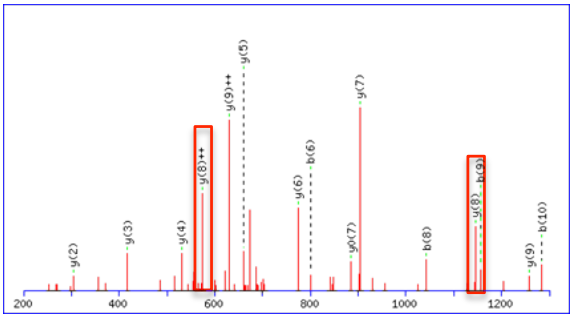
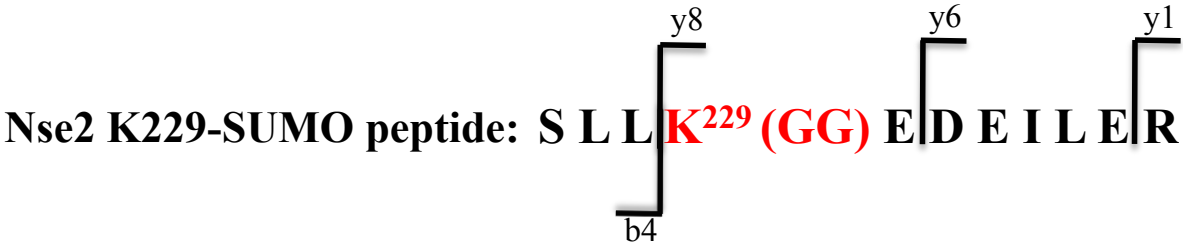
Following MASCOT search of the MS/MS spectrum, peptide mass fingerprints, sequence queries and MS/MS ion search (Perkins et al., 1999) (fig. 6.15) only one residue, K50, was identified as an *in vitro* sumoylation site for the SUMO conjugating enzyme. While Hus5 is highly conserved amongst species, K50 is not conserved in humans or *S. cerevisiae*. However, mammalian Ubc9 has a surface lysine residue at position 49 (fig. 6.16 C) and the crystal structure of *S. cerevisiae* Ubc9 (pdb id.: 3ONG) reveals that the SUMO modified K153 is at an approximate position within the 3D



#	b	b ⁺⁺	b ⁺	b ⁺⁺⁺	b ⁰	b ⁰⁺⁺	Seq.	y	y ⁺⁺	y ⁺	y ⁺⁺⁺	y ⁰	y ⁰⁺⁺	#
1	164.0706	82.5389					Y							12
2	221.0921	111.0497					G	1413.7009	707.3541	1396.6743	698.8408	1395.6903	698.3488	11
3	322.1397	161.5735			304.1292	152.5682	T	1356.6794	678.8433	1339.6529	670.3301	1338.6688	669.8381	10
4	450.1983	225.6028	433.1718	217.0895	432.1878	216.5975	Q	1255.6317	628.3195	1238.6052	619.8062	1237.6212	619.3142	9
5	507.2198	254.1135	490.1932	245.6003	489.2092	245.1083	G	1127.5732	564.2902	1110.5466	555.7769	1109.5626	555.2849	8
6	636.2624	318.6348	619.2358	310.1216	618.2518	309.6295	E	1070.5517	535.7795	1053.5251	527.2662	1052.5411	526.7742	7
7	799.3257	400.1665	782.2992	391.6532	781.3151	391.1612	Y	941.5091	471.2582	924.4825	462.7449	923.4985	462.2529	6
8	912.4098	456.7085	895.3832	448.1953	894.3992	447.7032	I	778.4458	389.7265	761.4192	381.2132	760.4352	380.7212	5
9	1041.4524	521.2298	1024.4258	512.7165	1023.4418	512.2245	E	665.3617	333.1845	648.3352	324.6712	647.3511	324.1792	4
10	1188.5208	594.7640	1171.4942	586.2508	1170.5102	585.7587	F	536.3191	268.6632	519.2926	260.1499			3
11	1430.6587	715.8330	1413.6321	707.3197	1412.6481	706.8277	K	389.2507	195.1290	372.2241	186.6157			2
12							K	147.1128	74.0600	130.0863	65.5468			1

Fig. 6.10 MS/MS fragmentation of Nse2 peptide sumoylated at K134

Highlighted in boxes are the b and y ions corresponding to K134



#	b	b ⁺⁺	b [*]	b ⁺⁺⁺	b ⁰	b ⁰⁺⁺	Seq.	y	y ⁺⁺	y [*]	y ⁺⁺⁺	y ⁰	y ⁰⁺⁺	#
1	88.0393	44.5233			70.0287	35.5180	S							11
2	201.1234	101.0653			183.1128	92.0600	L	1371.7478	686.3775	1354.7213	677.8643	1353.7373	677.3723	10
3	314.2074	157.6074			296.1969	148.6021	L	1258.6638	629.8355	1241.6372	621.3222	1240.6532	620.8302	9
4	556.3453	278.6763	539.3188	270.1630	538.3348	269.6710	K	1145.3797	573.2935	1128.5531	564.7802	1127.5691	564.2882	8
5	685.3879	343.1976	668.3614	334.6843	667.3773	334.1923	E	903.4418	452.2245	886.4153	443.7113	885.4312	443.2193	7
6	800.4149	400.7111	783.3883	392.1978	782.4043	391.7058	D	774.3992	387.7032	757.3727	379.1900	756.3886	378.6980	6
7	929.4575	465.2324	912.4309	456.7191	911.4469	456.2271	E	659.3723	330.1898	642.3457	321.6765	641.3617	321.1845	5
8	1042.5415	521.7744	1025.5150	513.2611	1024.5309	512.7691	I	530.3297	265.6685	513.3031	257.1552	512.3191	256.6632	4
9	1155.6256	578.3164	1138.5990	569.8032	1137.6150	569.3111	L	417.2456	209.1264	400.2191	200.6132	399.2350	200.1212	3
10	1284.6682	642.8377	1267.6416	634.3244	1266.6576	633.8324	E	304.1615	152.5844	287.1350	144.0711	286.1510	143.5791	2
11							R	175.1190	88.0631	158.0924	79.5498			1

Fig. 6.11 MS/MS fragmentation of Nse2 peptide sumoylated at K229

Highlighted in boxes are the b and y ions corresponding to K229

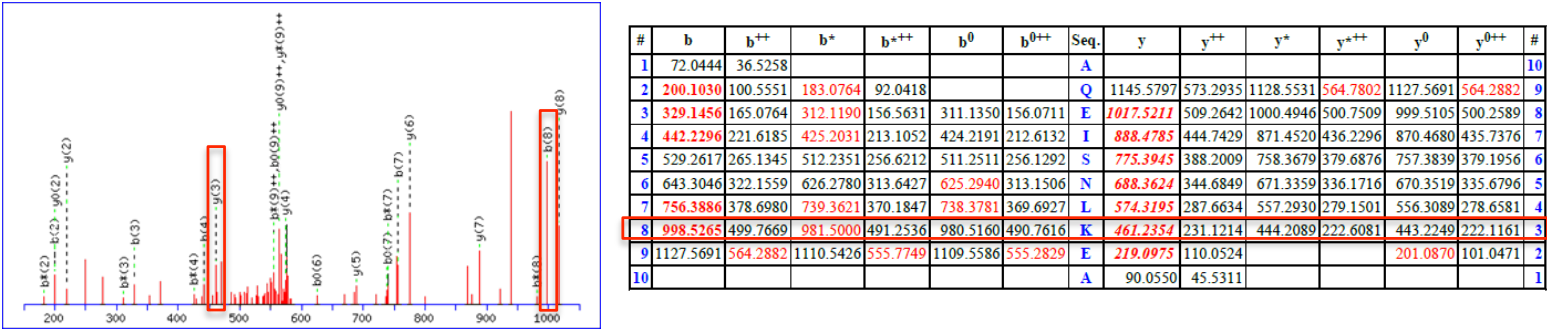
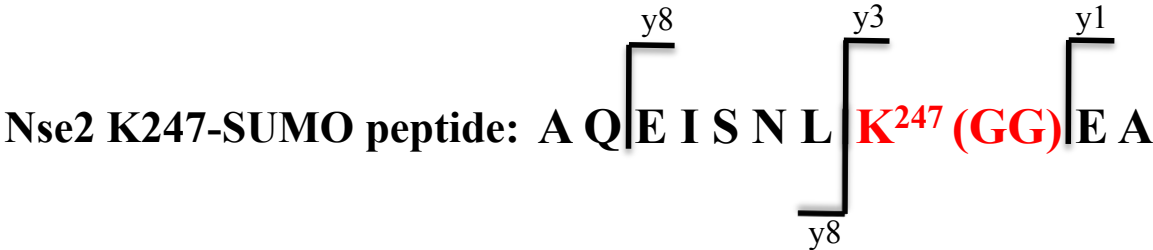


Fig. 6.12 MS/MS fragmentation of Nse2 peptide sumoylated at K247

Highlighted in boxes are the b and y ions corresponding to K247

```

Sp_Nse2.  1  ---MSEAQLKTSLEALSQNLLPGNQNHCSFDFQLKETDDSIKQVIKCAIVAAEIKNNE-
Hs_Nse2.  1  ---MPGRSSSNSTGTFISFSGVESALSSLKNFQACINSGMDTASSVALDLVESQTEVS
Sc_Mms21  1  MALNDNPPIPKSVPLHPKSGKMFHNLHARDLSNIYQQCYKQIDETINQIVDSTSPSTIGIE

Sp_Nse2.  56 CLDMIDSGIRELLDAKQRILLMQQSVDTLANKTSENISTFENKSLIDIYTQIFKELIQEY
Hs_Nse2.  57 SEYSMDKAMVEFATLDRQLNHVYKAVOSTINHVKE-----ERPEKIPDLKLIVEKKFIAL
Sc_Mms21  61 EQVADITSTYKILLSTYESNSFDEHIKDLKKNFQSSACPQIDISTWDKYRTGETTAP

Sp_Nse2.  116 EEKSLYGKMYCTQGEYIEFKKTIWHEQNTDGSDFPSMKTFNFVMNTEEQEADVMVYSATF
Hs_Nse2.  112 QSKNSDADEQNNEKEVQKKQIKELKKQCG-----LQADREADGTBQGVDEIIIVTQSQTN
Sc_Mms21  121 KLSELYLNMETPEPATMVNNTDTLKILKVLPIWNDPTCVIPDLQNPADDDLQIEGKI

Sp_Nse2.  176 DNRCLTLQPIVHPILSTACNHFYEKDAILSLN-----PTCVCFVVGCEARLQSSLK
Hs_Nse2.  167 -FTCPITKEEMKKPVKNKVCGHITYEEDAIVRMIESRQKRKKKAYCPQIGCSHTDIR---K
Sc_Mms21  181 ELTCPIITCKEYEAPLISRKCNHVFDRDGIQNYLQG----YTTRDCPQAACSQVVSMDRFV

Sp_Nse2.  230 EDEILERRLRRAQEISNLKKEA-----
Hs_Nse2.  223 SDLIQDEALRRAIENHNKKRHRHSE-----
Sc_Mms21  237 RDPIMELRCKIAKMKESQEQDKRSSQAIDVL

```

Fig. 6.13 Nse2 sumoylated lysine residues are conserved in humans but not *S. cerevisiae*

Sequence alignment of PIAS type SUMO E3 ligases Nse2^{Sp/Hs} and Mms21^{Sc}. Highlighted in yellow are the lysines sumoylated in *S. pombe* and the conserved lysine residues in *H. sapiens*.

Fig. 6.14 Structural mapping of the sumoylated lysines of *S.pombe* Nse2 and structurally conserved lysines of human Nse2 and *S. cerevisiae* Mms21

A. Cartoon representation of the crystal structure of *S. cerevisiae* Mms21 in complex with Smc5 (pdb id: 3HTK)

B. Cartoon representation of the structural model of *S. pombe* Nse2. Model created by PHYRE software based on the structure of *S. cerevisiae* Mms21 (pdb id: 3HTK).

C. Cartoon representation of the structural model of human Nse2. Model created by PHYRE software based on the crystal structure of *S.cerevisiae* complex Smc5-Mms21 (pdb id: 3HTK)

Highlighted:

Smc5 = blue; Nse2/Mms21 domain that interacts with Smc5 = pink;

Nse2/Mms21 Zn finger domain = wheat; Sumoylated lysines in *S.pombe*

Nse2 and possible structurally conserved lysines in human Nse2 and *S.*

cerevisiae Mms21 = red; active cysteine = yellow

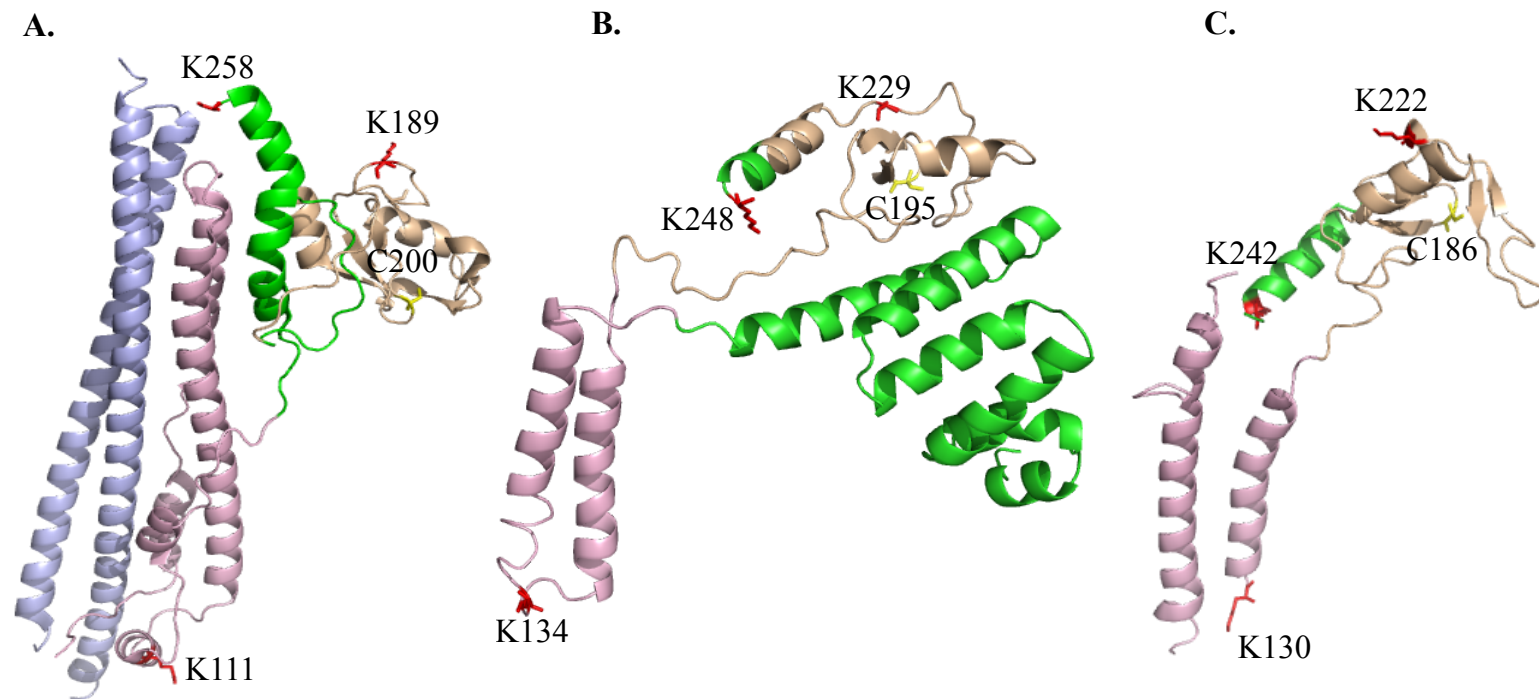
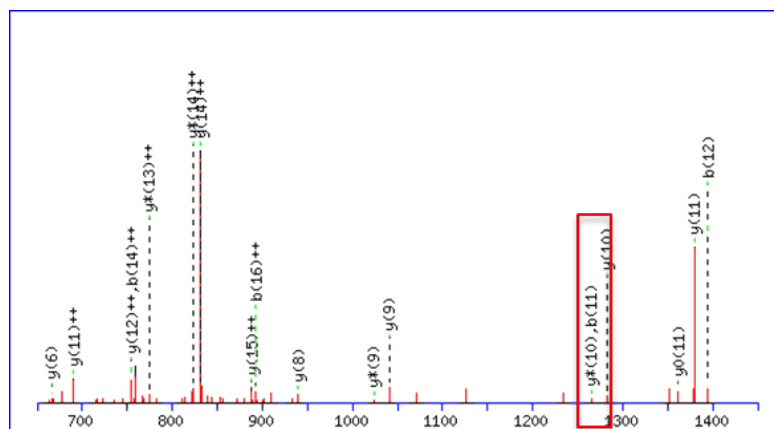
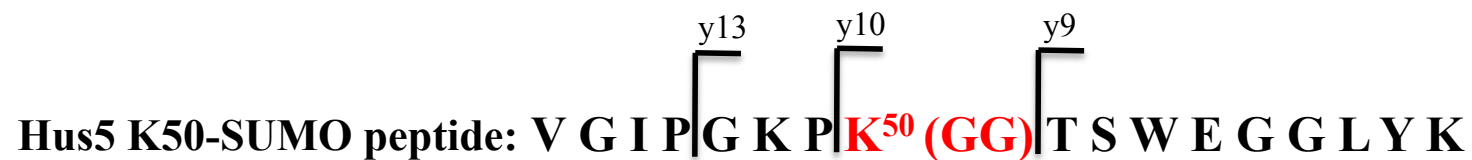


Fig. 6.14 Structural mapping of the sumoylated lysines of *S. pombe* Nse2 (B) and structurally conserved lysines of *H. sapiens* Nse2 (C) and *S. cerevisiae* Mms21 (A)



Seq.	y	y ⁺⁺	y [*]	y ⁺⁺	y ⁰	y ⁰⁺⁺	#
V							17
G	1831.9701	916.4887	1814.9436	907.9754	1813.9595	907.4834	16
I	1774.9486	887.9780	1757.9221	879.4647	1756.9381	878.9727	15
P	1661.8646	831.4359	1644.8380	822.9227	1643.8540	822.4306	14
G	1564.8118	782.9095	1547.7853	774.3963	1546.8013	773.9043	13
K	1507.7904	754.3988	1490.7638	745.8855	1489.7798	745.3935	12
P	1379.6954	690.3513	1362.6688	681.8381	1361.6848	681.3461	11
K	1282.6426	641.8250	1265.6161	633.3117	1264.6321	632.8197	10
T	1040.5047	520.7560	1023.4782	512.2427	1022.4942	511.7507	9
S	939.4571	470.2322	922.4305	461.7189	921.4465	461.2269	8
W	852.4250	426.7162	835.3985	418.2029	834.4145	417.7109	7
E	666.3457	333.6765	649.3192	325.1632	648.3352	324.6712	6
G	537.3031	269.1552	520.2766	260.6419			5
G	480.2817	240.6445	463.2551	232.1312			4
L	423.2602	212.1337	406.2336	203.6205			3
Y	310.1761	155.5917	293.1496	147.0784			2
K	147.1128	74.0600	130.0863	65.5468			1

Fig. 6.15 MS/MS fragmentation of Hus5 peptide sumoylated at K50

Highlighted in boxes is the y ion corresponding to K50

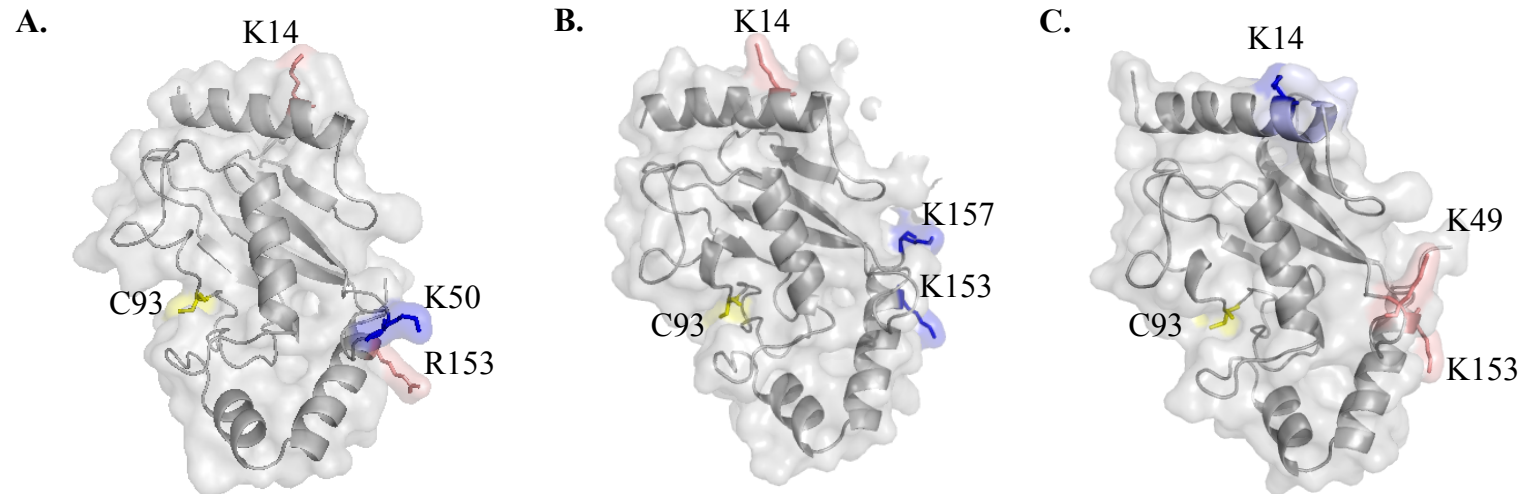


Fig. 6.16 Comparison of the position of the sumoylated lysines of the SUMO conjugator Hus5^{Sp}/Ubc9^{Hs/Sc}

A. Cartoon representation of the structural model of *S. pombe* Hus5. Model created by PHYRE software based on the structure of *Mus musculus* Ubc9 (pdb id: 2VVR).

B. Cartoon representation of the crystal structure of *S. cerevisiae* Ubc9 (pdb id: 2GJD).

C. Cartoon representation of the crystal structure of human Ubc9 (pdb id: 1A3S).

Active cysteine residues are highlighted in yellow. Identified sumoylated lysines are highlighted in blue. Structurally conserved residues that are potential sumoylation sites or functionally conserved are highlighted in red.

structure (fig. 6.16 A and B). None of the Hus5/Ubc9 lysine residues are within sumoylation consensus sequence. To further understand the role of autosumoylation, biochemical and genetic analysis was carried out on the SUMO modification of Hus5.

6.4 *In vitro* analysis of sumoylation of Hus5 at K50

Firstly, to confirm that K50 is the only sumoylated lysine, the *in vitro* sumoylation assay was carried out using a recombinant Hus5 mutant which had the lysine at position fifty mutated to an arginine residue. Arginine residues contribute to the structure and the non-covalent interactions of the protein in a similar manner to the lysine residues but they cannot be sumoylated and therefore are the ideal substitution for lysines when analyzing sumoylation. The mutant protein to be used was created from a previous bacterial construct of the wild-type *hus5*⁺, pGEX-KH-*hus5*⁺, by site directed mutagenesis (using primers 5K50-F: 5'GGAAAACCGAGAACGTCTTGG and 5K50-R: 5'CCAAGACGTCTTCGGTTTTCC). The protein was expressed in a bacterial culture and purified on a glutathione sepharose column (fig. 6.17 A). The sumoylation assay was carried out in parallel with the wild type Hus5 conjugating enzyme and the Hus5-K50R mutant (fig. 6.17 B). The sumoylation assay reaction mixture carried out with the Hus5-K50R mutant (fig. 6.17 B lane 4) does not display a band at the size where the sumoylated wild type Hus5 separates. This confirms that K50 is sumoylated *in vitro* and that no other lysine residues are modified. More interestingly, most of the high Mr bands present when wild type Hus5 is used (fig. 6.17 B lane 2) are absent when the mutant is employed. This suggests that sumoylation of Hus5 at K50 is required for the formation of high Mr sumoylated species *in vitro*. To assess the *in vitro* results, an *in vivo* analysis of how Hus5 defective in sumoylation affects the levels the cellular sumoylation was carried out.

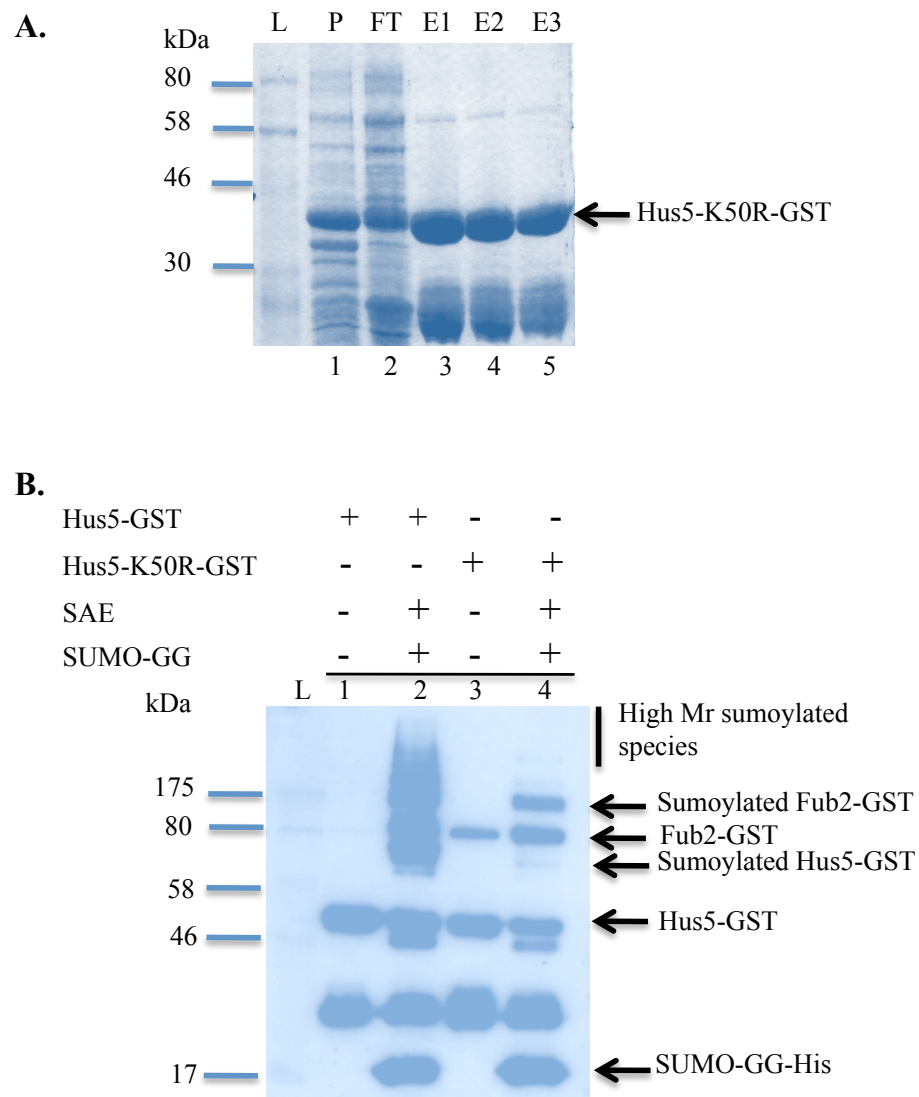


Fig. 6.17 Hus5-K50R is not sumoylated *in vitro*

- A. SDS-PAGE of purified Hus5-K50R-GST. P = pellet; FT = flow through; E = elution
- B. Colloidal blue staining of SDS-PAGE of *in vitro* sumoylation assay with wild type Hus5 (lane 2) and mutant Hus5-K50R (lane 4)

6.5 *hus5-K50R* mutant promotes hypersumoylation *in vivo*

For the ease of genetic manipulation of the *hus5*⁺ gene, a base strain was created (by Dr. F.Z. Watts, University of Sussex) employing the RMCE strategy (see section 2.1.4) and used to obtain the mutant strain with *hus5-K50R* as the sole copy of the *hus5* gene (fig. 6.18). The *hus5*⁺ base strain and the *hus5-K50R* mutant grow like the wild type strain at the physiological *S. pombe* temperature (30°C) and at 37°C (fig. 6.19 A) signifying that the foreign DNA at the 5' (loxP) and the 3' (lox M) does not interfere with the gene function and that mutating the lysine at position 50 to arginine does not affect the folding of the protein.

To determine whether by mutating K50 to arginine in the genome affects SUMO modification or formation of high Mr sumoylated species, whole cell extracts were prepared using TCA, analysed by SDS-PAGE and probed with anti-SUMO antibodies, with anti-tubulin antibodies as control. The effect of the mutation on the levels of sumoylation were compared to wild type, the *hus5* base strain which should behave like wild type, *pli1Δ*, which has reduced levels of cellular sumoylation, and *pmt3* null mutant strains (fig. 6.19 B). *pli1* and *pmt3* null mutant strains (lane 2 and 5 respectively) display reduced sumoylation and no sumoylated species respectively, as expected. The *hus5* base strain (lane 3 and 6) has similar levels of sumoylation to the wild type (lane 1) strain but, unexpectedly, the *hus5-K50R* strain (lane 4) has elevated levels of total sumoylation compared to wild type. This is consistent with *in vivo* results from *S. cerevisiae* (Ho et al., 2011) where the *ubc9-K153,K157R* mutant shows increased levels of cellular sumoylation. This phenotype is similar to that observed in *S. cerevisiae* in a null mutant of the SUMO protease *ulp2* (Bylebyl et al., 2003) and the STUbL mutant *slx8-1* (Prudden et al., 2007).

6.6 Phenotypic analysis of *hus5-K50R* mutant

The phenotypic characteristics of the *hus5-K50R* mutant were compared to those of a wild type strain, the *hus5* base strain, which should behave like a wild type strain, and

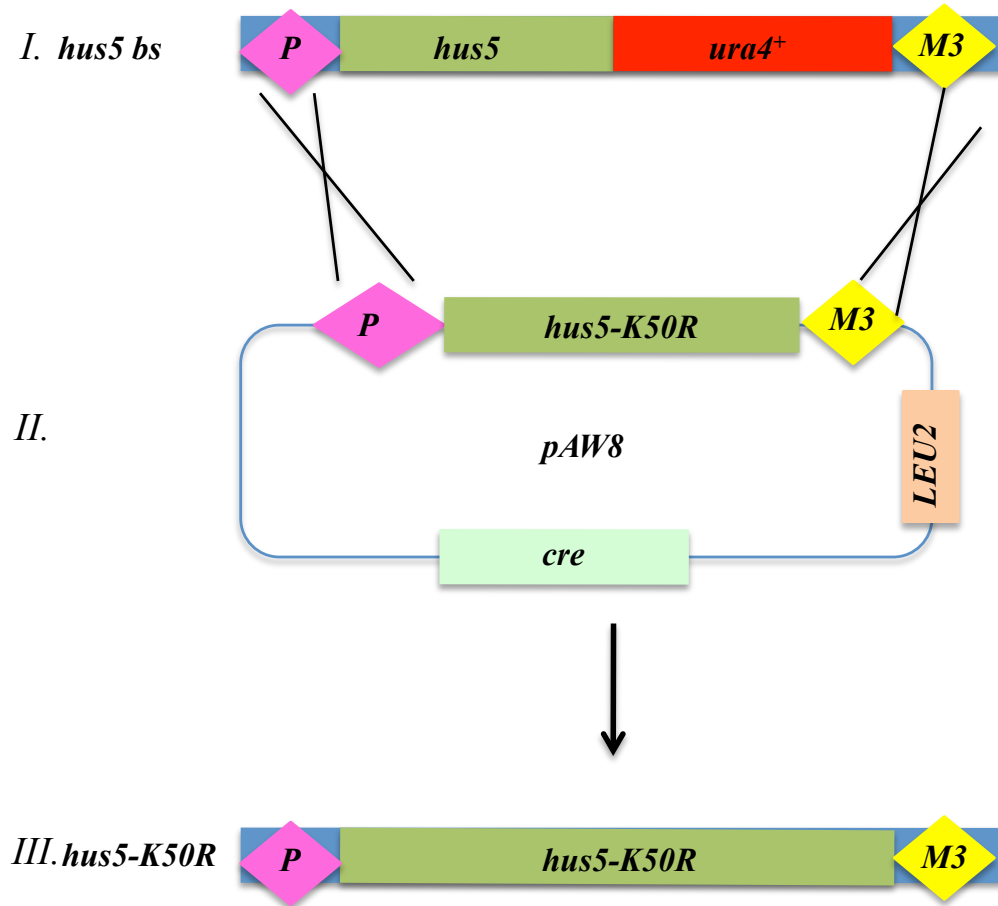


Fig. 6.18 Strategy to create *hus5-K50R* mutant using a *hus5* base strain (bs)

A *hus5* base strain (*ura⁺*) (I) was transformed with the *pAW8* plasmid containing the *hus5-k50R* mutant (obtained by site directed mutagenesis) flanked by the *loxP* (at 5' end') and *loxM3* (at the 3' end) (II). Cassette exchange by homologous recombination results in *hus5-K50R* strain (*ura⁻*) (III)

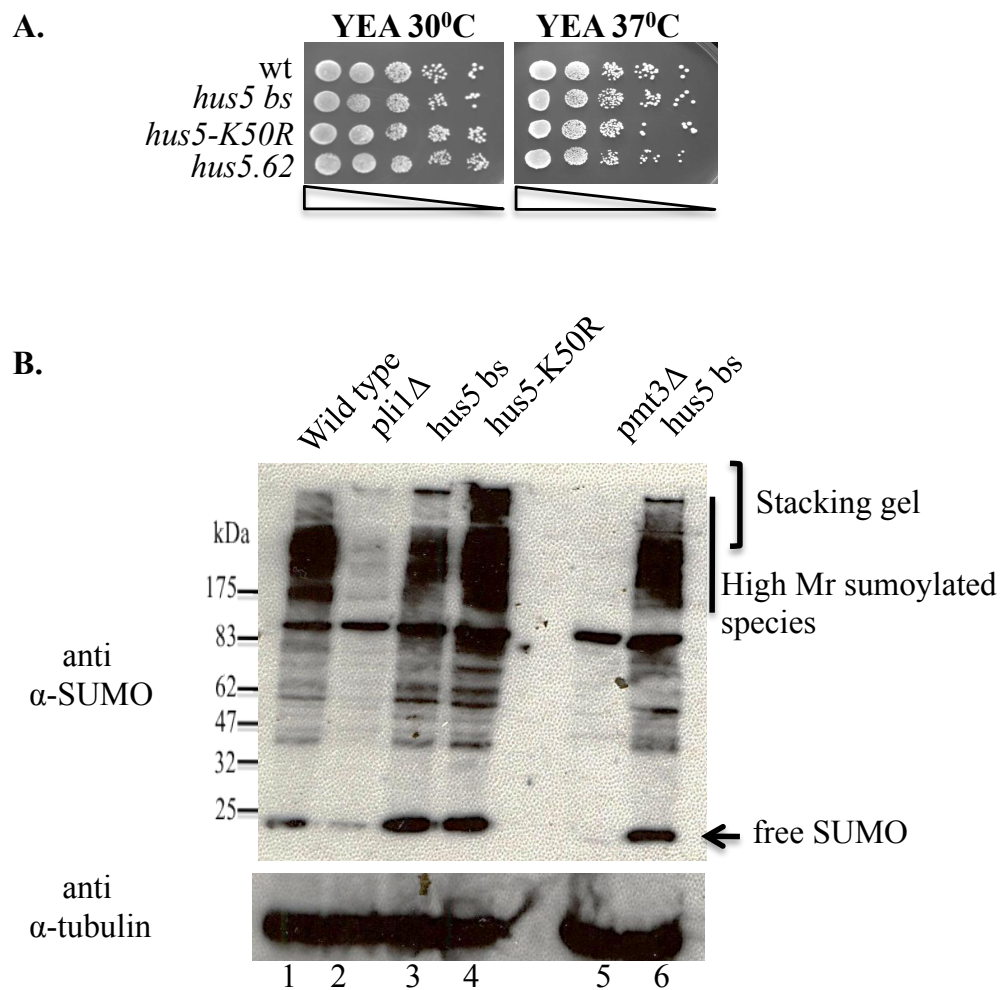



Fig. 6.19 *hus5-K50R* mutant promotes hypersumoylation

A. The *hus5-K50R* mutant is not temperature sensitive
10 μ l of 10 fold serially diluted cultures () were plated onto YEA media and incubated at 30°C and 37°C for 3 days as indicated.

B. Western blot of total cell extract from wild type, *hus5*⁺ base strain, *pli1* Δ , *pmt3* Δ and *hus5-K50R* mutant cells as indicated, probed with anti-SUMO antisera (upper panel) and anti-tubulin antisera (lower panel).

the *hus5-62* mutant of the SUMO conjugating enzyme which was comprehensively characterized (Ho and Watts, 2003) and is sensitive to most genotoxins. The microscopic analysis of the *hus5-K50R* mutant revealed cellular and nuclear aberrations and a ‘cut phenotype’ (fig. 6.20)

6.6.1 *hus5-K50R* is not sensitive to S-phase arrest

As the *hus5-62* mutant is sensitive to the DNA replication inhibitors HU, MMS and CPT, the response of *hus5*⁺ base strain and *hus5-K50R* to these genotoxins was evaluated (fig. 6.21). The results confirm that the *hus5*⁺ base strain behaves like wild type. The *hus5-K50R* displays no sensitivities to these DNA damaging agents, suggesting that sumoylation of the SUMO conjugating enzyme is not required during DNA replication.

6.6.2 Hus5 sumoylation is not required for chromosome segregation or protein synthesis

As the null mutant of the SUMO E3 ligase *pli1Δ* is sensitive to the microtubules inhibitor thiabendazole (TBZ) (Xhemalce et al., 2004) and in the light of recent reports that hypersumoylation occurs in response to the inhibition of protein translation (Castoralova et al., 2012) the sensitivity of *hus5-K50R* to TBZ and cycloheximide (CHX), a protein synthesis inhibitor, was tested (fig. 6.22). The mutant is not sensitive to either inhibitor, suggesting that sumoylation of Hus5 does not function in chromosome segregation or in protein translation.

6.6.3 *hus5-K50R* mutant sensitivity to IR is S phase-specific

The IR sensitivity of the *hus5-K50R* mutant was tested on asynchronous cell cultures in parallel with the *hus5*⁺ base strain and wild type cells (fig. 6.23 A). *hus5-K50R* exhibits a slight sensitivity at high doses of IR suggesting that the function of the sumoylation of Hus5 in IR induced cellular response could be phase specific.

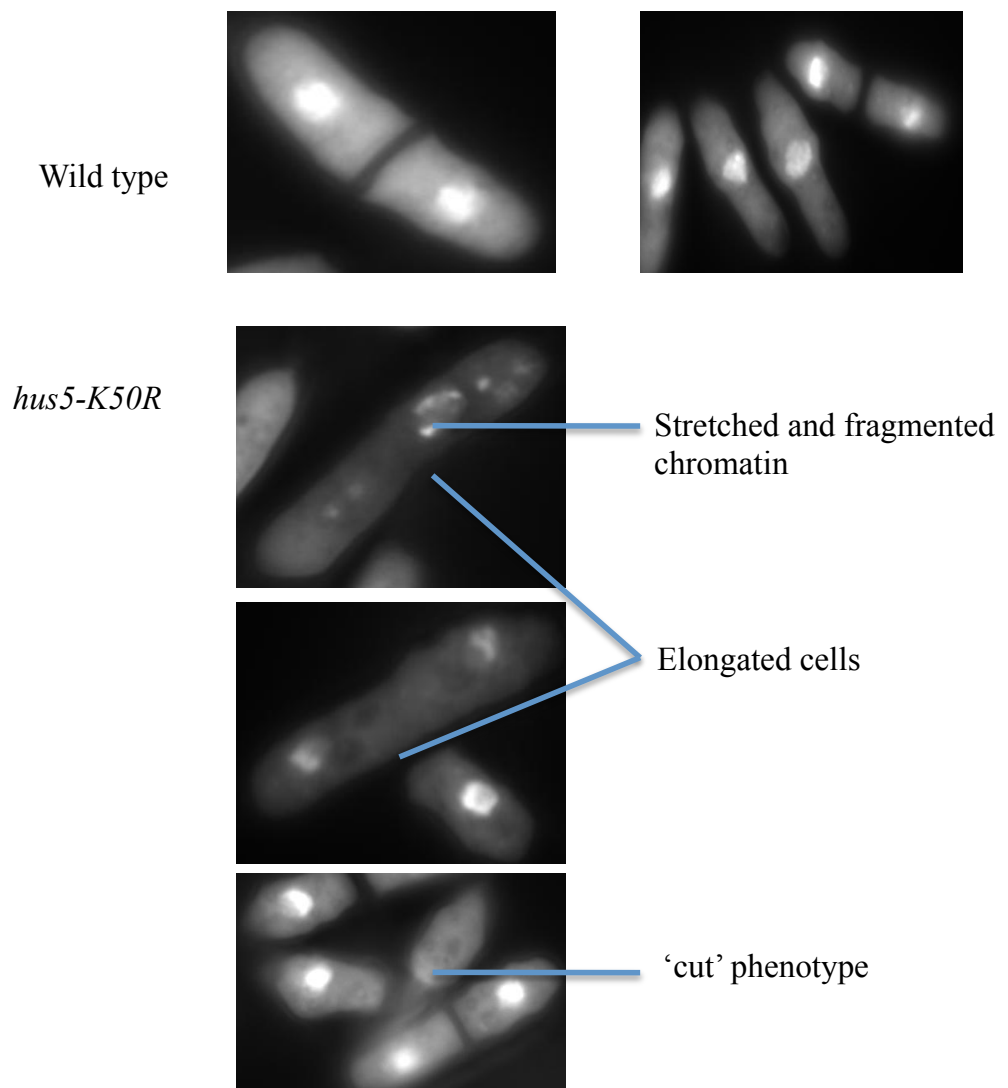


Fig. 6.20 *hus5-K50R* mutant display aberrant cell and nucleus morphology

Morphology of methanol fixed cells, stained with DAPI and calcofluor.

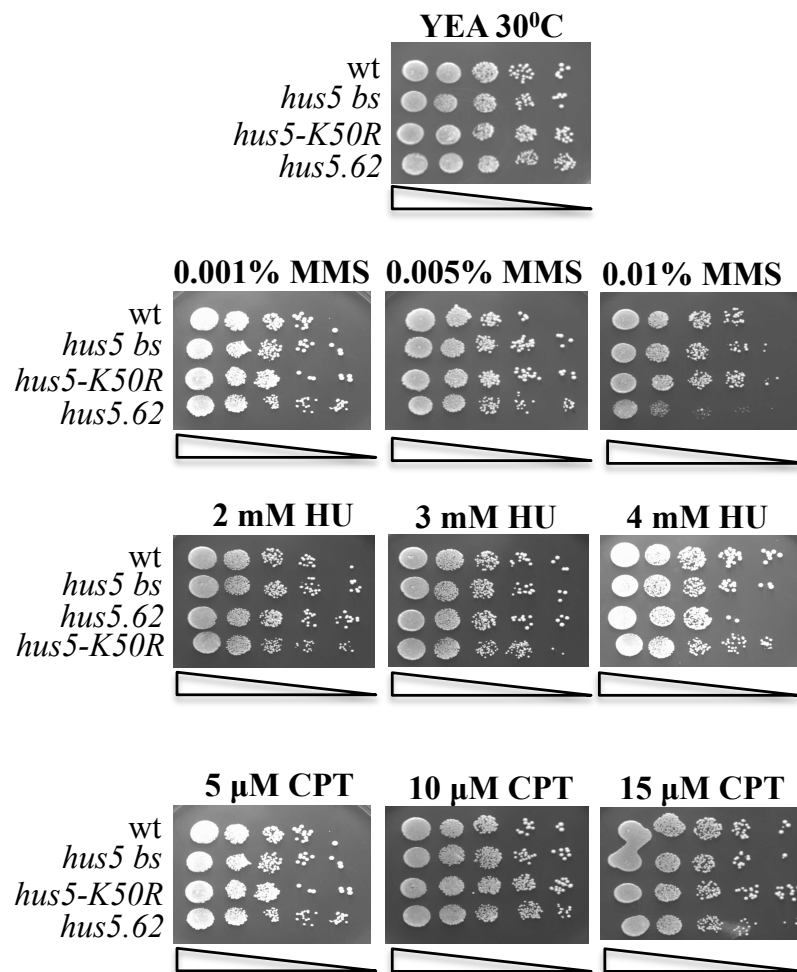



Fig. 6.21 The *hus5-K50R* mutant is not sensitive to S-phase genotoxins

10 μ l of 10 fold serially diluted cultures () were plated onto media containing genotoxins as indicated, and incubated at 30°C for 3 days.

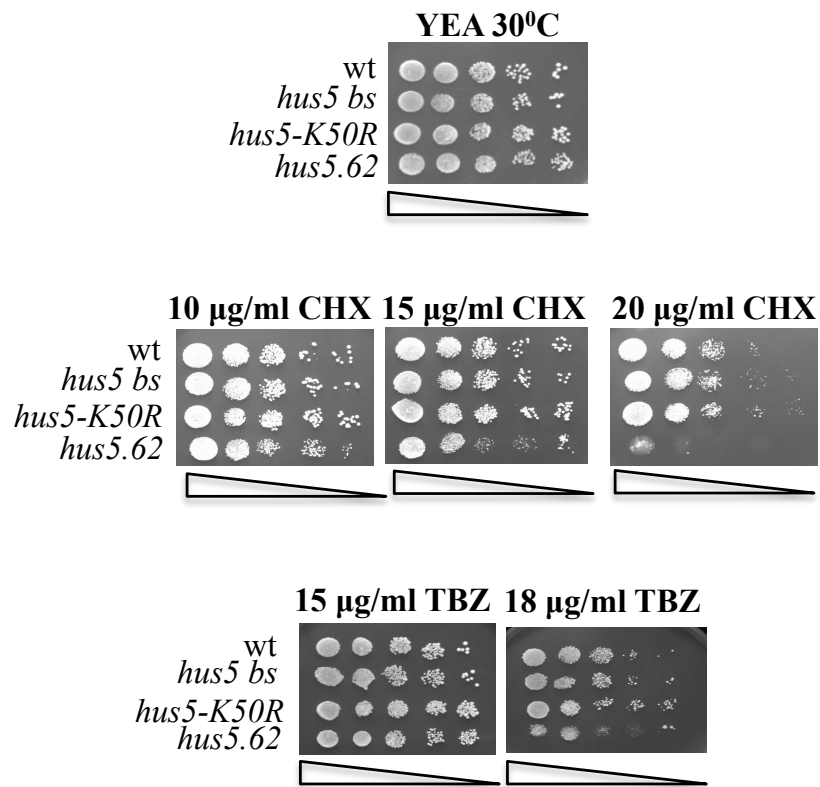


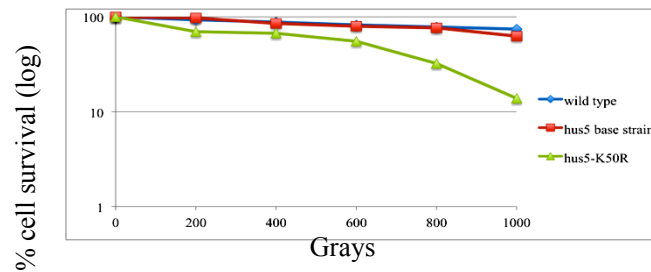
Fig. 6.22 The *hus5-K50R* mutant is not sensitive to protein synthesis and microtubules inhibition

10 µl of 10 fold serially diluted cultures () were plated onto media containing stressing agents as indicated, and incubated at 30°C for three days.

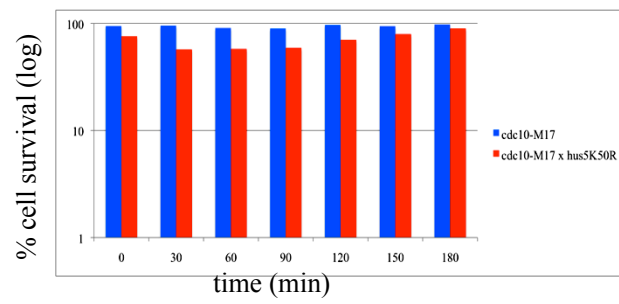
Fig. 6.23 The *hus5-K50R* sensitivity to ionizing radiation is reversed by over-expression of the SUMO protease Ulp2

- A. *hus5-K50R* is sensitive to high doses of ionizing radiation. IR survival curves of *hus5-K50R* compared to wild type and *hus5⁺* base strain. Log-phase cultures were irradiated with the stated dose and 500 cells were plated onto YEA and incubated at 30°C for three days to determine cell viability.
- B. *hus5-K50R* cells synchronized in S-phase are sensitive to low doses (200 Gy) of ionizing radiation. Measurements were taken at 30 minutes interval after release from G1 block. 500 cells were plated onto YEA and incubated at 30°C for three days to determine cell viability.
- C. Over-expression of Ulp2 can rescue the *hus5-K50R* sensitivity to ionizing radiation. Log-phase cultures were irradiated with the stated dose and 500 cells were plated onto YEA and incubated at 30°C for three days to determine cell viability.

A.



B.



C.

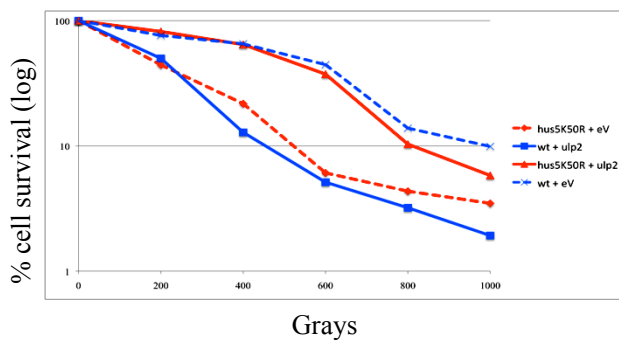


Fig. 6.23 The *hus5-K50R* sensitivity to ionizing radiation is reversed by over-expression of the SUMO protease Ulp2

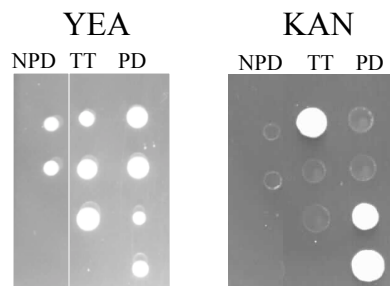
The S phase checkpoint is induced by DSBs and it delays the replication process until the damage is repaired. Many proteins involved in the intra-S-phase checkpoint are sumoylated such as ATM/ATR, BRCA1, FANCD2, PCNA. To investigate if the IR sensitivity of *hus5-K50R* mutant is phase specific, cultures of *hus5-K50R x cdc10-M17* were synchronized in late G1 phase. The *cdc10-M17* grows at 25°C, it blocks at late G1 phase at 36°C and the cell cycle can be restarted by reverting to 25°C. *hus5-K50R x cdc10-M17* cultures were blocked at 36°C for 3 hours and released at 25°C for 3 hours. After the release samples were taken at 30 minutes intervals and irradiated with 200 Gy (fig. 6.23 B; due to technical restrictions a higher dose of radiation could not be administered). The *hus5-K50R x cdc10-M17* mutant shows a smaller percent of cell viability compared to *cdc10-M17* single mutant and the difference is higher than that of the asynchronous cultures of *hus5-K50R* and wild type at 200 Gy. These data suggests that the autosumoylation of Hus5 could be required for DNA damage repair during S-phase.

Mutants that accumulate high Mr sumoylated species (*slx8-1* and *ulp2Δ*) are sensitive to IR. To see if the phenotype of *hus5-K50R* in response to IR is due to oversumoylation, the Ulp2 SUMO protease was over-expressed in the *hus5-K50R* strain from a *pREP41* vector (Maundrell, 1993) (fig. 6.23 C). Indeed, over-expressing Ulp2 reverses the *hus5-K50R* sensitivity to IR and this is consistent with previous reports that accumulation of sumoylated species interferes with the cellular response to the DNA damaging agents.

6.6.4 Sumoylation of Hus5 is required for cell viability when homologous recombination is impaired

As the homologous recombination defective mutants *rad22^{Sp}/rad52^{Hs/Sc}Δ* and *rhp51^{Sp}/rad51^{Hs/Sc}Δ* are sensitive to ionizing radiation it was interesting to see if the *hus5-K50R* mutant is epistatic with the recombination mutants. *hus5-K50R* strain (no marker) was crossed with opposite mating type of *rad22Δ::NAT* and *rhp51Δ::KAN* strains. The spores were dissected from asci on complete YEA media and were allowed to germinate for three days. The resulting colonies were replica plated onto YEA media containing nourseothricin (NAT) and geneticin (G418/KAN) to select for *rad22Δ::NAT* and *rhp51Δ::KAN* alleles (fig. 6.24). The pattern of the viable spores implies that the double

A.



B.

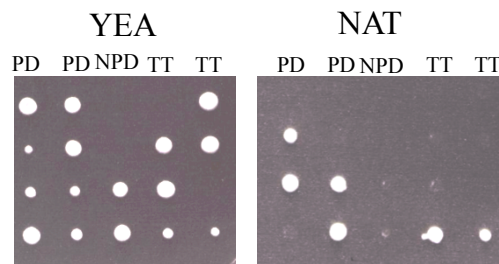


Fig. 6.24 Sumoylation of Hus5 is required for cell viability in homologous recombination mutant backgrounds

A. hus5-K50R is lethal with *rhp51^{Sp}/rad51^{Hs/Sc}Δ* mutant

B. hus5-K50R is lethal with *rad22^{Sp}/rad52^{Hs/Sc}Δ* mutant

NPD = non-parental di-type; TT = tetra-type; PD = parental di-type

Represented dissected tetrads were chosen from a pool of 20 dissected tetrads.

mutants *hus5-K50R:rad22Δ::NAT* and *hus5-K50R:rhp51Δ::KAN* are not viable. This phenotype is similar to that displayed by the null mutant of the SUMO E3 ligase Pli1, which is interesting as this mutant displays significant reduced levels of cellular sumoylation.

6.6.5 Sumoylation of Hus5 is required for DNA damage response when sumoylation of the Smc5/6 complex is impaired

Another important component of the homologous recombination repair pathway is the Smc5/6 complex. The Smc6 protein is sumoylated in a manner dependent on the SUMO E3 ligase Nse2, which is itself a component of the complex. The *nse2-SA* mutant, which is defective in Smc6 sumoylation, is sensitive to a range of genotoxins and to UV and IR radiation. To determine if the *hus5-K50R* mutant is epistatic with the *nse2-SA* mutant the *hus5-K50R* strain was crossed with a *nse2-SA::NAT* strain (fig. 6.25 A). The double mutant *hus5-K50R:nse2-SA::NAT* is slow growing and very sensitive to low doses of UV, IR and HU (fig. 6.25 B, C and D). These data imply that the mutants are not epistatic and that sumoylation of Hus5 is required for the DNA damage response machinery when the sumoylation of the Smc6 is impaired.

6.6.6 Sumoylation of Hus5 prevents gross chromosomal rearrangements

Both *pli1Δ* and *nse2-SA* mutants are defective in maintaining a minichromosome and in preventing gross chromosomal rearrangements at centromeric repeats (this study Chapter 5 and (Watts et al., 2007)). To determine if the sumoylation of Hus5 function in genomic maintenance, a *hus5-K50R* strain containing the artificial minichromosome Ch16-AGU (strain created as previously described in Chapter 5, section 5.1.3) was tested for loss of the minichromosome and loss of *ura4⁺* gene by means of fluctuation tests as previously described (Chapter 5, section 5.2). Three independent experiments, each using 5 cultures propagated from single colonies of wild type and *hus5-K50R* strains were performed (fig. 6.26).

Fig. 6.25 *hus5-K50R*; *nse2-SA* double mutant is hypersensitive to low doses of UV, IR and HU

- A. *hus5-K50R*; *nse2-SA* double mutant is slow growing
- B. *hus5-K50R*; *nse2-SA* double mutant is hypersensitive to low doses of UV radiation
- C. *hus5-K50R*; *nse2-SA* double mutant is hypersensitive to low doses of IR
- D. *hus5-K50R* \times *nse2-SA* double mutant is hypersensitive to low doses of hydroxyurea

NPD = non-parental di-type; TT = tetra-type; PD = parental di-type.
Represented dissected tetrads were chosen from a pool of 20 dissected tetrads.

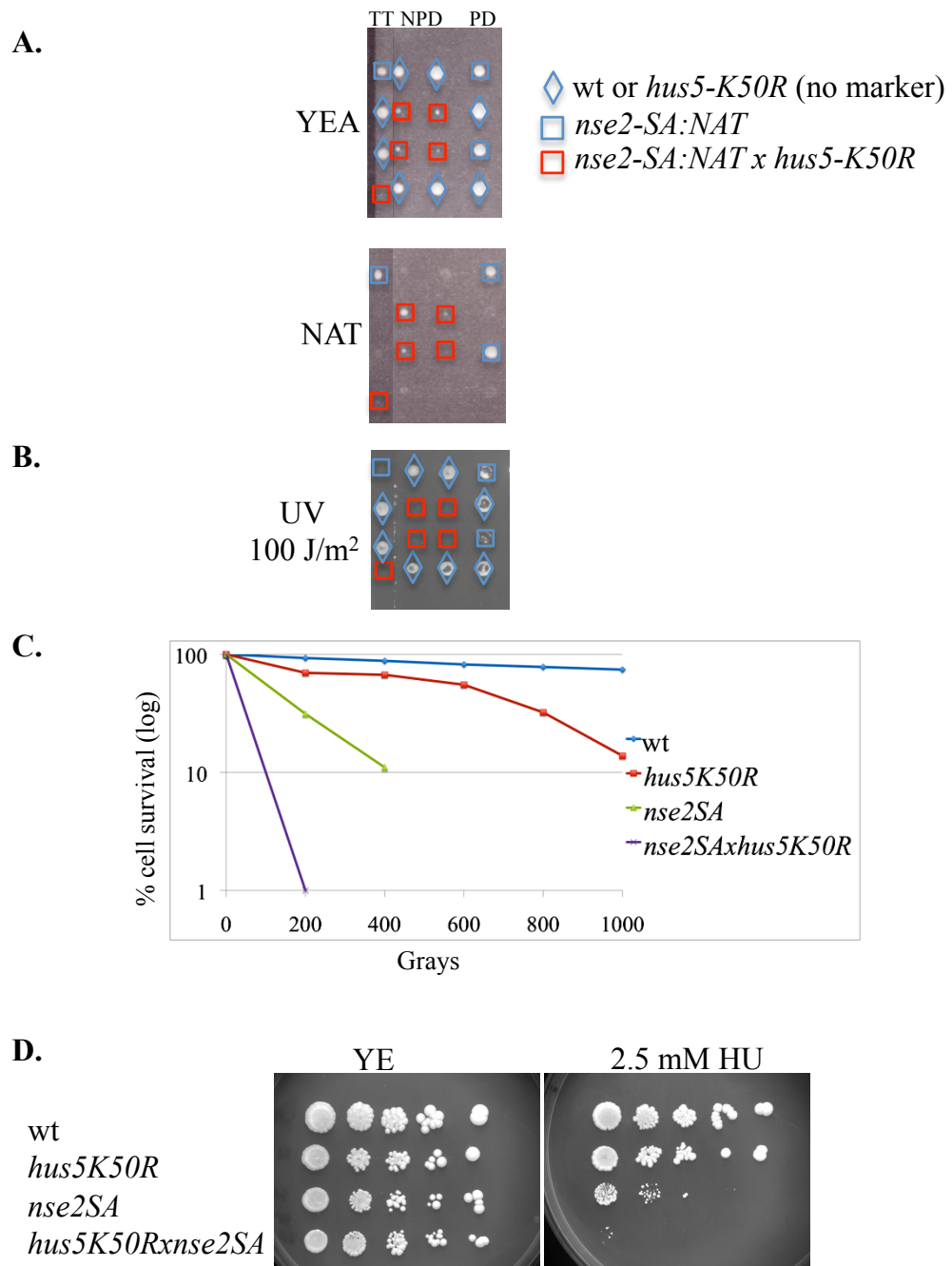


Fig. 6.25 *hus5-K50R x nse2-SA* double mutant is hypersensitive to low doses of UV, IR and HU

The *hus5-K50R* mutant is not defective in maintaining the minichromosome (fig.6.26 A) but shows an increased frequency of chromosomal rearrangements compared to wild type (fig. 6.26 B), at levels similar to those of other sumoylation mutants (see Chapter 5, section 5.2). These data suggests that the sumoylation of the SUMO conjugating enzyme is not involved in double strand break repair or chromosome segregation but has roles in maintaining the genome integrity.

6.7 Discussion

Sumoylation of the SUMO pathway components has emerged as an important regulatory mechanism of general cellular sumoylation levels and specific target discrimination. In this study, using an *in vitro* sumoylation assay and mass spectrometry, I identified specific sumoylated lysine residues of components of the sumoylation pathway, carried out an *in silico* analysis of sumoylated lysine residues of the SUMO activating enzyme Fub2, the SUMO conjugating enzyme Hus5 and the SUMO E3 ligase Nse2, and I conducted an *in vitro*, *in vivo* and genetic characterization of the Hus5 sumoylation at K50. Together with newly identified lysine residues, sumoylated K30 of the SUMO protein was identified by mass spectrometry (fig. 6.27), confirming the validity of the data presented in Chapter 3 of this study.

In silico analysis in this study and previous reports (Truong et al., 2012) reveal that SUMO isopeptide bond formation in Fub2 especially, and to some extent in Nse2, affect their enzymatic activity as the sumoylated lysine residues are present near the RING domain. It has been shown that the sumoylation of SAE2 inhibits the transfer of SUMO from E1 to E2 but not the Fub2/Uba2 adenylation or thioester formation at C173 (Truong et al., 2012). Therefore sumoylation of Fub2 at K86 could be a *S. pombe* specific mechanism of SUMO self-regulation through inhibition of E1 adenylation.

The sumoylated lysine, K50, of Hus5 is situated on an opposite surface to the catalytic cysteine and the domain involved in non-covalent interactions with target proteins, suggesting that it might not be involved in the conjugation function of Hus5. However it

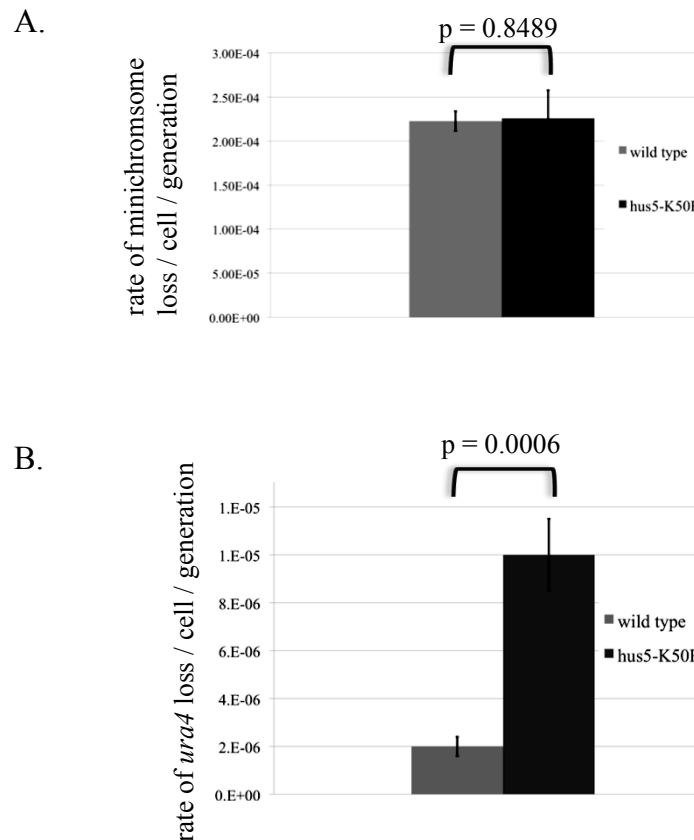


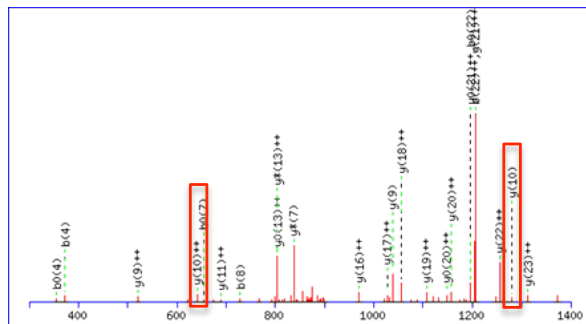
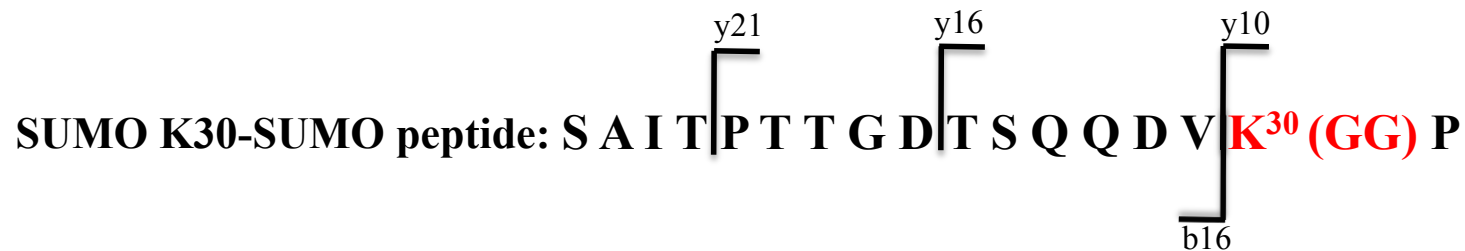
Fig. 6.26 *hus5-K50R* promotes gross chromosomal rearrangements

- A. Graphical representation of spontaneous loss of minichromosome of wild type and *hus5-K50R* strains.
- B. Graphical representation of spontaneous loss of *ura4*⁺ gene of wild type and *hus5-K50R* strains.

Bars represent s.e.m.

High p value (> 0.05): the sets of data are not significantly different.

Low p value (< 0.05): the sets of data are significantly different.



#	b	b ⁺⁺	b [*]	b ⁺⁺⁺	b ⁰	b ⁰⁺⁺	Seq.	y	y ⁺⁺	y [*]	y ⁺⁺⁺	y ⁰	y ⁰⁺⁺	#
1	88.0393	44.5233			70.0287	35.5180	S							25
2	159.0764	80.0418			141.0659	71.0366	A	2696.3373	1348.6723	2679.3108	1340.1590	2678.3268	1339.6670	24
3	272.1605	136.5839			254.1499	127.5786	I	2625.3002	1313.1538	2608.2737	1304.6405	2607.2897	1304.1485	23
4	373.2082	187.1077			355.1976	178.1024	T	2512.2162	1256.6117	2495.1896	1248.0984	2494.2056	1247.6064	22
5	470.2609	235.6341			452.2504	226.6288	P	2411.1685	1206.0879	2394.1419	1197.5746	2393.1579	1197.0826	21
6	571.3086	286.1579			553.2980	277.1527	T	2314.1157	1157.5615	2297.0892	1149.0482	2296.1052	1148.5562	20
7	672.3563	336.6818			654.3457	327.6765	T	2213.0680	1107.0377	2196.0415	1098.5244	2195.0575	1098.0324	19
8	729.3777	365.1925			711.3672	356.1872	G	2112.0204	1056.5138	2094.9938	1048.0005	2094.0098	1047.5085	18
9	844.4047	422.7060			826.3941	413.7007	D	2054.9989	1028.0031	2037.9724	1019.4898	2036.9883	1018.9978	17
10	945.4524	473.2298			927.4418	464.2245	T	1939.9720	970.4896	1922.9454	961.9763	1921.9614	961.4843	16
11	1032.4844	516.7458			1014.4738	507.7406	S	1838.9243	919.9658	1821.8977	911.4525	1820.9137	910.9605	15
12	1160.5430	580.7751	1143.5164	572.2619	1142.5324	571.7698	Q	1751.8923	876.4498	1734.8657	867.9365	1733.8817	867.4445	14
13	1289.5856	645.2964	1272.5590	636.7831	1271.5750	636.2911	Q	1623.8337	812.4205	1606.8071	803.9072	1605.8231	803.4152	13
14	1404.6125	702.8099	1387.5860	694.2966	1386.6019	693.8046	D	1494.7911	747.8992	1477.7645	739.3859	1476.7805	738.8939	12
15	1503.6809	752.3441	1486.6544	743.8308	1485.6704	743.3388	V	1379.7641	690.3857	1362.7376	681.8724	1361.7536	681.3804	11
16	1745.8188	873.4130	1728.7923	864.8998	1727.8083	864.4078	K	1280.6957	640.8515	1263.6692	632.3382	1262.6852	631.8462	10
17	1842.8716	921.9394	1825.8450	913.4262	1824.8610	912.9341	P	1038.5578	519.7826	1021.5313	511.2693	1020.5473	510.7773	9

Fig. 6.27 MS/MS fragmentation of SUMO peptide sumoylated at K30

Highlighted in boxes are the b, y and y⁺⁺ ions corresponding to K30

is in close proximity to the SUMO interacting domain like the mammalian sumoylated K14 (fig. 6.28). The non-covalent interaction between Ubc9 and SUMO is important for the interaction of the conjugating enzyme with the E3 ligases and the formation of high Mr poly-SUMO chains (Capili and Lima, 2007).

An *in vitro* sumoylation assay carried out with the Hus5-K50R mutant protein revealed that most high Mr sumoylated species are missing, including a band representing a covalent bond between the conjugating enzyme and one SUMO molecule. This is intriguing as the Hus5-SUMO thioester complex should still be present and the formation of SUMO chains should therefore not be affected. However, the thioester bond is transient and readily hydrolyses to facilitate the formation of the more stable isopeptide bond (Hershko and Ciechanover, 1998). This suggests that most of the high Mr sumoylated species observed in *in vitro* sumoylation assays are probably SUMO chains attached to the K50 of Hus5. The presence of the sumoylated form of Fub2 further confirms that the sumoylation of Hus5 at K50 does not affect its catalytic activity. As the SUMO E3 ligases enhance isopeptide bond and SUMO chain forming it would be interesting to see if Pli1 and Nse2 restore the formation of high Mr sumoylated species when the lysine at position 50 of Hus5 is mutated to an arginine, especially as the mammalian E3 ligase Rhes was shown to facilitate the sumoylation of the conjugating enzyme at multiple lysines (Subramaniam et al., 2010) .

It is interesting that, while *hus5-K50R* mutant has an opposite effect to total cellular level of sumoylation to *pli1* null mutant, both strains are lethal with the homologous recombination mutants *rad22Δ/rad52Δ* and *rhp51Δ/rad51Δ*. This suggests that strict control of overall sumoylation is required for cellular viability when the homologous recombination repair mechanism is impaired and /or both Pli1 and sumoylated Hus5 are required for an alternative repair mechanism. It would be interesting as well to analyze the levels of Hus5 in total cell extracts of *hus5-K50R* mutant.

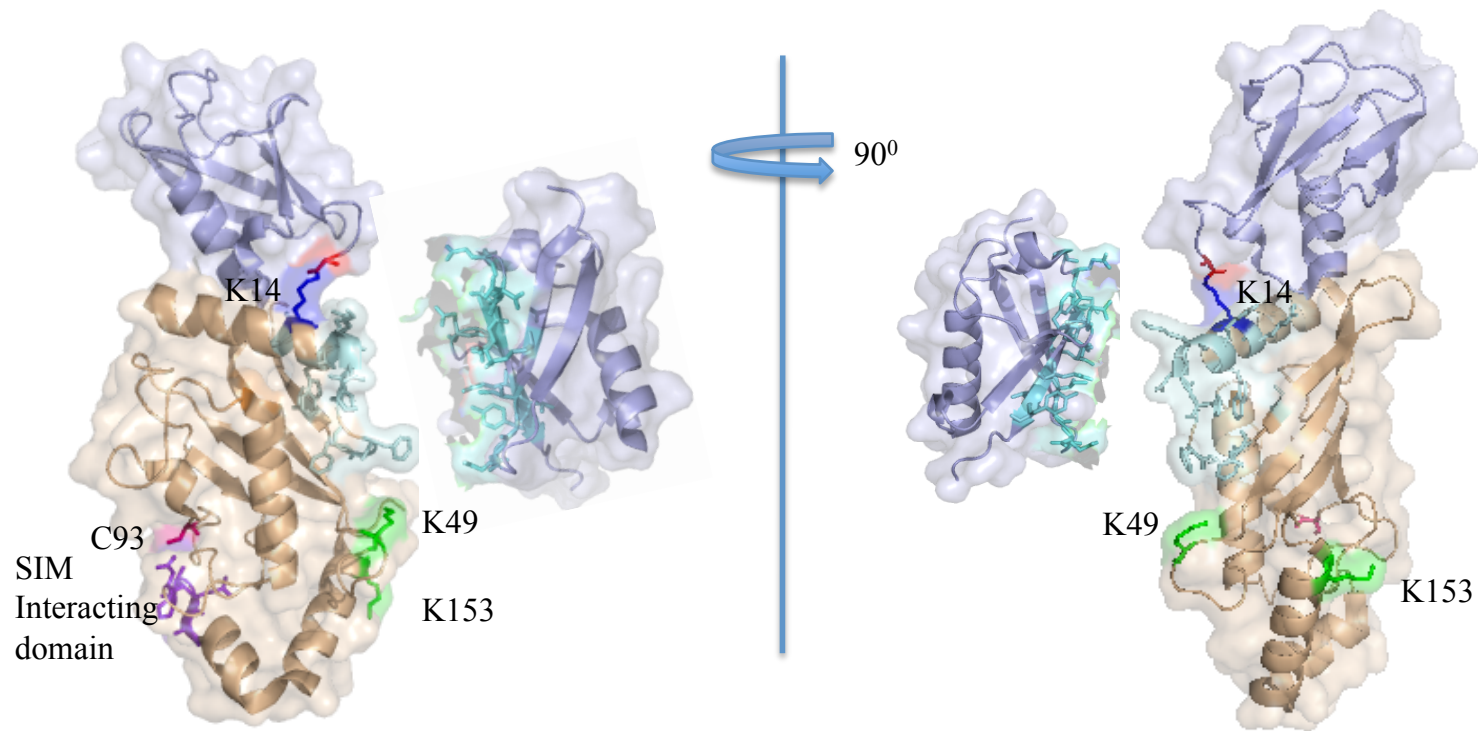


Fig. 6.28 Structural representation of non-covalent interaction of sumoylated Ubc9 with SUMO-1

Model created by PHYRE software based on the structures of *Mus musculus* Ubc9 modified by human SUMO-1 (pdb id: 2VVR) and the non-covalent complex between *Mus musculus* Ubc9 and human SUMO-1 (pdb id.: 2UYZ)

CHAPTER 7

SUMOYLATION OF RTF2 IS REQUIRED FOR RECOVERY FROM IR-INDUCED DNA DAMAGE DURING EARLY S PHASE

7.1 Introduction

Rtf2, Replication Termination factor 2, is required for the stabilization of replication forks at the RTS1 (Replication Termination Sequence 1) locus. It has been shown that the function of Rtf2 is dependent on its interactions with Pmt3 (*S. pombe* SUMO) and PCNA, the replication fork clamp loader (Inagawa et al., 2009). However the role of these interactions remains to be unveiled.

The role of sumoylation of PCNA in preventing unscheduled recombination events at stalled replication forks is well documented in *S. cerevisiae* and *H. sapiens* (Gali et al., 2012, Pfander et al., 2005). Rtf2 is the founder member of a newly discovered family of proteins (Inagawa et al., 2009) and its function is less well characterized than is that of PCNA. The interaction of Rtf2 with SUMO and the presence of a RING-type domain at its C-terminal (Inagawa et al., 2009) suggest that Rtf2 could be a sumoylation pathway component (ie an E3 ligase), but alternatively it could be a sumoylation substrate.

The *in vitro* sumoylation assay, previously developed in the lab and used to study SUMO chain formation and sumoylation of the pathway components, was employed here, together with tandem mass spectroscopy, for identification of specific modified lysine residues in Rtf2 and PCNA as previously described (see chapter 2, section 2.4.22)

7.2 PCNA is sumoylated at specific lysines *in vitro*

For use of PCNA as a substrate in the *in vitro* sumoylation assay, the protein was expressed and purified from a pET15b plasmid in *E. coli* as a His-tagged fusion protein (construct made by J. Ho, University of Sussex). It has been previously shown that in *S. cerevisiae* the sumoylation of PCNA is enhanced by the E3 ligase Siz1 (Hoege et al., 2002, Windecker and Ulrich, 2008), the homologue of *S. pombe* SUMO E3 ligase Pli1. To identify modified lysine residue in PCNA two sumoylation assays were carried out, one without Pli1 and the second one with Pli1, and the results were analysed by western blotting (fig. 7.1). The unmodified His-PCNA is clearly visible at ~ 30 kDa and one band corresponding to mono-sumoylated PCNA is visible at approximately 40kDa (SUMO runs at ~ 10 kDa on SDS-PAGE) on the assay without Pli1. As expected multiple bands at 10 kDa intervals are observed in the lane corresponding to the sumoylation assay with Pli1. Bands corresponding to the sumoylated form of PCNA were excised from colloidal stained gels and sent to mass spectrometry services for in-gel trypsin digestion, LC-MS/MS and MASCOT searches (Dr. L. Bowler and M. Daniels, Proteomics Department, University of Sussex). The PCNA lysine residues modified by SUMO identified by MS/MS in *S. pombe* together with those previously identified in *S. cerevisiae* and mammals are listed in table 7.1.

7.3 *In silico* analysis of sumoylation of PCNA in *S. pombe*

K13, K164, K176 and K253 of PCNA were identified from the MS/MS spectra, peptide mass fingerprints, sequence queries and MS/MS ion searches using the MASCOT search engine (see section 2.4.22; fig. 7.2, 7.3, 7.4 and 7.5 respectively) (Perkins et al., 1999). K164, the main sumoylation site of PCNA in *S. cerevisiae* and mammals, is within a non-consensus sumoylation sequence. To assess if the newly identified lysine residues are within consensus sumoylation sites, the sequence of PCNA was analyzed with the SUMOsp 2.0 site specific predictor software (Ren et al., 2009). Interestingly,

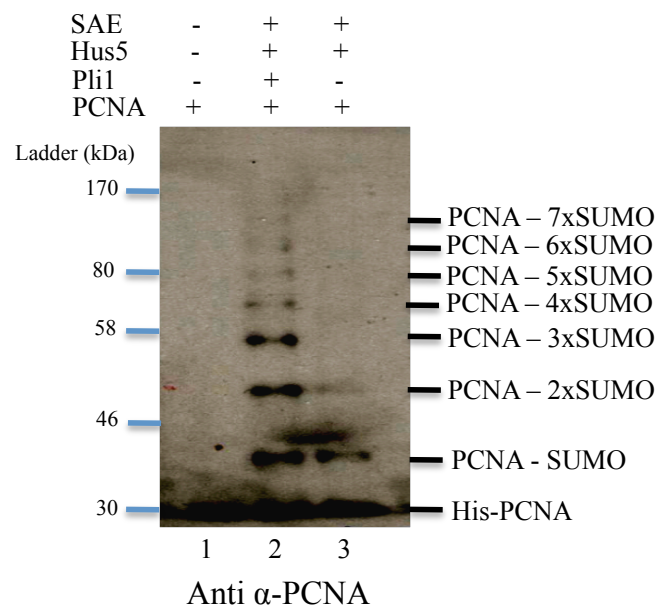


Fig. 7.1 *in vitro* poly-sumoylation of PCNA is facilitated by Pli1 E3 ligase

Western blotting of *in vitro* sumoylation assay with PCNA as target protein. Probed with α -PCNA antibodies.

Substrate	Sumoylated Ks identified in this study	Sumoylated Ks in <i>Hs</i>	Sumoylated Ks in <i>Sc</i>
PCNA	13, 164, 172, 253	164, 254 Gali <i>et. al.</i> , 2012	127, 164 Hoege <i>et. al.</i> , 2002

Table 7.1 Sumoylated lysine residues identified in PCNA

PCNA lysine position	Peptide	Type
13	ALLKLL	Non-consensus
164	NASKEGV	Non-consensus
172	FSCKGDI	Non-consensus
253	LAPKIGE	Non-consensus

Table 7.2 *S. pombe* PCNA possible sumoylation sites are within non-consensus motifs

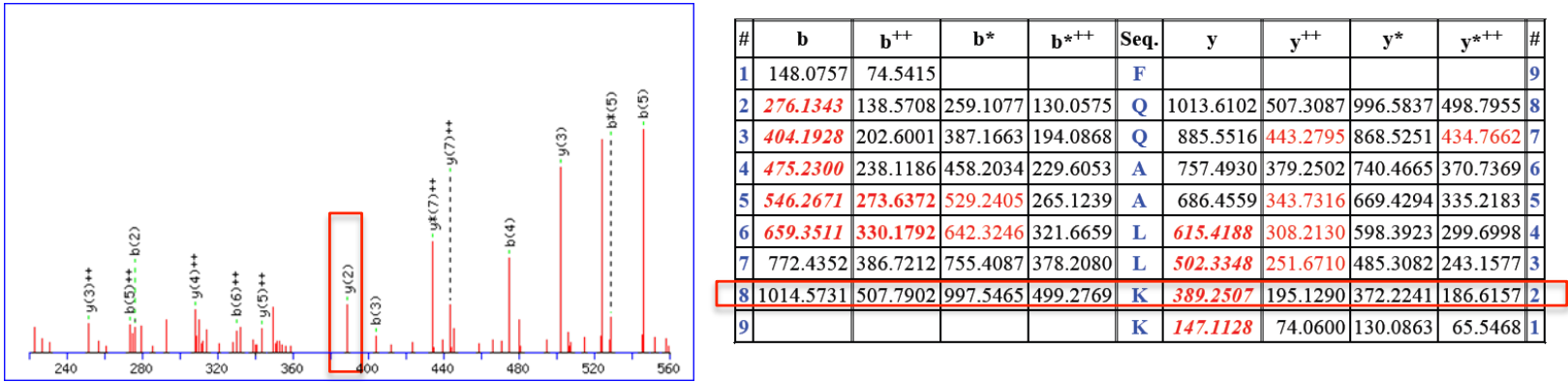
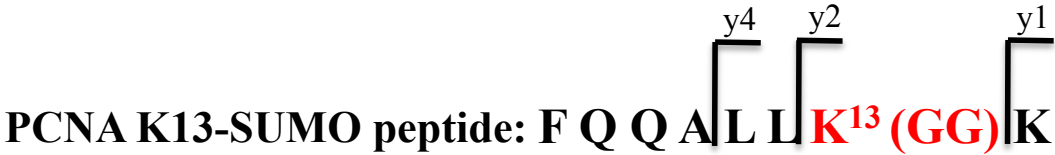
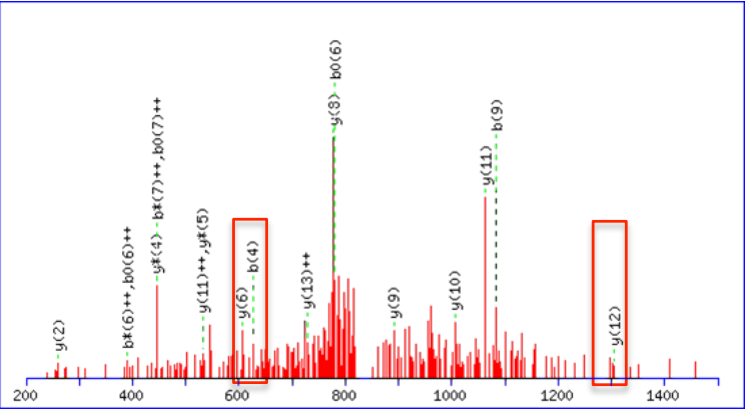
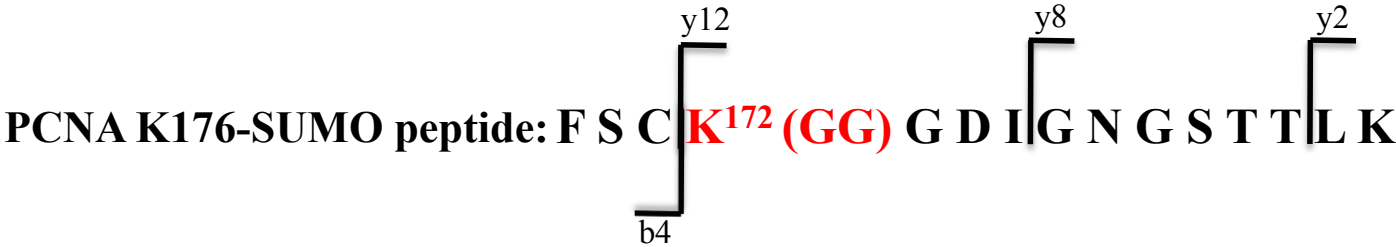


Fig. 7.2 MS/MS fragmentation of PCNA peptide sumoylated at K13

Highlighted in the red boxes are the b and y ions corresponding to K13



#	b	b ⁺⁺	b ⁺	b ⁺⁺⁺	b ⁰	b ⁰⁺⁺	Seq.	y	y ⁺⁺	y ⁺	y ⁺⁺⁺	y ⁰	y ⁰⁺⁺	#
1	148.0757	74.5415					F							15
2	235.1077	118.0575			217.0972	109.0522	S	1541.6934	771.3503	1524.6669	762.8371	1523.6829	762.3451	14
3	384.1046	192.5560			366.0941	183.5507	C	1454.6614	727.8343	1437.6348	719.3211	1436.6508	718.8291	13
4	626.2425	313.6249	609.2160	305.1116	608.2319	304.6196	K	1305.6645	653.3359	1288.6379	644.8226	1287.6539	644.3306	12
5	683.2640	342.1356	666.2374	333.6224	665.2534	333.1303	G	1063.5266	532.2669	1046.5000	523.7537	1045.5160	523.2617	11
6	798.2909	399.6491	781.2644	391.1358	780.2804	390.6438	D	1006.5051	503.7562	989.4786	495.2429	988.4946	494.7509	10
7	911.3750	456.1911	894.3484	447.6779	893.3644	447.1858	I	891.4782	446.2427	874.4516	437.7295	873.4676	437.2375	9
8	968.3964	484.7019	951.3699	476.1886	950.3859	475.6966	G	778.3941	389.7007	761.3676	381.1874	760.3836	380.6954	8
9	1083.4234	542.2153	1066.3968	533.7021	1065.4128	533.2101	N	721.3727	361.1900	704.3461	352.6767	703.3621	352.1847	7
10	1140.4449	570.7261	1123.4183	562.2128	1122.4343	561.7208	G	606.3457	303.6765	589.3192	295.1632	588.3352	294.6712	6
11	1227.4769	614.2421	1210.4503	605.7288	1209.4663	605.2368	S	549.3243	275.1658	532.2977	266.6525	531.3137	266.1605	5
12	1328.5246	664.7659	1311.4980	656.2526	1310.5140	655.7606	T	462.2922	231.6498	445.2657	223.1365	444.2817	222.6445	4
13	1429.5722	715.2898	1412.5457	706.7765	1411.5617	706.2845	T	361.2445	181.1259	344.2180	172.6126	343.2340	172.1206	3
14	1542.6563	771.8318	1525.6298	763.3185	1524.6457	762.8265	L	260.1969	130.6021	243.1703	122.0888			2
15							K	147.1128	74.0600	130.0863	65.5468			1

Fig. 7.4 MS/MS fragmentation of PCNA peptide sumoylated at K172

Highlighted in boxes are the y and b ions corresponding to K172

like K164, none of the identified sumoylated lysine residues are within consensus sequences (table 7.2).

To evaluate the significance of the identified sumoylation sites it was important to determine if they are evolutionarily conserved like K164. The sequence alignment of *S. cerevisiae*, *H. sapiens* and *S. pombe* PCNA (fig. 7.6) reveals that K13 is conserved in all three organisms. K172 is not conserved, like *S. cerevisiae* K127 that was identified as a sumoylation site (Hoege et al., 2002). K254 is conserved in all three organisms and was identified as a sumoylation site in mammalian cells (Gali et al., 2012) but not in *S. cerevisiae*. The crystal structures of *S. cerevisiae* and *H. sapiens* PCNA have been elucidated (Freudenthal et al., 2009, Punchihewa et al., 2012, Krishna et al., 1994), including the crystal structure of PCNA modified by SUMO at K164 (Armstrong et al., 2012) and PCNA in complex with DNA (McNally et al., 2010) (fig. 7.7 A, B and D). To map the identified sumoylation sites, the sequence of *S. pombe* PCNA was modeled onto the crystal structure of *H. sapiens* PCNA (Punchihewa et al., 2012) using the PHYRE protein-modeling server (fig. 7.7 C). Like K164, K172 and K253 are situated on the external β sheets of the homotrimer, shown to be implicated in the PCNA protein-protein interactions, while the K13 is positioned on the internal α helices, shown to be important for the interactions of PCNA with DNA (fig. 7.7 D).

This *in silico* analysis suggests that the lysine residues identified to be sumoylated *in vitro* could be important sumoylation sites *in vivo* with key functions in PCNA-protein and PCNA-DNA interactions.

7.4 Rtf2 does not function as a SUMO E3 ligase *in vitro*

Given the presence of a RING domain, characteristic to SUMO and ubiquitin ligases, and the interaction with SUMO, the possibility of Rtf2 to function as a SUMO E3 ligase was tested by means of *in vitro* sumoylation assays.

The Rtf2 protein was expressed and purified from a pET-21a plasmid in *E. coli* as a MBP-6xHis tagged fusion protein (construct made by J. Daalgard, University of

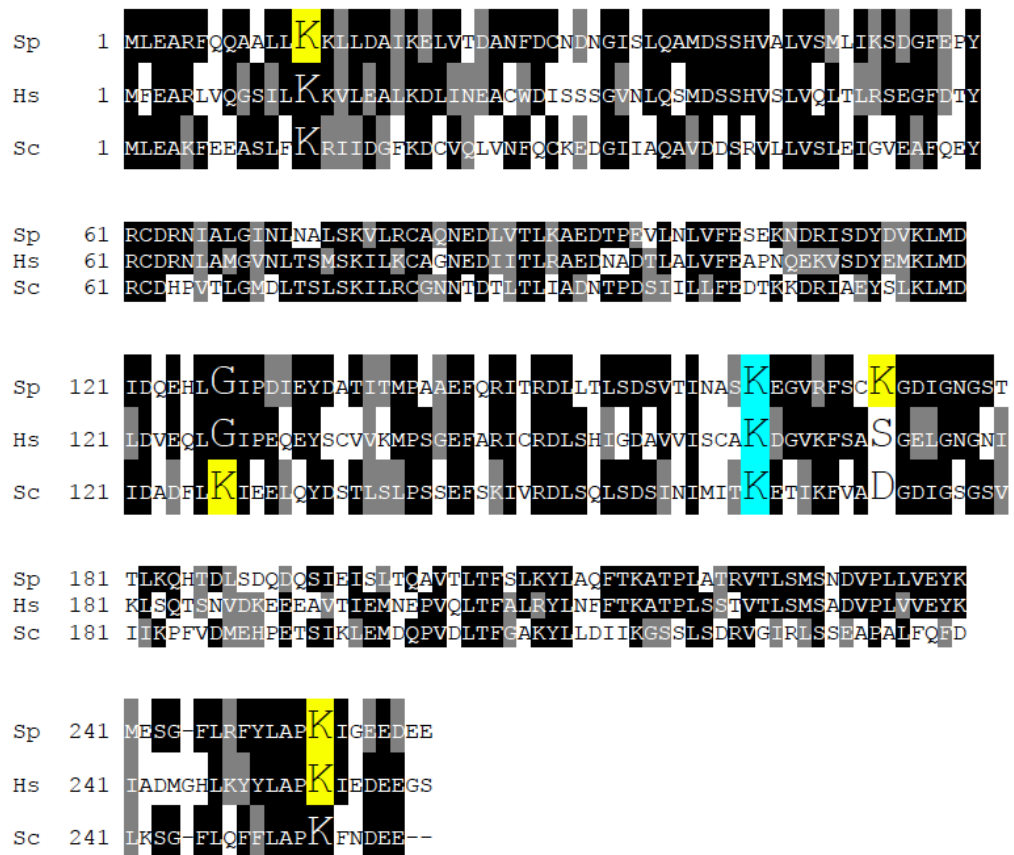


Fig. 7.6 *S. pombe* PCNA sumoylated lysine residues are sequentially conserved in humans and *S. cerevisiae*

Sequence alignment of *S. pombe*, *H. sapiens* and *S. cerevisiae* PCNA.

Highlighted in blue is K164 that is ubiquitinated and sumoylated in all three organisms. Highlighted in yellow are other lysines identified as sumoylation sites.

Fig. 7.7 Structural mapping of the sumoylated lysines and possible sumoylation sites of PCNA

- A. Cartoon representation of the crystal structure of *H. sapiens* PCNA (pdb id: 3VKX). Highlighted in blue and red are lysine residues identified to be sumoylated: K164 and K253 respectively.
- B. Cartoon representation of the crystal structure of *S. cerevisiae* PCNA conjugated to SUMO (in light blue) at K164 (blue) (pdb id: 3V60). Highlighted in red is K127 which was identified as a sumoylation site.
- C. Cartoon representation of the structural model of *S. pombe* PCNA. Model created by PHYRE software based on the crystal structure of *S. cerevisiae* PCNA (pdb id: 3V60). Highlighted in blue and red are lysine residues identified to be sumoylated in vitro: K164 and K13, K172 and K254 respectively.
- D. Cartoon representation of *S. cerevisiae* trimeric PCNA in complex with DNA (pink) (pdb id: 3K4X). Highlighted in blue is K164 residue identified to be sumoylated in all three organisms. Highlighted in red are sumoylated lysine residues specific to each organism.

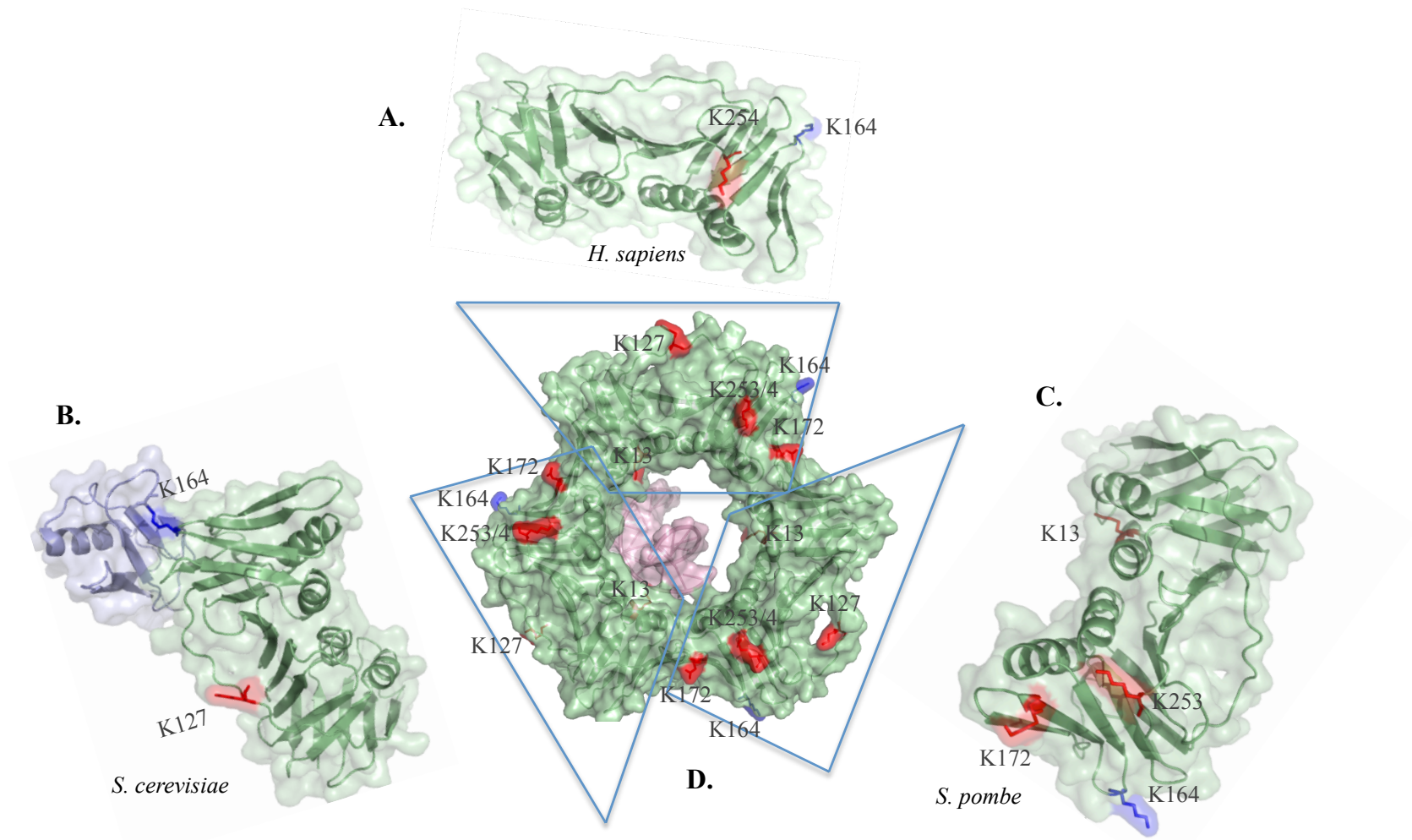


Fig. 7.7 Structural mapping of the sumoylated lysines and possible sumoylation sites of PCNA

Warwick). To determine whether Rtf2 can function as a SUMO E3 ligase, the sumoylation assay was carried out under the conditions used to test for ligase function (fig. 7.8). When Rtf2 was added to the assay carried out with a tenth of the required amount of Hus5, the formation of the high Mr sumoylated species was not restored (fig. 7.8 A and B, lane 6). However, when Rtf2 was added to the assay carried out with the full amount of Hus5 an additional band was identified above 80 kDa that could correspond to a sumoylated form of Rtf2 (fig. 7.8 A lane 9).

The results of the *in vitro* sumoylation assay suggest that Rtf2 does not function as a SUMO E3 ligase, but it cannot be excluded that Rtf2 is a specific SUMO E3 ligase, like Nse2, rather than a general one, like Pli1. *In vitro*, a ten-fold amount of Nse2 compared to Pli1 is required to restore high Mr sumoylated species when low amounts of the SUMO conjugating enzyme are present. To assess if this is the case for Rtf2, sumoylation assays were carried out with increasing amounts of Rtf2 (fig. 7.8 B) and compared with sumoylation assays with Pli1 and Nse2 (fig. 7.8 B lanes 3 and 7). Interestingly, increasing the amount of Rtf2 reduces the intensity of high Mr sumoylated species (fig. 7.8 B lanes 4.5 and 6) further confirming that Rtf2 does not function as a SUMO E3 ligase *in vitro*.

7.5 Rtf2 is sumoylated *in vitro* at specific lysine residues

The *in vitro* sumoylation assay was scaled up from 20 µl to 100 µl so that proteins could be visualized by colloidal blue staining. Bands matching the Rtf2 protein and possible sumoylated forms of it were excised from colloidal stained gels (fig. 7.9) and sent to mass spectrometry services for in-gel trypsin digestion, LC-MS/MS run and MASCOT search (Dr. L. Bowler and M. Daniels, Proteomics Department, University of Sussex). K184, K209 and K224 of Rtf2 were identified from the MS/MS spectra, peptide mass fingerprints, sequence queries and MS/MS ion searches using the MASCOT search engine (see section 2.4.22; fig. 7.10, 7.11 and 7.12 respectively) (Perkins et al., 1999).

Fig. 7.8 Rtf2 does not function as a SUMO E3 ligase *in vitro*

- A. Western blot of sumoylation assay with Rtf2. Probed with anti SUMO antibodies
- B. Western blot of sumoylation assay with E3 ligases Pli1 (lane3) and Nse2 (lane 7) and Rtf2 (lanes 4, 5 and 6). Probed with anti SUMO antibodies.

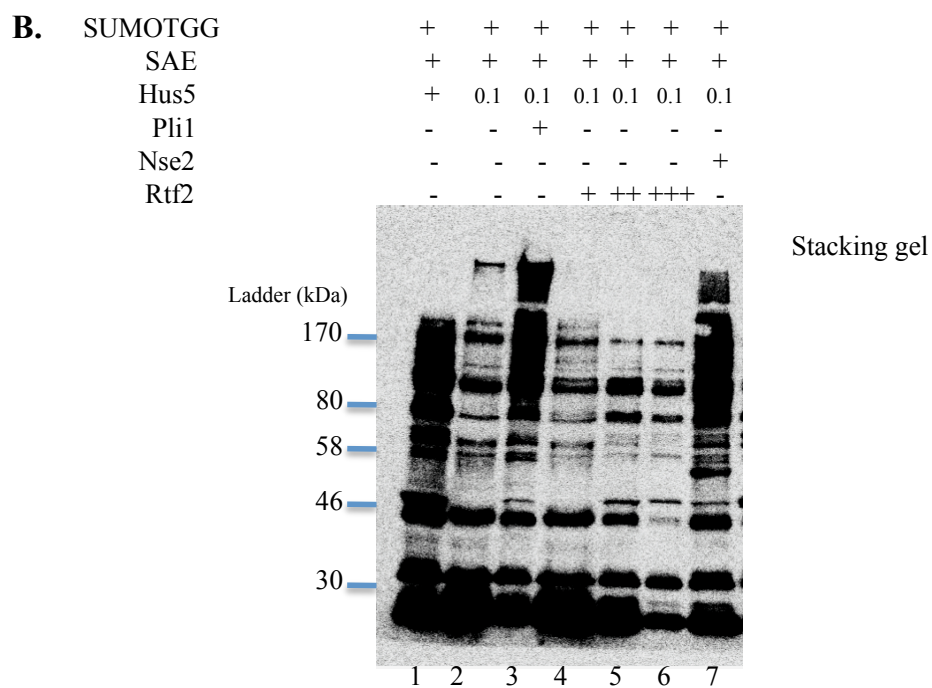
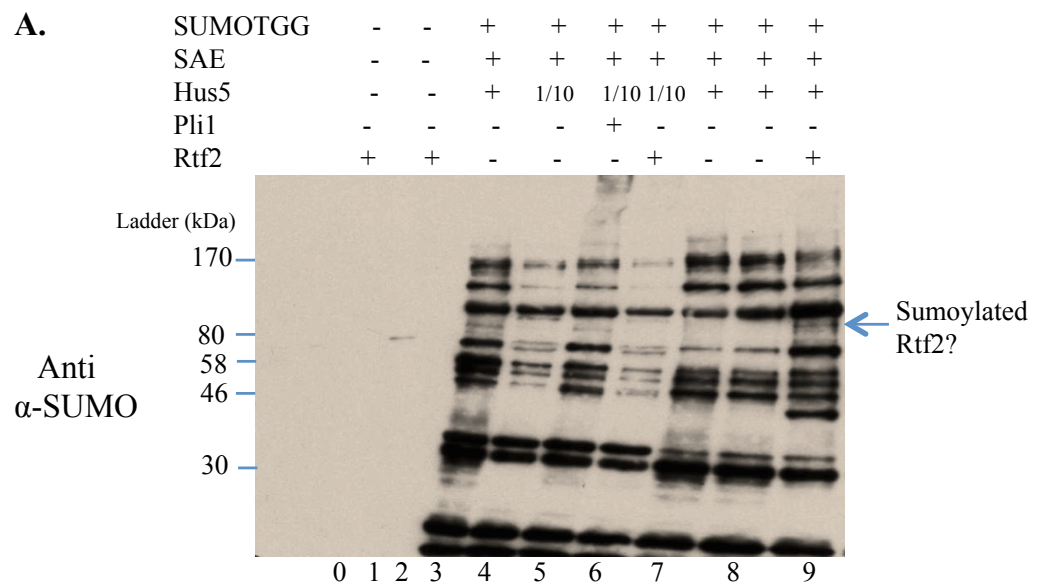


Fig. 7.8 Rtf2 does not function as a SUMO E3 ligase *in vitro*

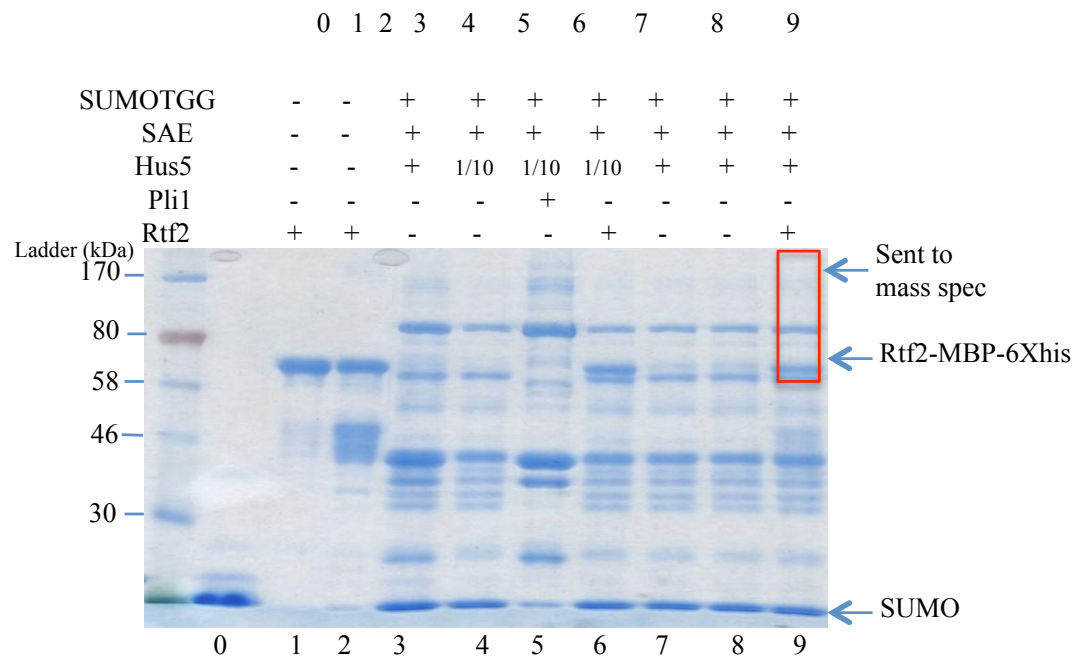


Fig. 7.9 Rtf2 is sumoylated *in vitro*

Colloidal blue staining of sumoylation assay with Rtf2 as target protein.

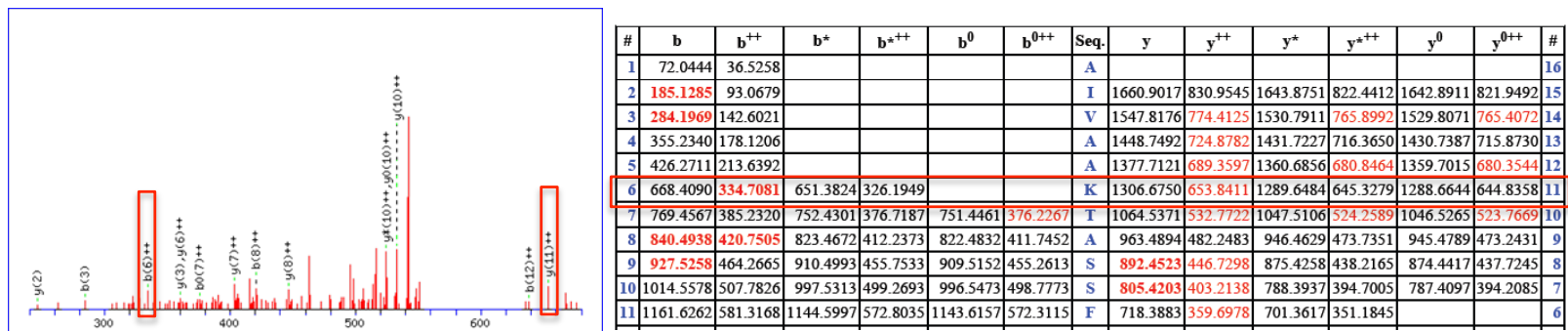
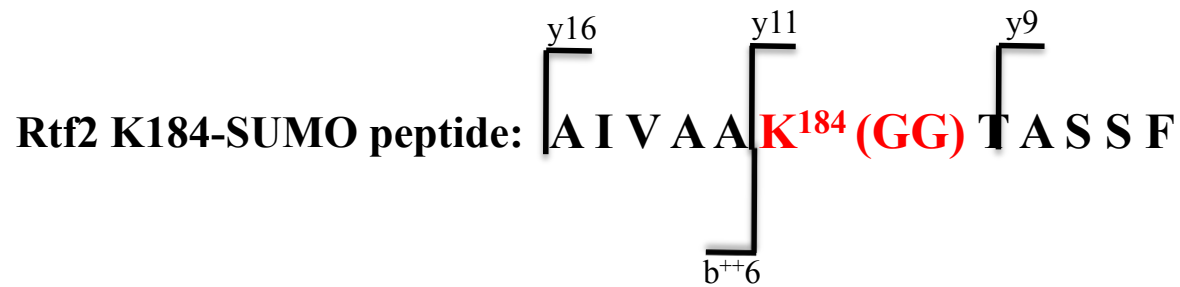
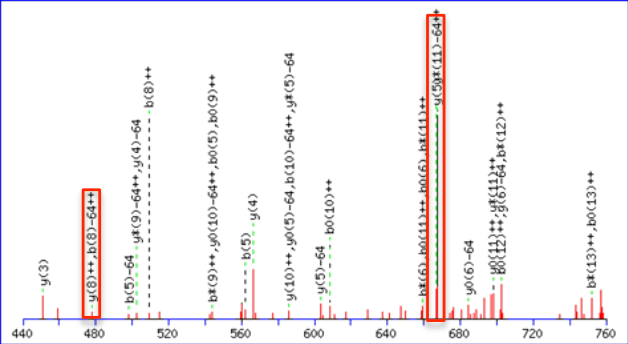


Fig. 7.10 MS/MS fragmentation of Rtf2 peptide sumoylated at K184

Highlighted in boxes are the b and y ions corresponding to K184



#	b	b ⁺⁺	b ⁺	b ⁺⁺⁺	b ⁰	b ⁰⁺⁺	Seq.	y	y ⁺⁺	y ⁺	y ⁺⁺⁺	y ⁰	y ⁰⁺⁺	#
1	148.0427	74.5250					M							18
2	261.1267	131.0670					L	2040.9026	1020.9549	2023.8761	1012.4417	2022.8921	1011.9497	17
3	376.1537	188.5805			358.1431	179.5752	D	1927.8186	964.4129	1910.7920	955.8996	1909.8080	955.4076	16
4	433.1751	217.0912			415.1646	208.0859	G	1812.7916	906.8994	1795.7651	898.3862	1794.7810	897.8942	15
5	562.2177	281.6125			544.2072	272.6072	E	1755.7701	878.3887	1738.7436	869.8754	1737.7596	869.3834	14
6	677.2447	339.1260	660.2181	330.6127	659.2341	330.1207	N	1626.7276	813.8674	1609.7010	805.3541	1608.7170	804.8621	13
7	776.3131	388.6602	759.2865	380.1469	758.3025	379.6549	V	1511.7006	756.3539	1494.6741	747.8407	1493.6900	747.3487	12
8	1018.4510	509.7291	1001.4244	501.2159	1000.4404	500.7238	K	1412.6322	706.8197	1395.6057	698.3065	1394.6216	697.8145	11
9	1105.4830	553.2451	1088.4565	544.7319	1087.4725	544.2399	S	1170.4943	585.7508	1153.4678	577.2375	1152.4837	576.7455	10
10	1234.5256	617.7664	1217.4991	609.2532	1216.5150	608.7612	E	1083.4623	542.2348	1066.4357	533.7215	1065.4517	533.2295	9

Fig. 7.12 MS/MS fragmentation of Rtf2 peptide sumoylated at K224

Highlighted in boxes is the y ion corresponding to K50

7.6 *In silico* analysis Rtf2

The three lysine residues in Rtf2 identified to be sumoylated *in vitro* are situated in different type of motifs: K184 is within a non-consensus sequence, while K209 and K224 are within canonical sumoylation motifs (table 7.3). Sequence alignment of *S. pombe* Rtf2 with the *H. sapiens* and *S. japonicus* homologues (fig. 7.13 A) reveals that K184 is conserved in all three organisms while K209 and K224 are not conserved. This suggests that sumoylation of Rtf2 at K184 could have an evolutionary conserved function. Human Rtf2 has lysine residues equivalent to the residues corresponding to K209 and K224, namely K254 and K269 respectively, suggesting that these residues could be structurally conserved. Sequence alignment of Rtf2 with the human ubiquitin ligase BRCA1 suggests that the C2HC2 RING domain of Rtf2 can adopt a similar fold as the C3HC4 RING domain of BRCA1 (Inagawa et al., 2009). It has been shown that the ubiquitin ligase activity of BRCA1 is stimulated by the sumoylation at a lysine residue situated just after the RING domain (K119) (Morris et al., 2009). Since the identified sumoylated lysines of Rtf2 are situated at the C-terminal just after the RING domain, it was interesting to determine whether extending the alignment with BRCA1 revealed any conserved lysine residues. Indeed the K209 of Rtf2 corresponds to the sumoylated K119 of BRCA1 (fig. 7.13 B). This suggests that Rtf2 could be a SRUbL (SUMO-Regulated Ubiquitin Ligase) like BRCA1.

To further understand if the K184, K209 and K224 of Rtf2 are of structural or functional importance, full-length Rtf2 modeling queries were submitted to PHYRE, SWISS-MODEL and I-TASSER protein modeling servers. Nearly all of the returned hits were models of the C2HC2 RING domain mostly based on RING domains of ubiquitin ligases, with one model based on the E3 SUMO ligase Nse2 and only the PHYRE server returned full length models of *S. pombe* and *H. sapiens* Rtf2 (fig. 7.14). Interestingly all lysines, *S. pombe* K184, K209 and K224, corresponding to human K230, K254 and K269 respectively, are surface residues that could be available for SUMO conjugation. More importantly they are all situated on a similar arrangement in *S. pombe* and humans in relation to the C2HC2 RING domain.

Rtf2 lysine position	Peptide	Type
184	SLN K ASK	Non-consensus
209	KHA K HEL	Ψ-K-X-E
224	ENV K SET	Ψ-K-X-E

Table 7.3 Rtf2 possible sumoylation sites are within non-consensus and canonical motifs

Fig. 7.13 Sequence alignment of Rtf2

- A. Sequence alignment of *S. pombe*, *S. japonicus* and *H. sapiens* Rtf2 protein. Highlighted in green are the U-box and C2HC2 RING domains. Highlighted in blue are lysines identified to be sumoylated *in vitro* in *S. pombe* and sequentially conserved. Highlighted in yellow are possible structurally conserved sumoylated lysines.
- B. Sequence alignment of *S. pombe* Rtf2 and *H.sapiens* BRCA1. Highlighted in yellow is the conserved RING domain. Boxed is the Rtf2 sumoylated K209 that corresponds to the sumoylation site K119 of BRCA1.

A.

```

Sp   1  -----MGNDGGSIPTRNELVKEEGKVPPLDID-----
Sj   1  MRLAKANLIKATDGEVLGGSIPLRQELVKQKSKVAQLDID-----
Hs   1  -----MGNDGGTIPKRHELVKGEKKVEKTWHLKNGKEWCSLHSEGKNKNGKE

                                     U-box

Sp  28  -----FKRSVKSSQFSQCAITDEHLYPPIVSCGLGKLYNKASILQMLLDR---SSVPK
Sj  41  -----LKRSLHKSLFTQCSLSGASLRDPIVSCGFGRLYNKEAILEMLLNR---SLYPN
Hs  48  WDMEDVDKDAELVAQNNYCTLSQELLRPIVACELGRLYNKDAVIEFLLDNSAEKALGK

                                     C2HC2 RING

Sp  78  SPSHIKSLKDVVQLQVE-----LDDSGKVLWLCPITRHVMSDTYQFAYI
Sj  91  APAHITSIKDVQLQSMK-----KNEE-TDRWMCPLSRHEENEAHKEVYI
Hs 108  AASHIKSIKNVTEIKLSDNPAWEGDKGNTKGDKHDDLQARFICPVVGLMNGRHRFCFL

Sp 122  VPCGHVFEYSALKQFGEKMGFCQCNQVYEEKDVIPINPNAEQIKTLKRLLDLALSEKTHS
Sj 134  VPCGHVFELSASFQTVGNECVLCSTAVNKDDIPINPSTEQEKALKERLEKLAQQGKTHS
Hs 168  RCCGCVBSERALKETKAENVCHTCGAAFQEDDVIMINGKEDVDVLKTRMEERRLRAKLEK

Sp 182  LNKASKKSNKNGDKKRKHVSKSNSKHAHELRTNRMLDGENVKSETSVTDMERVKRVKI
Sj 194  LKKIPN-SKKNSKKEKKKLPSEASTTEHRETKEHVHTDKLVA-----
Hs 228  KTKKPKAAESVSKPDIVSEEAPGEKKVKTG PEEASDSEKKTNLAPKST-----

```

B.

```

Rtf2_  1  MGNDGGSIPTRNELVKEPGKVPPLDIDFKRSVKSSQFSQCAITDEPLYPP      50
BRCA1   1  -----                                0

Rtf2_  51  IVSCGLGKLYNKASILQMLLDRSSVPKSPSHIKSLKDVVQLQVE-----L      95
                                     .|...|:|
BRCA1   1  -----MDLSALRVEEVQNVI      15

Rtf2_  96  DDSGKVLWLCPITRHVMSDTYQFAYIVPCGHVF-EYSALKQFGEK---M      140
      ...|:| .|||...:.. ..|:| :...|...:|
BRCA1  16  NAMQKIL-ECPICLELIKEPVS---TKCDHIFCKFCMLKLLNQKKGPSQ      60

Rtf2_ 141  CFQC-----NQVYEEKDVIPINPNAEQIKTLKRLLDLAL      175
      |..| :|:~| |..|:|...|..|
BRCA1  61  CPLCKNDITKRSIQESTRFSQLVE-----ELLKIICAFQLDTGL      99

Rtf2_ 176  SEKTHSLNKASKKSNKNGDKKRKHVSKSNSKHAHEL-----RTN      215
      |..|..|..|:~| :~|..|:~|
BRCA1 100  -EYANSYNFAKKENN-----SPEHLKDEVSIIQSMGYRNRK      135

Rtf2_ 216  RMLDGENVK---SETS---VTDMERVKRVKI-----      240
      |:|..|..• .||| :~...|:~...
BRCA1 136  RLLQSEPENPSLQETSLSVQLSNLGTVRTLRTKQRIQPQKTSVYIELGSD      185

```

Fig. 7.13 Sequence alignment of Rtf2

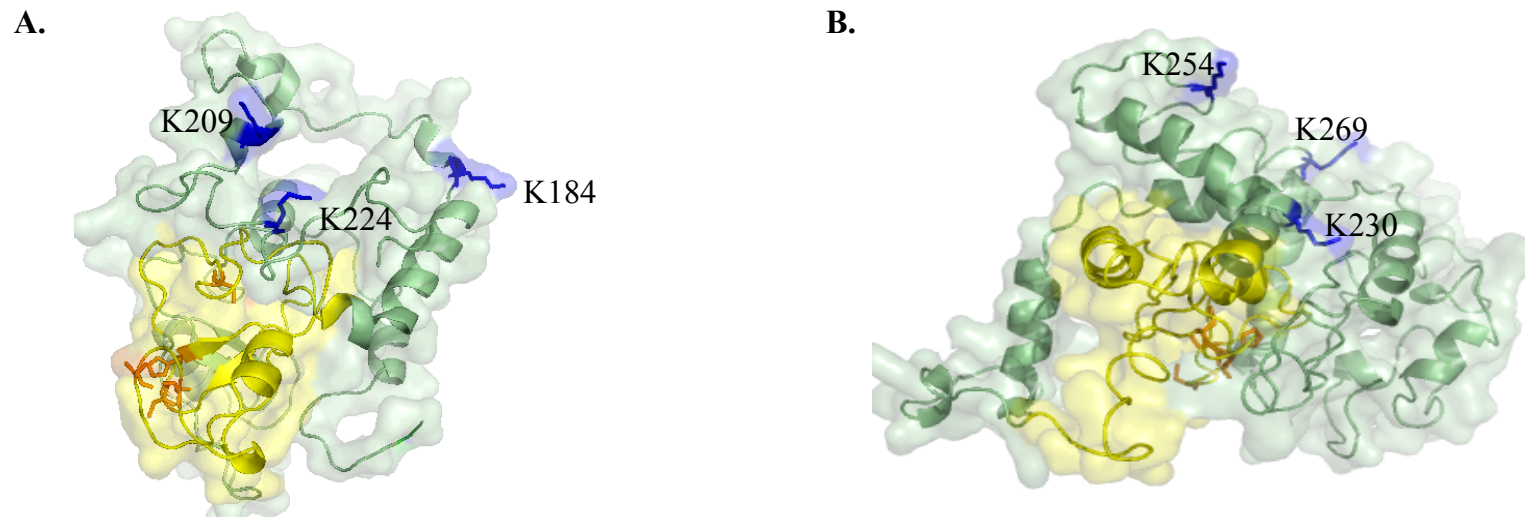


Fig. 7.14 Structural modeling of *S. pombe* and *H. sapiens* Rtf2 protein

A. Cartoon representation of structural model of *S. pombe* Rtf2

B. Cartoon representation of structural model of *H. sapiens* Rtf2

Highlighted in blue are sumoylated lysine residues identified in *S. pombe* and their corresponding lysines in *H. sapiens*.

Highlighted in yellow are the C2HC2 RING domains. Structural models created using the PHYRE server. Cartoon representation created using PYMOL software.

7.7 Creating the Rtf2 sumoylation mutants from a *rtf2*⁺ base strain

To facilitate the construction of the *rtf2* sumoylation mutants, a *rtf2* base strain was first created employing the RMCE strategy for non-essential genes (Watson et al., 2008)(see sections 2.1.3.2 and 2.1.4). The *ura4*⁺ gene flanked by the loxP and loxM sites was amplified from pAW1 plasmid with primers with homology to sequences upstream and downstream of loxP and loxM respectively, and to genomic sequences upstream of the *rtf2*⁺ promoter and downstream of the *rtf2*⁺ terminator (*rtf2*-W1_F: 5' CAGTCGTGGAATGTAAGCGCTTCTTTGAAATATGCTTACTTAACACTACTCA AATTTAATACACACAAGTAACTTATAGCTACATTATACGAA and *rtf2*-W1_R: 5' AAGTTGCTTTATTTATGGGTAAATTAATACACACATACATTTATCTTTTAA AAAAAAATCTACTATGTACATTTAAATATATAGCATACATTATCGAA) (fig. 7.15 A). The PCR product was used to transform a wild type strain to obtain the *rtf2::ura4* base strain. To create an *rtf2*⁺ strain the chromosomal *rtf2*⁺ gene together with the promoter and terminator was amplified with primers containing the sites for the SphI and SpeI enzymes present in the MCS of pAW8 plasmid (*rtf2*-W8_F: 5' GTAATATTTAATACACACAAGCATGC and *rtf2*-W8_R: 5' AATCTACTATGT ACATTACTAGT) (fig. 7.15 B). The PCR product was ligated into the MCS of pAW8 plasmid and the *rtf2*⁺ strain was obtained by transforming the *rtf2::ura4* base strain with the pAW8-*rtf2*⁺ plasmid due to homologous recombination between the heterospecific loxP and loxM sites (fig. 7.15 B).

To create the *rtf2* sumoylation mutants, site directed mutagenesis was carried out on pAW8-*rtf2* to mutate K184, K209 and K224 to arginine residues. The mutated pAW8-*rtf2* plasmids were used to transform the *rtf2::ura4* base strain to obtain the strains with one lysine mutated to arginine (*rtf2*-K184R, *rtf2*-K209R and *rtf2*-K224R), two lysine mutated to arginine (*rtf2*-K184R;K224R) and all three lysine residues mutated to arginine (*rtf2*-T) (fig. 7.16). Given the importance of the sumoylation of BRCA1 at K119, further genetical analysis was carried out on the *rtf2*-K209R mutant and

Fig. 7.15 Strategy to create a *rtf2*⁺ base strain using RMCE strategy

- A. A *rtf2* deletion strain was obtained by replacing the *rtf2* gene with *ura4* gene flanked by the heterospecific sites *loxP* (at 5' end) and *loxM3* (at the 3' end) in the *S. pombe* genome.
- B. A *rtf2*⁺ base strain was obtained by transforming the *rtf2::ura4* strain with a pAW8 plasmid containing the *rtf2* gene between the heterospecific sites *loxP* and *loxM*

○○○○○ = chromosomal DNA

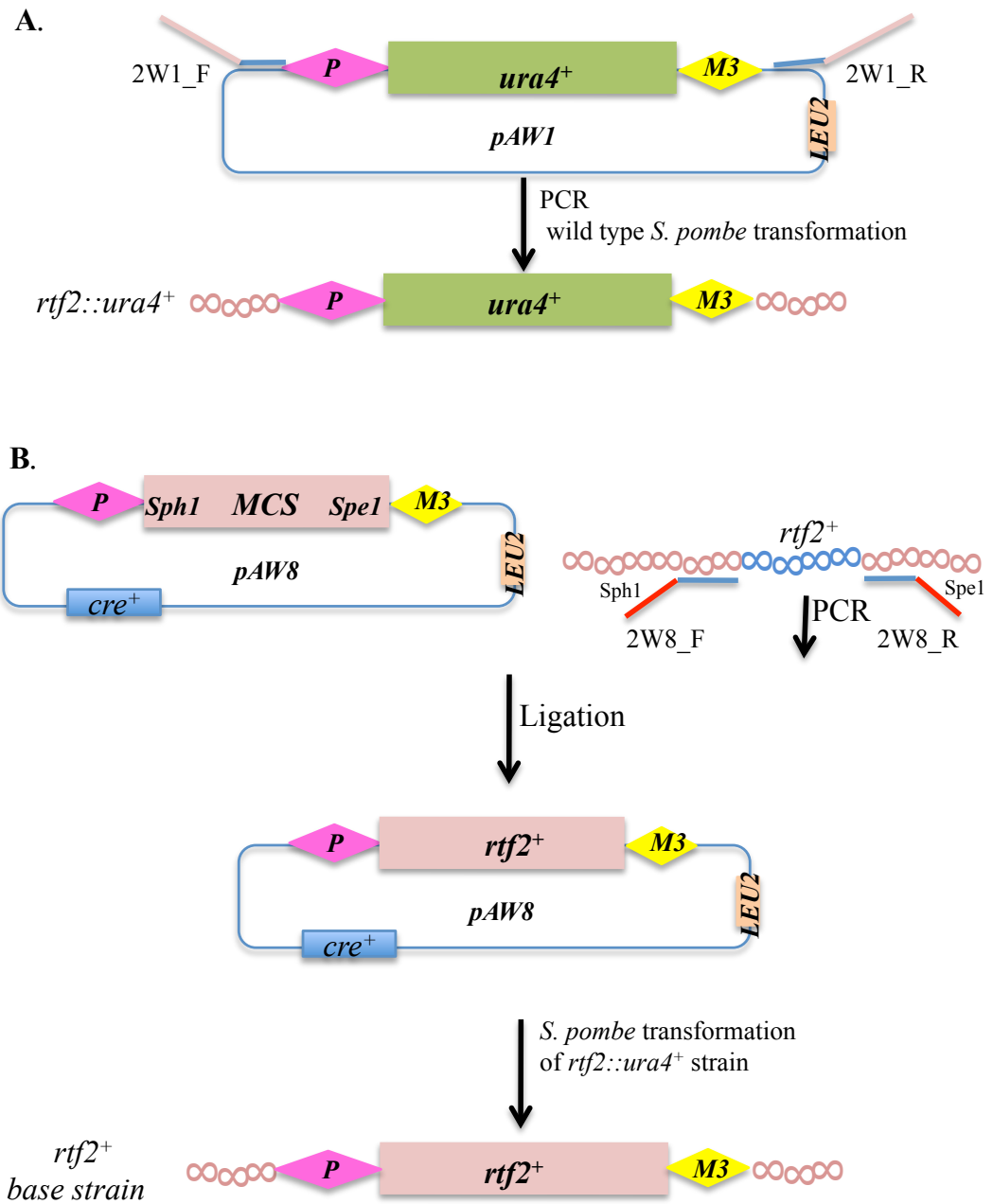


Fig. 7.15 Strategy to create a *rtf2⁺* base strain

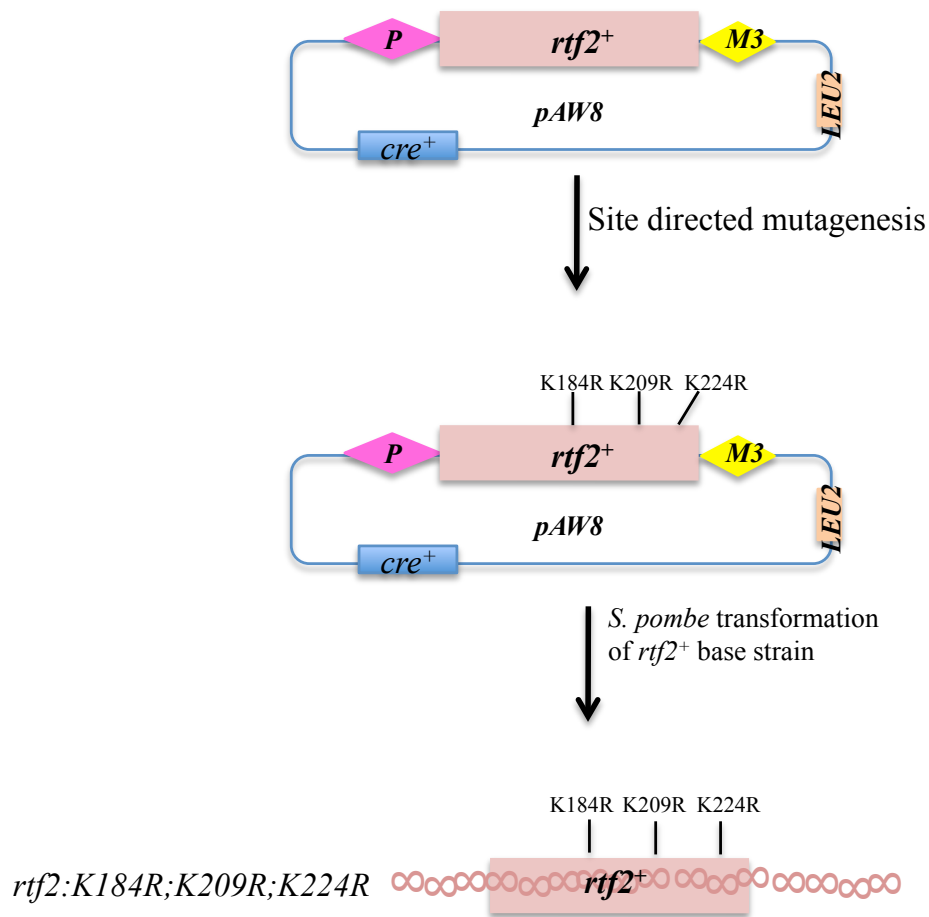


Fig. 7.16 Strategy to create *rtf2* sumoylation mutants

rtf2⁺ sumoylation mutants were obtained by transforming the *rtf2*⁺ base strain with a *pAW8* plasmid containing the mutated *rtf2* gene between the heterospecific sites loxP and loxM

compared with the *rtf2-K184R; K224R* (*rtf2-D*), *rtf2-T* and *rtf2::ura4* (*rtf2Δ*) mutant strains.

7.8 Phenotypic characterization of *rtf2*⁺ sumoylation mutants

The phenotypic characteristics of *rtf2* sumoylation mutants were compared to those of *rtf2*⁺ strain obtained from the *rtf2::ura4* base strain, *rtf2Δ* and *rtf2-I* mutant (kindly donated by J. Daalgard, University of Warwick). Microscopic analysis of *rtf2Δ* and *rtf2-T* mutants revealed cellular and nuclear aberrations such as elongated cells, with no nuclear division, consistent with defects in DNA replication, and stretched and fragmented chromatin, consistent with defects in DNA damage repair (fig. 7.17).

7.8.1 Rtf2 defective in sumoylation is sensitive to MMS and IR

To determine whether mutating the K184, K209 and K224 to arginine affects the response to restrictive temperatures, spot tests were carried out at the *S. pombe* physiological temperature (30°) and at 25°C and 37°C. The results suggest that the *rtf2* sumoylation mutants are not cold or heat sensitive (a characteristic of some sumoylation mutants), and that the mutations are unlikely to affect the folding of the Rtf2 protein (characterized by sensitivity at 37°C) (fig. 7.18 A).

It has been previously shown that *rtf2Δ* and *rtf2-I* mutants are not sensitive to hydroxyurea or camptothecin but are sensitive to the alkylating agent MMS (Inagawa et al., 2009). Since *rtf2-I* has a mutation that probably affects the RING motif, it suggests that the sensitivity of *rtf2Δ* to MMS could be due to a defect in the functionality of this domain. To determine whether sumoylation affects the function of the C2HC2, as in BRCA1, the response of the *rtf2* sumoylation mutants to MMS was tested (fig. 7.18 B). Interestingly *rtf2-K209R* mutant is only slightly sensitive while the *rtf2-D* and *rtf2-T* mutants are as sensitive as *rtf2Δ* at high doses of MMS. This result implies that sumoylation of Rtf2 is required for the cellular response to DNA alkylation and that all three lysine residues are important sumoylation sites.

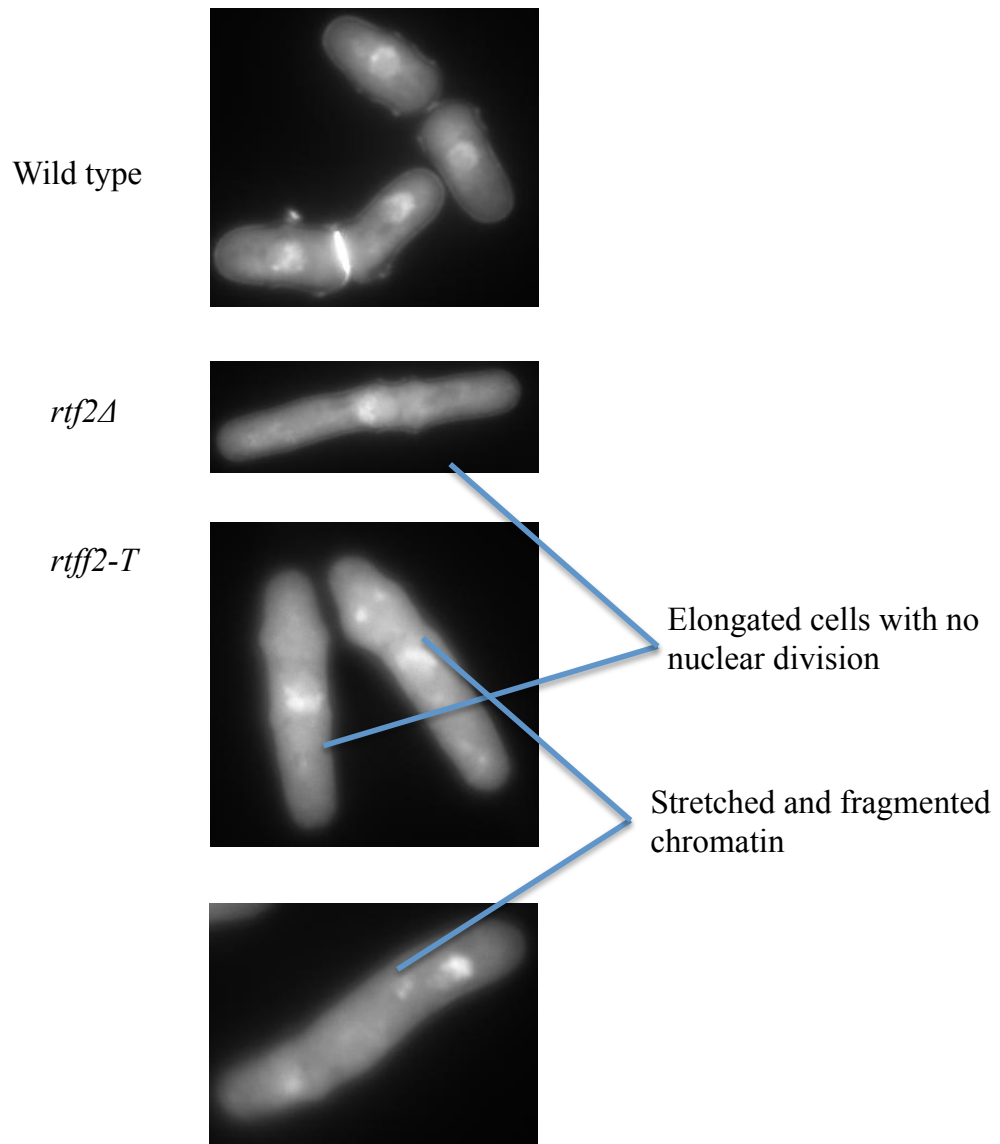
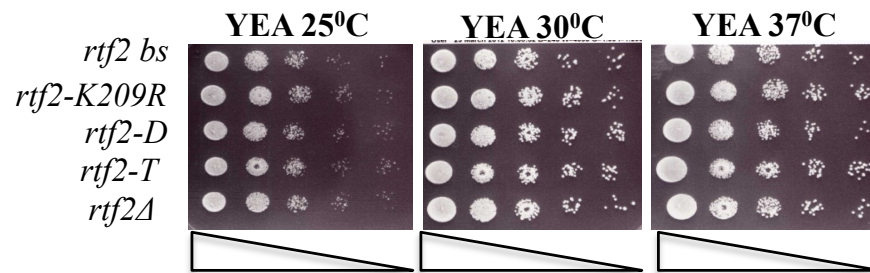


Fig. 7.17 *rtf2Δ* and *rtf2-T* mutants display aberrant cell and nucleus morphology

Morphology of methanol fixed cells, stained with DAPI and calcofluor.

A.



B.

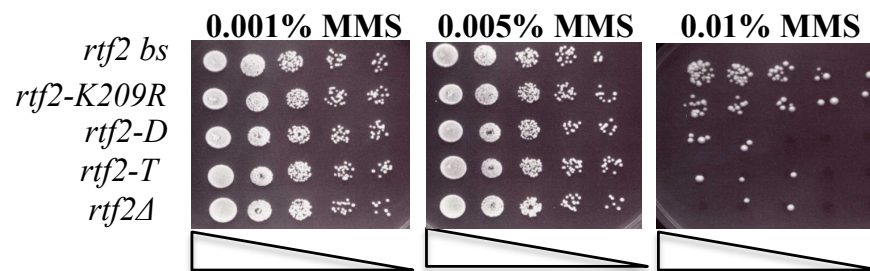



Fig. 7.18 *rtf2* sumoylation mutants are sensitive to MMS

A. Temperature sensitivity of *rtf2* mutants.

B. MMS sensitivity of *rtf2* mutants.

10 μ l of 10 fold serially diluted cultures () were plated onto media containing MMS as indicated, and incubated at 30°C for 3 days.

Since BRCA1 is sumoylated in response to ionizing radiation (Morris et al., 2009) it was of interest to determine whether *rtf2* sumoylation mutants were sensitive to IR. Firstly, the response to IR of an asynchronous culture of *rtf2*⁺ strain, constructed from the *rtf2::ura4* base strain, was compared to that of a wild type strain, to see if the loxP and loxM affect the *rtf2*⁺ gene, and with the *rtf2Δ* mutant (fig. 7.19 A). The *rtf2* null mutant is sensitive to high doses of IR and the *rtf2*⁺ strain has a response similar to that of a wild type strain. To determine whether the sensitivity of *rtf2Δ* is due to defects in its sumoylation, the IR sensitivity of asynchronous cultures of *rtf2-K184R*, *rtf2-K209R* and *rtf2-K224R* was tested and compared to that of *rtf2-T* (fig. 7.19 B). Interestingly all single sumoylation mutants display similar IR sensitivities to that of the triple mutant, further suggesting that the sumoylation of all three lysine residues is required for the function of the Rtf2 protein. The *rtf2-T* is less sensitive to IR than *rtf2Δ* but has similar sensitivity as the *rtf2-I* mutant (fig. 7.19 C).

As Rtf2 functions during S phase, and given that asynchronous cultures of *rtf2* mutants only shows sensitivity to high doses of IR, it was of interest to determine whether this sensitivity is specific to S phase. *rtf2* mutants were crossed with a *cdc10-M17* mutant which grows at 25°C and it blocks at late G1 phase at 36°C. Reverting to 25°C can restart the cell cycle of *cdc10-M17* mutant. Firstly, the response to IR of asynchronous cultures of *rtf2-T:cdc10-M17* and *rtf2-I:cdc10-M17* double mutants were determined and compared to that of the *cdc10-M17* single mutant. Interestingly the double mutants are very sensitive to 200 Gy (fig. 7.20 A) and the sensitivity of S phase synchronized cultures was tested at this dose. Cultures of *rtf2-T:cdc10-M17* and *rtf2-I:cdc10-M17* double mutants were grown in parallel with *cdc10-M17* at 36°C for 3 hours and released at 25°C for 3 hours. After the release, samples were taken at 30 minutes intervals and irradiated with 200 Gy (fig. 7.20 B). The *rtf2-T:cdc10-M17* and *rtf2-I:cdc10-M17* double mutants exhibit low cell viability in early S phase compared to *cdc10-M17* but recover slightly as S phase progresses. This further suggests that sumoylation of Rtf2 is required during DNA replication when DNA damage is present. Since recovery of replication forks stalled at damaged sites requires homologous recombination, it was of interest to determine whether the *rtf2* sumoylation mutants are epistatic with homologous recombination mutants.

Fig. 7.19 *rtf2* sumoylation mutants are sensitive to ionizing radiation

A. *rtf2::ura4⁺* deletion mutant is sensitive to ionizing radiation. IR survival curves of *rtf2::ura4⁺* compared to wild type and *rtf2⁺* base strain.

Log-phase cultures were irradiated with the stated dose and 500 cells were plated onto YEA and incubated at 30°C for three days to determine cell viability.

B. *rtf2* sumoylation mutants are sensitive to ionizing radiation. IR survival curves of *rtf2:K184R*, *rtf2:K184R*, *rtf2:K184R* and *rtf2:K184R; K209R; K224R (rtf2-T)* compared to wild type strain.

Log-phase cultures were irradiated with the stated dose and 500 cells were plated onto YEA and incubated at 30°C for three days to determine cell viability.

C. *rtf2-T* and *rtf2-I* mutants display similar IR sensitivities.

Log-phase cultures were irradiated with the stated dose and 500 cells were plated onto YEA and incubated at 30°C for three days to determine cell viability.

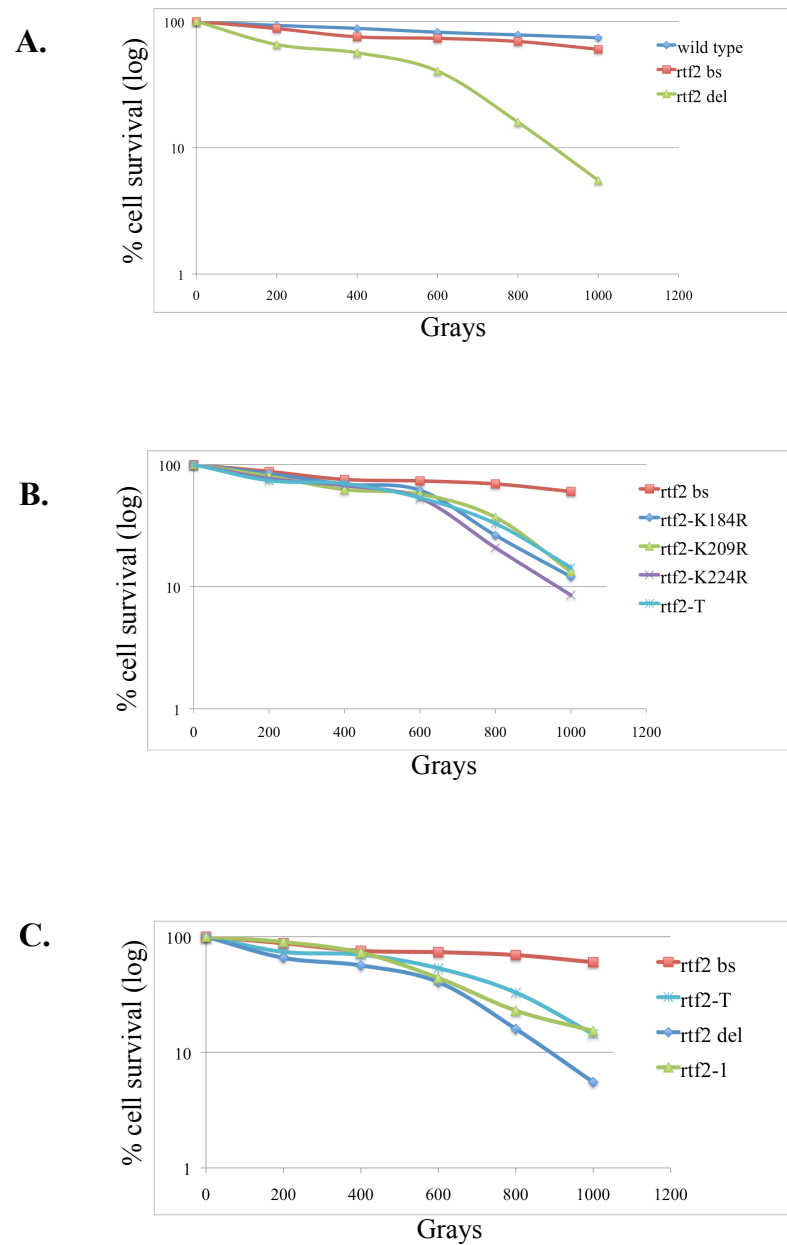
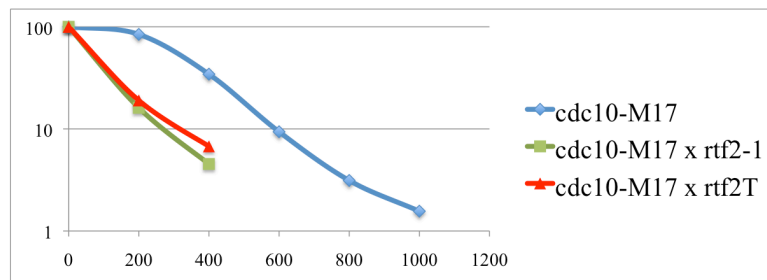


Fig. 7.19 *rtf2* sumoylation mutants are sensitive to ionizing radiation

A.



B.

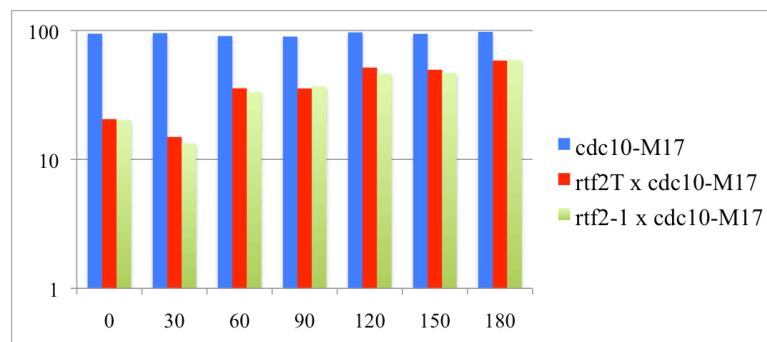


Fig. 7.20 *rtf2-T* and *rtf2-1* mutants are sensitive to low dose of IR during early S-phase

A. Unsynchronized *cdc17-M10 x rtf2-T* and *cdc17-M10 x rtf2-T* are sensitive to low doses (200 Grays) of ionizing radiation.

Log-phase cultures were irradiated with the stated dose and 500 cells were plated onto YEA and incubated at 30°C for three days to determine cell viability.

B. *cdc17-M10 x rtf2-T* and *cdc17-M10 x rtf2-T* cells synchronized in S-phase are sensitive to low doses (200 Grays) of ionizing radiation. Measurements were taken at 30 minutes interval after release from G1-S phase block. 500 cells were plated onto YEA and incubated at 30°C for three days to determine cell viability.

7.8.2 *rtf2* sumoylation mutants are lethal with recombination mutants

To assess whether the *rtf2* sumoylation mutants are epistatic with homologous recombination mutants *rad22Δ/rad52Δ* and *rhp51Δ/rad51Δ*, double mutants were created. Firstly, the *rtf2-T* strain (no marker) was crossed with *rad22Δ::NAT* and *rhp51Δ::KAN* strains. The spores were dissected from asci on complete YEA medium and were allowed to germinate for three days. The resulting colonies were replica plated onto YEA medium containing nourseothricin (NAT) and geneticin (G418/KAN) to select for *rad22Δ::NAT* and *rhp51Δ::KAN* alleles (fig. 7.21). The pattern of the viable spores implies that the double mutants *rtf2-T, rad22Δ::NAT* and *rtf2-T, rhp51Δ::KAN* are not viable (fig. 7.21). To further determine whether a specific lysine could be responsible for this lethality, *rtf2-K184R*, *rtf2-K209R* and *rtf2-K224R* single mutants were crossed with *rad22Δ::NAT* and *rhp51Δ::KAN* strains (fig. 7.22). Interestingly all single mutants are also lethal with the homologous recombination mutants, suggesting that sumoylation of Rtf2 at K184, K209 and K224 is required for cell viability in homologous recombination mutant backgrounds.

7.9 Discussion

7.9.1 Sumoylation of PCNA

Preliminary results in Watts lab suggested that PCNA is sumoylated in *S. pombe* but no specific sumoylated lysine residues have been reported. In this study I carried out an *in silico* analysis of the sumoylated lysine residues of *S. pombe* PCNA modified using an *in vitro* sumoylation assay and identified by MS/MS as K13, K164, K172 and K253. The *in silico* analysis suggests that K164 and K253 are more likely *in vivo* sumoylation sites while K172 could be a potential sumoylation site as, while not conserved amongst species, it is situated at a surface near K164 and K253. K13, while conserved in *S. cerevisiae* and *H. sapiens*, it is situated at the positively charged internal α helices of the clamp that interact with DNA and it has not been identified as a sumoylation site in *S. cerevisiae* or *H. sapiens*. However, before the sumoylation of PCNA was first detected in *S. cerevisiae* (Hoege et al., 2002), the mutation of N-terminal K13 to alanine was

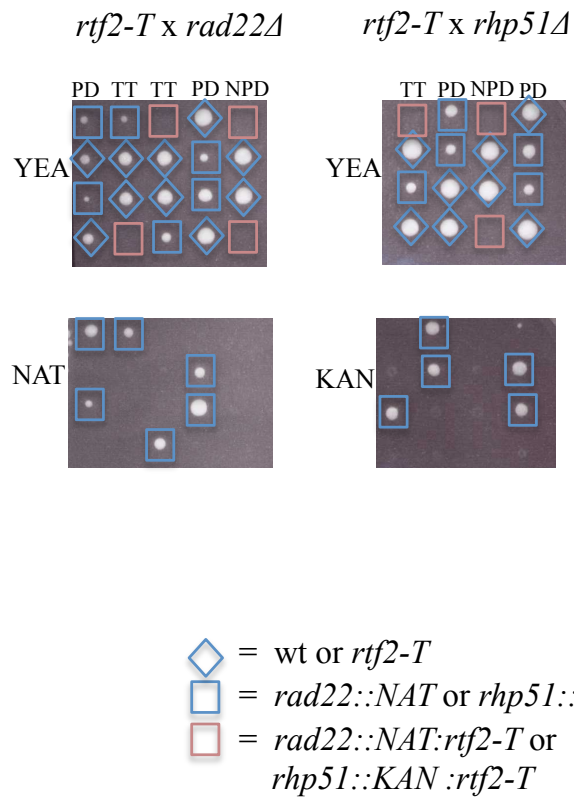


Fig. 7.21 Sumoylation of Rtf2 is required for cell viability on homologous recombination mutants background

rtf2-T is lethal with *rhp51^{Sp}/rad51^{Hs/Sc}Δ* and *rad22^{Sp}/rad52^{Hs/Sc}Δ* mutant

NPD = non-parental di-type; TT = tetra-type; PD = parental di-type
 Represented dissected tetrads were chosen from a pool of 20 dissected tetrads.

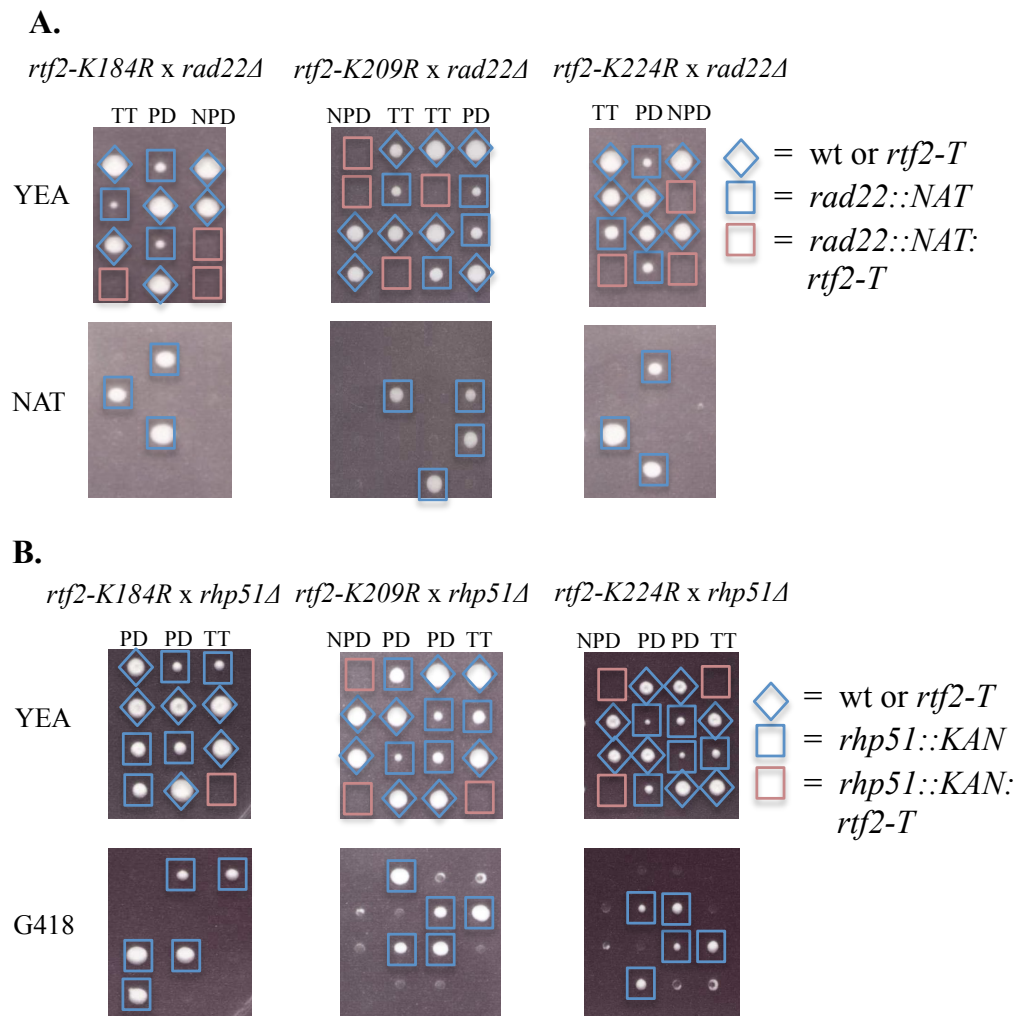


Fig. 7.22 Sumoylation of three lysine residues of Rtf2 is required for cell viability on homologous recombination mutants background

A. hus5-K50R is lethal with *rhp51^{Sp}/rad51^{Hs/Sc}Δ* mutant

B. hus5-K50R is lethal with *rad22^{Sp}/rad52^{Hs/Sc}Δ* mutant

NPD = non-parental di-type; TT = tetra-type; PD = parental di-type
 Represented dissected tetrads were chosen from a pool of 20 dissected tetrads.

shown to inhibit the DNA processivity of pol δ (Fukuda et al., 1995). The K253 was shown to be situated on an external loop involved in PCNA – protein interactions (Fien and Stillman, 1992). More recently the importance of all Ks and Rs cations at the N-terminal to the activity of pol δ have been highlighted in *H. sapiens* (Zhou and Hingorani, 2012) and the same study identifies that the sequence K²⁵⁴-E²⁵⁶ is required for RFC ATPase activity but not for pol δ activity. The identification of K13 as a sumoylation site *in vitro* opens new avenues in exploring DNA replication, as sumoylation of K13 could be a regulatory factor of pol δ activity while sumoylation at K253 could be a regulatory factor of RFC.

7.9.2 Sumoylation of Rtf2

Rtf2 is the founder member of a newly identified family of proteins that contain a modified RING domain that is characteristic to ubiquitin and SUMO ligases. After identifying specific sumoylated lysines K184, K209 and K224 by MS/MS, an *in silico* analysis reveals that these residues are partially conserved in *H. sapiens* and *S. japonicus* and an extended sequence alignment with the ubiquitin SUMO E3 ligase BRCA1 reveals that K209 corresponds to the sumoylation site K119 of BRCA1. Extended structural modeling of Rtf2 using multiple modeling servers shows that the lysine residues are situated at surfaces and not involved in interactions required to maintain the hydrophobic core of the protein and therefore are potential *in vivo* SUMO targets. Interestingly the I-TASSER modeling server identifies an U-box domain at the N-terminal (fig. 7.23 A). U-box domains share a fold with the RING domains but are missing the specific Cys and His residues specific to the RING motif (Ohi et al., 2003). More importantly U-box domains have been identified only in ubiquitin E3 ligases and have been specifically associated with poly-ubiquitination (Ohi et al., 2003). The putative U-box domain of Rtf2 can be modeled onto the U-box of the ubiquitin E3 ligase Prp19 (fig. 7.23 B) and the sequence alignment of the domains reveals high similarities (fig. 7.23 C).

Genetic analysis of *rtf2* sumoylation mutants is consistent with previous reports of *rtf2* null mutant sensitivity to DNA alkylation, their sensitivity to IR reminisce the IR sensitivity of homologous recombination mutants and some sumoylation mutants

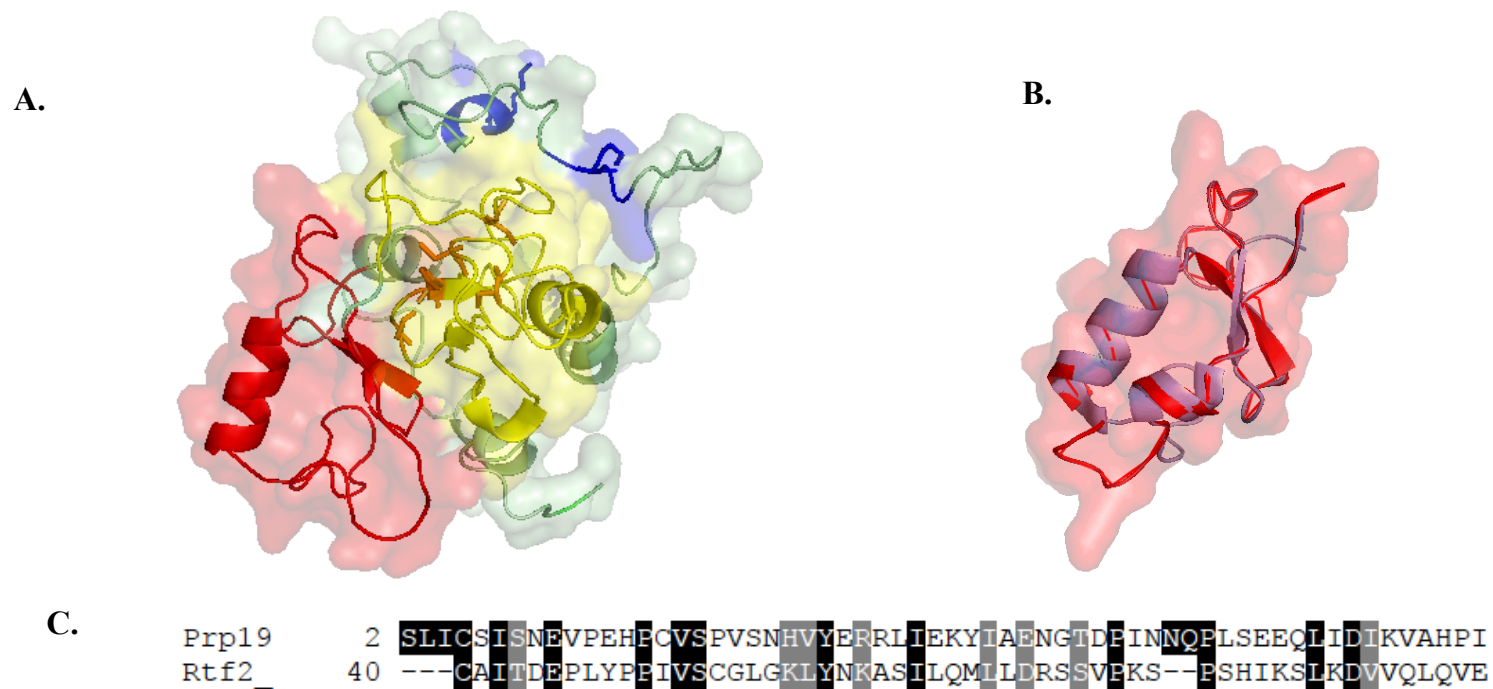


Fig. 7.23 Rtf2 contains a N-terminal U-box domain

- A. Cartoon representation of the structural model of *S. pombe* Rtf2. Highlighted are the putative U-box domain (in red), the C2HC2 RING domain (in yellow) and sumoylated lysines (in blue)
- B. Cartoon representation of the putative U-box domain of Rtf2 (in red) superimposed onto the U-box domain of Prp19 (in blue)
- C. Sequence alignment of Rtf2 putative U-box domain and the U-box domain of the ubiquitin E3 ligase Prp19

(*hus5.62* and *nse2-SA*). Interestingly, mutating each of the three lysine residues to arginine results in synthetic lethality with homologous recombination mutants like the sumoylation mutants *pli1Δ* and *hus5-K50R*.

The above data suggest that the Rtf2 sumoylation could function in a DNA damage repair mechanism during S-phase when the homologous recombination is impaired and that its sumoylation could be facilitated by the SUMO E3 ligase Pli1. Further, Rtf2 could function as an ubiquitin E3 ligase and this function could be dependent on its sumoylation, like BRCA1.

CHAPTER 8

DISCUSSION

Sumoylation has emerged as an important posttranslational modification of proteins involved in many biological processes required for normal cell proliferation. In this thesis, different approaches were employed to analyze various aspects of sumoylation in fission yeast.

Rad60 protein contains two SUMO-like domains, SLD1 and SLD2, identified from a bioinformatics analysis (Novatchkova et al., 2005). Key residues that maintain the β -grasp fold of SUMO, known as Bayer residues (Bayer et al., 1998), are conserved in the SLDs of Rad60. To see if these proposed SLDs adopt the stable β -grasp fold of SUMO, protein expression and stability assays were carried out on SLD2 with mutated Bayer residues. The mutants are insoluble under the conditions that SLD2 can be expressed as a stable protein, suggesting that the conserved Bayer residues that maintain the structure of SUMO are required for maintaining the structure of SLD2 and imply that SLD2 adopts the β -grasp fold of SUMO. Further, a putative SUMO-binding motif (SBM3), situated within SLD2, has been proposed to be required for the function of Rad60 by facilitating its dimerization (Raffa et al., 2006). Using gel filtration, dynamic light scattering (DLS) and protein stability assays, I show that this motif is required for maintaining the structure of SLD2. A genetic analysis of *rad60-SBM3* mutant (*rad60* with point mutations within SBM3) has a more severe phenotype than *rad60-SLD2 Δ* , suggesting that a misfolded SLD2 induces greater defects than a deletion of this domain. A model of SLD2 was generated based on the crystal structure of mammalian SUMO-1 and it showed that SBM3 forms the β 5 sheet of the β -grasp fold of SUMO. Taken together, these data suggest that SBM3 is an essential element of the hydrophobic core of SLD2 and unlikely to be available for intermolecular interactions. Recently new SUMO-like domains have been identified in the human protein UAF1 (Yang et al., 2011). The UAF1 protein, which is part of the USP1/UAF1 complex, has been shown to contain two SUMO-like domains. While the SLDs of RENi proteins are

more similar to SUMO-1, the SLDs of UAF1 have similarities with SUMO-2 and SUMO-3 and, more interestingly, they both have the diglycin motif conserved at the C-terminal, though no proteolytic cleavage have been identified. The USP1/UAF complex promotes DSB repair through HR by de-ubiquitinating the Fanconi anaemia protein FANCD2-Ub (Murai et al., 2011) and PCNA-Ub through interactions between SLD2 and ‘SUMO-like domain-interacting motifs’ (SLIMs) present in FANCD2 and Elg1, a PCNA-interacting protein, respectively. This is consistent with data presented in this thesis that putative SBMs present within the SLDs of Rad60 are unlikely to interact with the SLDs to promote Rad60 dimerisation as previously suggested.

The *in vitro* interaction of SLD2 with the SUMO conjugating enzyme Hus5 identified in this work, together with the interactions of SLD1 with the SUMO components Fub2 and Pli1 and the STUbL component Slx8, shown by Prudden *et al.*, suggests that Rad60 plays a multifaceted role in the sumoylation pathway. Given the interaction of Rad60 with the Smc5/6 complex, it could be that Rad60 is required for the regulation of the sumoylation/desumoylation of this multifunctional essential complex (fig. 8.1). The interaction of Rad60 with Pli1, the SUMO E3 ligase required for SUMO-chain formation, and Slx8, the ubiquitin E3 ligase responsible for proteasomal degradation of proteins marked by SUMO chains, suggests that Rad60 function is linked to the regulation of sumoylation.

SUMO chain formation has been shown to occur in *S. cerevisiae* and mammals at lysine residues situated at the disordered N-terminal of SUMO (Bylebyl et al., 2003, Tatham et al., 2001). *S. pombe* SUMO has an extended disordered N-terminal with two lysine residues as potential sites of sumoylation. In the second chapter of this thesis I show that *in vitro* and *in vivo* both lysine residues can be substrates for chain formation and that the E3 ligases facilitate SUMO chain formation, albeit Pli1 with an increased efficiency compared to Nse2. A genetic analysis of the mutant *SUMO-RR* (K14R; K30R) suggests that SUMO chain formation is required for the cellular responses to DNA replication arrest, and for DNA damage repair when the homologous recombination repair is defective.

Pli1, the SUMO E3 ligase that facilitate SUMO chain formation, has been shown to function in maintaining genomic stability at heterochromatic regions (Xhemalce et al.,

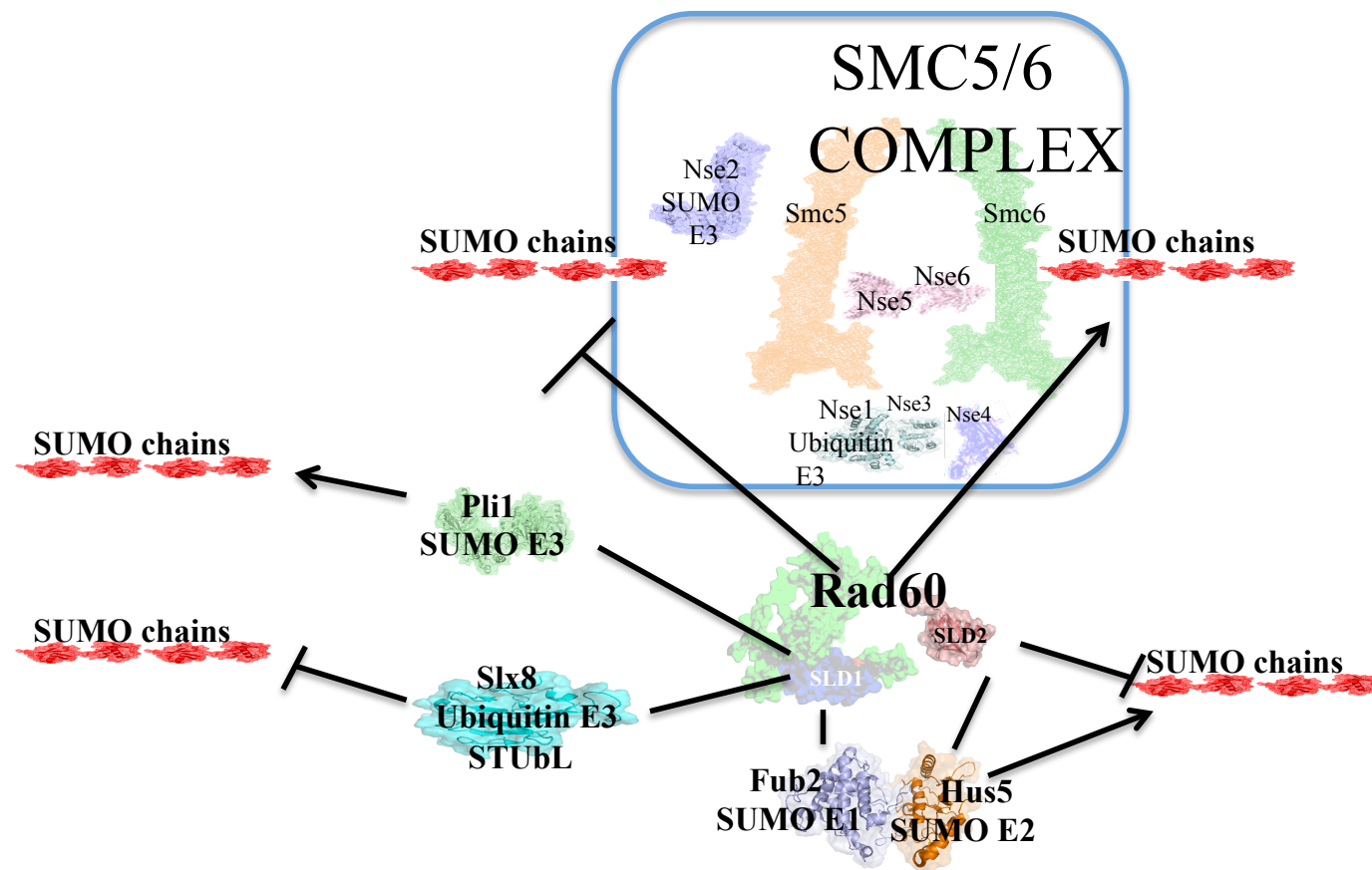


Fig. 8.1 Rad60 interactions with sumoylation machinery may control the levels of sumoylated Smc5/6 complex

→ activating interaction; —| inhibitory interaction

2004). An investigation into the function of Pli1 at heterochromatic centromeric regions, using an artificial minichromosome, was undertaken. Results from an assay to detect spontaneous mutations show that Pli1 is required for maintaining the minichromosome and for preventing minichromosomal rearrangements. PFGE was employed to analyse minichromosomal rearrangements, and a survey carried out on *pli1Δ* and wild type strains suggests that Pli1 is required to prevent illicit homologous recombination between the artificial minichromosome and the endogenous chromosome III. Using PCR, the centromeric repeats *otr-imr* were identified as the region at which the minichromosomal rearrangements occurred.

In *S. pombe* and *S. cerevisiae* STUbL mutants defective in targeting poly-SUMO species for proteasomal degradation display a similar increase in poly-SUMO species and sensitivity to hydroxyurea like *ulp2Δ* mutants. In fission yeast the *slx8-1* mutant (temperature sensitive) defect in response to hydroxyurea is suppressed in a *pli1Δ* background while the level of poly-SUMO species is reduced to that of *pli1Δ* rather than the intermediate level of a wild type strain (Prudden et al., 2007). Further, the sensitivity to hydroxyurea of the *slx8-29^{I230T}* mutant (mutation in the E3 ubiquitin ligase RING domain) and the high level of poly-SUMO species are suppressed by the *pli1Δ* and *pmt3-RR* mutants (Prudden et al., 2011). Mutants of the *slx8-rnf* complex and *ulp2* gene display severe phenotypes, while *pli1* and *pmt3-RR* mutants have mild or no obvious phenotypes. This suggests that SUMO chain formation can have a negative effect on DNA replication and/or DNA damage response mechanisms and that STUbLs and Ulp proteases are both required to maintain the physiological levels of SUMO chains.

The analysis of sumoylation, and the identification of specific modified lysine residues in particular, has been challenging due to the fact that, at any one point under normal physiological conditions, only a small fraction of a target protein exists in a sumoylated form. In recent years, the development of new mass spectrometry techniques enabled the identification of post-translational modified amino acids present in trace quantities in the sample. Using an *in vitro* sumoylation assay and mass spectrometry techniques, provided by the mass spectrometry services at the University of Sussex, sumoylated lysine residues were detected in the SUMO activating component Fub2, the SUMO conjugating enzyme, Hus5, and the SUMO E3 ligase Nse2. An *in vitro* sumoylation

assay with a mutant of the conjugating enzyme that cannot be sumoylated, Hus5-K50R, results in a reduced level of high Mr SUMO species. This suggests that, at least *in vitro*, SUMO chains are mostly attached to the K50 of Hus5 rather than be present in a free form. *In vivo* analysis of the *hus5-K50R* reveals an increased level of high Mr sumoylated species compared to wild type. This contradicts the *in vitro* results but is consistent with data from *S. cerevisiae*, where a mutant of the SUMO conjugating enzyme that cannot be sumoylated shows increased levels of cellular sumoylation (Knipscheer et al., 2008). These results suggest that sumoylation of Hus5 inhibits its activity towards illicit sumoylation. Further *in vivo* analysis, carried out in the Watts lab with an HA (hemagglutinin) epitope tag on the wild type Hus5 and the mutant *hus5-K50R*, suggests that Hus5 is mono-sumoylated *in vivo* and confirms experimental results from this work that K50 is the only lysine residue at which sumoylation can occur (experimental work carried out by Lauren Small, University of Sussex). A genetic characterization of *hus5-K50R*, carried out in this project, suggests that sumoylation of Hus5 is required for repair of IR-induced DNA damage during S-phase and for DNA damage repair when homologous recombination repair is defective. The latter phenotype is reminiscent of the phenotype of the SUMO chain formation and *pli1* null mutants that are synthetically sick and lethal, respectively, with homologous recombination mutants. Taken together, these data suggests that a strict control sumoylation levels is required for cell viability on a homologous recombination mutant background, as both lower and increased levels of sumoylated species are lethal when homologous recombination is impaired.

The optimization of the *in vitro* sumoylation assay, carried out during the analysis of SUMO chain formation, brought about a collaborative work with Dr. J. Dalgaard, University of Warwick, on the Rtf2 protein. Rtf2 is associated with the replication termination site RTS1 and it has been shown to interact with SUMO and PCNA (Inagawa et al., 2009). A sequence analysis of Rtf2 identified a RING domain, raising the possibility that Rtf2 might function as a SUMO E3ligase that might facilitate the sumoylation of PCNA. *In vitro* sumoylation assays carried put with PCNA, Rtf2 and Pli1 show that Pli1 facilitate the sumoylation of PCNA *in vitro* but Rtf2 does not. However, the results show that Rtf2 is sumoylated itself. Mass spectrometry analysis identified that sumoylation of PCNA occur at four lysine residues, including the highly conserved K164, while sumoylation of Rtf2 occur at three lysine residues at the C-

terminal, proximal to the RING domain. A genetic analysis suggests that sumoylation of Rtf2 is required for MMS and IR-induced DNA damage repair during S phase, and for cell viability when homologous recombination repair is defective. A sequence analysis of Rtf2 suggests that, apart of the RING domain at the C-terminal, there is a U-box domain at the N-terminal. Tandem U-box and RING domains are a characteristic of some ubiquitin E3 ligases. Further, the RING domain of Rtf2, together with the sumoylated lysine K209, is conserved with the RING domain and the sumoylation site K119 of BRCA1. Sumoylation of K119 of BRCA1 is required for its activity as an ubiquitin E3 ligase (Morris et al., 2009). Taken together with the experimental data presented, these facts raise the possibility that Rtf2 can function as an ubiquitin E3 ligase, either as a STUbL or a SRUbL (SUMO-regulated ubiquitin ligase) like BRCA1, and that PCNA could be the target protein. *In vitro* ubiquitination assays have been developed and this would be a first experimental step towards identifying if Rtf2 function as an ubiquitin ligase. As Rtf2 is required to stabilize the replication fork at the replication termination chromosomal locus RTS1, it could be that its function is to modify PCNA, either by sumoylation or ubiquitination, such that the appropriate mechanism is employed to resume DNA replication at RTS1.

The functions Rad60, SUMO chain formation, sumoylation of the E1, E2 and E3 SUMO enzymes, modification of PCNA by SUMO and ubiquitin, and the sumoylation of targets, such as the Smc5/6 and Rtf2, seem to be closely interconnected. The experimental data from this work suggests that sumoylation has important roles in maintaining genomic stability by regulating many facets of the homologous recombination repair, especially during DNA replication. Further work should target the understanding of the interactions between the many factors involved. Determining the structure of Rad60 and the nature of its interactions with its many partner proteins would bring new avenues in understanding complex cellular processes such as replication fork progression and DNA damage repair by homologous recombination. Expression and purification of a stable full-length recombinant Rad60 has not been possible using *E. coli* systems. However, new protein expression systems have been developed, such as baculovirus systems. Further work should exploit these new systems in expressing not only the Rad60 protein, but also complexes of Rad60 with the

sumoylation pathway components, the Slx8-Rnf complex and with the Smc5/6 complex.

Many sumoylation mutants described in this thesis are defective in cellular responses to DNA replication perturbations, IR induced DNA damage and when homologous recombination is impaired. This reoccurring observation is consistent with results from other studies of the sumoylation functions in genomic stability. With the advance of mass spectrometry techniques and *in vivo* labeling techniques, such as SILAC, the identification of SUMO targets, and particularly the identification of specific sumoylated lysine residues, has become more accessible. Identification of specific sumoylated lysine residues will assist genetical and biochemical experimental work that could bring new insights into the role of sumoylation in maintaining genomic stability.

CHAPTER 9

References

- ADAR, S., IZHAR, L., HENDEL, A., GEACINTOV, N. & LIVNEH, Z. (2009) Repair of gaps opposite lesions by homologous recombination in mammalian cells. *Nucleic Acids Res*, 37, 5737-48.
- AL-KHODAIRY, F. & CARR, A. M. (1992) DNA repair mutants defining G2 checkpoint pathways in *Schizosaccharomyces pombe*. *EMBO J*, 11, 1343-50.
- AL-KHODAIRY, F., ENOCH, T., HAGAN, I. M. & CARR, A. M. (1995) The *Schizosaccharomyces pombe* hus5 gene encodes a ubiquitin conjugating enzyme required for normal mitosis. *J Cell Sci*, 108 (Pt 2), 475-86.
- AL-KHODAIRY, F., FOTOUE, E., SHELDRIK, K. S., GRIFFITHS, D. J., LEHMANN, A. R. & CARR, A. M. (1994) Identification and characterization of new elements involved in checkpoint and feedback controls in fission yeast. *Mol Biol Cell*, 5, 147-60.
- ALLEVA, J. L. & DOETSCH, P. W. (1998) Characterization of *Schizosaccharomyces pombe* Rad2 protein, a FEN-1 homolog. *Nucleic Acids Res*, 26, 3645-50.
- ALLSHIRE, R. C., NIMMO, E. R., EKWALL, K., JAVERZAT, J. P. & CRANSTON, G. (1995) Mutations derepressing silent centromeric domains in fission yeast disrupt chromosome segregation. *Genes Dev*, 9, 218-33.
- ALMEDAWAR, S., COLOMINA, N., BERMUDEZ-LOPEZ, M., POCINO-MERINO, I. & TORRES-ROSELL, J. (2012) A SUMO-dependent step during establishment of sister chromatid cohesion. *Curr Biol*, 22, 1576-81.
- ALTMANNOVA, V., ECKERT-BOULET, N., ARNERIC, M., KOLESAR, P., CHALOUKHOVA, R., DAMBORSKY, J., SUNG, P., ZHAO, X., LISBY, M. & KREJCI, L. (2010) Rad52 SUMOylation affects the efficiency of the DNA repair. *Nucleic Acids Res*, 38, 4708-21.
- ANDREWS EA, PALECEK J, SERGEANT J, TAYLOR E, LEHMANN AR & FZ., W. (2005) Nse2, a component of the Smc5-6 complex, is a SUMO ligase required for the response to DNA damage. *Mol Cell Biol*, 25, 185-96.
- ANDREWS, E. A., PALECEK, J., SERGEANT, J., TAYLOR, E., LEHMANN, A. R. & WATTS, F. Z. (2005) Nse2, a component of the Smc5-6 complex, is a SUMO ligase required for the response to DNA damage. *Mol Cell Biol*, 25, 185-96.

- ANTONY, E., TOMKO, E. J., XIAO, Q., KREJCI, L., LOHMAN, T. M. & ELLENBERGER, T. (2009) Srs2 disassembles Rad51 filaments by a protein-protein interaction triggering ATP turnover and dissociation of Rad51 from DNA. *Mol Cell*, 35, 105-15.
- ARAVIND, L. & KOONIN, E. V. (2000) SAP - a putative DNA-binding motif involved in chromosomal organization. *Trends Biochem Sci*, 25, 112-4.
- ARMSTRONG, A. A., MOHIDEEN, F. & LIMA, C. D. (2012) Recognition of SUMO-modified PCNA requires tandem receptor motifs in Srs2. *Nature*, 483, 59-63.
- AZUMA Y, T. S., CAVENAGH MM, AINSZTEIN AM, SAITOH H, DASSO M. (2001) Expression and regulation of the mammalian SUMO-1 E1 enzyme. *FASEB J.*, 15, 1825-1827.
- BANIN, S., MOYAL, L., SHIEH, S., TAYA, Y., ANDERSON, C. W., CHESSA, L., SMORODINSKY, N. I., PRIVES, C., REISS, Y., SHILOH, Y. & ZIV, Y. (1998) Enhanced phosphorylation of p53 by ATM in response to DNA damage. *Science*, 281, 1674-7.
- BANNO, K., SUSUMU, N., HIRAO, T., YANOKURA, M., HIRASAWA, A., AOKI, D., UDAGAWA, Y., SUGANO, K. & NOZAWA, S. (2004) Two Japanese kindreds occurring endometrial cancer meeting new clinical criteria for hereditary non-polyposis colorectal cancer (HNPCC), Amsterdam Criteria II. *J Obstet Gynaecol Res*, 30, 287-92.
- BARTEK, J., LUKAS, C. & LUKAS, J. (2004) Checking on DNA damage in S phase. *Nat Rev Mol Cell Biol*, 5, 792-804.
- BAUM, M., NGAN, V. K. & CLARKE, L. (1994) The centromeric K-type repeat and the central core are together sufficient to establish a functional *Schizosaccharomyces pombe* centromere. *Mol Biol Cell*, 5, 747-61.
- BAYER, P., ARNDT, A., METZGER, S., MAHAJAN, R., MELCHIOR, F., JAENICKE, R. & BECKER, J. (1998) Structure determination of the small ubiquitin-related modifier SUMO-1. *J Mol Biol*, 280, 275-86.
- BECKER, J., MELCHIOR, F., GERKE, V., BISCHOFF, F. R., PONSTINGL, H. & WITTINGHOFFER, A. (1995) RNA1 encodes a GTPase-activating protein specific for Gsp1p, the Ran/TC4 homologue of *Saccharomyces cerevisiae*. *J Biol Chem*, 270, 11860-5.
- BENNETT-LOVSEY, R. M., HERBERT, A. D., STERNBERG, M. J. & KELLEY, L. A. (2008) Exploring the extremes of sequence/structure space with ensemble fold recognition in the program Phyre. *Proteins*, 70, 611-25.

- BENTLEY, N. J., HOLTZMAN, D. A., FLAGGS, G., KEEGAN, K. S., DEMAGGIO, A., FORD, J. C., HOEKSTRA, M. & CARR, A. M. (1996) The *Schizosaccharomyces pombe* rad3 checkpoint gene. *EMBO J*, 15, 6641-51.
- BODDY, M. N., FURNARI, B., MONDESERT, O. & RUSSELL, P. (1998) Replication checkpoint enforced by kinases Cds1 and Chk1. *Science*, 280, 909-12.
- BODDY, M. N., SHANAHAN, P., MCDONALD, W. H., LOPEZ-GIRONA, A., NOGUCHI, E., YATES, I. J. & RUSSELL, P. (2003) Replication checkpoint kinase Cds1 regulates recombinational repair protein Rad60. *Mol Cell Biol*, 23, 5939-46.
- BOE, C. A., KNUTSEN, J. H., BOYE, E. & GRALLERT, B. (2012) Hpz1 modulates the G1-S transition in fission yeast. *PLoS One*, 7, e44539.
- BOTTA, E., NARDO, T., BROUGHTON, B. C., MARINONI, S., LEHMANN, A. R. & STEFANINI, M. (1998) Analysis of mutations in the XPD gene in Italian patients with trichothiodystrophy: site of mutation correlates with repair deficiency, but gene dosage appears to determine clinical severity. *Am J Hum Genet*, 63, 1036-48.
- BOYD, L. K., MERCER, B., THOMPSON, D., MAIN, E. & WATTS, F. Z. (2010) Characterisation of the SUMO-like domains of *Schizosaccharomyces pombe* Rad60. *PLoS One*, 5, e13009.
- BRANZEI, D. & FOIANI, M. (2008) Regulation of DNA repair throughout the cell cycle. *Nat Rev Mol Cell Biol*, 9, 297-308.
- BRANZEI D, S. J., LIBERI G, ZHAO X, MAEDA X, SEKI M, ENOMOTO T, OHTA K, FOIANI M. (2006) Ubc9- and Mms21-Mediated Sumoylation Counteracts Recombinogenic Events at Damaged Replication Forks *Cell*, 127, 509-522.
- BRANZEI, D., SOLLIER, J., LIBERI, G., ZHAO, X., MAEDA, D., SEKI, M., ENOMOTO, T., OHTA, K. & FOIANI, M. (2006) Ubc9- and mms21-mediated sumoylation counteracts recombinogenic events at damaged replication forks. *Cell*, 127, 509-22.
- BRUDERER, R., TATHAM, M. H., PLECHANOVOVA, A., MATIC, I., GARG, A. K. & HAY, R. T. (2011) Purification and identification of endogenous polySUMO conjugates. *EMBO Rep*, 12, 142-8.
- BURNETT, G. & KENNEDY, E. P. (1954) The enzymatic phosphorylation of proteins. *J Biol Chem*, 211, 969-80.

- BYLEBYL, G. R., BELICHENKO, I. & JOHNSON, E. S. (2003) The SUMO isopeptidase Ulp2 prevents accumulation of SUMO chains in yeast. *J Biol Chem*, 278, 44113-20.
- CAPILI, A. D. & LIMA, C. D. (2007) Structure and analysis of a complex between SUMO and Ubc9 illustrates features of a conserved E2-Ubl interaction. *J Mol Biol*, 369, 608-18.
- CARR, A. M. (2002) DNA structure dependent checkpoints as regulators of DNA repair. *DNA Repair (Amst)*, 1, 983-94.
- CASTORALOVA, M., BREZINOVA, D., SVEDA, M., LIPOV, J., RUMIL, T. & KNEJZLIK, Z. (2012) SUMO-2/3 conjugates accumulating under heat shock or MG132 treatment result largely from new protein synthesis. *Biochim Biophys Acta*, 1823, 911-9.
- CLARKE, L., AMSTUTZ, H., FISHEL, B. & CARBON, J. (1986) Analysis of centromeric DNA in the fission yeast *Schizosaccharomyces pombe*. *Proc Natl Acad Sci U S A*, 83, 8253-7.
- COOPER, H. J., TATHAM, M. H., JAFFRAY, E., HEATH, J. K., LAM, T. T., MARSHALL, A. G. & HAY, R. T. (2005) Fourier transform ion cyclotron resonance mass spectrometry for the analysis of small ubiquitin-like modifier (SUMO) modification: identification of lysines in RanBP2 and SUMO targeted for modification during the E3 autoSUMOylation reaction. *Anal Chem*, 77, 6310-9.
- CORELLOU, F., BISGROVE, S. R., KROPF, D. L., MEIJER, L., KLOAREG, B. & BOUGET, F. Y. (2000) A S/M DNA replication checkpoint prevents nuclear and cytoplasmic events of cell division including centrosomal axis alignment and inhibits activation of cyclin-dependent kinase-like proteins in fucoid zygotes. *Development*, 127, 1651-60.
- CULLEN, J. K., HUSSEY, S. P., WALKER, C., PRUDDEN, J., WEE, B. Y., DAVE, A., FINDLAY, J. S., SAVORY, A. P. & HUMPHREY, T. C. (2007) Break-induced loss of heterozygosity in fission yeast: dual roles for homologous recombination in promoting translocations and preventing de novo telomere addition. *Mol Cell Biol*, 27, 7745-57.
- D'URSO, G., GRALLERT, B. & NURSE, P. (1995) DNA polymerase alpha, a component of the replication initiation complex, is essential for the checkpoint coupling S phase to mitosis in fission yeast. *J Cell Sci*, 108 (Pt 9), 3109-18.
- DALGAARD, J. Z., EYDMANN, T., KOULINTCHENKO, M., SAYRAC, S., VENGROVA, S. & YAMADA-INAGAWA, T. (2009) Random and site-specific replication termination. *Methods Mol Biol*, 521, 35-53.

- DALGAARD, J. Z. & KLAR, A. J. (2000) swi1 and swi3 perform imprinting, pausing, and termination of DNA replication in *S. pombe*. *Cell*, 102, 745-51.
- DALGAARD, J. Z. & KLAR, A. J. (2001) A DNA replication-arrest site RTS1 regulates imprinting by determining the direction of replication at mat1 in *S. pombe*. *Genes Dev*, 15, 2060-8.
- DE LAHONDES, R., RIBES, V. & ARCANGIOLI, B. (2003) Fission yeast Sap1 protein is essential for chromosome stability. *Eukaryot Cell*, 2, 910-21.
- DECOTTIGNIES, A., SANCHEZ-PEREZ, I. & NURSE, P. (2003) *Schizosaccharomyces pombe* essential genes: a pilot study. *Genome Res*, 13, 399-406.
- DENISON, C., RUDNER, A. D., GERBER, S. A., BAKALARSKI, C. E., MOAZED, D. & GYGI, S. P. (2005) A proteomic strategy for gaining insights into protein sumoylation in yeast. *Mol Cell Proteomics*, 4, 246-54.
- DESHPANDE, A. M. & NEWLON, C. S. (1996) DNA replication fork pause sites dependent on transcription. *Science*, 272, 1030-3.
- DESTERRO, J. M., RODRIGUEZ, M. S. & HAY, R. T. (1998) SUMO-1 modification of IkappaBalpha inhibits NF-kappaB activation. *Mol Cell*, 2, 233-9.
- DOU, H., HUANG, C., SINGH, M., CARPENTER, P. B. & YEH, E. T. (2010) Regulation of DNA repair through deSUMOylation and SUMOylation of replication protein A complex. *Mol Cell*, 39, 333-45.
- DOYLE, J. M., GAO, J., WANG, J., YANG, M. & POTTS, P. R. (2010) MAGE-RING protein complexes comprise a family of E3 ubiquitin ligases. *Mol Cell*, 39, 963-74.
- DUAN, X., SARANGI, P., LIU, X., RANGI, G. K., ZHAO, X. & YE, H. (2009a) Structural and functional insights into the roles of the Mms21 subunit of the Smc5/6 complex. *Mol Cell*, 35, 657-68.
- DUAN, X., YANG, Y., CHEN, Y. H., ARENZ, J., RANGI, G. K., ZHAO, X. & YE, H. (2009b) Architecture of the Smc5/6 Complex of *Saccharomyces cerevisiae* Reveals a Unique Interaction between the Nse5-6 Subcomplex and the Hinge Regions of Smc5 and Smc6. *J Biol Chem*, 284, 8507-15.
- DULIC, V., KAUFMANN, W. K., WILSON, S. J., TLSTY, T. D., LEES, E., HARPER, J. W., ELLEDGE, S. J. & REED, S. I. (1994) p53-dependent inhibition of cyclin-dependent kinase activities in human fibroblasts during radiation-induced G1 arrest. *Cell*, 76, 1013-23.

- DUVAL, D., DUVAL, G., KEDINGER, C., POCH, O. & BOEUF, H. (2003) The 'PINIT' motif, of a newly identified conserved domain of the PIAS protein family, is essential for nuclear retention of PIAS3L. *FEBS Lett*, 554, 111-8.
- EDENBERG, H. J. & HUBERMAN, J. A. (1975) Eukaryotic chromosome replication. *Annu Rev Genet*, 9, 245-84.
- EDWARDS, R. J., BENTLEY, N. J. & CARR, A. M. (1999) A Rad3-Rad26 complex responds to DNA damage independently of other checkpoint proteins. *Nat Cell Biol*, 1, 393-8.
- EGGLER, A. L., INMAN, R. B. & COX, M. M. (2002) The Rad51-dependent pairing of long DNA substrates is stabilized by replication protein A. *J Biol Chem*, 277, 39280-8.
- EKWALL, K., NIMMO, E. R., JAVERZAT, J. P., BORGSTROM, B., EGEL, R., CRANSTON, G. & ALLSHIRE, R. (1996) Mutations in the fission yeast silencing factors *clr4+* and *rik1+* disrupt the localisation of the chromo domain protein Swi6p and impair centromere function. *J Cell Sci*, 109 (Pt 11), 2637-48.
- ELLENBERGER, T. & TOMKINSON, A. E. (2008) Eukaryotic DNA ligases: structural and functional insights. *Annu Rev Biochem*, 77, 313-38.
- ENOCH, T., CARR, A. & NURSE, P. (1993) Checkpoint check. *Nature*, 361, 26.
- EYDMANN, T., SOMMARIVA, E., INAGAWA, T., MIAN, S., KLAR, A. J. & DALGAARD, J. Z. (2008) Rtf1-mediated eukaryotic site-specific replication termination. *Genetics*, 180, 27-39.
- FACHINETTI, D., BERMEJO, R., COCITO, A., MINARDI, S., KATOU, Y., KANO, Y., SHIRAHIGE, K., AZVOLINSKY, A., ZAKIAN, V. A. & FOIANI, M. (2010) Replication termination at eukaryotic chromosomes is mediated by Top2 and occurs at genomic loci containing pausing elements. *Mol Cell*, 39, 595-605.
- FALCK, J., PETRINI, J. H., WILLIAMS, B. R., LUKAS, J. & BARTEK, J. (2002) The DNA damage-dependent intra-S phase checkpoint is regulated by parallel pathways. *Nat Genet*, 30, 290-4.
- FENECH, M., CARR, A. M., MURRAY, J., WATTS, F. Z. & LEHMANN, A. R. (1991) Cloning and characterization of the *rad4* gene of *Schizosaccharomyces pombe*; a gene showing short regions of sequence similarity to the human XRCC1 gene. *Nucleic Acids Res*, 19, 6737-41.
- FERREIRA, M. G. & COOPER, J. P. (2004) Two modes of DNA double-strand break repair are reciprocally regulated through the fission yeast cell cycle. *Genes Dev*, 18, 2249-54.

- FIEN, K. & STILLMAN, B. (1992) Identification of replication factor C from *Saccharomyces cerevisiae*: a component of the leading-strand DNA replication complex. *Mol Cell Biol*, 12, 155-63.
- FLOTHO, A., WERNER, A., WINTER, T., FRANK, A. S., EHRET, H. & MELCHIOR, F. (2012) Recombinant reconstitution of sumoylation reactions in vitro. *Methods Mol Biol*, 832, 93-110.
- FOUSTERI MI, L. A. (2000.) A novel SMC protein complex in *Schizosaccharomyces pombe* contains the Rad18 DNA repair protein. *EMBO J.*, 19, 1691-1702.
- FREUDENTHAL, B. D., GAKHAR, L., RAMASWAMY, S. & WASHINGTON, M. T. (2009) A charged residue at the subunit interface of PCNA promotes trimer formation by destabilizing alternate subunit interactions. *Acta Crystallogr D Biol Crystallogr*, 65, 560-6.
- FUKUDA, K., MORIOKA, H., IMAJOU, S., IKEDA, S., OHTSUKA, E. & TSURIMOTO, T. (1995) Structure-function relationship of the eukaryotic DNA replication factor, proliferating cell nuclear antigen. *J Biol Chem*, 270, 22527-34.
- FURUYA, K. & NIKI, H. (2012) Hyphal differentiation induced via a DNA damage checkpoint-dependent pathway engaged in crosstalk with nutrient stress signaling in *Schizosaccharomyces japonicus*. *Curr Genet*, 58, 291-303.
- GALI, H., JUHASZ, S., MOROCZ, M., HAJDU, I., FATYOL, K., SZUKACSOV, V., BURKOVICS, P. & HARACSKA, L. (2012) Role of SUMO modification of human PCNA at stalled replication fork. *Nucleic Acids Res*.
- GAO C, H. C., REINEKE E, LAM M, CHENG X, STANYA KJ, LIU Y, CHAKRABORTY S, SHIH HM, KAO HY. (2008) Histone deacetylase 7 promotes PML sumoylation and is essential for PML nuclear body formation. *Mol Biol Cell.*, 28, 5658-5667.
- GARY, R., KIM, K., CORNELIUS, H. L., PARK, M. S. & MATSUMOTO, Y. (1999) Proliferating cell nuclear antigen facilitates excision in long-patch base excision repair. *J Biol Chem*, 274, 4354-63.
- GERBER, J. K., GOGEL, E., BERGER, C., WALLISCH, M., MULLER, F., GRUMMT, I. & GRUMMT, F. (1997) Termination of mammalian rDNA replication: polar arrest of replication fork movement by transcription termination factor TTF-I. *Cell*, 90, 559-67.
- GOLEBIEWSKI, F., MATIC, I., TATHAM, M. H., COLE, C., YIN, Y., NAKAMURA, A., COX, J., BARTON, G. J., MANN, M. & HAY, R. T. (2009) System-wide changes to SUMO modifications in response to heat shock. *Sci Signal*, 2, ra24.

- GONG, L., MILLAS, S., MAUL, G. G. & YEH, E. T. (2000) Differential regulation of sentrinized proteins by a novel sentrin-specific protease. *J Biol Chem*, 275, 3355-9.
- GONG, L. & YEH, E. T. (2006) Characterization of a family of nucleolar SUMO-specific proteases with preference for SUMO-2 or SUMO-3. *J Biol Chem*, 281, 15869-77.
- GRALLERT, B. & NURSE, P. (1996) The ORC1 homolog orp1 in fission yeast plays a key role in regulating onset of S phase. *Genes Dev*, 10, 2644-54.
- GREGOIRE S, Y. X.-J. (2005) Association with Class IIa Histone Deacetylases Upregulates the Sumoylation of MEF2 Transcription Factors. *Mol Biol Cell*, 25, 2273-2287.
- GRIEP, M. A. (1995) Primase structure and function. *Indian J Biochem Biophys*, 32, 171-8.
- GUERINEAU, M., KRIZ, Z., KOZAKOVA, L., BEDNAROVA, K., JANOS, P. & PALECEK, J. (2012) Analysis of the Nse3/MAGE-binding domain of the Nse4/EID family proteins. *PLoS One*, 7, e35813.
- GUO, Z., ZHENG, L., XU, H., DAI, H., ZHOU, M., PASCUA, M. R., CHEN, Q. M. & SHEN, B. (2010) Methylation of FEN1 suppresses nearby phosphorylation and facilitates PCNA binding. *Nat Chem Biol*, 6, 766-73.
- GYGI, S. P., CORTHALS, G. L., ZHANG, Y., ROCHON, Y. & AEBERSOLD, R. (2000) Evaluation of two-dimensional gel electrophoresis-based proteome analysis technology. *Proc Natl Acad Sci U S A*, 97, 9390-5.
- HANNICH, J. T., LEWIS, A., KROETZ, M. B., LI, S. J., HEIDE, H., EMILI, A. & HOCHSTRASSER, M. (2005) Defining the SUMO-modified proteome by multiple approaches in *Saccharomyces cerevisiae*. *J Biol Chem*, 280, 4102-10.
- HARTWELL, L., WEINERT, T., KADYK, L. & GARVIK, B. (1994) Cell cycle checkpoints, genomic integrity, and cancer. *Cold Spring Harb Symp Quant Biol*, 59, 259-63.
- HARTWELL, L. H. & WEINERT, T. A. (1989) Checkpoints: controls that ensure the order of cell cycle events. *Science*, 246, 629-34.
- HASHIGUCHI, K., OZAKI, M., KURAOKA, I. & SAITOH, H. (2013) Establishment of a human cell line stably overexpressing mouse Nip45 and characterization of Nip45 subcellular localization. *Biochem Biophys Res Commun*, 430, 72-7.

- HASTINGS, P. J., IRA, G. & LUPSKI, J. R. (2009) A microhomology-mediated break-induced replication model for the origin of human copy number variation. *PLoS Genet*, 5, e1000327.
- HENRICKSEN, L. A., UMBRICHT, C. B. & WOLD, M. S. (1994) Recombinant replication protein A: expression, complex formation, and functional characterization. *J Biol Chem*, 269, 11121-32.
- HERSCHLEB, J., ANANIEV, G. & SCHWARTZ, D. C. (2007) Pulsed-field gel electrophoresis. *Nat Protoc*, 2, 677-84.
- HERSHKO, A. & CIECHANOVER, A. (1998) The ubiquitin system. *Annu Rev Biochem*, 67, 425-79.
- HERSHKO, A., EYTAN, E., CIECHANOVER, A. & HAAS, A. L. (1982) Immunochemical analysis of the turnover of ubiquitin-protein conjugates in intact cells. Relationship to the breakdown of abnormal proteins. *J Biol Chem*, 257, 13964-70.
- HIRANO, M., ANDERSON, D. E., ERICKSON, H. P. & HIRANO, T. (2001) Bimodal activation of SMC ATPase by intra- and inter-molecular interactions. *EMBO J*, 20, 3238-50.
- HIRANO T, M. T. (1994) A heterodimeric coiled-coil protein required for mitotic chromosome condensation in vitro *Cell*, 79, 449-458.
- HO, C. W., CHEN, H. T. & HWANG, J. (2011) UBC9 autosumoylation negatively regulates sumoylation of septins in *Saccharomyces cerevisiae*. *J Biol Chem*, 286, 21826-34.
- HO, J. C., WARR, N. J., SHIMIZU, H. & WATTS, F. Z. (2001) SUMO modification of Rad22, the *Schizosaccharomyces pombe* homologue of the recombination protein Rad52. *Nucleic Acids Res*, 29, 4179-86.
- HO, J. C. & WATTS, F. Z. (2003) Characterization of SUMO-conjugating enzyme mutants in *Schizosaccharomyces pombe* identifies a dominant-negative allele that severely reduces SUMO conjugation. *Biochem J*, 372, 97-104.
- HOCHSTRASSER, M. (2001) SP-RING for SUMO: new functions bloom for a ubiquitin-like protein. *Cell*, 107, 5-8.
- HOEGE, C., PFANDER, B., MOLDOVAN, G. L., PYROWOLAKIS, G. & JENTSCH, S. (2002) RAD6-dependent DNA repair is linked to modification of PCNA by ubiquitin and SUMO. *Nature*, 419, 135-41.
- HOYT, M. A., TOTIS, L. & ROBERTS, B. T. (1991) *S. cerevisiae* genes required for cell cycle arrest in response to loss of microtubule function. *Cell*, 66, 507-17.

- HUMPHREY, T. (2000) DNA damage and cell cycle control in *Schizosaccharomyces pombe*. *Mutat Res*, 451, 211-26.
- INAGAWA, T., YAMADA-INAGAWA, T., EYDMANN, T., MIAN, I. S., WANG, T. S. & DALGAARD, J. Z. (2009) *Schizosaccharomyces pombe* Rtf2 mediates site-specific replication termination by inhibiting replication restart. *Proc Natl Acad Sci U S A*, 106, 7927-32.
- IRA, G. & HABER, J. E. (2002) Characterization of RAD51-independent break-induced replication that acts preferentially with short homologous sequences. *Mol Cell Biol*, 22, 6384-92.
- JASCUR, T. & BOLAND, C. R. (2006) Structure and function of the components of the human DNA mismatch repair system. *Int J Cancer*, 119, 2030-5.
- JOHNSON ES, G. A. (2001) An E3-like factor that promotes SUMO conjugation to the yeast septins. *Cell*, 106.
- JOHNSON, E. S. & GUPTA, A. A. (2001) An E3-like factor that promotes SUMO conjugation to the yeast septins. *Cell*, 106, 735-44.
- JOHNSON, E. S., SCHWIENHORST, I., DOHMEN, R. J. & BLOBEL, G. (1997) The ubiquitin-like protein Smt3p is activated for conjugation to other proteins by an Aos1p/Uba2p heterodimer. *EMBO J*, 16, 5509-19.
- KAGEY MH, M. T., WOTTON D. (2003) The polycomb protein Pc2 is a SUMO E3. *Cell*, 113, 127-137.
- KAMILERI, I., KARAKASILITI, I. & GARINIS, G. A. (2012) Nucleotide excision repair: new tricks with old bricks. *Trends Genet*, 28, 566-73.
- KANG, L. E. & SYMINGTON, L. S. (2000) Aberrant double-strand break repair in rad51 mutants of *Saccharomyces cerevisiae*. *Mol Cell Biol*, 20, 9162-72.
- KELMAN, Z., LEE, J. K. & HURWITZ, J. (1999) The single minichromosome maintenance protein of *Methanobacterium thermoautotrophicum* DeltaH contains DNA helicase activity. *Proc Natl Acad Sci U S A*, 96, 14783-8.
- KNIPSCHER, P., FLOTHO, A., KLUG, H., OLSEN, J. V., VAN DIJK, W. J., FISH, A., JOHNSON, E. S., MANN, M., SIXMA, T. K. & PICHLER, A. (2008) Ubc9 sumoylation regulates SUMO target discrimination. *Mol Cell*, 31, 371-82.
- KODAKI, T., WOSCHOLSKI, R., EMR, S., WATERFIELD, M. D., NURSE, P. & PARKER, P. J. (1994) Mammalian phosphatidylinositol 3'-kinase induces a lethal phenotype on expression in *Schizosaccharomyces pombe*; comparison with the VPS34 gene product. *Eur J Biochem*, 219, 775-80.

- KOGOMA, T. (1996) Recombination by replication. *Cell*, 85, 625-7.
- KOSOY, A., CALONGE, T. M., OUTWIN, E. A. & O'CONNELL, M. J. (2007) Fission yeast Rnf4 homologs are required for DNA repair. *J Biol Chem*, 282, 20388-94.
- KREJCI, L., ALTMANNOVA, V., SPIREK, M. & ZHAO, X. (2012) Homologous recombination and its regulation. *Nucleic Acids Res*, 40, 5795-818.
- KRISHNA, T. S., KONG, X. P., GARY, S., BURGERS, P. M. & KURIYAN, J. (1994) Crystal structure of the eukaryotic DNA polymerase processivity factor PCNA. *Cell*, 79, 1233-43.
- LAANE, E., TAMM, K. P., BUENTKE, E., ITO, K., KHARAZIHA, P., OSCARSSON, J., CORCORAN, M., BJORKLUND, A. C., HULTENBY, K., LUNDIN, J., HEYMAN, M., SODERHALL, S., MAZUR, J., PORWIT, A., PANDOLFI, P. P., ZHIVOTOVSKY, B., PANARETAKIS, T. & GRANDER, D. (2009) Cell death induced by dexamethasone in lymphoid leukemia is mediated through initiation of autophagy. *Cell Death Differ*, 16, 1018-29.
- LAMBERT, S., MIZUNO, K., BLAISONNEAU, J., MARTINEAU, S., CHANET, R., FREON, K., MURRAY, J. M., CARR, A. M. & BALDACCI, G. (2010) Homologous recombination restarts blocked replication forks at the expense of genome rearrangements by template exchange. *Mol Cell*, 39, 346-59.
- LARSEN, M. R., TRELLE, M. B., THINGHOLM, T. E. & JENSEN, O. N. (2006) Analysis of posttranslational modifications of proteins by tandem mass spectrometry. *Biotechniques*, 40, 790-8.
- LEA DE, C. C. (1949) The distribution of the numbers of mutants in bacterial populations. *J Genetics*, 49, 264-284.
- LEA, D. E. & COULSON, C. A. (1949) The distribution of numbers of mutants in bacterial populations. *J Genet*, 49, 264-85.
- LEE, J. H. & PAULL, T. T. (2004) Direct activation of the ATM protein kinase by the Mre11/Rad50/Nbs1 complex. *Science*, 304, 93-6.
- LEE, M. G. & NURSE, P. (1987) Complementation used to clone a human homologue of the fission yeast cell cycle control gene *cdc2*. *Nature*, 327, 31-5.
- LEHMANN, A. R. (1972) Postreplication repair of DNA in ultraviolet-irradiated mammalian cells. *J Mol Biol*, 66, 319-37.
- LEHMANN, A. R., NIIMI, A., OGI, T., BROWN, S., SABBIONEDA, S., WING, J. F., KANNOUCHE, P. L. & GREEN, C. M. (2007) Translesion synthesis: Y-family polymerases and the polymerase switch. *DNA Repair (Amst)*, 6, 891-9.

- LEHMANN AR, W. M., GRIFFITHS DJ, MURRAY JM, WATTS FZ, MCCREADY S, CARR AM. (1995) The rad18 gene of *Schizosaccharomyces pombe* defines a new subgroup of the SMC superfamily involved in DNA repair. *Mol Cell Biol.*, 15, 7067–7080.
- LEUPOLD, U. (1957) [Physiologic and genetic studies of adenine-dependant mutants of *Schizosaccharomyces pombe*; a contribution to the problem of pseudoallele]. *Schweiz Z Pathol Bakteriologie*, 20, 535-44.
- LI, W., HESABI, B., BABBO, A., PACIONE, C., LIU, J., CHEN, D. J., NICKOLOFF, J. A. & SHEN, Z. (2000) Regulation of double-strand break-induced mammalian homologous recombination by UBL1, a RAD51-interacting protein. *Nucleic Acids Res*, 28, 1145-53.
- LI, Y. J., STARK, J. M., CHEN, D. J., ANN, D. K. & CHEN, Y. (2010) Role of SUMO:SIM-mediated protein-protein interaction in non-homologous end joining. *Oncogene*, 29, 3509-18.
- LIANG, M. P., BANATAO, D. R., KLEIN, T. E., BRUTLAG, D. L. & ALTMAN, R. B. (2003) WebFEATURE: An interactive web tool for identifying and visualizing functional sites on macromolecular structures. *Nucleic Acids Res*, 31, 3324-7.
- LIBERI, G., MAFFIOLETTI, G., LUCCA, C., CHIOLO, I., BARYSHNIKOVA, A., COTTA-RAMUSINO, C., LOPES, M., PELLICOLI, A., HABER, J. E. & FOIANI, M. (2005) Rad51-dependent DNA structures accumulate at damaged replication forks in *sgs1* mutants defective in the yeast ortholog of BLM RecQ helicase. *Genes Dev*, 19, 339-50.
- LIMBO, O., PORTER-GOFF, M. E., RHIND, N. & RUSSELL, P. (2010) Mre11 nuclease activity and Ctp1 regulate Chk1 activation by Rad3ATR and Tel1ATM checkpoint kinases at double-strand breaks. *Mol Cell Biol*, 31, 573-83.
- LIN, D. Y., HUANG, Y. S., JENG, J. C., KUO, H. Y., CHANG, C. C., CHAO, T. T., HO, C. C., CHEN, Y. C., LIN, T. P., FANG, H. I., HUNG, C. C., SUEN, C. S., HWANG, M. J., CHANG, K. S., MAUL, G. G. & SHIH, H. M. (2006) Role of SUMO-interacting motif in Daxx SUMO modification, subnuclear localization, and repression of sumoylated transcription factors. *Mol Cell*, 24, 341-54.
- LIU, Q., JIN, C., LIAO, X., SHEN, Z., CHEN, D. J. & CHEN, Y. (1999) The binding interface between an E2 (UBC9) and a ubiquitin homologue (UBL1). *J Biol Chem*, 274, 16979-87.
- LOBRICH, M. & JEGGO, P. A. (2007) The impact of a negligent G2/M checkpoint on genomic instability and cancer induction. *Nat Rev Cancer*, 7, 861-9.

- LOIS, L. M. & LIMA, C. D. (2005) Structures of the SUMO E1 provide mechanistic insights into SUMO activation and E2 recruitment to E1. *EMBO J*, 24, 439-51.
- LOK, B. H. & POWELL, S. N. (2012) Molecular pathways: understanding the role of Rad52 in homologous recombination for therapeutic advancement. *Clin Cancer Res*, 18, 6400-6.
- LOSADA A, H. M., HIRANO T. (1998) Identification of Xenopus SMC protein complexes required for sister chromatid cohesion *Genes & Dev.*, 12, 1986-1997.
- LUNDBLAD, V. (2012) Telomere end processing: unexpected complexity at the end game. *Genes Dev*, 26, 1123-7.
- LURIA, S. E. & DELBRUCK, M. (1943) Mutations of Bacteria from Virus Sensitivity to Virus Resistance. *Genetics*, 28, 491-511.
- LYDEARD, J. R., JAIN, S., YAMAGUCHI, M. & HABER, J. E. (2007) Break-induced replication and telomerase-independent telomere maintenance require Pol32. *Nature*, 448, 820-3.
- MAHAJAN, R., DELPHIN, C., GUAN, T., GERACE, L. & MELCHIOR, F. (1997) A small ubiquitin-related polypeptide involved in targeting RanGAP1 to nuclear pore complex protein RanBP2. *Cell*, 88, 97-107.
- MAIN, E. R., FULTON, K. F. & JACKSON, S. E. (1998) Context-dependent nature of destabilizing mutations on the stability of FKBP12. *Biochemistry*, 37, 6145-53.
- MAKNEVYCH T, S. Y., XIN X, SRIKUMAR T, VIZEACOMAR FJ, JERAM SM, LI Z, BAHR S, ANDREWS BJ, BOONE C, RAUGHT B. (2008) Global Map of SUMO Function Revealed by Protein-Protein Interaction and Genetic Networks *Molecular Cell*, 33, 124-135.
- MANOLIS, K. G., NIMMO, E. R., HARTSUIKER, E., CARR, A. M., JEGGO, P. A. & ALLSHIRE, R. C. (2001) Novel functional requirements for non-homologous DNA end joining in *Schizosaccharomyces pombe*. *EMBO J*, 20, 210-21.
- MARTI, T. M., MANSOUR, A. A., LEHMANN, E. & FLECK, O. (2003) Different frameshift mutation spectra in non-repetitive DNA of MutSalph α - and MutLalph α -deficient fission yeast cells. *DNA Repair (Amst)*, 2, 571-80.
- MASUDA, K., BANNO, K., YANOKURA, M., KOBAYASHI, Y., KISU, I., UEKI, A., ONO, A., ASAHARA, N., NOMURA, H., HIRASAWA, A., SUSUMU, N. & AOKI, D. (2011) Relationship between DNA Mismatch Repair Deficiency and Endometrial Cancer. *Mol Biol Int*, 2011, 256063.
- MASUDA, Y., SUZUKI, M., KAWAI, H., HISHIKI, A., HASHIMOTO, H., MASUTANI, C., HISHIDA, T., SUZUKI, F. & KAMIYA, K. (2012) En bloc

transfer of polyubiquitin chains to PCNA in vitro is mediated by two different human E2-E3 pairs. *Nucleic Acids Res*, 40, 10394-407.

- MATSUURA, A., NAITO, T. & ISHIKAWA, F. (1999) Genetic control of telomere integrity in *Schizosaccharomyces pombe*: rad3(+) and tel1(+) are parts of two regulatory networks independent of the downstream protein kinases chk1(+) and cds1(+). *Genetics*, 152, 1501-12.
- MATUNIS MJ, W. J., BLOBEL G. (1998) SUMO-1 Modification and Its Role in Targeting the Ran GTPase-activating Protein, RanGAP1, to the Nuclear Pore Complex. *J Cell Biol*, 140, 499-509.
- MAUNDRELL, K. (1993) Thiamine-repressible expression vectors pREP and pRIP for fission yeast. *Gene*, 123, 127-30.
- MAYANAGI, K., KIYONARI, S., NISHIDA, H., SAITO, M., KOHDA, D., ISHINO, Y., SHIRAI, T. & MORIKAWA, K. (2011) Architecture of the DNA polymerase B-proliferating cell nuclear antigen (PCNA)-DNA ternary complex. *Proc Natl Acad Sci U S A*, 108, 1845-9.
- MCALEENAN, A., CORDON-PRECIADO, V., CLEMENTE-BLANCO, A., LIU, I. C., SEN, N., LEONARD, J., JARMUZ, A. & ARAGON, L. (2012) SUMOylation of the alpha-kleisin subunit of cohesin is required for DNA damage-induced cohesion. *Curr Biol*, 22, 1564-75.
- MCNALLY, R., BOWMAN, G. D., GOEDKEN, E. R., O'DONNELL, M. & KURIYAN, J. (2010) Analysis of the role of PCNA-DNA contacts during clamp loading. *BMC Struct Biol*, 10, 3.
- MELBY, T. E., CIAMPAGLIO, C. N., BRISCOE, G. & ERICKSON, H. P. (1998) The symmetrical structure of structural maintenance of chromosomes (SMC) and MukB proteins: long, antiparallel coiled coils, folded at a flexible hinge. *J Cell Biol*, 142, 1595-604.
- MELUH PB, K. D. (1995) Evidence that the MIF2 gene of *Saccharomyces cerevisiae* encodes a centromere protein with homology to the mammalian centromere protein CENP-C. *Mol Biol Cell*, 6, 793-807.
- MERALDI, P., MCAINSH, A. D., RHEINBAY, E. & SORGER, P. K. (2006) Phylogenetic and structural analysis of centromeric DNA and kinetochore proteins. *Genome Biol*, 7, R23.
- MEULMEESTER, E., KUNZE, M., HSIAO, H. H., URLAUB, H. & MELCHIOR, F. (2008) Mechanism and consequences for paralog-specific sumoylation of ubiquitin-specific protease 25. *Mol Cell*, 30, 610-9.

- MICHEL, B., GROMPONE, G., FLORES, M. J. & BIDNENKO, V. (2004) Multiple pathways process stalled replication forks. *Proc Natl Acad Sci U S A*, 101, 12783-8.
- MINTY, A., DUMONT, X., KAGHAD, M. & CAPUT, D. (2000) Covalent modification of p73 α by SUMO-1. Two-hybrid screening with p73 identifies novel SUMO-1-interacting proteins and a SUMO-1 interaction motif. *J Biol Chem*, 275, 36316-23.
- MIRKIN, S. M. (2006) DNA structures, repeat expansions and human hereditary disorders. *Curr Opin Struct Biol*, 16, 351-8.
- MITCHISON, J. M. (1957) The growth of single cells. I. *Schizosaccharomyces pombe*. *Exp Cell Res*, 13, 244-62.
- MIYACHI, K., FRITZLER, M. J. & TAN, E. M. (1978) Autoantibody to a nuclear antigen in proliferating cells. *J Immunol*, 121, 2228-34.
- MOLDOVAN, G. L., PFANDER, B. & JENTSCH, S. (2006) PCNA controls establishment of sister chromatid cohesion during S phase. *Mol Cell*, 23, 723-32.
- MORISHITA, T., TSUTSUI, Y., IWASAKI, H. & SHINAGAWA, H. (2002) The *Schizosaccharomyces pombe* rad60 gene is essential for repairing double-strand DNA breaks spontaneously occurring during replication and induced by DNA-damaging agents. *Mol Cell Biol*, 22, 3537-48.
- MORRIS, J. R. (2009) SUMO in the mammalian response to DNA damage. *Biochemical Society Transactions* 38, 92-97.
- MORRIS, J. R., BOUTELL, C., KEPPLER, M., DENSHAM, R., WEEKES, D., ALAMSHAH, A., BUTLER, L., GALANTY, Y., PANGON, L., KIUCHI, T., NG, T. & SOLOMON, E. (2009) The SUMO modification pathway is involved in the BRCA1 response to genotoxic stress. *Nature*, 462, 886-90.
- MUKHOPADHYAY, D., AYAYDIN, F., KOLLI, N., TAN, S. H., ANAN, T., KAMETAKA, A., AZUMA, Y., WILKINSON, K. D. & DASSO, M. (2006) SUSP1 antagonizes formation of highly SUMO2/3-conjugated species. *J Cell Biol*, 174, 939-49.
- MUKHOPADHYAY, D. & DASSO, M. (2007) Modification in reverse: the SUMO proteases. *Trends Biochem Sci*, 32, 286-95.
- MULLEN, J. R., KALIRAMAN, V., IBRAHIM, S. S. & BRILL, S. J. (2001) Requirement for three novel protein complexes in the absence of the Sgs1 DNA helicase in *Saccharomyces cerevisiae*. *Genetics*, 157, 103-18.

- MURAI, J., YANG, K., DEJSUPHONG, D., HIROTA, K., TAKEDA, S. & D'ANDREA, A. D. (2011) The USP1/UAF1 complex promotes double-strand break repair through homologous recombination. *Mol Cell Biol*, 31, 2462-9.
- MURRAY, J. M., TAVASSOLI, M., AL-HARITHY, R., SHELDRIK, K. S., LEHMANN, A. R., CARR, A. M. & WATTS, F. Z. (1994) Structural and functional conservation of the human homolog of the *Schizosaccharomyces pombe* rad2 gene, which is required for chromosome segregation and recovery from DNA damage. *Mol Cell Biol*, 14, 4878-88.
- MUSACCHIO, A. (2011) Spindle assembly checkpoint: the third decade. *Philos Trans R Soc Lond B Biol Sci*, 366, 3595-604.
- NAKAMURA, K., OKAMOTO, A., KATOU, Y., YADANI, C., SHITANDA, T., KAWETEERAWAT, C., TAKAHASHI, T. S., ITOH, T., SHIRAHIGE, K., MASUKATA, H. & NAKAGAWA, T. (2008) Rad51 suppresses gross chromosomal rearrangement at centromere in *Schizosaccharomyces pombe*. *EMBO J*, 27, 3036-46.
- NAKASEKO, Y., ADACHI, Y., FUNAHASHI, S., NIWA, O. & YANAGIDA, M. (1986) Chromosome walking shows a highly homologous repetitive sequence present in all the centromere regions of fission yeast. *EMBO J*, 5, 1011-21.
- NAKASEKO, Y., KINOSHITA, N. & YANAGIDA, M. (1987) A novel sequence common to the centromere regions of *Schizosaccharomyces pombe* chromosomes. *Nucleic Acids Res*, 15, 4705-15.
- NISHIDA, T., KANEKO, F., KITAGAWA, M. & YASUDA, H. (2001) Characterization of a novel mammalian SUMO-1/Smt3-specific isopeptidase, a homologue of rat axam, which is an axin-binding protein promoting beta-catenin degradation. *J Biol Chem*, 276, 39060-6.
- NOVATCHKOVA, M., BACHMAIR, A., EISENHABER, B. & EISENHABER, F. (2005) Proteins with two SUMO-like domains in chromatin-associated complexes: the RENi (Rad60-Esc2-NIP45) family. *BMC Bioinformatics*, 6, 22.
- OHI, M. D., VANDER KOOI, C. W., ROSENBERG, J. A., CHAZIN, W. J. & GOULD, K. L. (2003) Structural insights into the U-box, a domain associated with multi-ubiquitination. *Nat Struct Biol*, 10, 250-5.
- OHYA, T., ARAI, H., KUBOTA, Y., SHINAGAWA, H. & HISHIDA, T. (2008) A SUMO-like domain protein, Esc2, is required for genome integrity and sister chromatid cohesion in *Saccharomyces cerevisiae*. *Genetics*, 180, 41-50.
- OKAZAKI, R., OKAZAKI, T., SAKABE, K. & SUGIMOTO, K. (1967) Mechanism of DNA replication possible discontinuity of DNA chain growth. *Jpn J Med Sci Biol*, 20, 255-60.

- OKUMA, T., HONDA, R., ICHIKAWA, G., TSUMAGARI, N. & YASUDA, H. (1999) In vitro SUMO-1 modification requires two enzymatic steps, E1 and E2. *Biochem Biophys Res Commun*, 254, 693-8.
- OSTAPCHUK, P., DIFFLEY, J. F., BRUDER, J. T., STILLMAN, B., LEVINE, A. J. & HEARING, P. (1986) Interaction of a nuclear factor with the polyomavirus enhancer region. *Proc Natl Acad Sci U S A*, 83, 8550-4.
- PALECEK, J., VIDOT, S., FENG, M., DOHERTY, A. J. & LEHMANN, A. R. (2006) The Smc5-Smc6 DNA repair complex. bridging of the Smc5-Smc6 heads by the KLEISIN, Nse4, and non-Kleisin subunits. *J Biol Chem*, 281, 36952-9.
- PANSE, V. G., HARDELAND, U., WERNER, T., KUSTER, B. & HURT, E. (2004) A proteome-wide approach identifies sumoylated substrate proteins in yeast. *J Biol Chem*, 279, 41346-51.
- PAPOULI, E., CHEN, S., DAVIES, A. A., HUTTNER, D., KREJCI, L., SUNG, P. & ULRICH, H. D. (2005) Crosstalk between SUMO and ubiquitin on PCNA is mediated by recruitment of the helicase Srs2p. *Mol Cell*, 19, 123-33.
- PARDEE, A. B. (1989) G1 events and regulation of cell proliferation. *Science*, 246, 603-8.
- PARKER, J. L. & ULRICH, H. D. (2009) Mechanistic analysis of PCNA poly-ubiquitylation by the ubiquitin protein ligases Rad18 and Rad5. *EMBO J*, 28, 3657-66.
- PARRILLA-CASTELLAR, E. R., ARLANDER, S. J. & KARNITZ, L. (2004) Dial 9-1-1 for DNA damage: the Rad9-Hus1-Rad1 (9-1-1) clamp complex. *DNA Repair (Amst)*, 3, 1009-14.
- PARSONS, C. A., BAUMANN, P., VAN DYCK, E. & WEST, S. C. (2000) Precise binding of single-stranded DNA termini by human RAD52 protein. *EMBO J*, 19, 4175-81.
- PEBERNARD, S., MCDONALD, W. H., PAVLOVA, Y., YATES, J. R., 3RD & BODDY, M. N. (2004) Nse1, Nse2, and a novel subunit of the Smc5-Smc6 complex, Nse3, play a crucial role in meiosis. *Mol Biol Cell*, 15, 4866-76.
- PEBERNARD, S., SCHAFFER, L., CAMPBELL, D., HEAD, S. R. & BODDY, M. N. (2008) Localization of Smc5/6 to centromeres and telomeres requires heterochromatin and SUMO, respectively. *EMBO J*, 27, 3011-23.
- PEBERNARD S, S. L., CAMPBELL D, HEAD SR, BODDY MN. (2008) Localization of Smc5/6 to centromeres and telomeres requires heterochromatin and SUMO, respectively *EMBO J*, 27, 3011-3023.

- PEBERNARD S, W. J., MCDONALD WH, YATES JR, BODDY MN. (2006) The Nse5-Nse6 dimer mediates DNA repair roles of the Smc5-Smc6 complex. *Mol Cell Biol*, 26, 1617-30.
- PERKINS, D. N., PAPPIN, D. J., CREASY, D. M. & COTTRELL, J. S. (1999) Probability-based protein identification by searching sequence databases using mass spectrometry data. *Electrophoresis*, 20, 3551-67.
- PERRY, J. J., TAINER, J. A. & BODDY, M. N. (2008) A simultaneous role for SUMO and ubiquitin. *Trends Biochem Sci*, 33, 201-8.
- PFANDER, B., MOLDOVAN, G. L., SACHER, M., HOEGE, C. & JENTSCH, S. (2005) SUMO-modified PCNA recruits Srs2 to prevent recombination during S phase. *Nature*, 436, 428-33.
- PICHLER A, G. A., SEELER JS, DEJEAN A, MELCHIOR F. (2002) The nucleoporin RanBP2 has SUMO1 E3 ligase activity. *Cell*, 108, 109-120.
- PICHLER, A., GAST, A., SEELER, J. S., DEJEAN, A. & MELCHIOR, F. (2002) The nucleoporin RanBP2 has SUMO1 E3 ligase activity. *Cell*, 108, 109-20.
- PICHLER, A., KNIPSCHER, P., OBERHOFER, E., VAN DIJK, W. J., KORNER, R., OLSEN, J. V., JENTSCH, S., MELCHIOR, F. & SIXMA, T. K. (2005) SUMO modification of the ubiquitin-conjugating enzyme E2-25K. *Nat Struct Mol Biol*, 12, 264-9.
- PIERRON, D., CHANG, I., ARACHICHE, A., HEISKE, M., THOMAS, O., BORLIN, M., PENNARUN, E., MURAIL, P., THORAVALL, D., ROCHER, C. & LETELLIER, T. (2011) Mutation rate switch inside Eurasian mitochondrial haplogroups: impact of selection and consequences for dating settlement in Europe. *PLoS One*, 6, e21543.
- POTTS, P. R. & YU, H. (2005) Human MMS21/NSE2 is a SUMO ligase required for DNA repair. *Mol Cell Biol*, 25, 7021-32.
- PRUDDEN, J., PEBERNARD, S., RAFFA, G., SLAVIN, D. A., PERRY, J. J., TAINER, J. A., MCGOWAN, C. H. & BODDY, M. N. (2007) SUMO-targeted ubiquitin ligases in genome stability. *EMBO J*, 26, 4089-101.
- PRUDDEN, J., PERRY, J. J., ARVAI, A. S., TAINER, J. A. & BODDY, M. N. (2009) Molecular mimicry of SUMO promotes DNA repair. *Nat Struct Mol Biol*, 16, 509-16.
- PRUDDEN, J., PERRY, J. J., NIE, M., VASHISHT, A. A., ARVAI, A. S., HITOMI, C., GUENTHER, G., WOHLSCHEGEL, J. A., TAINER, J. A. & BODDY, M. N. (2011) DNA repair and global sumoylation are regulated by distinct Ubc9 noncovalent complexes. *Mol Cell Biol*, 31, 2299-310.

- PUNCHIHEWA, C., INOUE, A., HISHIKI, A., FUJIKAWA, Y., CONNELLY, M., EVISON, B., SHAO, Y., HEATH, R., KURAOKA, I., RODRIGUES, P., HASHIMOTO, H., KAWANISHI, M., SATO, M., YAGI, T. & FUJII, N. (2012) Identification of small molecule proliferating cell nuclear antigen (PCNA) inhibitor that disrupts interactions with PIP-box proteins and inhibits DNA replication. *J Biol Chem*, 287, 14289-300.
- RAFFA GD, WOHLSCHLEGEL J, YATES JR & MN., B. (2006) SUMO-binding motifs mediate the Rad60-dependent response to replicative stress and self-association. *J Biol Chem*, 281, 27973-81.
- RAFFA, G. D., WOHLSCHLEGEL, J., YATES, J. R., 3RD & BODDY, M. N. (2006) SUMO-binding motifs mediate the Rad60-dependent response to replicative stress and self-association. *J Biol Chem*, 281, 27973-81.
- REENAN, R. A. & KOLODNER, R. D. (1992) Characterization of insertion mutations in the *Saccharomyces cerevisiae* MSH1 and MSH2 genes: evidence for separate mitochondrial and nuclear functions. *Genetics*, 132, 975-85.
- REINDLE, A., BELICHENKO, I., BYLEBYL, G. R., CHEN, X. L., GANDHI, N. & JOHNSON, E. S. (2006) Multiple domains in Siz SUMO ligases contribute to substrate selectivity. *J Cell Sci*, 119, 4749-57.
- REIS, C. C., BATISTA, S. & FERREIRA, M. G. (2012) The fission yeast MRN complex tethers dysfunctional telomeres for NHEJ repair. *EMBO J*, 31, 4576-86.
- REN, J., GAO, X., JIN, C., ZHU, M., WANG, X., SHAW, A., WEN, L., YAO, X. & XUE, Y. (2009) Systematic study of protein sumoylation: Development of a site-specific predictor of SUMOsp 2.0. *Proteomics*, 9, 3409-3412.
- REVERTER, D. & LIMA, C. D. (2005) Insights into E3 ligase activity revealed by a SUMO-RanGAP1-Ubc9-Nup358 complex. *Nature*, 435, 687-92.
- RHIND, N. & RUSSELL, P. (2000) Chk1 and Cds1: linchpins of the DNA damage and replication checkpoint pathways. *J Cell Sci*, 113 (Pt 22), 3889-96.
- ROBERTSON, A. B., KLUNGLAND, A., ROGNES, T. & LEIROS, I. (2009) DNA repair in mammalian cells: Base excision repair: the long and short of it. *Cell Mol Life Sci*, 66, 981-93.
- RODRIGUEZ MS, D. C., HAY RT. (2001) SUMO-1 conjugation in vivo requires both a consensus modification motif and nuclear targeting. *J Biol Chem.*, 276, 12654-12659.

- SACHER, M., PFANDER, B., HOEGE, C. & JENTSCH, S. (2006) Control of Rad52 recombination activity by double-strand break-induced SUMO modification. *Nat Cell Biol*, 8, 1284-90.
- SAITO, K., KAGAWA, W., SUZUKI, T., SUZUKI, H., YOKOYAMA, S., SAITOH, H., TASHIRO, S., DOHMAE, N. & KURUMIZAKA, H. (2010) The putative nuclear localization signal of the human RAD52 protein is a potential sumoylation site. *J Biochem*, 147, 833-42.
- SAKA, Y., ESASHI, F., MATSUSAKA, T., MOCHIDA, S. & YANAGIDA, M. (1997) Damage and replication checkpoint control in fission yeast is ensured by interactions of Crb2, a protein with BRCT motif, with Cut5 and Chk1. *Genes Dev*, 11, 3387-400.
- SANTA MARIA, S. R., GANGAVARAPU, V., JOHNSON, R. E., PRAKASH, L. & PRAKASH, S. (2007) Requirement of Nse1, a subunit of the Smc5-Smc6 complex, for Rad52-dependent postreplication repair of UV-damaged DNA in *Saccharomyces cerevisiae*. *Mol Cell Biol*, 27, 8409-18.
- SAPETSCHNIG A, R. G., BRAUN H, DOLL A, SCHERGAUT M, MELCHIOR F, SUSKE G. (2002) Transcription factor Sp3 is silenced through SUMO modification by PIAS1. *EMBO J.*, 5206-5215.
- SCHULMAN, B. A. & HARPER, J. W. (2009) Ubiquitin-like protein activation by E1 enzymes: the apex for downstream signalling pathways. *Nat Rev Mol Cell Biol*, 10, 319-31.
- SCOTT, K. C., MERRETT, S. L. & WILLARD, H. F. (2006) A heterochromatin barrier partitions the fission yeast centromere into discrete chromatin domains. *Curr Biol*, 16, 119-29.
- SEKIYAMA, N., ARITA, K., IKEDA, Y., HASHIGUCHI, K., ARIYOSHI, M., TOCHIO, H., SAITOH, H. & SHIRAKAWA, M. (2010) Structural basis for regulation of poly-SUMO chain by a SUMO-like domain of Nip45. *Proteins*, 78, 1491-502.
- SERGEANT J, T. E., PALECEK J, FOUSTERI M, ANDREWS EA, SWEENEY S, SHINAGAWA H, WATTS FZ, LEHMANN AR. (2005) Composition and architecture of the *Schizosaccharomyces pombe* Rad18 (Smc5-6) complex. *Mol Cell Biol.* , 25, 172-184.
- SEUFERT, W., FUTCHER, B. & JENTSCH, S. (1995) Role of a ubiquitin-conjugating enzyme in degradation of S- and M-phase cyclins. *Nature*, 373, 78-81.
- SHANNON, K. B., CANMAN, J. C. & SALMON, E. D. (2002) Mad2 and BubR1 function in a single checkpoint pathway that responds to a loss of tension. *Mol Biol Cell*, 13, 3706-19.

- SHAYEGHI, M., DOE, C. L., TAVASSOLI, M. & WATTS, F. Z. (1997) Characterisation of *Schizosaccharomyces pombe* rad31, a UBA-related gene required for DNA damage tolerance. *Nucleic Acids Res*, 25, 1162-9.
- SHIN, J. A., CHOI, E. S., KIM, H. S., HO, J. C., WATTS, F. Z., PARK, S. D. & JANG, Y. K. (2005) SUMO modification is involved in the maintenance of heterochromatin stability in fission yeast. *Mol Cell*, 19, 817-28.
- SONG, J., DURRIN, L. K., WILKINSON, T. A., Krontiris, T. G. & CHEN, Y. (2004) Identification of a SUMO-binding motif that recognizes SUMO-modified proteins. *Proc Natl Acad Sci U S A*, 101, 14373-8.
- SONG, J., ZHANG, Z., HU, W. & CHEN, Y. (2005) Small ubiquitin-like modifier (SUMO) recognition of a SUMO binding motif: a reversal of the bound orientation. *J Biol Chem*, 280, 40122-9.
- SPELL, R. M. & JINKS-ROBERTSON, S. (2004) Determination of mitotic recombination rates by fluctuation analysis in *Saccharomyces cerevisiae*. *Methods Mol Biol*, 262, 3-12.
- STEINACHER, R., OSMAN, F., DALGAARD, J. Z., LORENZ, A. & WHITBY, M. C. (2012) The DNA helicase Pfh1 promotes fork merging at replication termination sites to ensure genome stability. *Genes Dev*, 26, 594-602.
- STELTER, P. & ULRICH, H. D. (2003) Control of spontaneous and damage-induced mutagenesis by SUMO and ubiquitin conjugation. *Nature*, 425, 188-91.
- SU, Y. F., YANG, T., HUANG, H., LIU, L. F. & HWANG, J. (2012) Phosphorylation of Ubc9 by Cdk1 enhances SUMOylation activity. *PLoS One*, 7, e34250.
- SUBRAMANIAM, S., MEALER, R. G., SIXT, K. M., BARROW, R. K., USIELLO, A. & SNYDER, S. H. (2010) Rhes, a physiologic regulator of sumoylation, enhances cross-sumoylation between the basic sumoylation enzymes E1 and Ubc9. *J Biol Chem*, 285, 20428-32.
- SUN, L. & CHEN, Z. J. (2004) The novel functions of ubiquitination in signaling. *Curr Opin Cell Biol*, 16, 119-26.
- SUNG, P., KREJCI, L., VAN KOMEN, S. & SEHORN, M. G. (2003) Rad51 recombinase and recombination mediators. *J Biol Chem*, 278, 42729-32.
- TAKAHASHI, Y., DULEV, S., LIU, X., HILLER, N. J., ZHAO, X. & STRUNNIKOV, A. (2008) Cooperation of sumoylated chromosomal proteins in rDNA maintenance. *PLoS Genet*, 4, e1000215.
- TAKAHASHI Y, K. Y. (2005) Yeast PIAS-type Ull1/Siz1 is composed of SUMO ligase and regulatory domains. *J Biol Chem*, 280, 35822-35828.

- TAKAHASHI, Y., TOH, E. A. & KIKUCHI, Y. (2003) Comparative analysis of yeast PIAS-type SUMO ligases in vivo and in vitro. *J Biochem*, 133, 415-22.
- TANAKA K, N. J., OKAZAKI K, KATO H, NIWA O, NAKAGAWA T, MATSUDA H, KAWAMUKAI M, MURAKAMI Y. (1999) Characterization of a fission yeast SUMO-1 homologue, pmt3p, required for multiple nuclear events, including the control of telomere length and chromosome segregation. *Mol Cell Biol.*, 19, 8660-8672.
- TANAKA, K. & RUSSELL, P. (2001) Mrc1 channels the DNA replication arrest signal to checkpoint kinase Cds1. *Nat Cell Biol*, 3, 966-72.
- TATHAM, M. H., GEOFFROY, M. C., SHEN, L., PLECHANOVOVA, A., HATTERSLEY, N., JAFFRAY, E. G., PALVIMO, J. J. & HAY, R. T. (2008) RNF4 is a poly-SUMO-specific E3 ubiquitin ligase required for arsenic-induced PML degradation. *Nat Cell Biol*, 10, 538-46.
- TATHAM, M. H., JAFFRAY, E., VAUGHAN, O. A., DESTERRO, J. M., BOTTING, C. H., NAISMITH, J. H. & HAY, R. T. (2001) Polymeric chains of SUMO-2 and SUMO-3 are conjugated to protein substrates by SAE1/SAE2 and Ubc9. *J Biol Chem*, 276, 35368-74.
- TATHAM, M. H., MATIC, I., MANN, M. & HAY, R. T. (2011) Comparative proteomic analysis identifies a role for SUMO in protein quality control. *Sci Signal*, 4, rs4.
- TAYLOR, D. L., HO, J. C., OLIVER, A. & WATTS, F. Z. (2002) Cell-cycle-dependent localisation of Ulp1, a *Schizosaccharomyces pombe* Pmt3 (SUMO)-specific protease. *J Cell Sci*, 115, 1113-22.
- TAYLOR, E. M., BROUGHTON, B. C., BOTTA, E., STEFANINI, M., SARASIN, A., JASPERS, N. G., FAWCETT, H., HARCOURT, S. A., ARLETT, C. F. & LEHMANN, A. R. (1997) Xeroderma pigmentosum and trichothiodystrophy are associated with different mutations in the XPD (ERCC2) repair/transcription gene. *Proc Natl Acad Sci U S A*, 94, 8658-63.
- TINLINE-PURVIS, H., SAVORY, A. P., CULLEN, J. K., DAVE, A., MOSS, J., BRIDGE, W. L., MARGUERAT, S., BAHLE, J., RAGOISSIS, J., MOTT, R., WALKER, C. A. & HUMPHREY, T. C. (2009) Failed gene conversion leads to extensive end processing and chromosomal rearrangements in fission yeast. *EMBO J*, 28, 3400-12.
- TOM, S., HENRICKSEN, L. A. & BAMBARA, R. A. (2000) Mechanism whereby proliferating cell nuclear antigen stimulates flap endonuclease 1. *J Biol Chem*, 275, 10498-505.

- TORRES-ROSELL, J., SUNJEVARIC, I., DE PICCOLI, G., SACHER, M., ECKERT-BOULET, N., REID, R., JENTSCH, S., ROTHSTEIN, R., ARAGON, L. & LISBY, M. (2007) The Smc5-Smc6 complex and SUMO modification of Rad52 regulates recombinational repair at the ribosomal gene locus. *Nat Cell Biol*, 9, 923-31.
- TRUONG, K., LEE, T. D. & CHEN, Y. (2012) Small Ubiquitin-like Modifier (SUMO) Modification of E1 Cys Domain Inhibits E1 Cys Domain Enzymatic Activity. *J Biol Chem*, 287, 15154-63.
- ULRICH, H. D. (2005) Mutual interactions between the SUMO and ubiquitin systems: a plea of no contest. *Trends Cell Biol*, 15, 525-32.
- WATSON, A. T., GARCIA, V., BONE, N., CARR, A. M. & ARMSTRONG, J. (2008) Gene tagging and gene replacement using recombinase-mediated cassette exchange in *Schizosaccharomyces pombe*. *Gene*, 407, 63-74.
- WATTS FZ, A. S., J.C.-Y. HO2, L.K. BOYD, M.A.M. TRICKEY3, L. GARDNER, F.-X. OGI AND E.A. OUTWIN4 (2007) The role of *Schizosaccharomyces pombe* SUMO ligases in genome stability. *Biochemical Society Transactions*, 35, 1379–1384.
- WATTS, F. Z., SKILTON, A., HO, J. C., BOYD, L. K., TRICKEY, M. A., GARDNER, L., OGI, F. X. & OUTWIN, E. A. (2007) The role of *Schizosaccharomyces pombe* SUMO ligases in genome stability. *Biochem Soc Trans*, 35, 1379-84.
- WETERINGS, E. & CHEN, D. J. (2008) The endless tale of non-homologous end-joining. *Cell Res*, 18, 114-24.
- WINDECKER, H. & ULRICH, H. D. (2008) Architecture and assembly of poly-SUMO chains on PCNA in *Saccharomyces cerevisiae*. *J Mol Biol*, 376, 221-31.
- WOOD, V., GWILLIAM, R., RAJANDREAM, M. A., LYNE, M., LYNE, R., STEWART, A., SGOUROS, J., PEAT, N., HAYLES, J., BAKER, S., BASHAM, D., BOWMAN, S., BROOKS, K., BROWN, D., BROWN, S., CHILLINGWORTH, T., CHURCHER, C., COLLINS, M., CONNOR, R., CRONIN, A., DAVIS, P., FELTWELL, T., FRASER, A., GENTLES, S., GOBLE, A., HAMLIN, N., HARRIS, D., HIDALGO, J., HODGSON, G., HOLROYD, S., HORNSBY, T., HOWARTH, S., HUCKLE, E. J., HUNT, S., JAGELS, K., JAMES, K., JONES, L., JONES, M., LEATHER, S., MCDONALD, S., MCLEAN, J., MOONEY, P., MOULE, S., MUNGALL, K., MURPHY, L., NIBLETT, D., ODELL, C., OLIVER, K., O'NEIL, S., PEARSON, D., QUAIL, M. A., RABBINOWITSCH, E., RUTHERFORD, K., RUTTER, S., SAUNDERS, D., SEEGER, K., SHARP, S., SKELTON, J., SIMMONDS, M., SQUARES, R., SQUARES, S., STEVENS, K., TAYLOR, K., TAYLOR, R. G., TIVEY, A., WALSH, S., WARREN, T., WHITEHEAD, S., WOODWARD, J., VOLCKAERT, G., AERT, R., ROBBEN, J.,

- GRYMONPREZ, B., WELTJENS, I., VANSTREELS, E., RIEGER, M., SCHAFER, M., MULLER-AUER, S., GABEL, C., FUCHS, M., DUSTERHOFT, A., FRITZC, C., HOLZER, E., MOESTL, D., HILBERT, H., BORZYM, K., LANGER, I., BECK, A., LEHRACH, H., REINHARDT, R., POHL, T. M., EGER, P., ZIMMERMANN, W., WEDLER, H., WAMBUTT, R., PURNELLE, B., GOFFEAU, A., CADIEU, E., DREANO, S., GLOUX, S., et al. (2002) The genome sequence of *Schizosaccharomyces pombe*. *Nature*, 415, 871-80.
- WU, N., KONG, X., JI, Z., ZENG, W., POTTS, P. R., YOKOMORI, K. & YU, H. (2012) Scc1 sumoylation by Mms21 promotes sister chromatid recombination through counteracting Wapl. *Genes Dev*, 26, 1473-85.
- XHEMALCE, B., SEELER, J. S., THON, G., DEJEAN, A. & ARCANGIOLI, B. (2004) Role of the fission yeast SUMO E3 ligase Pli1p in centromere and telomere maintenance. *EMBO J*, 23, 3844-53.
- XHEMALCE B, S. J., THON G, DEJEAN A, ARCANGIOLI B. (2004) Role of the fission yeast SUMO E3 ligase Pli1p in centromere and telomere maintenance. *EMBO J*, 23, 3844–3853.
- XIE, Y., KERSCHER, O., KROETZ, M. B., MCCONCHIE, H. F., SUNG, P. & HOCHSTRASSER, M. (2007) The yeast Hex3.Slx8 heterodimer is a ubiquitin ligase stimulated by substrate sumoylation. *J Biol Chem*, 282, 34176-84.
- YAMASHITA, Y. M., NAKASEKO, Y., KUMADA, K., NAKAGAWA, T. & YANAGIDA, M. (1999) Fission yeast APC/cyclosome subunits, Cut20/Apc4 and Cut23/Apc8, in regulating metaphase-anaphase progression and cellular stress responses. *Genes Cells*, 4, 445-63.
- YANG, K., MOLDOVAN, G. L., VINCIGUERRA, P., MURAI, J., TAKEDA, S. & D'ANDREA, A. D. (2011) Regulation of the Fanconi anemia pathway by a SUMO-like delivery network. *Genes Dev*, 25, 1847-58.
- YANG, M., HSU, C. T., TING, C. Y., LIU, L. F. & HWANG, J. (2006) Assembly of a polymeric chain of SUMO1 on human topoisomerase I in vitro. *J Biol Chem*, 281, 8264-74.
- YEAP, L. S., HAYASHI, K. & SURANI, M. A. (2009) ERG-associated protein with SET domain (ESET)-Oct4 interaction regulates pluripotency and represses the trophectoderm lineage. *Epigenetics Chromatin*, 2, 12.
- YU, Q., KUZMIAK, H., OLSEN, L., KULKARNI, A., FINK, E., ZOU, Y. & BI, X. (2010) *Saccharomyces cerevisiae* Esc2p interacts with Sir2p through a small ubiquitin-like modifier (SUMO)-binding motif and regulates transcriptionally silent chromatin in a locus-dependent manner. *J Biol Chem*, 285, 7525-36.

- YUNUS, A. A. & LIMA, C. D. (2009) Structure of the Siz/PIAS SUMO E3 ligase Siz1 and determinants required for SUMO modification of PCNA. *Mol Cell*, 35, 669-82.
- ZHAO, H., TRAGANOS, F., ALBINO, A. P. & DARZYNKIEWICZ, Z. (2008) Oxidative stress induces cell cycle-dependent Mre11 recruitment, ATM and Chk2 activation and histone H2AX phosphorylation. *Cell Cycle*, 7, 1490-5.
- ZHOU, Y. & HINGORANI, M. M. (2012) Impact of Individual Proliferating Cell Nuclear Antigen-DNA Contacts on Clamp Loading and Function on DNA. *J Biol Chem*, 287, 35370-81.
- ZOU, H. (2012) The sister bonding of duplicated chromosomes. *Semin Cell Dev Biol*, 22, 566-71.

PUBLICATIONS

Characterisation of the SUMO-Like Domains of *Schizosaccharomyces pombe* Rad60

Lara K. Boyd¹, Brenda Mercer¹, Darren Thompson², Ewan Main³, Felicity Z. Watts^{1*}

¹ Genome Damage and Stability Centre, School of Life Sciences, University of Sussex, Brighton, United Kingdom, ² Division of Biochemistry and Biomedical Sciences, School of Life Sciences, University of Sussex, Brighton, United Kingdom, ³ Division of Chemistry, School of Life Sciences, University of Sussex, Brighton, United Kingdom

Abstract

The *S. pombe* Rad60 protein is required for the repair of DNA double strand breaks, recovery from replication arrest, and is essential for cell viability. It has two SUMO-like domains (SLDs) at its C-terminus, an SXS motif and three sequences that have been proposed to be SUMO-binding motifs (SBMs). SBM1 is located in the middle of the protein, SBM2 is in SLD1 and SBM3 is at the C-terminus of SLD2. We have probed the functions of the two SUMO-like domains, SLD1 and SLD2, and the putative SBMs. SLD1 is essential for viability, while SLD2 is not. *rad60-SLD2Δ* cells are sensitive to DNA damaging agents and hydroxyurea. Neither ubiquitin nor SUMO can replace SLD1 or SLD2. Cells in which either SBM1 or SBM2 has been mutated are viable and are wild type for response to MMS and HU. In contrast mutation of SBM3 results in significant sensitivity to MMS and HU. These results indicate that the lethality resulting from deletion of SLD1 is not due to loss of SBM2, but that mutation of SBM3 produces a more severe phenotype than does deletion of SLD2. Using chemical denaturation studies, FPLC and dynamic light scattering we show this is likely due to the destabilisation of SLD2. Thus we propose that the region corresponding to the putative SBM3 forms part of the hydrophobic core of SLD2 and is not a SUMO-interacting motif. Over-expression of Hus5, which is the SUMO conjugating enzyme and known to interact with Rad60, does not rescue *rad60-SLD2Δ*, implying that as well as having a role in the sumoylation process as previously described [1], Rad60 has a Hus5-independent function.

Citation: Boyd LK, Mercer B, Thompson D, Main E, Watts FZ (2010) Characterisation of the SUMO-Like Domains of *Schizosaccharomyces pombe* Rad60. PLoS ONE 5(9): e13009. doi:10.1371/journal.pone.0013009

Editor: Anja-Katrin Bielinsky, University of Minnesota, United States of America

Received: June 29, 2010; **Accepted:** August 24, 2010; **Published:** September 27, 2010

Copyright: © 2010 Boyd et al. This is an open-access article distributed under the terms of the Creative Commons Attribution License, which permits unrestricted use, distribution, and reproduction in any medium, provided the original author and source are credited.

Funding: This work was supported by Biotechnology and Biological Sciences Research Council (BBSRC) S03/G152, <http://www.bbsrc.ac.uk/>; BBSRC BB/D526861/1; and Leverhulme Trust RFG/10839, <http://www.leverhulme.ac.uk/>. The funders had no role in study design, data collection and analysis, decision to publish, or preparation of the manuscript.

Competing Interests: The authors have declared that no competing interests exist.

* E-mail: f.z.watts@sussex.ac.uk

Introduction

SUMO is a small ubiquitin-like modifier. It is implicated in numerous cellular processes, including chromosome segregation, DNA repair and recombination, and transcriptional control e.g. [2,3,4,5,6]. More specifically, SUMO-modification of proteins affects protein-protein or protein-DNA interactions e.g. between PCNA and Srs2 in *Saccharomyces cerevisiae* [7,8] or between thymine DNA glycosylase [9] or mammalian transcription factors, such as p53, Sp3 and Elk-1 and DNA (reviewed in [6,10]). In addition, it has recently been demonstrated that SUMO-modified proteins interact with SUMO-targeted ubiquitin ligases (STUbLs) that target the modified proteins for proteasomal degradation [11,12,13].

SUMO is produced as a precursor protein and processed to the mature form to reveal a diglycine (GG) motif at the C-terminus which is used for attachment to one or more lysine residues in target proteins (reviewed in [10]). Sumoylation requires activation of the mature form of SUMO by a heterodimeric activating (E1) protein. SUMO is then passed to a SUMO conjugating (E2) protein, called Ubc9 or Hus5 in *S. pombe* [14,15]. SUMO is subsequently attached to target proteins either in a ligase-dependent or -independent manner. In *S. pombe* the SUMO ligases (E3s) are Nse2 and Pli1 [16,17].

SUMO is capable of forming both covalent and non-covalent interactions with proteins. In many instances, formation of a

covalent bond occurs via the lysine residue within the ψ K χ E consensus motif e.g. [18,19]. Non-covalent interactions occur via SUMO-interacting motifs (SIMs). The SXS motif is one of two types of SIMs, and was first identified in a peptide derived from the SUMO ligase PIASx in complex with human SUMO-1 [20]. The second type of SIM comprises [V/I]-X-[V/I]-[V/I], and is present in another SUMO ligase, RanBP2, and a variety of proteins including TTRAP and MCAF [21].

Rad60 is a founder member of the RENi (Rad60 Esc2 NIP45) family of proteins which have two SUMO-like domains (SLDs) at the C-terminus [22]. As the name suggests, other members of the RENi family include *S. cerevisiae* Esc2 and human NIP45 [22]. The *ESC2* gene was initially identified in a screen for proteins that restored silencing when tethered to a telomere [23] and more recently has been shown to have a role in genome integrity [24] and S phase repair [25,26]. NIP45 is implicated as having a function in gene regulation [27]. *S. pombe rad60* is required for response to DNA damaging agents and recovery from S phase arrest [28,29,30]. Unlike *S. cerevisiae ESC2*, *rad60* is essential for viability [28].

In addition to the SLDs, Rad60 contains an SXS motif that is thought to be a SIM [31]. It also has three hydrophobic regions that each contain a sequence conforming to the [V/I]-X-[V/I]-[V/I] SIM consensus and these have been termed putative SUMO-binding motifs (SBMs) [31].

Rad60 was originally identified in a screen for mutants defective in homologous recombination [24]. It has been proposed that control of Rad60 regulates recombination events when replication is stalled. It is delocalised from the nucleus in an HU-dependent manner on activation of Cds1, the fission yeast S phase checkpoint kinase, but becomes essential for viability on recovery from replication arrest [29]. Genetic and biochemical studies indicate that Rad60 functions with the Smc5/6 (structural maintenance of chromosomes) complex required for recombinational repair and recovery from replication fork stalling [29,32].

The *S. pombe* Smc5/6 complex comprises eight tightly associated proteins: two large proteins, Smc5 and Smc6, and six smaller, non-SMC proteins, Nse1-6 [33,34]. All of these proteins apart from Nse5 and Nse6, are essential for viability in *S. pombe*. The role of these proteins is beginning to be elucidated. Nse1 has a RING-like domain frequently associated with ubiquitin E3 ligase activity (e.g. [35]) although no ligase activity has yet been demonstrated for the protein. Nse2 is a SUMO ligase [16,36,37]. Nse4 is a kleisin that bridges the Smc5/6 heads [38]. Nse5 and Nse6 form a heterodimer that interacts with the hinge regions of Smc5 and Smc6 [39]. In response to DNA damage, components of the Smc5/6 complex are modified post-translationally by SUMO (e.g. [16,36,37]).

In order to further our understanding of the organisation and function of the Smc5/6 complex, we have undertaken a study into the function of domains and motifs in the Rad60 protein. These studies extend those of Raffa et al [31] and Prudden et al [1]. In particular we have investigated the function(s) of the SUMO-like domains (SLDs) and the three putative SUMO binding motifs (SBMs). We show that SLD1 but not SLD2 is essential for viability. Deletion of SLD2 results in sensitivity to DNA damage. We show that while the SLDs resemble SUMO, their function cannot be

replaced by SUMO. Additionally, we have analysed the role of three hydrophobic regions that have been proposed to be SBMs. Genetic and biophysical studies indicate that SBM3 is not likely to be a SUMO-interacting motif, but is part of the hydrophobic core of SLD2.

Materials and Methods

Strains and plasmids

The strains used in this work are detailed in Table 1. *rad60-SLD2Δ* (sp.1174) and *rad60-FL* (sp.1175) (created as a wild type control for *rad60-SLD2Δ*) were created by the method of Bahler et al [40]. The recombinase-mediated cassette exchange (RMCE) system described by Watson et al [41] was used for the creation of other strains. Briefly, a *rad60* haploid 'base strain' was created as follows: the *loxP* site was integrated 300bp upstream of the *rad60* coding sequence, and *ura4⁺* and the *loxM3* site were integrated immediately downstream of the *rad60* coding sequence. The base strain was checked to ensure that the *rad60* gene was still functional, and that the integration events had not disrupted the function of adjacent genes. A diploid strain heterozygous for this altered *rad60* locus was created by crossing the haploid *h⁻* base strain containing the *ade6-210* allele with a *rad⁺*, *h⁺*, *ura4-D18*, *leu1-32*, *ade6-216* strain. The base strain (either haploid or diploid as required) was then transformed with wild type and mutant versions of *rad60* flanked by *loxP* and *loxM3* loci, cloned into the *LEU2*-containing plasmid pAW8, and *LEU⁺* colonies selected. Recombination was subsequently induced by expression of the Cre recombinase following growth of cells in thiamine-free medium. Strains in which the original copy of *rad60* had been replaced were selected on medium containing 5-FOA. Other plasmids used for *S. pombe* transformation were based on pREP41 or pREP42 [42].

Table 1. Strains used in this study.

Strain	Genotype	Reference:
sp.011	<i>ade6-704, ura4-D18, leu1-32, h⁻</i>	[52]
sp.432	<i>rhp51::ura4, ade6-704, ura4-D18, leu1-32, h⁺</i>	[53]
sp.473	<i>rqh1::ura4, ade6-704, ura4-D18, leu1-32, h⁻</i>	[55]
sp.480	<i>brc1::LEU2, ade6-704, ura4-D18, leu1-32, h⁻</i>	This work
sp.714	<i>pli1::ura4, ade6-704, ura4-D18, leu1-32, h⁻</i>	[2]
sp.1123	<i>nse2-SA, ade6-704, ura4-D18, leu1-32, h⁻</i>	[16]
sp.1125	<i>smc6-X, ade6-704, ura4-D18, leu1-32, h⁺</i>	[54]
sp.1126	<i>smc6-74, ade6-704, ura4-D18, leu1-32, h⁺</i>	[46]
sp.1174	<i>rad60-SLD2Δ, ade6-704, ura4-D18, leu1-32, h⁻</i>	This work
sp.1175	<i>rad60-FL:kan, ade6-704, ura4-D18, leu1-32, h⁻</i>	This work
sp.1179	<i>rad60-1, ura4-D18, leu1-32, h⁻</i>	[28]
sp.1305	<i>rad60-SLD2Δ, nse2-SA, ade6-704, ura4-D18, leu1-32, h⁻</i>	This work
sp.1408	<i>rad60-SLD2Δ, rhp51::ura4, ade6-704, ura4-D18, leu1-32, h⁺</i>	This work
sp.1701	<i>rad60 base strain, ade6-704, leu1-32, h⁻</i>	This work
sp.1704	<i>rad60-SBM2, ade6-704, ura4-D18, leu1-32, h⁻</i>	This work
sp.1778	<i>rad60-SBM1, ade6-704, ura4-D18, leu1-32, h⁻</i>	This work
sp.1845	<i>rad60 base strain heterozygous diploid, ade6-210, ade6-216, leu1-32, h⁺/h⁻</i>	This work
sp.1925	<i>rad60-SBM3, ade6-704, ura4-D18, leu1-32, h⁻</i>	This work
sp.2026	<i>rad60-SLD2Δ-SUMO, ade6-704, ura4-D18, leu1-32, h⁻</i>	This work
sp.2027	<i>rad60-SLD2Δ-SUMO-M, ade6-704, ura4-D18, leu1-32, h⁻</i>	This work
sp.2045	<i>rad60-SBM1,SBM2, ade6-704, ura4-D18, leu1-32, h⁻</i>	This work

doi:10.1371/journal.pone.0013009.t001

pREP41-*rad60-SLD1A* was created by deleting aa 227–308, pREP41-*rad60-SLD2A* lacked aa 334–406 and pREP41-*rad60-SLD2A-SUMO* contained the coding sequence for aa 1–109 of *S. pombe* SUMO cloned in-frame with *rad60-SLD2A* in pREP41-*rad60-SLD2A*. *rad60-SLD2A-SUMO-M* was created by Quik-Change site-directed mutagenesis (Stratagene) according to the manufacturers instructions. The *hus5* gene was from A Carr (U. of Sussex) [15].

Analysis of DNA damage responses

UV irradiation was carried out on freshly plated cells using a Stratagene Stratalinker. Ionising radiation sensitivity was assayed using a ^{137}Cs source at a dose of 10 Gymin^{-1} . Sensitivities to hydroxyurea (HU) and methyl methanesulphonate (MMS) were analysed on YE agar (YEA) at the doses stated.

Microscopy

Methanol-fixed cells were stained with DAPI ($1\text{ }\mu\text{g/ml}$) and viewed using an Applied Precision Deltavision Spectris microscope with deconvolution software.

Protein purification

His-tagged proteins expressed from pET15b, were purified using Ni^{2+} agarose (Novagen) according to the manufacturer's instructions.

Equilibrium Denaturation Studies

Preparation of samples: A stock solution of guanidinium HCl (8 M) was diluted to obtain a large range of denaturant concentrations using a Hamilton Microlab dispenser; $100\text{ }\mu\text{l}$ of a stock solution of SLD2 protein ($9\text{ }\mu\text{M}$) containing 450 mM phosphate, 9 mM DTT (pH 7.0) was added to each denaturant sample ($800\text{ }\mu\text{l}$). This gave a final buffer concentration of 50 mM phosphate pH 7.0 and a protein concentration of $1\text{ }\mu\text{M}$. The protein/denaturant solutions were pre-equilibrated at 25°C for at least three hours (This was sufficient time for every solution to reach equilibrium [data not shown]).

Fluorescence measurements: All measurements were performed in a thermostatted cuvette holder at 25°C using Varian Cary Eclipse Fluorescence Spectrophotometer. The excitation wavelength was 280 nm, band passes were set at 5 nm for excitation and emission and the fluorescence was measured at the λ_{max} for the denatured state of 352 nm.

Equilibrium data analysis

Two state folding model: The entire fluorescence monitored denaturation of SLD2 was fitted to equation (1) using the non-linear regression analysis program *Kaleidagraph* (version 4.0 Synergy Software, PCS Inc.):

$$\lambda_{\text{obs}} = \frac{(\alpha_N + \beta_N[\text{D}]) + ((\alpha_D + \beta_D[\text{D}])\exp((m_{D-N}[\text{D}] - [\text{D}]_{50\%}))/RT)}{1 + \exp(m_{D-N}[\text{D}] - [\text{D}]_{50\%})/RT} \quad (1)$$

where λ_{obs} is the observed fluorescence signal, α_N and α_D are the intercepts, and β_N and β_D are the slopes of the baselines at the low (N) and high (D) denaturant concentrations, $[\text{D}]_{50\%}$ is the midpoint of unfolding, $[\text{D}]$ is the concentration of denaturant and m_{D-N} is a constant that is proportional to the increase in degree of exposure of the protein on denaturation.

Size exclusion chromatography

$250\text{ }\mu\text{l}$ of protein was loaded onto a superose 6 column (volume 24 ml) connected to an Amersham Biosciences FPLC and eluted

with 20 mM Tris HCl pH 7.9, 150 mM NaCl, 1 mM DTT. Protein elutions were monitored with an in-line UV detector and fractions collected.

Dynamic Light Scattering

$50\text{ }\mu\text{l}$ samples were analyzed at 4°C using a Malvern Instruments Nano S Dynamic Light Scattering instrument. Samples were spun at 14k rpm for 10 minutes and allowed to equilibrate at collection temperature for 2 minutes prior to data collection. Scattering data were analysed for peak position and width to identify particle size and polydispersity.

Results

Relationship of the Rad60 SLDs to ubiquitin and SUMO

Rad60 has two domains (SLD1 and SLD2) at its C-terminus (Figure 1A) that were initially reported to be ubiquitin-like [28]. However, sequence comparisons indicate that SLD2 at least, resembles SUMO more closely than ubiquitin. SLD1 has identity with *S. pombe* ubiquitin and SUMO of 18.4% and 19.7% respectively. For SLD2 the identity with ubiquitin and SUMO is 14.3% and 23.4% respectively. The similarity between SLD2 and SUMO is further demonstrated by the recent publication of the structure of *S. pombe* and human SLD2 [1,43]. Comparison of the structures of SUMO, ubiquitin and SLD2 and the predicted structure of SLD1 indicates similar overall structures (Figure S1A,B). Interestingly, the amino acids in SLD1 and SLD2 that are the same as, or similar to, amino acids in SUMO, are, in most cases, not the same in the two domains (Figure S2).

SLD1, but not SLD2 is required for the essential function of Rad60

The importance of the SLDs for Rad60 function is attested to by the fact that the majority of the mutations within three characterised *rad60-ts* mutants lie within SLD1, namely K263E (*rad60-1*) [28], F272V (*rad60-3*), and I232S and Q250R (*rad60-4*) [29] (Figure 1A) (*rad60-4* also contains two mutations outside of SLD1, T72A, and K312N) [29] (Figure 1A). This suggests that SLD1 at least, has a key role in Rad60 function. Additionally, a point mutation within SLD2 (*rad60-E380R*) [1] results in sensitivity to DNA damaging agents. In order to investigate the roles of the SLDs, we attempted to create strains containing versions of Rad60 deleted for both SLD1 and SLD2 and, separately, deleted for a single domain (either SLD1 or SLD2). Using both haploid and diploid strains (see Materials and Methods) we were unable to produce haploid strains in which Rad60 was missing either SLD1+SLD2 (aa 228–406) or missing solely SLD1 (aa 228–307). In contrast, deletion of SLD2 (aa 334–406) resulted in viable cells (*rad60-SLD2A*). Thus, consistent with the presence of the *ts* mutations in SLD1, SLD1, but not SLD2, is essential.

SLD2 is required for response to DNA damaging agents

rad60-SLD2A is slightly temperature sensitive for growth at 36°C (Figure 1B) when compared to wild-type and *rad60-FL* strains (*rad60-FL* was created in parallel with *rad60-SLD2A* as a full length Rad60 control), but less sensitive than *rad60-1*. At permissive temperatures, *rad60-SLD2A* cells are slightly elongated compared to wild-type (Figure 1C). *rad60-SLD2A* is slightly sensitive to UV (Figure 1D, Figure S3B) and ionising radiation (Figure S3B). However, it is significantly sensitive to HU, (DNA synthesis inhibitor) and MMS (alkylating agent) (Figure 1D) similar to *smc6-X*, which contains a point mutation (R706C) in the hinge region of Smc6 [44], but more sensitive than *rad60-1*. This is consistent with Rad60's reported role in recovery from HU arrest, i.e. in

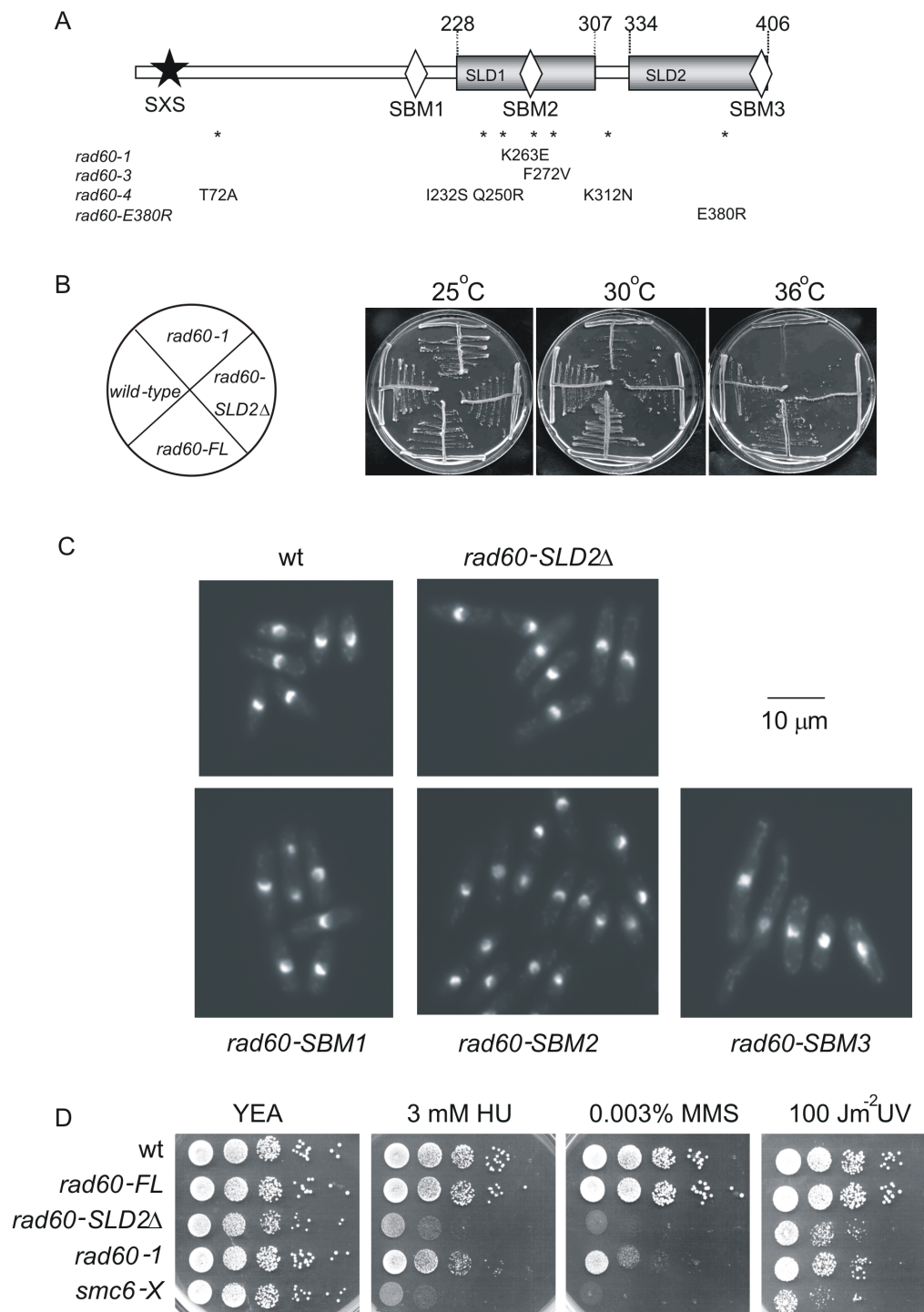


Figure 1. *rad60-SLD2Δ* is *ts* and sensitive to DNA damaging agents. A. Organisation of the Rad60 protein, indicating the position of the SXS motif (star), the putative SBMs (diamonds) and the *rad60* mutations (*). B. *rad60-SLD2Δ* is slightly temperature-sensitive for growth at 36°C. Strains were streaked onto YEA and incubated at the indicated temperatures for 5 days. C. Morphology of DAPI-stained cells. D. Spot tests to assess sensitivity to HU, MMS and UV. 10 μ l of serially diluted cells were spotted onto media as indicated. Plates were incubated at 25°C.
doi:10.1371/journal.pone.0013009.g001

processing of intermediates following exposure to DNA damaging agents or replication fork arrest by HU [30].

To determine whether *rad60-SLD2Δ* behaves differently to other *rad60* mutants we undertook epistasis analysis with *rad60-SLD2Δ* and mutants defective in the Smc5/6 complex and homologous recombination. The results are summarised in Table S1.

Consistent with the published analyses of other *rad60* mutants [1,28,29,45], *rad60-SLD2Δ* was synthetically lethal with *smc6-X*, *smc6-74* (contains a point mutation A151T, close to the ATP-binding site [46]), *brc1-d* (deleted for a 6 BRCT domain-containing protein [46]), *rgh1-d* (deleted for the *S. pombe* homologue of the RecQ helicase [47]) and *pli1-d* (deleted for the Pli1 SUMO ligase).

Additionally, it is epistatic with *nse2-SA* (contains 2 point mutations, C195S, H197A, in the SP-RING domain of the Nse2 SUMO ligase [16]) and *rhp51-d* (deleted for the Rad51 homologue) (Table S1 and Figure S3). Thus *rad60-SLD2Δ* is a hypomorphic mutant which displays a similar sensitivity to DNA damaging agents or the inhibition of replication and genetic interactions as previously described for *rad60-1*.

Neither ubiquitin nor SUMO can replace the functions of SLD1 or SLD2

The sequences and structural similarities of the SLDs with ubiquitin and SUMO prompted us to investigate whether the SLDs can be replaced by either ubiquitin or SUMO (both lacking the GG motifs and C-terminal extensions downstream of the GG motifs), or a combination of the two. Figure S4 shows the combinations that we tested. In no case were we able to obtain viable haploid cells with ubiquitin replacing SLD1 or SLD2. Additionally, we were unable to obtain strains in which SLD1 was replaced by SUMO. However, viable cells were obtained when SLD2 was replaced by SUMO (Figure S4, construct 7, *rad60-SLD2Δ-SUMO*).

To determine whether SUMO can replace the function of SLD2, *rad60-SLD2Δ-SUMO* was tested for sensitivity to HU and MMS. Figure 2 indicates that *rad60-SLD2Δ-SUMO* has similar sensitivity to HU and MMS as *rad60-SLD2Δ*. To determine why SUMO is not capable of functionally replacing SLD2, differences between the two were sought. While the overall structure of SLD2 resembles that of SUMO, a detailed comparison of the structure of SLD2 with that of SUMO identified some key differences between the two structures [1]. These are (i) that SLD2 lacks the C-terminal tail present in the mature form of SUMO, which is required for interaction with the SUMO activating E1 protein, and (ii) that SUMO has a positively charged cleft formed between β -strand 2 and α -helix 1 which interacts non-covalently with SIMs on interacting proteins. In SLD2 this is obscured by the side chains of P351, F354, R362 and E366. Thus the inability of SUMO to restore wild type function in *Rad60-SLD2Δ-SUMO* may be due to inappropriate interactions involving SUMO. We therefore introduced a series of mutations into SUMO in *rad60-SLD2Δ-SUMO* to produce *rad60-SLD2Δ-SUMO-M*. The mutant fusion protein lacks two amino acids at the C-terminus of SUMO, namely Q108 and L109 (see Figure S2B) and has four substitutions in amino acids corresponding to those in SLD2 that are proposed to be obscuring the charged cleft, namely K53P, T56F, I64R, R68E. *rad60-SLD2Δ-SUMO-M* was then integrated into the *S. pombe* genome. Figure 2 indicates that the mutations do not restore a wild type response to MMS or HU.

Intermolecular complementation is not observed with *rad60-SLD1* and *rad60-SLD2* mutants

Rad60 has been shown to form homodimers via the SLDs [31]. This raises the question as to whether the two molecules both need to contain SLD1 and SLD2. We investigated this by testing whether Rad60 function could be restored through inter-

molecular complementation by two Rad60 molecules defective in one case, in SLD1 and in the other in SLD2. Figure 3A indicates that unlike over-expression of full length Rad60, over-expression of Rad60-SLD1 Δ (lacking aa 227–308) does not complement the HU and MMS sensitive phenotypes of *rad60-SLD2Δ*.

We extended these studies to test whether Rad60-SLD2 Δ can suppress the ts and DNA damage sensitive phenotypes of *rad60-1* (which has a point mutation in SLD1, Figure 1A). As expected, over-expression of full length Rad60 complements the ts and DNA damage sensitivities of *rad60-1* (Figure 3B). In contrast, over-expression of Rad60-SLD2 Δ rescues the temperature sensitivity of *rad60-1*, but is less proficient than full length Rad60 in restoring resistance to HU and MMS, particularly at high doses. Since these responses to HU and MMS are similar to those observed when Rad60-SLD2 Δ is over-expressed in a *rad60-SLD2Δ* strain (Figure 3A), it is likely that the growth on these plates is due solely to the over-expression of Rad60-SLD2 Δ rather than to intramolecular complementation with Rad60-SLD1 Δ .

Probing the role of three putative SUMO binding motifs

It has been proposed that Rad60 contains a SIM (SUMO-interacting motif) in its N-terminus (SXS) [31]. Additionally, three hydrophobic regions within the protein which conform to the [V/I]-X-[V/I]-[V/I] SIM consensus have been identified. These have been termed putative SBMs (SUMO binding motifs), although no interactions with SUMO have been reported for them. Since these putative SBMs are either in, or close to, the SLDs (SBM2 (aa 268–271) lies within SLD1 and SBM3 (aa 401–406) comprises the last six amino acids of SLD2, Figure 1A), we were interested in their contribution to Rad60 function. If these putative SBMs are important motifs it might be expected that they would be highly conserved, at least within *Schizosaccharomyces* species. We therefore compared the sequence of *S. pombe* Rad60 with the recently elucidated Rad60 sequences from *S. japonicus*, *S. cryophilus* and *S. octosporus* (http://www.broadinstitute.org/annotation/genome/schizosaccharomyces_group) (Figure S5). Interestingly, while the SLDs are highly conserved, the regions corresponding to the proposed SBMs are not, particularly SBM1 and SBM2. For example, in *S. cryophilus* and *S. octosporus*, the region corresponding to the putative SBM1 contains Pro, while that corresponding to the putative SBM2 contains Phe. SIMs generally have adjacent acidic sequences e.g. [21]. Only in the case of the putative SBM3 is there a significant stretch of adjacent acidic amino acids, suggesting that SBM1 and 2 may not be SUMO-interacting motifs. Interestingly, the corresponding sequences in *S. cerevisiae* Esc2 are not conserved.

Rad60 and purified SLD2 do not interact with free SUMO

We next tested whether the putative SBMs interact with SUMO. Using GST-pull down assays (as described in File S1) we do not detect any interaction of full length Rad60 or SLD2 with free SUMO, under conditions where Hus5 and SUMO interact (Figure S6).

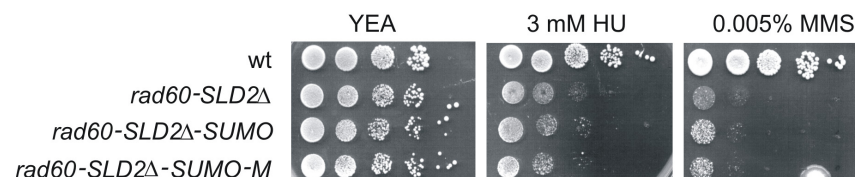


Figure 2. SUMO is unable to functionally replace SLD2. Response of strains, as indicated, to HU and MMS. Plates were incubated at 30°C. doi:10.1371/journal.pone.0013009.g002

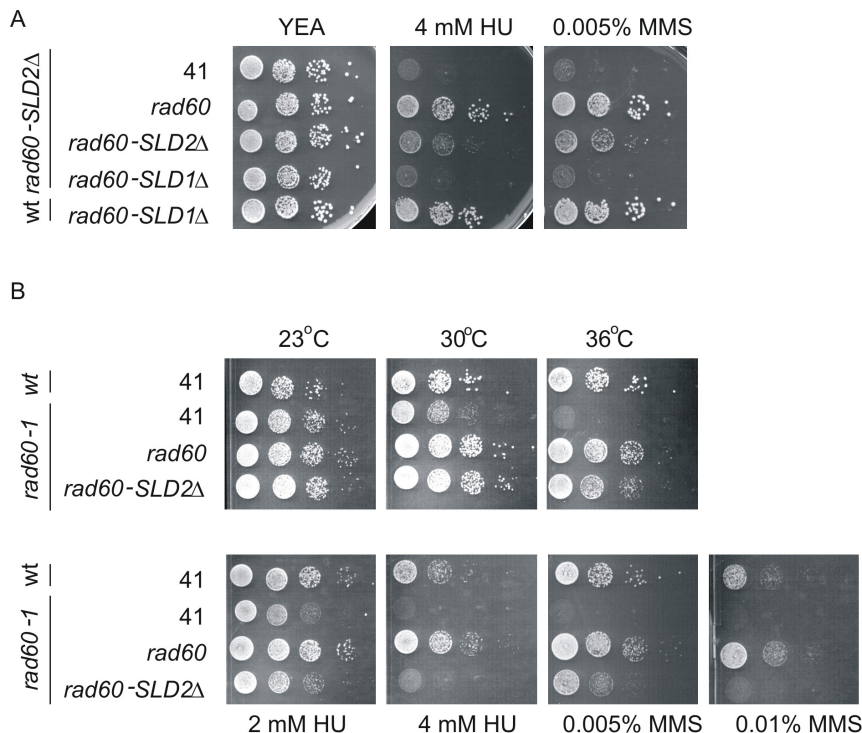


Figure 3. Testing the requirements for Rad60 dimerisation. A. wt and *rad60-SLD2Δ* strains were transformed with pREP41 (41), pREP41-*rad60* (*rad60*), pREP41-*rad60-SLD2Δ* (*rad60-SLD2Δ*) or pREP41-*rad60-SLD1Δ* (*rad60-SLD1Δ*) as indicated. Cells were plated on YEA containing HU and MMS as indicated and incubated at 30°C. B. wt or *rad60-1* cells were transformed with plasmids as indicated. Top row: cells were plated on YEA and incubated at 23°C, 30°C or 36°C as indicated. Bottom row: cells were plated on YEA containing HU or MMS at the doses stated and incubated at 25°C. doi:10.1371/journal.pone.0013009.g003

The phenotypes observed for *rad60-SLD1Δ* and *rad60-SLD2Δ* are not due to loss of the SUMO binding motifs SBM2 and SBM3

The three putative SBMs are not present in SUMO (Figure S2). Thus, a possible reason for the inability of SUMO to replace the SLDs may be their lack of SBMs. We therefore analysed the effect of mutating SBM2 and SBM3. In addition, we were interested to determine whether the phenotypes that we detect for *rad60-SLD1Δ* and *rad60-SLD2Δ* (namely lethality and sensitivity to DNA damaging agents respectively) are due to deletion of SBM2 or SBM3. We therefore mutated SBM2 (from VVLV to VALA, to produce *rad60-SBM2*), SBM3 (from VSVVLD to ASAVLD, producing *rad60-SBM3*) and in parallel, SBM1 (from ISVV to ISAA, producing *rad60-SBM1*). Mutagenesis of either SBM1 or SBM2 did not have any effect on cell viability, morphology or response to DNA damage (Figure 1C, 4A,B). Mutation of both SBM1 and SBM2 (to produce *rad60-SBM1,SBM2*) also had no effect on the response to HU, MMS or UV (Figure 4B). These results indicate that SBM1 and SBM2 do not contribute important functions to the recovery from S phase arrest or the DNA damage response, and do not function redundantly with each other.

In contrast to the results with SBM1 and SBM2 mutants, mutation of SBM3 has a severe effect on cell morphology, growth and response to DNA damaging agents (Figure 1C and 4A,B). *rad60-SBM3* cells are both heat and cold sensitive (25°C and 36°C) (Figure 4A), showing a greater sensitivity to high temperature than *rad60-SLD2Δ*. Thus, mutating SBM3 has a more severe effect on Rad60 function than deletion of the entire SLD2 domain.

Since the structure of Rad60 SLD2 has recently been determined [1] we are able to map the positions of the amino acids in SBM3 that we have mutated (Figure 5A). This shows that

they are located within the hydrophobic core of the protein and are completely buried. They are both, therefore, likely to be critical for the stability of the domain. To define the effect of these mutations on the Rad60 protein, we determined the stability of SLD2 using a chemical denaturation assay at 298K. We found this to be 6.2 kcalmol⁻¹ (Figure 5B). It has been shown that removing individual core residues generally leads to a loss of stability of at least 1 kcalmol⁻¹ per methylene group removed [48,49,50]. Thus, as the two amino acid substitutions in SBM3 each remove four methylene groups, it is likely that in the *rad60-SBM3* mutant, the SLD2 domain would be completely unfolded.

To further investigate the effect of the SBM3 mutation on the stability of SLD2, we attempted to purify SLD2-SBM3. Using our standard conditions for over-expression in *E. coli*, where the majority of wild type SLD2 is soluble, we observed that SLD2-SBM3 is predominantly in the insoluble fraction (data not shown). However, a small amount of soluble mutant protein was purified (Figure 5C). Analysis of wild type and SBM3 mutant forms of SLD2 were then analysed by size exclusion chromatography (Figure 5D). The majority of wild type SLD2 migrated as a discrete peak (V3), while most of the SBM3 mutant form of SLD2 eluted in the void volume (V1). SDS PAGE (Figure 5C) confirms that the majority of wild type SLD2 is in V3, and that the SBM3 mutant form is mainly present in high Mr fractions (V1–V2), but not in V3 as is the case with the wild type SLD2. This suggests that the SBM3 mutant form of SLD2 forms soluble aggregates. This was confirmed using dynamic light scattering (Figure 5E). The two samples clearly show peaks at different positions, the wild type giving a calculated diameter of 4 nm and the mutant a diameter of 10 nm. This suggests an increase in volume of 16 times. Thus the severe phenotype that we observe for *rad60-SBM3* is likely due to misfolding of SLD2.

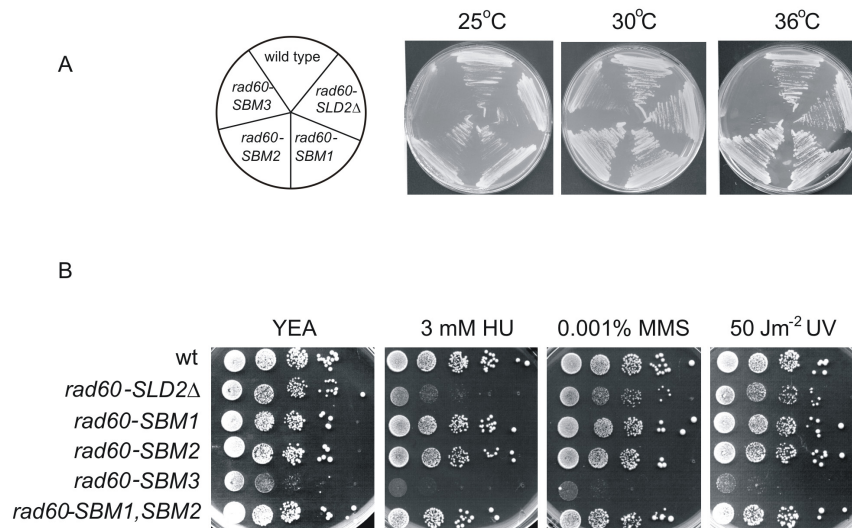


Figure 4. Effect of mutating the three putative Rad60-SBMs. A. *rad60-SBM3* is temperature sensitive. Strains were streaked onto YEA and incubated at the indicated temperatures for 5 days. B. Response of mutants to HU, MMS and UV. 5 fold more cells were plated for *rad60-SBM3* than other strains. Plates were incubated at 30°C for 5 days.
doi:10.1371/journal.pone.0013009.g004

Genetic relationship of *rad60-SLD2Δ* with components of the sumoylation system

The Rad60 SLDs interact with components of the sumoylation machinery [1]. In particular, the SLD2s of Rad60, Esc2 and Nip45 interact with the SUMO conjugating enzyme (E2), Hus5/Ubc9 [1,25,26,43]. The *hus5-62* strain is extremely slow growing and prone to accumulate suppressors, making it unreliable to use for epistasis analysis. To overcome these problems, we investigated whether over-expressing Hus5 in *rad60-SLD2Δ* could rescue the sensitivities to HU and MMS. Wild type and *rad60-SLD2Δ* cells were transformed with pREP41-Hus5 and the effect compared with over-expression of full-length Rad60 and Rad60-SLD2Δ. Wild type cells were not affected by over-expression of any versions of Rad60 or Hus5 (Figure 6A,B upper panel). As expected, over-expression of full length Rad60 reverses the HU and MMS sensitivities of *rad60-SLD2Δ* cells. However, over-expression of Hus5 does not reverse this phenotype. This supports the hypothesis that while SLD2 and Hus5 interact, SLD2 has some functions independent of the sumoylation system.

Over-expression of full length Rad60 has previously been shown to partially rescue the MMS sensitivity of *smc6-X* [28]. We next investigated whether over-expression of Rad60-SLD2Δ has any effect in *smc6-X*. We confirm that over-expression of Rad60 can reverse the sensitivity of *smc6-X* to MMS, and has a slight effect on the response to HU (Figure 6B). In contrast, over-expression of Rad60-SLD2Δ is unable to rescue these sensitivities. We next tested the effect of over-expression of Hus5. Over-expression of Hus5 either on its own, or with Rad60, has no effect on the response of *smc6-X* to HU or MMS. Additionally, over-expression of Hus5 with Rad60-SLD2Δ does not restore resistance to HU or MMS in *smc6-X*. This is consistent with the proposal that Rad60 has function(s) independent of the sumoylation system.

Discussion

In this study we have analysed the requirement for the SUMO-like domains (SLDs) and the putative SBMs for Rad60 function. We show that SLD1 is essential for cell viability under normal growth conditions, whereas SLD2 is not. Deletion of SLD2 results

in slight temperature sensitivity and sensitivity to DNA damaging agents, particularly MMS, and the DNA synthesis inhibitor, HU.

We show that despite the structural similarities with ubiquitin and SUMO, the functions of SLD1 and SLD2 cannot be provided by either ubiquitin or SUMO. Since the Rad60 SLDs interact with components of the SUMO modification machinery [1], it is perhaps not surprising that ubiquitin cannot substitute for either of the SLDs. In contrast, since the SLDs more closely resemble SUMO, the reason for the inability of SUMO to functionally replace either or both SLDs in Rad60 is less clear, particularly since a single copy of SUMO can functionally replace the two SLDs in *S. cerevisiae* Esc2 [24].

We tested whether the inability of SUMO to replace SLD2 is due to inappropriate interactions involving SUMO, by removing two amino acids (Q108, L109) from the C-terminus that are required for interaction of SUMO with the E1, and then mutated four amino acids in the region required for interaction with SUMO-interacting motifs (SIMs). Mutation of these regions in SUMO in *rad60-SLD2Δ-SUMO-M* did not restore wild type function to the hybrid molecule and thus imply a specific role for SLD2 not undertaken by SUMO.

Two possible explanations for the ability of SUMO to replace SLD2 in Esc2 but not in Rad60 are that either, the similarity between *S. cerevisiae* SUMO and Esc2 SLD2 is greater than that between *S. pombe* SUMO and Rad60 SLD2, or that Esc2 and Rad60 have somewhat different roles in cells, such that SUMO can replace the SLDs in Esc2, but not in Rad60. Pair wise sequence comparisons do not indicate gross differences in similarities between the SLDs and the respective SUMO sequences (Esc2 SLD2 and SUMO are 17.6% identical and 40% similar, while Rad60 SLD2 and SUMO are 20% identical and 36.9% similar). This suggests that sequence similarity may not account for the ability of SUMO to replace the Esc2 SLDs, although it is possible that certain key epitopes in Esc2 SLD2 may be present in *S. cerevisiae* SUMO, while the same may not be true for Rad60 SLD2 and *S. pombe* SUMO. Alternatively, and our preferred hypothesis, the difference may be related to the different functions of Esc2 and Rad60 in cells. Rad60 is essential for cell viability, while Esc2 is not. Additionally, an *esc2* null mutant is

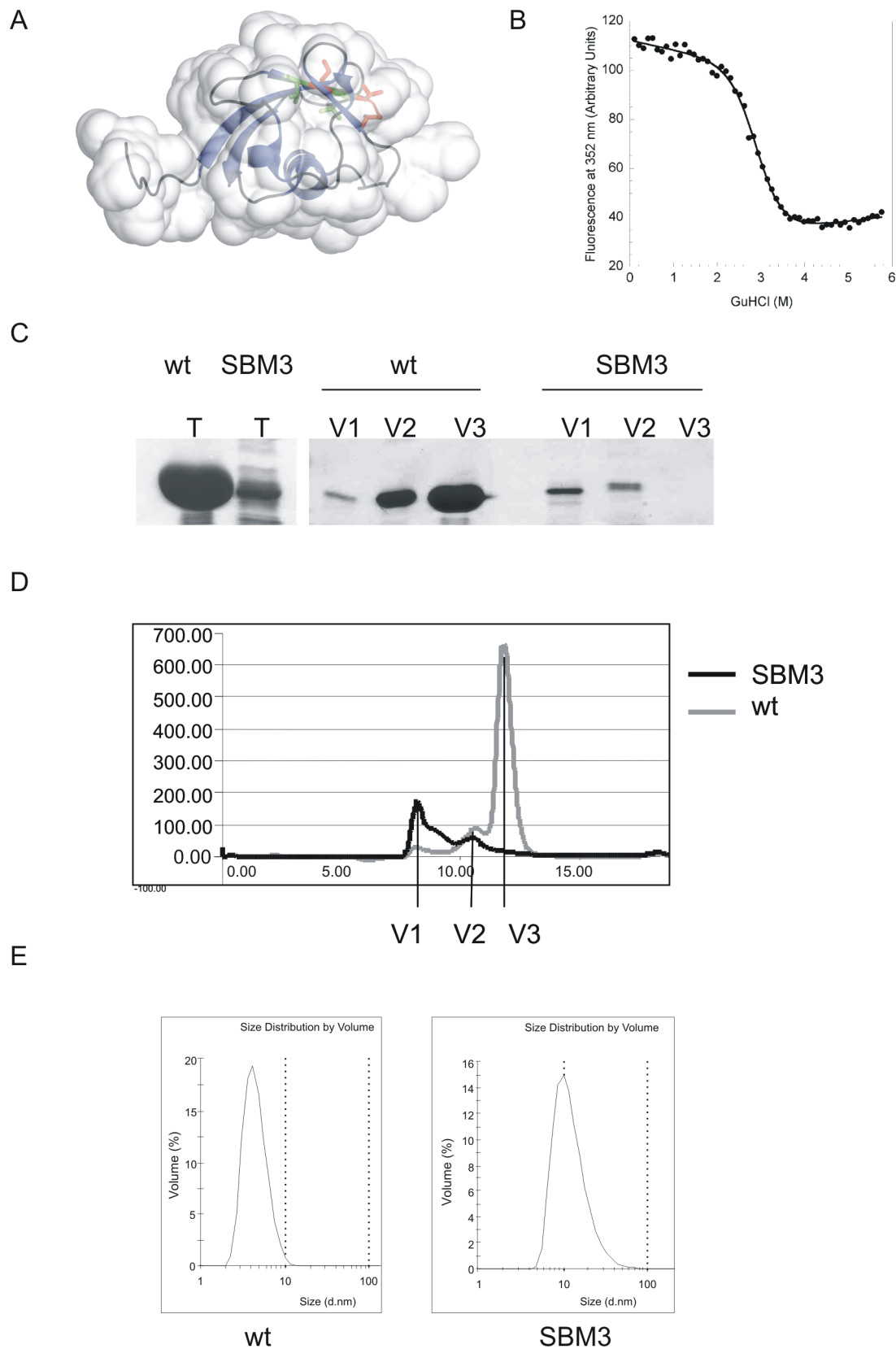


Figure 5. Mutation of SBM3 affects SLD2 structure. A. Position of SBM3 in crystal structure of SLD2 = red and green [1]. SBM3 point mutations created in this study are in green. B. Thermal stability of SLD2. C. SDS PAGE. T = SLD2 protein purified from Ni^{+2} agarose. In both cases (wt and SBM3), 8 μl of 500 μl eluate was loaded onto gel. V1–V3 8 μl of the FPLC fractions indicated in D, was loaded in each case. D. FPLC trace of wt SLD2 and SLD2-SBM3 mutant on Superose 6. SBM3 shows an elution peak after 7 ml whereas the wild type shows elution peaks at 11 ml and 12 ml). E.

Dynamic Light Scattering spectra showing solution sizes of wild type and SBM3. The wild type shows a peak indicating a size of diameter 4 nm whereas SBM3 shows a peak indicating a size of diameter of 10 nm.
doi:10.1371/journal.pone.0013009.g005

sensitive to MMS but not to HU, UV or IR, unlike *rad60* mutants. It has therefore been proposed that Esc2 probably acts to prevent, or process only limited types of DNA damage, unlike the case with Rad60 [26]. This suggests that Rad60 may be involved in a more complex set of molecular interactions than is Esc2. Despite the likely similarity in structure, the two SLDs in Rad60 have been demonstrated to be involved in distinctly different interactions with components of the sumoylation pathway [1]. This may account for the fact that Rad60 needs to contain two SLDs neither of which can be replaced by SUMO,

Raffa et al [31] demonstrated that Rad60 homodimerises via the SLDs. We observe using FPLC and GST-pulldowns (data not shown) that SLD2 does not interact with itself. This suggests that homodimerisation occurs either between two SLD1s or between SLD1 and SLD2. We tested this latter possibility by investigating whether intermolecular complementation occurred between two mutant Rad60 proteins defective in one case in SLD1 and in the other in SLD2. No intermolecular complementation was observed. This suggest two possibilities. The first is that homodimerisation occurs between two SLD1s. As SLD1 protein is not very soluble we have been unable to test this. The second possibility is, that since our assay is for Rad60 function and not specifically for homodimerisation, that a Rad60 function unrelated to homo-

dimerisation, e. g. involving intramolecular folding, requires that both SLD1 and SLD2 need to be present in the same molecule. This issue will be resolved with the elucidation of the crystal structure of the full-length Rad60 protein.

Raffa et al [31] proposed that three hydrophobic regions in Rad60 were putative SUMO binding motifs (SBMs), and that SBM3 is required for homodimerisation. We have tested the requirement for these putative SBMs *in vivo*. Mutation of SBM1 and SBM2 has no effect on cell viability or DNA damage responses. Since mutation of SBM2 results in viable cells, removal of this SBM likely does not account for the loss of viability observed in *rad60-SLD1Δ* cells, and the inability of SUMO to substitute for SLD1. Since some proteins (e.g. STUbLs) contain more than one SIM (e.g. [51]) we tested the effect of mutating both SBM1 and SBM2. Since the *rad60-SBM1,SBM2* double mutant grows as wild type and is not sensitive to HU or MMS, we conclude that SBM1 and SBM2 do not function redundantly. In contrast to the results with the SBM1 and SBM2 mutants, we see a striking effect when we mutate two residues in SBM3. From the published structure of SLD2 and our results from chemical denaturation studies we propose that the mutations would drastically affect the stability of SLD2, with the likely result that the domain would not be correctly folded. This is also likely to be

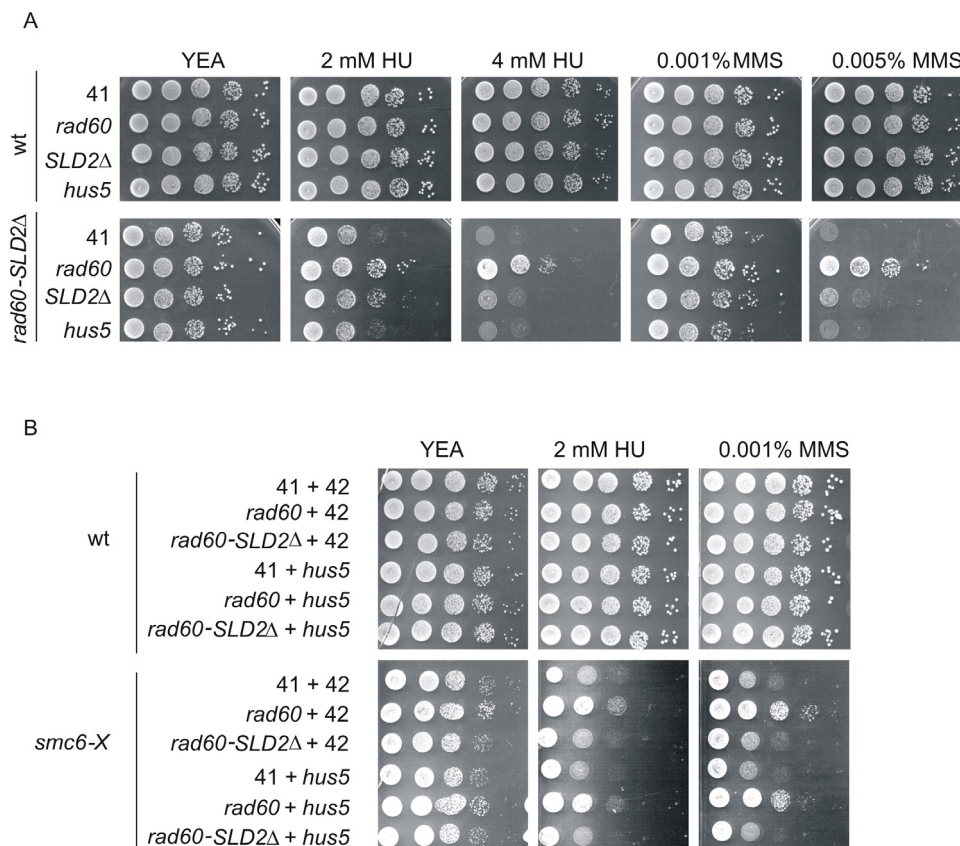


Figure 6. Relationship of *Rad60-SLD2Δ* to *Hus5*. A. wt and *rad60-SLD2Δ* cells were transformed with pREP41 (41), pREP41-*rad60* (*rad60*) or pREP41-*rad60-SLD2Δ* (*SLD2Δ*) or pREP41-*Hus5* (*hus5*) as indicated. Cells were plated on YEA with supplements at 30°C. B. wt and *smc6-X* cells were transformed with combinations of pREP41 (41), pREP42 (42), pREP41-*rad60* (*rad60*), pREP41-*rad60-SLD2Δ* (*SLD2Δ*), pREP42-*hus5* (*hus5*) as indicated.
doi:10.1371/journal.pone.0013009.g006

the case in [31], where 6 aa (comprising an entire β -sheet) were deleted from the C-terminus of Rad60.

Since SLD2 interacts with Ubc9/Hus5 [1,25,26], it has been proposed that Rad60 may recruit SUMO-charged Ubc9 to mediate sumoylation of specific proteins, or that it may sequester Ubc9 in an inactive complex to down-regulate sumoylation [1]. We observe that over-expression of Hus5 does not rescue the phenotypes of *rad60-SLD2A*. Thus, SLD2 likely has a function, in addition to its role in sumoylation, that is independent of Hus5. This conclusion is supported by the fact that, while over-expression of full length Rad60 suppresses the HU and MMS sensitivity of *smc6-X*, co-over-expression of Hus5 and Rad60-SLD2A in *smc6-X* does not. This suggests that Rad60 function is not simply to recruit the SUMO conjugating enzyme Hus5 to the Smc5/6 complex and into close proximity with the Nse2 SUMO ligase subunit. The viability and mild DNA damage sensitivities of the SUMO ligase dead *nse2-SA* mutant [16] is further support for both Smc5/6 and Rad60 having functions independent of the sumoylation system.

In conclusion, we have demonstrated that SLD1 but not SLD2 is required for the essential function of Rad60, and that neither can be replaced by ubiquitin or SUMO. Mutational analysis indicates that the inability of SUMO to functionally replace SLD2 is not due to the slightly extended C-terminus or the presence of the SIM-interacting region. *rad60-SLD2A* is sensitive to HU and MMS. Mutation of the SBMs indicates that neither SBM1 nor SBM2 is required for the DNA damage response. Since mutation of SBM3, which is present in the hydrophobic core of SLD2, destabilises SLD2, we conclude that SBM3 does not interact with SUMO, but is required for maintaining SLD2 structure. Our over-expression studies indicate that although SLD2 interacts with the SUMO conjugating enzyme Hus5/Ubc9, Rad60 also has a Hus5/sumoylation-independent role.

Supporting Information

File S1 Supplementary materials and methods.

Found at: doi:10.1371/journal.pone.0013009.s001 (0.03 MB DOC)

Table S1 Epistasis analysis of *rad60-SLD2A-S*. E = epistatic.

Found at: doi:10.1371/journal.pone.0013009.s002 (0.03 MB DOC)

Figure S1 Comparison of actual structures of ubiquitin, SUMO, Rad60-SLD2 and the predicted structure of Rad60-SLD1.

References

- Prudden J, Perry JJ, Arvai AS, Tainer JA, Boddy MN (2009) Molecular mimicry of SUMO promotes DNA repair. *Nat Struct Mol Biol* 16: 509–516.
- Watts FZ (2007) The role of SUMO in chromosome segregation. *Chromosoma* 116: 15–20.
- Hoegel C, Pfander B, Moldovan GL, Pyrowolakis G, Jentsch S (2002) RAD6-dependent DNA repair is linked to modification of PCNA by ubiquitin and SUMO. *Nature* 419: 135–141.
- Stelter P, Ulrich HD (2003) Control of spontaneous and damage-induced mutagenesis by SUMO and ubiquitin conjugation. *Nature* 425: 188–191.
- Sacher M, Pfander B, Hoegel C, Jentsch S (2006) Control of Rad52 recombination activity by double-strand break-induced SUMO modification. *Nat Cell Biol* 8: 1284–1290.
- Gill G (2005) Something about SUMO inhibits transcription. *Curr Opin Genet Dev* 15: 536–541.
- Pfander B, Moldovan GL, Sacher M, Hoegel C, Jentsch S (2005) SUMO-modified PCNA recruits Srs2 to prevent recombination during S phase. *Nature* 436: 428–433.
- Papouli E, Chen S, Davies AA, Huttner D, Krejci L, et al. (2005) Crosstalk between SUMO and ubiquitin on PCNA is mediated by recruitment of the helicase Srs2p. *Mol Cell Biol* 25: 123–133.
- Hardeland U, Steinacher R, Jiricny J, Schar P (2002) Modification of the human thymine-DNA glycosylase by ubiquitin-like proteins facilitates enzymatic turnover. *Embo J* 21: 1456–1464.
- Hay RT (2005) SUMO: a history of modification. *Mol Cell Biol* 25: 1–12.
- Prudden J, Pebernard S, Raffa G, Slavin DA, Perry JJ, et al. (2007) SUMO-targeted ubiquitin ligases in genome stability. *Embo J* 26: 4089–4101.
- Xie Y, Kerscher O, Kroetz MB, McConchie HF, Sung P, et al. (2007) The yeast Hex3.Slx8 heterodimer is a ubiquitin ligase stimulated by substrate sumoylation. *J Biol Chem* 282: 34176–34184.
- Tatham MH, Geoffroy MC, Shen L, Plechanovova A, Hattersley N, et al. (2008) RNF4 is a poly-SUMO-specific E3 ubiquitin ligase required for arsenic-induced PML degradation. *Nat Cell Biol* 10: 538–546.
- Johnson ES, Blobel G (1997) Ubc9p is the conjugating enzyme for the ubiquitin-like protein Smt3p. *J Biol Chem* 272: 26799–26802.
- al-Khodairy F, Enoch T, Hagan IM, Carr AM (1995) The Schizosaccharomyces pombe hus5 gene encodes a ubiquitin conjugating enzyme required for normal mitosis. *J Cell Sci* 108: 475–486.
- Andrews EA, Palecek J, Sergeant J, Taylor E, Lehmann AR, et al. (2005) Nse2, a component of the Smc5-6 complex, is a SUMO ligase required for the response to DNA damage. *Mol Cell Biol* 25: 185–196.

Human ubiquitin (ubiquitin): 1ubq, human SUMO-1 (SUMO): 2asq, Rad60-SLD2 (SLD2): 3GOE. The models were aligned using the least-squares fit program for the whole polypeptide. A. Position of α -helices and β -sheets. B. Surface charge, red negative, blue positive.

Found at: doi:10.1371/journal.pone.0013009.s003 (1.85 MB TIF)

Figure S2 Alignment of Rad60-SLD1 and -SLD2 with SUMO and each other. Hs = human, Sp = *S. pombe*. # = positions of putative SBMs in SLD1 and SLD2. * = amino acids conserved between SLDs but not with SUMO. \$ = aa removed in Rad60-SLD2A-SUMO-M, ~ = aa mutated in Rad60-SLD2A-SUMO-M. Found at: doi:10.1371/journal.pone.0013009.s004 (0.03 MB DOC)

Figure S3 Response of *rad60-SLD2A* to DNA damaging agents. A. and B. Epistasis analysis with *nse2-SA* and *rhp51-d*. A. Spot tests. B. Survival curves. Experiments were done in triplicate. Averages and standard deviations plotted.

Found at: doi:10.1371/journal.pone.0013009.s005 (1.51 MB TIF)

Figure S4 Scheme indicating ubiquitin and SUMO replacement constructs. Constructs were created in pAW8 (37) and used to transform haploid and diploid *rad60* base strains. Star = SXS motif, diamond = putative SBM.

Found at: doi:10.1371/journal.pone.0013009.s006 (0.47 MB TIF)

Figure S5 Alignment of Rad60 sequences. Scry = *S. cryophilus*, Soct = *S. octosporos*, Spom = *S. pombe*, Sjap = *S. japonicus*, Scer = *S. cerevisiae*. # = putative SBMs.

Found at: doi:10.1371/journal.pone.0013009.s007 (0.03 MB DOC)

Figure S6 Rad60 and SLD2 do not interact with free SUMO GST pulldown assays. A. GST-Rad60 + His-SUMO. B. GST-Rad60-SLD2 + His-SUMO, GST-Hus5 + His-SUMO. G = GST, S = SUMO, I = input, U = unbound, B = bound.

Found at: doi:10.1371/journal.pone.0013009.s008 (1.09 MB TIF)

Acknowledgments

We thank Jo Murray, Tony Carr and Alan Lehmann for helpful discussions.

Author Contributions

Conceived and designed the experiments: DT EM FZW. Performed the experiments: LKB BM. Analyzed the data: LKB.

17. Xhemalce B, Seeler JS, Thon G, Dejean A, Arcangeli B (2004) Role of the fission yeast SUMO E3 ligase Plp1p in centromere and telomere maintenance. *Embo J* 23: 3844–3853.
18. Johnson ES, Blobel G (1999) Cell cycle-regulated attachment of the ubiquitin-related protein SUMO to the yeast septins. *J Cell Biol* 147: 981–994.
19. Seeler JS, Marchio A, Losson R, Desterro JM, Hay RT, et al. (2001) Common properties of nuclear body protein sp100 and ttf1alpha chromatin factor: role of sumo modification. *Mol Cell Biol* 21: 3314–3324.
20. Minty A, Dumont X, Kaghad M, Caput D (2000) Covalent modification of p73alpha by SUMO-1. Two-hybrid screening with p73 identifies novel SUMO-1-interacting proteins and a SUMO-1 interaction motif. *J Biol Chem* 275: 36316–36323.
21. Hecker CM, Rabiller M, Haglund K, Bayer P, Dikic I (2006) Specification of SUMO1- and SUMO2-interacting motifs. *J Biol Chem* 281: 16117–16127.
22. Novatchkova M, Bachmair A, Eisenhaber B, Eisenhaber F (2005) Proteins with two SUMO-like domains in chromatin-associated complexes: the RENi (Rad60-Esc2-NIP45) family. *BMC Bioinformatics* 6: 22.
23. Cuperus G, Shore D (2002) Restoration of silencing in *Saccharomyces cerevisiae* by tethering of a novel Sir2-interacting protein, Esc8. *Genetics* 162: 633–645.
24. Ohya T, Arai H, Kubota Y, Shinagawa H, Hishida T (2008) A SUMO-like domain protein, Esc2, is required for genome integrity and sister chromatid cohesion in *Saccharomyces cerevisiae*. *Genetics* 180: 41–50.
25. Sollier J, Driscoll R, Castellucci F, Foiani M, Jackson SP, et al. (2009) The *Saccharomyces cerevisiae* Esc2 and Smc5-6 proteins promote sister chromatid junction-mediated intra-S repair. *Mol Biol Cell* 20: 1671–1682.
26. Mankouri HW, Ngo HP, Hickson ID (2009) Esc2 and Sgs1 act in functionally distinct branches of the homologous recombination repair pathway in *Saccharomyces cerevisiae*. *Mol Biol Cell* 20: 1683–1694.
27. Hodge MR, Chun HJ, Rengarajan J, Alt A, Lieberman R, et al. (1996) NF-AT-Driven interleukin-4 transcription potentiated by NIP45. *Science* 274: 1903–1905.
28. Morishita T, Tsutsui Y, Iwasaki H, Shinagawa H (2002) The *Schizosaccharomyces pombe* rad60 gene is essential for repairing double-strand DNA breaks spontaneously occurring during replication and induced by DNA-damaging agents. *Mol Cell Biol* 22: 3537–3548.
29. Boddy MN, Shanahan P, McDonald WH, Lopez-Girona A, Noguchi E, et al. (2003) Replication checkpoint kinase Cds1 regulates recombinational repair protein Rad60. *Mol Cell Biol* 23: 5939–5946.
30. Miyabe I, Morishita T, Hishida T, Yonei S, Shinagawa H (2006) Rhp51-dependent recombination intermediates that do not generate checkpoint signal are accumulated in *Schizosaccharomyces pombe* rad60 and smc5/6 mutants after release from replication arrest. *Mol Cell Biol* 26: 343–353.
31. Raffa GD, Wohlschlegel J, Yates JR, 3rd, Boddy MN (2006) SUMO-binding motifs mediate the Rad60-dependent response to replicative stress and self-association. *J Biol Chem* 281: 27973–27981.
32. Murray JM, Carr AM (2008) Smc5/6: a link between DNA repair and unidirectional replication? *Nat Rev Mol Cell Biol* 9: 177–182.
33. Sergeant J, Taylor E, Palecek J, Foustier M, Andrews EA, et al. (2005) Composition and architecture of the *Schizosaccharomyces pombe* Rad18 (Smc5-6) complex. *Mol Cell Biol* 25: 172–184.
34. Pebernard S, Wohlschlegel J, McDonald WH, Yates JR, 3rd, Boddy MN (2006) The Nse5-Nse6 dimer mediates DNA repair roles of the Smc5-Smc6 complex. *Mol Cell Biol* 26: 1617–1630.
35. Pebernard S, Perry JJ, Tainer JA, Boddy MN (2008) Nse1 RING-like domain supports functions of the Smc5-Smc6 holocomplex in genome stability. *Mol Biol Cell* 19: 4099–4109.
36. Potts PR, Yu H (2005) Human MMS21/NSE2 is a SUMO ligase required for DNA repair. *Mol Cell Biol* 25: 7021–7032.
37. Zhao X, Blobel G (2005) A SUMO ligase is part of a nuclear multiprotein complex that affects DNA repair and chromosomal organization. *Proc Natl Acad Sci U S A* 102: 4777–4782.
38. Palecek J, Vidot S, Feng M, Doherty AJ, Lehmann AR (2006) The Smc5-Smc6 DNA repair complex: bridging of the Smc5-Smc6 heads by the KLEISIN, Nse4, and non-Kleisin subunits. *J Biol Chem* 281: 36952–36959.
39. Duan X, Yang Y, Chen YH, Arenz J, Rangi GK, et al. (2009) Architecture of the Smc5/6 Complex of *Saccharomyces cerevisiae* Reveals a Unique Interaction between the Nse5-6 Subcomplex and the Hinge Regions of Smc5 and Smc6. *J Biol Chem* 284: 8507–8515.
40. Bahler J, Wu JQ, Longtine MS, Shah NG, McKenzie A, 3rd, et al. (1998) Heterologous modules for efficient and versatile PCR-based gene targeting in *Schizosaccharomyces pombe*. *Yeast* 14: 943–951.
41. Watson AT, Garcia V, Bone N, Carr AM, Armstrong J (2008) Gene tagging and gene replacement using recombinase-mediated cassette exchange in *Schizosaccharomyces pombe*. *Gene* 407: 63–74.
42. Basi G, Schmid E, Maundrell K (1993) TATA box mutations in the *Schizosaccharomyces pombe* nmt1 promoter affect transcription efficiency but not the transcription start point or thiamine repressibility. *Gene* 123: 131–136.
43. Sekiyama N, Arita K, Ikeda Y, Hashiguchi K, Ariyoshi M, et al. Structural basis for regulation of poly-SUMO chain by a SUMO-like domain of Nip45. *Proteins* 78: 1491–1502.
44. Foustier MI, Lehmann AR (2000) A novel SMC protein complex in *Schizosaccharomyces pombe* contains the Rad18 DNA repair protein. *Embo J* 19: 1691–1702.
45. Morikawa H, Morishita T, Kawane S, Iwasaki H, Carr AM, et al. (2004) Rad62 protein functionally and physically associates with the smc5/smc6 protein complex and is required for chromosome integrity and recombination repair in fission yeast. *Mol Cell Biol* 24: 9401–9413.
46. Verkade HM, Bugg SJ, Lindsay HD, Carr AM, O'Connell MJ (1999) Rad18 is required for DNA repair and checkpoint responses in fission yeast. *Mol Biol Cell* 10: 2905–2918.
47. Laursen LV, Ampatzidou E, Andersen AH, Murray JM (2003) Role for the fission yeast RecQ helicase in DNA repair in G2. *Mol Cell Biol* 23: 3692–3705.
48. Serrano L, Kellis JT, Jr., Cann P, Matouschek A, Fersht AR (1992) The folding of an enzyme. II. Substructure of barnase and the contribution of different interactions to protein stability. *J Mol Biol* 224: 783–804.
49. Main ER, Fulton KF, Jackson SE (1998) Context-dependent nature of destabilizing mutations on the stability of FKBP12. *Biochemistry* 37: 6145–6153.
50. Jackson SE, Moracci M, eMasry N, Johnson CM, Fersht AR (1993) Effect of cavity-creating mutations in the hydrophobic core of chymotrypsin inhibitor 2. *Biochemistry* 32: 11259–11269.
51. Perry JJ, Tainer JA, Boddy MN (2008) A SIM-ultaneous role for SUMO and ubiquitin. *Trends Biochem Sci* 33: 201–208.
52. Murray JM, Carr AM, Lehmann AR, Watts FZ (1991) Cloning and characterisation of the rad9 DNA repair gene from *Schizosaccharomyces pombe*. *Nucleic Acids Res* 19: 3525–3531.
53. Muris DF, Vreeken K, Carr AM, Broughton BC, Lehmann AR, et al. (1993) Cloning the RAD51 homologue of *Schizosaccharomyces pombe*. *Nucleic Acids Res* 21: 4586–4591.
54. Lehmann AR, Walicka M, Griffiths DJ, Murray JM, Watts FZ, et al. (1995) The rad18 gene of *Schizosaccharomyces pombe* defines a new subgroup of the SMC superfamily involved in DNA repair. *Mol Cell Biol* 15: 7067–7080.
55. Murray JM, Lindsay HD, Munday CA, Carr AM (1997) Role of *Schizosaccharomyces pombe* RecQ homolog, recombination, and checkpoint genes in UV damage tolerance. *Mol Cell Biol* 17: 6868–6875.

SUMO Chain Formation Is Required for Response to Replication Arrest in *S. pombe*

Andrew Skilton, Jenny C. Y. Ho[‡], Brenda Mercer, Emily Outwin, Felicity Z. Watts*

Genome Damage and Stability Centre, University of Sussex, Falmer, Brighton, United Kingdom

Abstract

SUMO is a ubiquitin-like protein that is post-translationally attached to one or more lysine residues on target proteins. Despite having only 18% sequence identity with ubiquitin, SUMO contains the conserved $\beta\beta\alpha\beta\beta\alpha\beta$ fold present in ubiquitin. However, SUMO differs from ubiquitin in having an extended N-terminus. In *S. pombe* the N-terminus of SUMO/Pmt3 is significantly longer than those of SUMO in *S. cerevisiae*, human and *Drosophila*. Here we investigate the role of this N-terminal region. We have used two dimensional gel electrophoresis to demonstrate that *S. pombe* SUMO/Pmt3 is phosphorylated, and that this occurs on serine residues at the extreme N-terminus of the protein. Mutation of these residues (in *pmt3-1*) results in a dramatic reduction in both the levels of high Mr SUMO-containing species and of total SUMO/Pmt3, indicating that phosphorylation of SUMO/Pmt3 is required for its stability. Despite the significant reduction in high Mr SUMO-containing species, *pmt3-1* cells do not display an aberrant cell morphology or sensitivity to genotoxins or stress. Additionally, we demonstrate that two lysine residues in the N-terminus of *S. pombe* SUMO/Pmt3 (K14 and K30) can act as acceptor sites for SUMO chain formation *in vitro*. Inability to form SUMO chains results in aberrant cell and nuclear morphologies, including stretched and fragmented chromatin. SUMO chain mutants are sensitive to the DNA synthesis inhibitor, hydroxyurea (HU), but not to other genotoxins, such as UV, MMS or CPT. This implies a role for SUMO chains in the response to replication arrest in *S. pombe*.

Citation: Skilton A, Ho JCY, Mercer B, Outwin E, Watts FZ (2009) SUMO Chain Formation Is Required for Response to Replication Arrest in *S. pombe*. PLoS ONE 4(8): e6750. doi:10.1371/journal.pone.0006750

Editor: Gustavo Goldman, Universidade de Sao Paulo, Brazil

Received: April 4, 2009; **Accepted:** July 15, 2009; **Published:** August 25, 2009

Copyright: © 2009 Skilton et al. This is an open-access article distributed under the terms of the Creative Commons Attribution License, which permits unrestricted use, distribution, and reproduction in any medium, provided the original author and source are credited.

Funding: AS was funded by an MRC studentship (G122/18), EO and BM by BBSRC studentships (G/07462 and BD/D526861/1) and JH by a BBSRC project grant (85/C15586). BBSRC <http://www.bbsrc.ac.uk/>, MRC <http://www.mrc.ac.uk/> The funders had no role in study design, data collection and analysis, decision to publish, or preparation of the manuscript.

Competing Interests: The authors have declared that no competing interests exist.

* E-mail: f.z.watts@sussex.ac.uk

[‡] Current address: Department of Medicine, Faculty of Medicine, University of Hong Kong, Pokfulam, Hong Kong, China

Introduction

Post-translational modification is an efficient and rapid way of controlling the activity of proteins. A variety of species have been identified that can be attached post-translationally to proteins. In many cases, modification involves small species, e.g. in the phosphorylation, acetylation and methylation of proteins, while in others the modifying species are larger, e.g. in the case of ubiquitination and sumoylation, which involve the proteins ubiquitin and SUMO respectively e.g. [1,2].

SUMO is a member of the Ubl (ubiquitin-like) family of post-translational modifiers. Although it has only 18% sequence identity with ubiquitin, its structure resembles that of ubiquitin, in that it contains the conserved ubiquitin $\beta\beta\alpha\beta\beta\alpha\beta$ fold [3,4]. Ubiquitin comprises 76 aa, while SUMO is larger, having an extended N-terminus (in the order of 15–30 aa) that is not present in ubiquitin. The major role of ubiquitin is in targeting proteins for proteasome-mediated proteolysis (reviewed in [5]). However, ubiquitin also has important roles in modifying the function of individual proteins required for specific processes, e.g. ubiquitination of PCNA (proliferating cell nuclear antigen) is required for bypass of replication blocking lesions in DNA [6,7,8]. SUMO modification has a variety of cellular functions, including roles in transcription, DNA damage responses, the cell cycle and nuclear transport e.g. [9,10,11]. Recently it has been shown to be required

for STUbL- (SUMO-targeted ubiquitin ligase)-dependent ubiquitination of target proteins e.g. [12,13,14].

The process of sumoylation resembles that of ubiquitination (reviewed in [15]). Like ubiquitin, SUMO is produced as a precursor protein that needs to be cleaved to the mature form by one or more specific SUMO proteases (Ulp). This processing reveals a GG motif at the C-terminus of SUMO, which is required for its subsequent activation and conjugation to target proteins. Mature SUMO is first activated by a heterodimeric activator protein via the formation of a thioester linkage. It is then transferred to a SUMO conjugator, again forming a thioester link. From here, SUMO is attached to one or more lysine residues on the target protein via an ϵ -amino bond. In many cases, the acceptor lysine is present within the context $\psi Kx\epsilon$, where ψ is a bulky hydrophobic amino acid and x is any residue. In some instances attachment of SUMO to target proteins is enhanced by one of relatively few SUMO ligases.

It is well documented that ubiquitin forms chains (e.g. [16]). This can occur through a number of lysine residues within ubiquitin, predominantly K6, K29, K48 and K63. Initial reports on SUMO modification suggested that, unlike ubiquitin, SUMO did not form chains. However, several findings have established that SUMO is capable of forming chains, both *in vitro* and *in vivo* [17,18,19,20]. Despite evidence for their existence *in vivo*, the biological role of SUMO chains is less obvious. An *S. cerevisiae*

mutant (*smt3-allR*) in which all potential SUMO acceptor lysines have been mutated to alanine, shows little phenotype during vegetative growth [20]. More recently it has been demonstrated that SUMO chains can interact with STUbLs (via SIMs – SUMO-interacting motifs) [21], implying that they can act as a signal to target proteins for ubiquitin-mediated proteolysis.

The process of sumoylation is generally conserved between eukaryotic organisms. In *S. pombe*, SUMO is encoded by the *pmt3* gene [22]. The ubiquitin-like region of *S. pombe* SUMO/Pmt3 resembles SUMO in other organisms. However its N-terminus is distinctly longer than those in *S. cerevisiae* SUMO/Smt3 or in human SUMO-1/-2/-3 (Figure S1). While SUMO is essential for viability in *S. cerevisiae* and mammals, deletion of the *pmt3* gene is not lethal, although null mutant cells are temperature sensitive for growth and extremely sensitive to a range of toxins [22]. Mutants defective in the *S. pombe* SUMO activator subunit (Rad31), the SUMO conjugator (Hus5) or one of the SUMO ligases, Nse2, are sensitive to DNA damaging agents [23,24,25,26]. In contrast, a null mutant deleted for the *S. pombe* SUMO ligase Pli1 has little phenotype, apart from a mild sensitivity to the microtubule inhibitor thiabendazole (TBZ) [27].

Here we investigate sequence requirements for SUMO/Pmt3 function in *S. pombe*. We show that SUMO/Pmt3 is phosphorylated on serine residues at its extreme N-terminus and that inability to phosphorylate SUMO/Pmt3 results in reduced levels of total SUMO/Pmt3 and reduced levels of high Mr SUMO-containing species *in vivo*. Additionally, we demonstrate that two lysines (K14 and K30) are required for SUMO chain formation, both *in vitro* and *in vivo*. A *pmt3-K14R,K30R* mutant shows cellular abnormalities and sensitivity to HU, indicating that SUMO chain formation is necessary for response to S phase arrest.

Results

S. pombe SUMO/Pmt3 is phosphorylated

As part of our investigation into sumoylated species in *S. pombe* we undertook 2D PAGE. An example of a typical gel (using a low level of protein, 50 µg, and isoelectric focussing range pH 3–6) stained with colloidal Coomassie Blue is shown in Figure S2. Western blotting of a similar 2D gel with anti-SUMO antisera

(Figure 1A) showed multiple species, including five which migrate with pIs and Mr similar to that of SUMO/Pmt3. (*S. pombe* SUMO/Pmt3 has a predicted pI of 4.6 and migrates at approximately 18 kDa, e.g. [28]).

One possible explanation for the presence of these species is that they could be intermediates arising during the processing of the precursor form of SUMO/Pmt3 to the mature form. We therefore compared the pattern of species in wild type and *pmt3-GG* cells (where only the mature form of SUMO/Pmt3 is present) (Figure 1B). No difference in the relative amount of the species was observed indicating that the species do not represent processing intermediates.

The pattern of the anti-SUMO antibody cross-reacting species suggests that the species may represent modified forms of SUMO/Pmt3. Since the forms are very similar in size, but have different pIs, it could be postulated that the modifying species is/are small, but charged. One candidate for such a modifying species is phosphate. To determine whether any of these species represent phosphorylated forms, we treated protein extracts with calf intestinal phosphatase (CIP) before analysis by 2D PAGE. Figure 1B and Figure 2 indicate that two prominent acidic forms (A,B) are lost following CIP treatment, consistent with them being phosphorylated forms.

We next analysed the SUMO/Pmt3 sequence for possible phosphorylation sites (Ser or Thr residues). Figure 2 shows that SUMO/Pmt3 has nine Ser residues and eight Thr residues (Figure 2, left hand panel). To identify which of these residues is phosphorylated, we created a series of mutations in *pmt3* (*pmt3-1* – *pmt3-8*) and used 2D PAGE to analyse the pattern of species present in each mutant (Figure 2, right hand panel). In all mutants the Ser or Thr residues were mutated to alanine. As a control we included a wild type extract treated with CIP. Of the eight mutants tested, seven had a similar number of species to that observed in wild type cells. In only one mutant, *pmt3-1* (*pmt3-S2A,S4A,S6A*), did the pattern of species resemble that observed following treatment with CIP. This indicates that phosphorylation occurs at the N-terminus of SUMO/Pmt3, likely on two of the three Ser residues (S2, S4, S6).

We next investigated whether inability to phosphorylate the N-terminus of SUMO/Pmt3 affected the levels of high Mr SUMO-

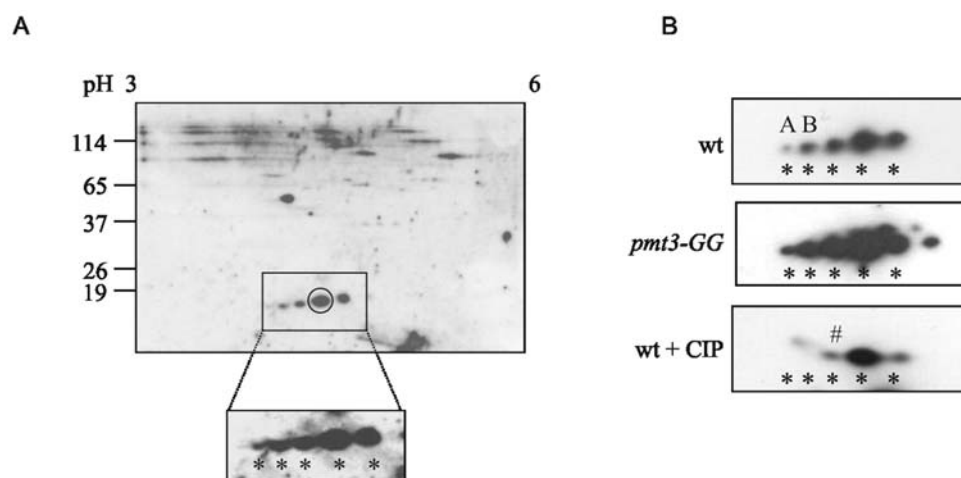


Figure 1. Western analysis of 2D PAGE of *S. pombe* proteins. A. 50 µg of a wild-type total cell extract was separated by IEF (pH 3–6) followed by SDS-PAGE (12.5%) and Western blotted with anti-SUMO antisera. Boxed region is an expanded version of a longer exposure of the same blot. B. Comparison of species in extracts from wt, *pmt3-GG* and wt extracts+CIP (5 units/50 µg protein). * presumed forms of SUMO monomer, A,B, forms not observed after CIP treatment, # possible acetylated form.
doi:10.1371/journal.pone.0006750.g001

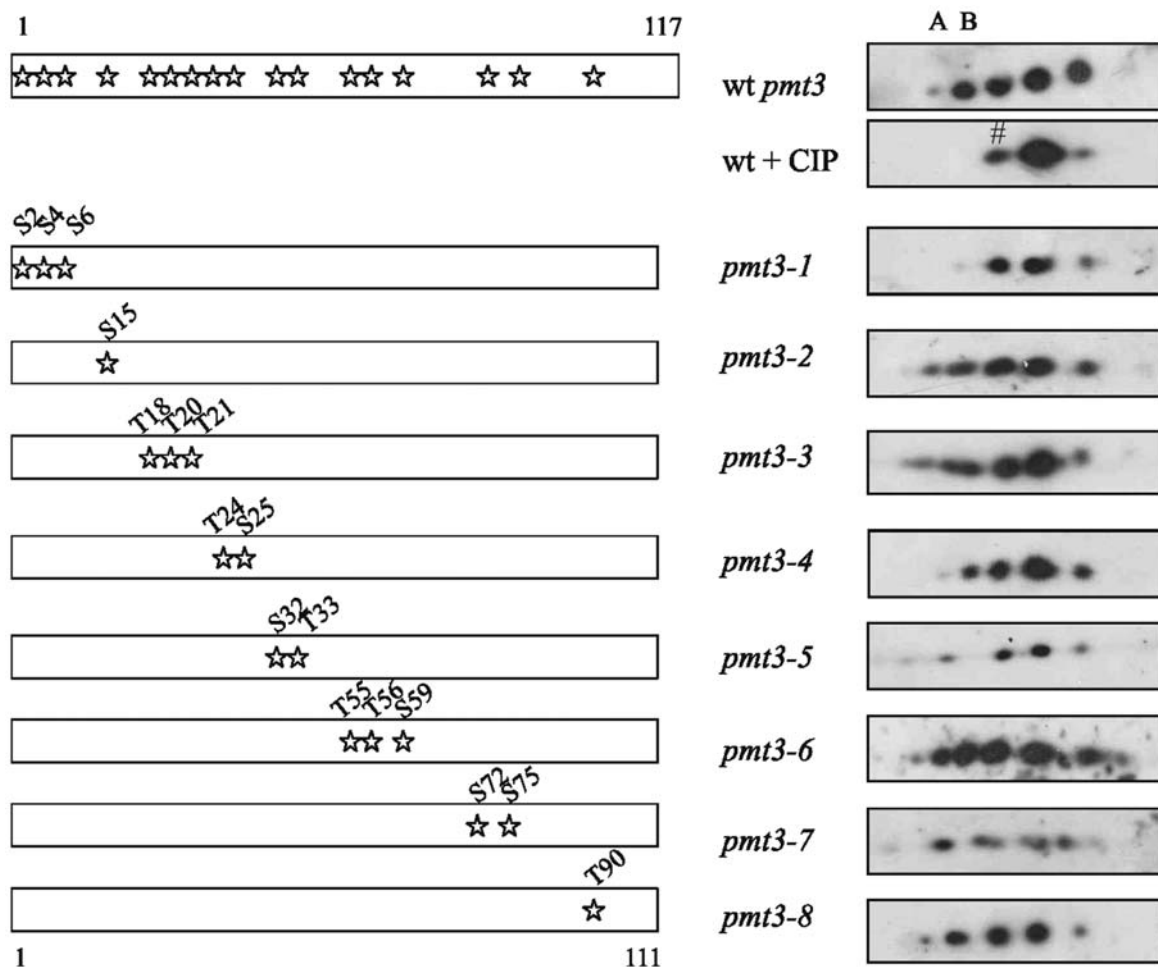


Figure 2. Position of serine and threonine residues and effects of mutations in SUMO/Pmt3. Position of serine and threonine residues in SUMO/Pmt3 are indicated by stars. Left hand panel: sites of mutations in *pmt3* mutants. Right hand panel: Western analysis with anti-SUMO antisera of 2D PAGE (1st dimension pH range 3–6, 2nd dimension 12.5% acrylamide) of extracts from wild type (wt), wild type+CIP and *pmt3* mutants. A,B, forms not observed after CIP treatment, # possible acetylated form.
doi:10.1371/journal.pone.0006750.g002

containing species in cells. The *pmt3-1* mutant is the only mutant of the eight that we tested that has altered levels of these high Mr species (Figure 3A). In *pmt3-1* the level of high Mr SUMO-containing species is similar to the level observed in *pmt3-nfl* cells (encoding a version of Pmt3 deleted for the first 29 aa), but is still greater than that observed in the SUMO ligase null mutant *pli1-d*.

To determine whether the reduced level of high Mr species in *pmt3-1* cells was due to reduced levels of total SUMO, or reduced ability to incorporate SUMO into chains we compared the levels of free SUMO/Pmt3 in the Ser/Thr mutants and *pli1-d* with that in wild type (Figure 3B and data not shown). Of all the mutants tested, only *pmt3-1* has reduced levels of free SUMO/Pmt3. This was not observed with *pli1-d* cells, where the absence of a SUMO ligase reduces the level of high Mr SUMO-containing species, but not the total amount of SUMO within cells. This suggests that the inability to phosphorylate SUMO/Pmt3 in *pmt3-1* cells affects its stability, and hence the amount of SUMO/Pmt3 available for sumoylation.

pmt3-1 is not sensitive to DNA damaging agents

We were interested to determine whether inability to phosphorylate SUMO/Pmt3 affected the response of cells to DNA damaging agents and other stresses. *pmt3-1* is not sensitive to HU, MMS, CPT or TBZ (Figure 4) or UV, IR or 1M sorbitol (data not shown),

despite having significantly reduced levels of high Mr SUMO-containing species and free SUMO/Pmt3. This lack of phenotype is reminiscent of *pli1-d* cells which also have little sensitivity to these agents, apart from slight sensitivity to TBZ (Figure 4 and [27])

pmt3-2 is sensitive to camptothecin and MMS

Analysis of the sensitivities of the remaining seven *pmt3* mutants, (*pmt3-2* – *pmt3-8*) (Figure 4) indicates that *pmt3-2* (*pmt3-S15A*) is sensitive to the topoisomerase I inhibitor, camptothecin (CPT), and slightly sensitive to MMS. The reason for this is not known but may reflect a requirement for S15 in a process required for replication of a damaged DNA template.

Sequence requirements for SUMO chain formation

The N-termini of *S. cerevisiae* SUMO/Smt3 and human SUMO-2/3 contain lysine residues that are involved in SUMO chain formation. Specifically, mutational analysis indicates that the major branch sites used during SUMO chain formation are K15 and K11 in *S. cerevisiae* Smt3 and human SUMO-2/3 respectively [17,19,20]. These lysine residues both occur within the SUMO acceptor consensus motif, ψ KxE. The N-terminal region of *S. pombe* SUMO/Pmt3 does not contain a KxE motif (Figure S1). This suggests that the sequence requirement(s) for SUMO chain formation may be less

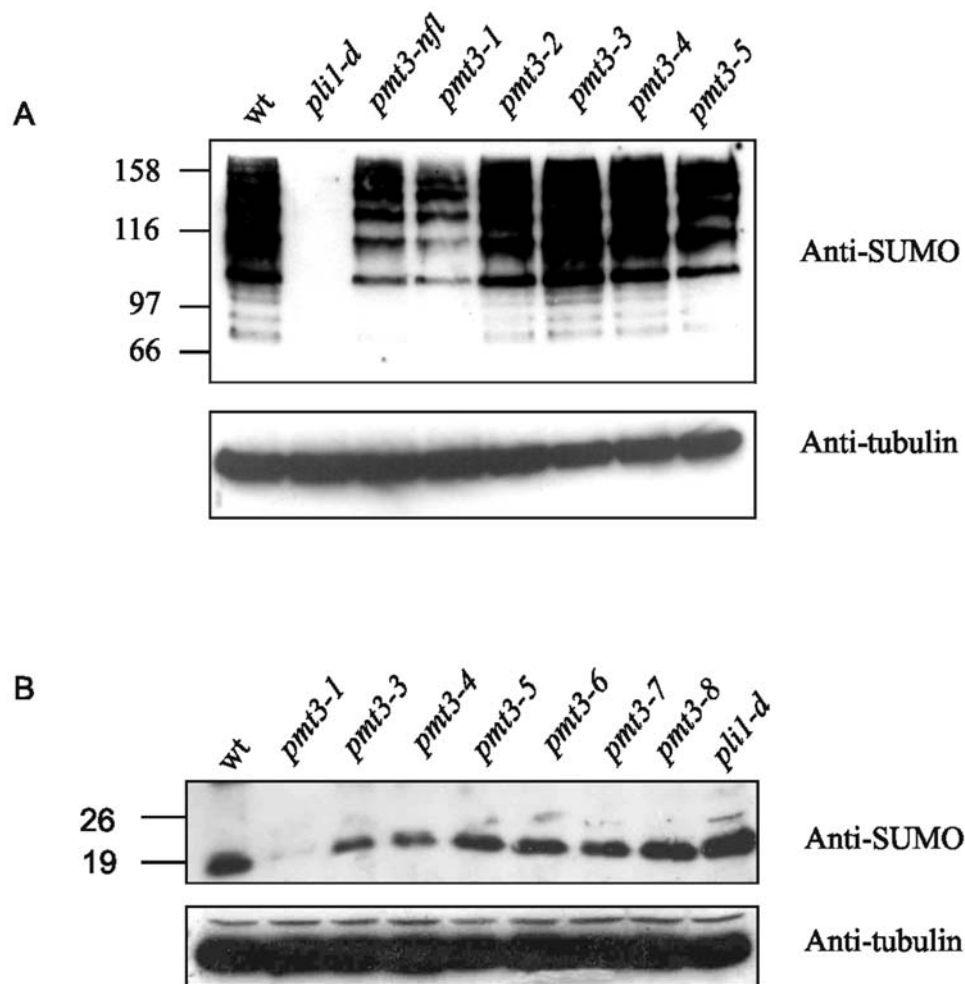


Figure 3. Effect of *pmt3* mutations on levels of sumoylated species and free SUMO/Pmt3 *in vivo*. A. Western blot 7.5% SDS PAG of total cell extracts from wt, *pli1-d* and *pmt3* mutant cells as indicated, probed with anti-SUMO antisera (upper panel) and anti-tubulin antisera (lower panel). B. Western blot 12.5% SDS PAG of total cell extracts from wt, *pli1-d* and *pmt3* mutant cells as indicated, probed with anti-SUMO antisera (upper panel) and anti-tubulin antisera (lower panel).
doi:10.1371/journal.pone.0006750.g003

stringent in *S. pombe* than in other organisms. Instead, SUMO/Pmt3 contains the sequence DVKPST (aa 28–33), adjacent to the highly conserved region of the molecule, and which corresponds to EVKPET (aa 17–22) in *S. cerevisiae*. In addition to K30, SUMO/Pmt3 has another lysine residue (K14) in its N-terminus. We have previously shown that K30 can act as a SUMO acceptor for chain formation in *S. pombe* [26]. We also demonstrated that the SUMO ligase, Nse2, can enhance SUMO chain formation.

We were interested in whether K14 can also be used as a SUMO acceptor, and whether the other *S. pombe* SUMO ligase, Pli1, can facilitate SUMO chain formation. Figure 5A indicates that under our standard *in vitro* SUMO modification conditions in the absence of either of the SUMO ligases, Nse2 or Pli1, mutation of lysine 14 to arginine (Pmt3-K14R) (lane 2), results in a similar decrease in SUMO chain formation as is observed with Pmt3-K30R (lane 3) when compared to wild type SUMO/Pmt3 (lane 1). Replacement of both lysine residues with arginine (Pmt3-K14R,K30R) further decreases chain formation (lane 4). These results indicate that both K14 and K30 act as SUMO acceptors *in vitro*, and that it is unlikely that there are other lysine residues within SUMO/Pmt3 involved in chain formation.

We next compared the effect of the K14R, K30R and K14R+K30R mutations on chain formation facilitated by the

two SUMO ligases. Figure 5B shows that, as previously described [26], using Nse2 as a ligase, chain formation is reduced with Pmt3-K30R (lane 7) when compared to wild type Pmt3 (lane 3). Using Pmt3-K14R (lane 5) chain formation is also reduced, but to a somewhat lesser extent than with Pmt3-K30R (lane 7). Mutation of both lysines (Pmt3-K14R,K30R) essentially abolishes chain formation (lane 9). When Pli1 is used as a ligase, there is only a small reduction in chain formation with either Pmt3-K14R (Figure 5C, lane 4) or Pmt3-K30R (lane 6) as compared to wild type Pmt3 (lane 2). As is observed with Nse2, mutation of both lysine residues (Pmt3-K14R,K30R, lane 8) abolishes chain formation. Taken together, these results show that both K14 and K30 can act as SUMO acceptor sites *in vitro* when chain formation is facilitated by either of the SUMO ligases. Since mutation of both residues abolishes chain formation, it is likely that K14 and K30 are the only SUMO acceptor sites in SUMO/Pmt3.

Inability to form SUMO chains results in aberrant cellular morphology and sensitivity to hydroxyurea

We were next interested in determining whether any of the *pmt3* K to R mutations affect SUMO modification or chain formation when the mutant alleles are present in cells as the sole copy of

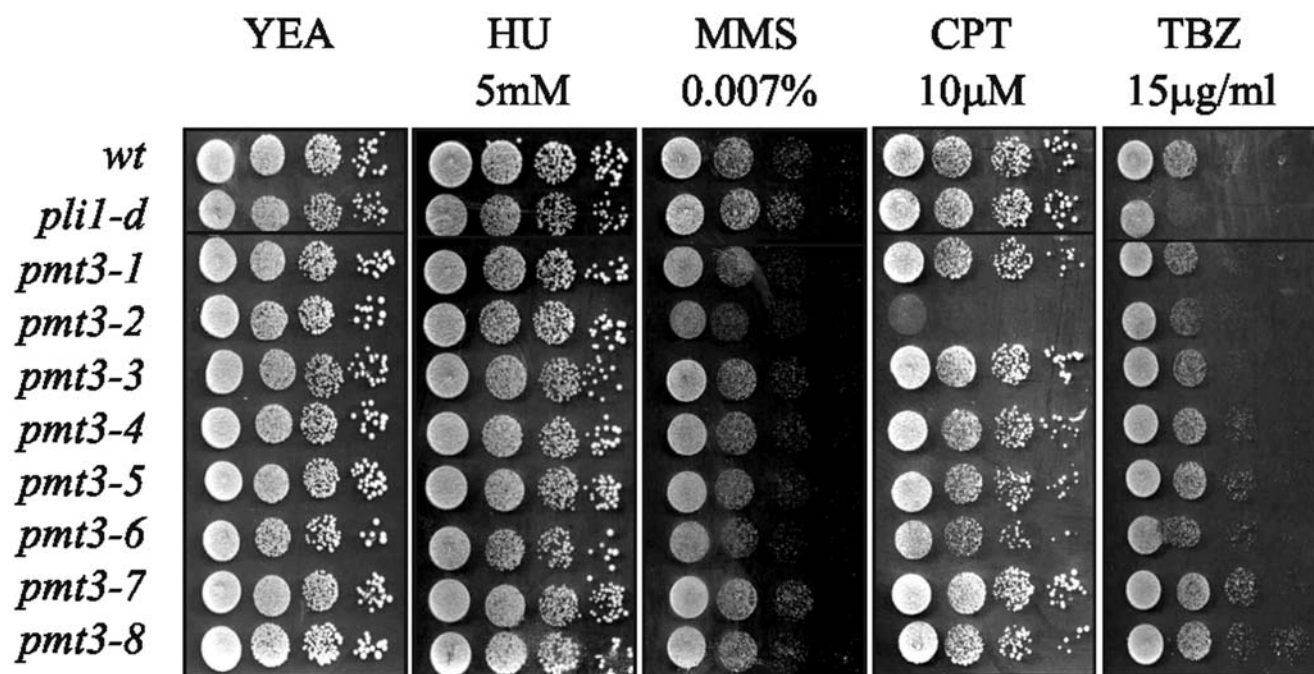


Figure 4. Effect of *pmt3* mutations on sensitivity to DNA damaging agents, HU and microtubule inhibitors. 10 µl of 10 fold serial dilutions were plated onto media as indicated, and incubated at 30°C for 5 days.
doi:10.1371/journal.pone.0006750.g004

SUMO/Pmt3 and whether they affect cell viability or morphology. All three mutants are viable, although *pmt3-K14R*, *K30R* colonies grow slightly slower than wild type (data not shown). Western blotting with anti-SUMO antisera indicates that, compared to wild type, *pmt3-K14R* has substantially reduced levels of high Mr SUMO-containing species (Figure 6A, lanes 2), compared to wild type cells (lanes 1,5). Cells containing *pmt3-K30R* (lane 3) have a similar level of high Mr SUMO/Pmt3-containing species to that observed in wild type cells (lanes 1,5), but the double mutant *pmt3-K14R,K30R* has significantly reduced levels high Mr species (lane 4), intermediate between those observed in *pli1-d* and *hus5-62* cells (defective in the SUMO conjugator, [24,25]). These data show that K14 and, to a lesser extent, K30 are required for SUMO chain formation *in vivo*.

Mutants defective in sumoylation e.g. *rad31-d* (deleted for one subunit of the SUMO activator [23]) and *hus5-62* have aberrant cell and nuclear morphologies under normal growth conditions, and are sensitive to DNA damaging agents and the DNA synthesis inhibitor hydroxyurea (HU) [24,25]. Comparison of the morphologies of *pmt3-K14R* and *pmt3-K30R* with that of wild type cells, indicates that replacement of a single lysine residue has no effect on cell or nuclear morphology, as cells resemble wild type (Figure 6B). However *pmt3-K14R,K30R* cells display a range of cellular morphologies, including elongated cells, aberrant nuclear structure (labelled a) and stretched and fragmented chromatin (labelled b). This phenotype is reminiscent of the phenotypes of *rad31-d* and *hus5-62* cells [23,24,25] and indicates that SUMO chain formation is important for normal growth under vegetative conditions.

We next investigated whether any of these *pmt3* mutants were sensitive to HU or other toxins. All the SUMO chain mutants resemble wild type in their response to UV, MMS, CPT and TBZ (Figure 6C and data not shown). The *pmt3-K14R* and *pmt3-K14R,K30R* mutants are both sensitive to HU (5 mM), while *pmt3-K30R* is very slightly sensitive to HU. These data indicate that

K14, and possibly K30, is required for response of cells to replication arrest. The HU sensitivities of *pmt3-K14R* and *pmt3-K14R,K30R* are significantly less than that observed for *hus5-62*, indicating that as well as a requirement for SUMO chains, modification of target proteins by single SUMO/Pmt3 moieties is also likely to be necessary for the response to S phase arrest.

Discussion

We show here that SUMO/Pmt3 is phosphorylated at its extreme N-terminus. While this manuscript was in preparation, results from mass spectrometry studies were published [29] which indicate that human SUMO-1 and *S. cerevisiae* SUMO/Smt3 are phosphorylated on S2. Our results described here, which show that *S. pombe* SUMO/Pmt3 is likely phosphorylated on two of three serine residues, S2, S4 and S6 (or diphosphorylated on one of them), are consistent with these data. [29]. In addition to being phosphorylated, Matic et al. observed that SUMO is acetylated on its N-terminus. Acetylation of SUMO/Pmt3 would account for the species labelled # (Figures 1 and 2) that remains after treatment with CIP.

Interestingly, inability to phosphorylate SUMO/Pmt3 in *pmt3-1*, results in a reduction in the level of high Mr SUMO containing species. Despite this, *pmt3-1* cells grow as wild type and are not sensitive to DNA damaging agents, HU or TBZ. Another feature of *pmt3-1* cells is the reduced level of free SUMO/Pmt3 (Figure 3B) suggesting that phosphorylation of SUMO/Pmt3 is required for stability of the molecule. The fact that *pli1-d* cells have normal levels of free SUMO/Pmt3 indicates that the low level of free SUMO/Pmt3 in *pmt3-1* is not likely to be due to the fact that in these cells, it is inefficiently conjugated onto target molecules.

It is now well documented that SUMO is capable of forming chains [17,18,20,30] and reviewed in [31]. We show here that *S. pombe* SUMO/Pmt3 can form chains using two lysine residues in the N-terminus (K14 and K30). Interestingly, the K30R mutation has a

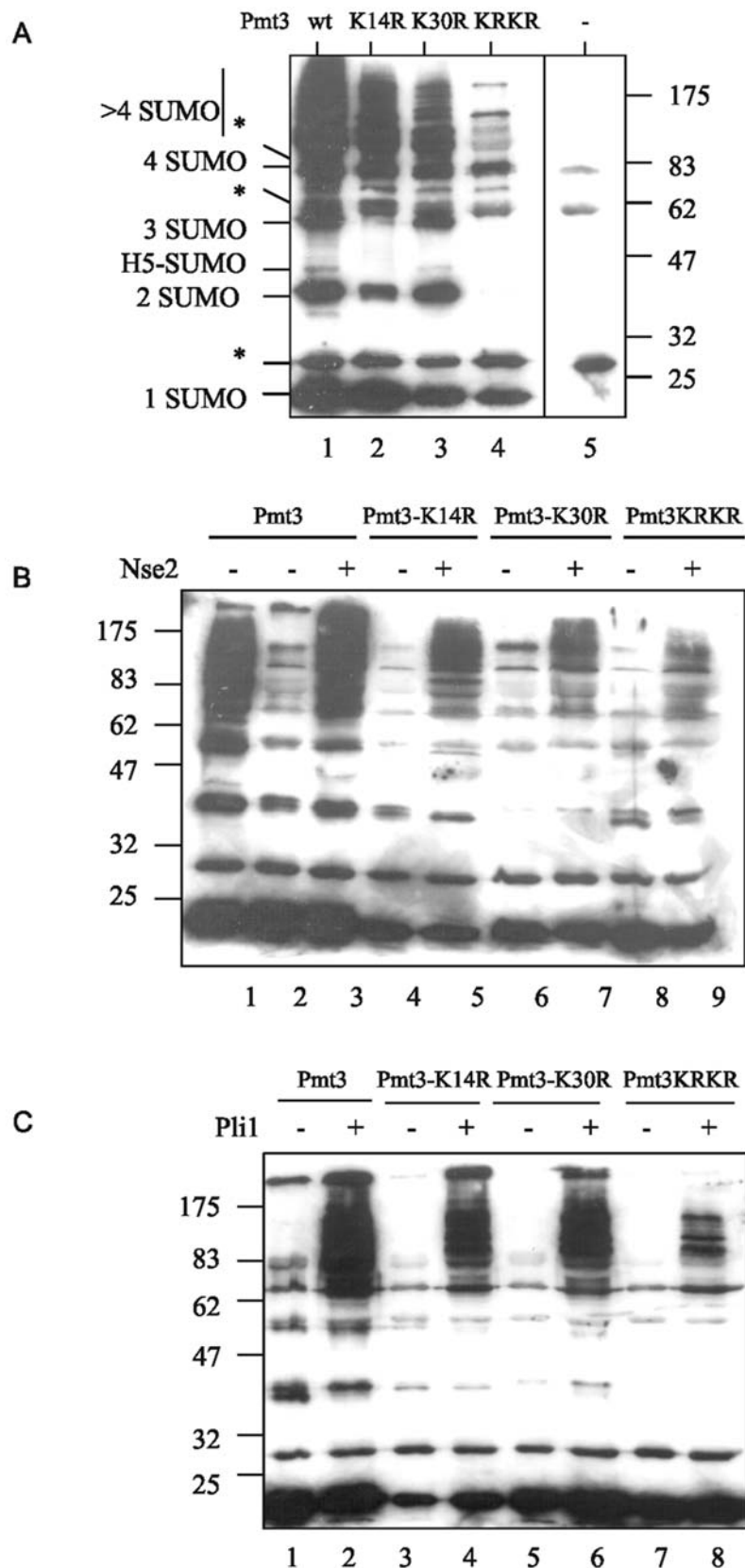
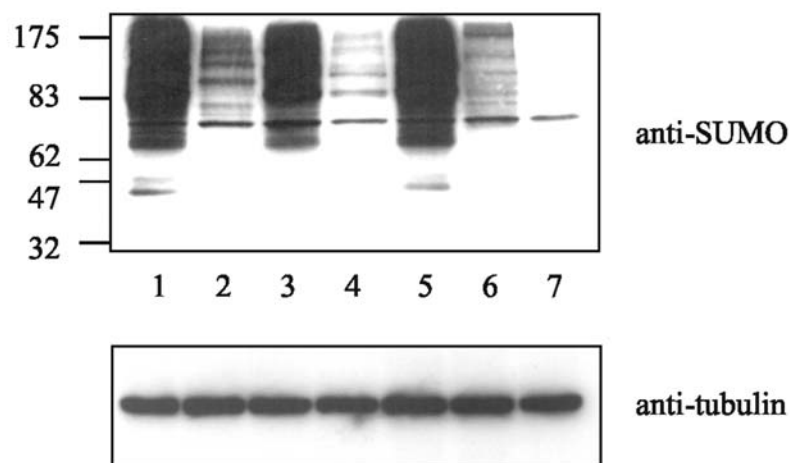
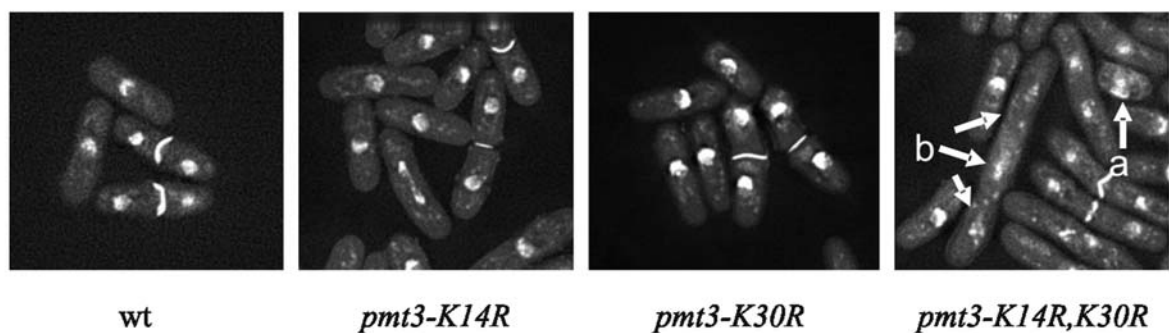


Figure 5. Pmt3 sequence requirements for chain formation. A–C. Mutant forms of Pmt3 tested for ability to form Pmt3 chains using the *in vitro* sumoylation assay in the absence of target protein. A. Lanes 1 Pmt3-GG, Lane 2 Pmt3-K14R,GG, Lane 3 Pmt3-K30R,GG, lane 4 Pmt3-K14R,K30R,GG, lane 5 no Pmt3. Reactions were carried out with 3 μ g Hus5. B. Lane 1 3 μ g Hus5, Lanes 2–9 0.3 μ g Hus5, otherwise as indicated. C. Lanes 1–8 0.3 μ g Hus5. * indicates cross-reaction with SAE proteins. H5-SUMO represents sumoylated Hus5.
doi:10.1371/journal.pone.0006750.g005

A



B



C

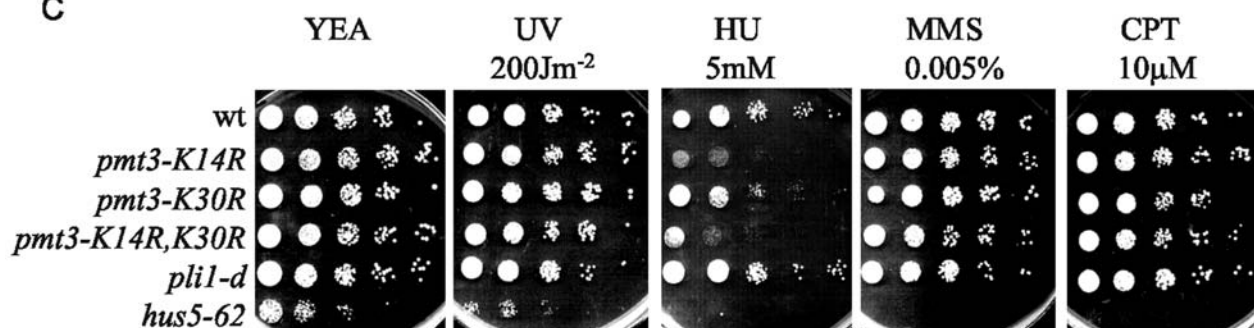


Figure 6. Phenotype of mutants defective in SUMO/Pmt3 chain formation. A. Western analysis of total cell extracts from cells containing mutant versions of SUMO/Pmt3. Lane 1,5 wt, lane 2 *pmt3-K14R*, lane 3 *pmt3-K30R*, lane 4 *pmt3-K14R,K30R*, lane 6 *pli1-d*, lane 7 *hus5-62*. B. Morphology of methanol fixed cells, stained with DAPI and calcofluor. C. Phenotype of *pmt3* mutants. 10 μl of 10 fold serially diluted cultures were plated onto media as indicated, and incubated at 25°C for 5 days.

doi:10.1371/journal.pone.0006750.g006

somewhat greater effect on Nse2-dependent chain formation [26] than it does on Pli1-dependent chain formation (Figure 5B,C). The reason for this is not known, i.e. whether it reflects the fact that the

two SUMO ligases have different specificities, or whether Pli1 behaves in a more promiscuous manner and can select K14 as an acceptor site if K30 is mutated. The sensitivities of the three SUMO

chain mutants to HU, but not to a range of other genotoxins indicates a role for SUMO chains in the cell's response to S phase arrest. The fact that *pmt3-K14R,K30R* cells have aberrant cell and nuclear morphologies, while the two single mutants appear morphologically wild type indicates a role for both lysine residues. The morphology of *pmt3-K14R,K30R* is reminiscent of *rad31-d* and *hus5-62* mutants [23,24,25]. These results are in contrast to what has been observed in *S. cerevisiae*, where an *smt3-allR* mutation has no effect on vegetative growth or sensitivity to toxins [20].

It has recently been shown that SUMO chains interact with STUbLs, and can be ubiquitinated by them [21]. If one of the functions of chain formation is to facilitate the interaction of SUMO/Pmt3 with the STUbLs it might be expected that the phenotype of a mutant defective in chain formation would share similarities with the phenotypes of STUbL mutants. In *S. pombe* the STUbL proteins include Slx8, Rfp1 and Rfp2 [14,32]. Deletion of *slx8* or of both *rfp1* and *rfp2* is lethal, while a conditional mutant of *slx8* (*slx8-1*) is sensitive to HU, MMS and CPT [14]. *pmt3-K14R,K30R* has a similar sensitivity to HU as *slx8-1*, but is wild type for response to MMS and CPT. The reason for the difference in MMS and CPT sensitivity between *slx8-1* and the SUMO chain mutants could be explained if the *S. pombe* STUbLs do not necessarily need to interact with SUMO chains in order to be targeted to substrates, but could recognise single SUMO species. This would be consistent with the fact that unlike the human STUbL, RNF4, that contains multiple SIMs which are proposed to recognise SUMO chains [21], *S. pombe* STUbLs only contain one or two SIMs [14,32], suggesting that they interact with mono-sumoylated species.

In summary, the N-terminus of SUMO/Pmt3 is required for the formation of SUMO chains and is phosphorylated. Surprisingly, a *pmt3* allele encoding a non-phosphorylatable version of SUMO/Pmt3 behaves as wild type. In contrast, abolition of SUMO chain formation has a substantial effect on cell and nuclear morphology. In particular, SUMO chain formation is required for a process associated with S phase arrest, perhaps involving the STUbLs. The precise role of SUMO chains in this event i.e. the identity of protein(s) required for the response to S phase arrest, that are modified by SUMO chains remains to be determined.

Materials and Methods

Strains and plasmids

Strains were constructed using standard genetic techniques. The *pli1-d* mutant was created by deleting the ORF using the method of Bahler *et al.* [33], *hus5-62* was from A. Carr, Sussex [24]. Full length *pmt3* and *pmt3-GG* were amplified as described in [28]. *pmt3-nfl*, lacking the coding sequence for 29 aa at the N terminus, was produced by PCR. *pmt3* mutant alleles were produced by Quikchange PCR mutagenesis (Stratagene) according to the manufacturer's instructions. Mutant *pmt3* alleles were subsequently subcloned into pET15b (Novagen) for expression in *E. coli*, or integrated into the *S. pombe* genome along with 0.5 kb 5' and 3' *pmt3* flanking sequences and the *ura4* gene as selectable marker.

Protein and Immunological methods

Whole cell *S. pombe* extracts were prepared using TCA as described in [34]. 1D SDS PAGE and Western blotting was carried

out as described in [35]. 2D PAGE was undertaken using standard techniques [36]. Total cell protein from 10 OD₅₉₅ units of cells were precipitated with TCA. The precipitate was resuspended in ice-cold acetone and protein precipitated at 4°C for 30 min. The precipitate was harvested by centrifugation at 13 krpm for 30 min, and allowed to dry. The pellet was resuspended in rehydration buffer (9M urea, 4% CHAPS, 2% IPG buffer (25 µl/µg pellet). DTT was added to 0.5%. 50 µg protein was added to modified rehydration buffer (6M urea, 2M thiourea, 2% CHAPS, 2% IPG buffer) to produce a total volume of 125 µl. 7 cm IPG strips pH 3–6 were used for the first dimension. 12.5% acrylamide was used for the second dimension. Anti-SUMO/Pmt3 antiserum was produced against full length SUMO/Pmt3 using standard methods [35]. Western analysis using purified recombinant proteins indicates that the antisera recognises equally well full length SUMO/Pmt3, N-terminally truncated SUMO/Pmt3 (Pmt3-nfl), Pmt3-1, and Pmt3 K to R mutants (Figure S3). Monoclonal anti-tubulin antibodies were from Sigma. The *in vitro* sumoylation assay was used as described previously [28].

Phenotypic analysis of mutants

Sensitivities to hydroxyurea (HU), methyl methanesulphonate (MMS), camptothecin, (CPT) and thiabendazole (TBZ) were analysed on YEP agar at the doses stated. Plates were incubated at 30°C or 25°C for 5 days as stated. Cell morphology was analysed using methanol-fixed cells stained with DAPI (1 µg/ml) and calcofluor (0.5 µg/ml) using an Applied Precision Deltavision Spectris microscope.

Supporting Information

Figure S1 SUMO sequence alignments Comparison of *S. pombe* (Sp), *S. cerevisiae* (Sc), human (Hs), *D. melanogaster* (Dm) and *C. elegans* (Ce) SUMO sequences, created using the ClustalW program. * indicates K14 and K30

Found at: doi:10.1371/journal.pone.0006750.s001 (9.49 MB TIF)

Figure S2 2D PAGE of total *S. pombe* proteins. 50 µg of a wild-type total cell extract was separated using IEF strip pH 3–6, followed by SDS PAGE (12.5% acrylamide). Gel was stained with colloidal Coomassie Blue.

Found at: doi:10.1371/journal.pone.0006750.s002 (9.29 MB TIF)

Figure S3 Anti-SUMO antisera recognise wt and mutant SUMO/Pmt3 Coomassie Brilliant Blue (CBB) staining and western analysis of recombinant wild type and mutant SUMO/Pmt3 with anti-SUMO antisera.

Found at: doi:10.1371/journal.pone.0006750.s003 (9.42 MB TIF)

Acknowledgments

We would like to thank Simon Morley and Jo Murray for helpful discussions.

Author Contributions

Conceived and designed the experiments: FZW. Performed the experiments: AS JCYH BM EO. Analyzed the data: AS EO. Wrote the paper: FZW.

References

1. Sims RJ 3rd, Reinberg D (2008) Is there a code embedded in proteins that is based on post-translational modifications? *Nat Rev Mol Cell Biol* 9: 815–820.
2. Kerscher O, Felberbaum R, Hochstrasser M (2006) Modification of proteins by ubiquitin and ubiquitin-like proteins. *Annu Rev Cell Dev Biol* 22: 159–180.
3. Vijay-Kumar S, Bugg CE, Cook WJ (1987) Structure of ubiquitin refined at 1.8 Å resolution. *J Mol Biol* 194: 531–544.
4. Bayer P, Arndt A, Metzger S, Mahajan R, Melchior F, et al. (1998) Structure determination of the small ubiquitin-related modifier SUMO-1. *J Mol Biol* 280: 275–286.

5. Rechsteiner M (1987) Ubiquitin-mediated pathways for intracellular proteolysis. *Annu Rev Cell Biol* 3: 1–30.
6. Hoege C, Pfander B, Moldovan GL, Pyrowolakis G, Jentsch S (2002) RAD6-dependent DNA repair is linked to modification of PCNA by ubiquitin and SUMO. *Nature* 419: 135–141.
7. Stelter P, Ulrich HD (2003) Control of spontaneous and damage-induced mutagenesis by SUMO and ubiquitin conjugation. *Nature* 425: 188–191.
8. Kannouche PL, Wing J, Lehmann AR (2004) Interaction of human DNA polymerase η with monoubiquitinated PCNA: a possible mechanism for the polymerase switch in response to DNA damage. *Mol Cell* 14: 491–500.
9. Hay RT (2005) SUMO: a history of modification. *Mol Cell* 18: 1–12.
10. Klein HL (2006) A SUMOry of DNA replication: synthesis, damage, and repair. *Cell* 127: 455–457.
11. Watts FZ (2007) The role of SUMO in chromosome segregation. *Chromosoma* 116: 15–20.
12. Lallemand-Breitenbach V, Jeanne M, Benhenda S, Nasr R, Lei M, et al. (2008) Arsenic degrades PML or PML-RAR α through a SUMO-triggered RNF4/ubiquitin-mediated pathway. *Nat Cell Biol* 10: 547–555.
13. Mullen JR, Brill SJ (2008) Activation of the Slx5-Slx8 ubiquitin ligase by poly-small ubiquitin-like modifier conjugates. *J Biol Chem* 283: 19912–19921.
14. Prudden J, Pebernard S, Raffa G, Slavin DA, Perry JJ, et al. (2007) SUMO-targeted ubiquitin ligases in genome stability. *Embo J* 26: 4089–4101.
15. Hay RT (2001) Protein modification by SUMO. *Trends Biochem Sci* 26: 332–333.
16. Pickart CM, Fushman D (2004) Polyubiquitin chains: polymeric protein signals. *Curr Opin Chem Biol* 8: 610–616.
17. Tatham MH, Jaffray E, Vaughan OA, Desterro JM, Botting CH, et al. (2001) Polymeric chains of SUMO-2 and SUMO-3 are conjugated to protein substrates by SAE1/SAE2 and Ubc9. *J Biol Chem* 276: 35368–35374.
18. Pichler A, Gast A, Seeler JS, Dejean A, Melchior F (2002) The nucleoporin RanBP2 has SUMO1 E3 ligase activity. *Cell* 108: 109–120.
19. Bencsath KP, Podgorski MS, Pagala VR, Slaughter CA, Schulman BA (2002) Identification of a multifunctional binding site on Ubc9p required for Smt3p conjugation. *J Biol Chem* 277: 47938–47945.
20. Bylebyl GR, Belichenko I, Johnson ES (2003) The SUMO isopeptidase Ulp2 prevents accumulation of SUMO chains in yeast. *J Biol Chem* 278: 44113–44120.
21. Tatham MH, Geoffroy MC, Shen L, Plechanovova A, Hattersley N, et al. (2008) RNF4 is a poly-SUMO-specific E3 ubiquitin ligase required for arsenic-induced PML degradation. *Nat Cell Biol* 10: 538–546.
22. Tanaka K, Nishide J, Okazaki K, Kato H, Niwa O, et al. (1999) Characterization of a fission yeast SUMO-1 homologue, pmt3p, required for multiple nuclear events, including the control of telomere length and chromosome segregation. *Mol Cell Biol* 19: 8660–8672.
23. Shayeghi M, Doe CL, Tavassoli M, Watts FZ (1997) Characterisation of *Schizosaccharomyces pombe* rad31, a UBA-related gene required for DNA damage tolerance. *Nucleic Acids Res* 25: 1162–1169.
24. al-Khodairy F, Enoch T, Hagan IM, Carr AM (1995) The *Schizosaccharomyces pombe* hus5 gene encodes a ubiquitin conjugating enzyme required for normal mitosis. *J Cell Sci* 108: 475–486.
25. Ho JC, Watts FZ (2003) Characterization of SUMO-conjugating enzyme mutants in *Schizosaccharomyces pombe* identifies a dominant-negative allele that severely reduces SUMO conjugation. *Biochem J* 372: 97–104.
26. Andrews EA, Palecek J, Sergeant J, Taylor E, Lehmann AR, et al. (2005) Nse2, a component of the Smc5-6 complex, is a SUMO ligase required for the response to DNA damage. *Mol Cell Biol* 25: 185–196.
27. Xhemalce B, Seeler JS, Thon G, Dejean A, Arcangioli B (2004) Role of the fission yeast SUMO E3 ligase Plilp in centromere and telomere maintenance. *Embo J* 23: 3844–3853.
28. Ho JC, Warr NJ, Shimizu H, Watts FZ (2001) SUMO modification of Rad22, the *Schizosaccharomyces pombe* homologue of the recombination protein Rad52. *Nucleic Acids Res* 29: 4179–4186.
29. Matic I, Macek B, Hilger M, Walther TC, Mann M (2008) Phosphorylation of SUMO-1 occurs in vivo and is conserved through evolution. *J Proteome Res* 7: 4050–4057.
30. Takahashi Y, Toh EA, Kikuchi Y (2003) Comparative Analysis of Yeast PIAS-Type SUMO Ligases In Vivo and In Vitro. *J Biochem (Tokyo)* 133: 415–422.
31. Ulrich HD (2008) The fast-growing business of SUMO chains. *Mol Cell* 32: 301–305.
32. Sun H, Levenson JD, Hunter T (2007) Conserved function of RNF4 family proteins in eukaryotes: targeting a ubiquitin ligase to SUMOylated proteins. *EMBO J* 26: 4102–4112.
33. Bahler J, Wu JQ, Longtine MS, Shah NG, McKenzie A 3rd, et al. (1998) Heterologous modules for efficient and versatile PCR-based gene targeting in *Schizosaccharomyces pombe*. *Yeast* 14: 943–951.
34. Caspari T, Dahlen M, Kanter-Smoler G, Lindsay HD, Hofmann K, et al. (2000) Characterization of *Schizosaccharomyces pombe* Hus1: a PCNA-related protein that associates with Rad1 and Rad9. *Mol Cell Biol* 20: 1254–1262.
35. Harlow E, Lane D (1988) Antibodies: a laboratory manual. Cold Spring Harbor Laboratory.
36. Gorg A, Obermaier C, Boguth G, Harder A, Scheibe B, et al. (2000) The current state of two-dimensional electrophoresis with immobilized pH gradients. *Electrophoresis* 21: 1037–1053.